TARGETING NEURO-IMMUNO-VASCULAR INTERACTIONS IN THE BRAIN AND THE PERIPHERY

EDITED BY: Imola Wilhelm, Istvan A. Krizbai, Mihaela Gherghiceanu, Éva Szőke and Zsuzsanna Helyes

PUBLISHED IN: Frontiers in Pharmacology

frontiers Research Topics

ISSN 1664-8714
ISBN 978-2-88976-172-2
DOI 10.3389/978-2-88976-172-2

About Frontiers

Frontiers is more than just an open-access publisher of scholarly articles: it is a pioneering approach to the world of academia, radically improving the way scholarly research is managed. The grand vision of Frontiers is a world where all people have an equal opportunity to seek, share and generate knowledge. Frontiers provides immediate and permanent online open access to all its publications, but this alone is not enough to realize our grand goals.

Frontiers Journal Series

The Frontiers Journal Series is a multi-tier and interdisciplinary set of open-access, online journals, promising a paradigm shift from the current review, selection and dissemination processes in academic publishing. All Frontiers journals are driven by researchers for researchers; therefore, they constitute a service to the scholarly community. At the same time, the Frontiers Journal Series operates on a revolutionary invention, the tiered publishing system, initially addressing specific communities of scholars, and gradually climbing up to broader public understanding, thus serving the interests of the lay society, too.

Dedication to Quality

Each Frontiers article is a landmark of the highest quality, thanks to genuinely collaborative interactions between authors and review editors, who include some of the world's best academicians. Research must be certified by peers before entering a stream of knowledge that may eventually reach the public - and shape society; therefore, Frontiers only applies the most rigorous and unbiased reviews.
Frontiers revolutionizes research publishing by freely delivering the most outstanding research, evaluated with no bias from both the academic and social point of view. By applying the most advanced information technologies, Frontiers is catapulting scholarly publishing into a new generation.

What are Frontiers Research Topics?

Frontiers Research Topics are very popular trademarks of the Frontiers Journals Series: they are collections of at least ten articles, all centered on a particular subject. With their unique mix of varied contributions from Original Research to Review Articles, Frontiers Research Topics unify the most influential researchers, the latest key findings and historical advances in a hot research area! Find out more on how to host your own Frontiers Research Topic or contribute to one as an author by contacting the Frontiers Editorial Office: frontiersin.org/about/contact

TARGETING NEURO-IMMUNO-VASCULAR INTERACTIONS IN THE BRAIN AND THE PERIPHERY

Topic Editors:
Imola Wilhelm, Biological Research Centre, Hungary
Istvan A. Krizbai, Biological Research Centre, Hungary
Mihaela Gherghiceanu, Victor Babes National Institute of Pathology (INCDVB), Romania
Éva Szőke, University of Pécs, Hungary
Zsuzsanna Helyes, University of Pécs, Hungary

Citation: Wilhelm, I., Krizbai, I. A., Gherghiceanu, M., Szőke, E., Helyes, Z., eds. (2022). Targeting Neuro-Immuno-Vascular Interactions in the Brain and the Periphery. Lausanne: Frontiers Media SA. doi: 10.3389/978-2-88976-172-2

Table of Contents

frontiers | Frontiers in Pharmacology

EDITORIAL
published: 26 April 2022
doi: 10.3389/fphar.2022.893384

Editorial: Targeting Neuro-Immuno-Vascular Interactions in the Brain and the Periphery

Imola Wilhelm[1]*, *István A. Krizbai*[1], *Mihaela Gherghiceanu*[2], *Éva Szőke*[3] and *Zsuzsanna Helyes*[3]

[1]Institute of Biophysics, Biological Research Centre, Szeged, Hungary, [2]Victor Babeș National Institute of Pathology (INCDVB), Bucharest, Romania, [3]Department of Pharmacology and Pharmacotherapy, Medical School and Szentágothai Research Centre, University of Pécs, Pécs, Hungary

Keywords: neuroinflammation, inflammasome, pain, neuropathy, ischemic stroke

Editorial on the Research Topic

Targeting Neuro-Immuno-Vascular Interactions in the Brain and the Periphery

Complex neuro-immune-vascular interactions play key roles in the development of both neuroinflammation (an inflammatory response within the nervous system) and neurogenic inflammation (sensory nerve-released neuropeptides inducing inflammation in different tissues). Both phenomena have a substantial importance in the pathogenesis of several diseases and might be targets for pharmacological interventions.

Therefore, the present Research Topic was designed to collect papers on the molecular mechanisms and pharmacology of pathological processes affecting neuro-immune-vascular interfaces, focusing on neurodegeneration, stroke, headache, neuropathic and other types of pain, as well as peripheral inflammatory diseases, such as arthritis or dermatitis. In addition, interactions between the peripheral and central nervous systems have also been explored.

Neuroinflammation is usually accompanied by vascular reactions, including opening of the blood-brain barrier. In the present Research Topic, Gabbert et al. (2020) describe the important role of protocadherins, especially PcdhgC3 in regulating the barrier integrity of brain microvascular endothelial cells in control and inflammatory conditions. One of the most frequent inflammatory conditions affecting brain vessels is ischemic stroke. Recanalization with tissue plasminogen activator (tPA) is the only approved agent available in this condition. The systematic review by Ye et al. (2020) identifies the possible protective effect of immunomodulators on a lethal side effect of tPA treatment, namely hemorrhagic transformation. In addition, Chen et al. (2021) found that inflammasome proteins were upregulated in neutrophil extracellular traps present in thrombi of patients with acute ischemic stroke, contributing to poor outcomes after tPA treatment.

Inflammasomes were in the focus of the work of Nógrádi et al. (2020) as well. However, they studied not vascular cells, but neurons and found that peripheral nerve injury induced inflammasome activation in motoneurons. The thiazide structure oral antidiabetic diazoxide proved to be protective in this model. Interlocking of peripheral and central processes has been investigated by Lovrenčić et al. (2020) too. They found that intranasal inflammatory reactions provoke distant intracranial changes, including headache.

Inflammatory reactions may affect the peripheral nervous system as well. Inflammatory neuropathies are characterized by leukocyte infiltration of peripheral nerves, demyelination and axonal degeneration. Therefore, inflammation and pain control in chronic neuropathies is essential to improve the outcomes of the disease. Somatostatin released from capsaicin-sensitive peptidergic sensory nerve endings leads to anti-inflammatory and anti-hyperalgesic actions at distant parts of the body,

OPEN ACCESS

Edited and reviewed by:
Frontiers Editorial Office, Frontiers Media SA, Switzerland

***Correspondence:**
Imola Wilhelm
wilhelm.imola@brc.hu

Specialty section:
This article was submitted to Inflammation Pharmacology, a section of the journal Frontiers in Pharmacology

Received: *10 March 2022*
Accepted: *24 March 2022*
Published: *26 April 2022*

Citation:
Wilhelm I, Krizbai IA, Gherghiceanu M, Szőke É and Helyes Z (2022) Editorial: Targeting Neuro-Immuno-Vascular Interactions in the Brain and the Periphery. Front. Pharmacol. 13:893384. doi: 10.3389/fphar.2022.893384

through activation of the somatostatin receptor subtype 4 (SST4). Based on this knowledge, Kántás et al. (2021) demonstrated the anti-nociceptive actions of orally active novel pyrollo-pyrimidine SST4 agonists, which are promising drug candidates in neuropathic pain.

A specific subgroup of neuropathies, immune axonal neuropathies are described in the review of Tulbă et al. (2021). These immune-mediated neuropathies occasionally accompany autoimmune rheumatic diseases, which in turn may also have cardiovascular comorbidities. These latter conditions have been explored by Mong et al. (2020), who found that arterial aging is faster in rheumatoid arthritis patients than in control subjects, and inhibiting inflammation is essential to attenuate the associated cardiovascular risk.

Finally, the paper of Szöllősi et al. (2022) reviews a symptom arising from cutaneous immune-neuronal crosstalks, i.e., pruritus or itch, which may involve the excitation of itch-sensitive neurons or damage of the itch-processing neural network.

Altogether, as a result of the common effort of the Frontiers in Pharmacology team and the five guest editors, a balanced collection of original and review papers have been included in the Research Topic. Nine articles originating from six different countries cover a wide thematic range focused around inflammatory processes affecting the central and peripheral nervous systems.

AUTHOR CONTRIBUTIONS

IW drafted the paper. All authors read and approved the final version.

REFERENCES

Chen, S. H., Scott, X. O., Ferrer Marcelo, Y., Almeida, V. W., Blackwelder, P. L., Yavagal, D. R., et al. (2021). Netosis and Inflammasomes in Large Vessel Occlusion Thrombi. *Front Pharmacol.* 11, 607287. doi:10.3389/fphar.2020.607287

Gabbert, L., Dilling, C., Meybohm, P., and Burek, M. (2020). Deletion of Protocadherin Gamma C3 Induces Phenotypic and Functional Changes in Brain Microvascular Endothelial Cells In Vitro. *Front Pharmacol.* 11, 590144. doi:10.3389/fphar.2020.590144

Kántás, B., Szöke, É., Börzsei, R., Bánhegyi, P., Asghar, J., Hudhud, L., et al. (2021). In Silico, In Vitro and In Vivo Pharmacodynamic Characterization of Novel Analgesic Drug Candidate Somatostatin SST4 Receptor Agonists. *Front Pharmacol.* 11, 601887–17. doi:10.3389/fphar.2020.601887

Lovrenčić, L., Matak, I., and Lacković, Z. (2020). Association of Intranasal and Neurogenic Dural Inflammation in Experimental Acute Rhinosinusitis. *Front Pharmacol.* 11, 586037. doi:10.3389/fphar.2020.586037

Mong, N., Tarjanyi, Z., Tothfalusi, L., Bartykowszki, A., Nagy, A. I., Szekely, A., et al. (2020). Largely Accelerated Arterial Aging in Rheumatoid Arthritis Is Associated With Inflammatory Activity and Smoking in the Early Stage of the Disease. *Front Pharmacol.* 11, 523962–120099. doi:10.3389/fphar.2020.601344

Nógrád, B., Nyúl-Tóth, Á., Kozma, M., Molnár, K., Patai, R., Siklós, L., et al. (2020). Upregulation of Nucleotide-Binding Oligomerization Domain-, LRR- and Pyrin Domain-Containing Protein 3 in Motoneurons Following Peripheral Nerve Injury in Mice. *Front Pharmacol.* 11, 584184. doi:10.3389/fphar.2020.584184

Szöllősi, A. G., Oláh, A., Lisztes, E., Griger, Z., and Tóth, B. I. (2022). Pruritus: A Sensory Symptom Generated in Cutaneous Immuno-Neuronal Crosstalk. *Front Pharmacol.* 13, 745658. doi:10.3389/fphar.2022.745658

Tulbă, D., Popescu, B. O., Manole, E., and Băicuś, C. (2021). Immune Axonal Neuropathies Associated With Systemic Autoimmune Rheumatic Diseases. *Front Pharmacol.* 12, 610585. doi:10.3389/fphar.2021.610585

Ye, Y., Zhu, Y. T., Tong, H. X., and Han, J. Y. (2020). The Protective Role of Immunomodulators on Tissue-Type Plasminogen Activator-Induced Hemorrhagic Transformation in Experimental Stroke: A Systematic Review and Meta-Analysis. *Front Pharmacol.* 11, 615166. doi:10.3389/fphar.2020.615166

Conflict of Interest: The authors declare that the research was conducted in the absence of any commercial or financial relationships that could be construed as a potential conflict of interest.

frontiers in Pharmacology

BRIEF RESEARCH REPORT
published: 15 October 2020
doi: 10.3389/fphar.2020.586037

Association of Intranasal and Neurogenic Dural Inflammation in Experimental Acute Rhinosinusitis

*Luka Lovrenčić, Ivica Matak and Zdravko Lacković**

Laboratory of Molecular Neuropharmacology, Department of Pharmacology, University of Zagreb School of Medicine, Zagreb, Croatia

OPEN ACCESS

Edited by:
Éva Szőke,
University of Pécs, Hungary

Reviewed by:
Mária Dux,
University of Szeged, Hungary
Andy Wai Kan Yeung,
The University of Hong Kong, Hong Kong
László Vécsei,
University of Szeged, Hungary

***Correspondence:**
Zdravko Lacković
zdravko.lackovic@mef.hr

Specialty section:
This article was submitted to Inflammation Pharmacology, a section of the journal Frontiers in Pharmacology

Received: *22 July 2020*
Accepted: *18 September 2020*
Published: *15 October 2020*

Citation:
Lovrenčić L, Matak I and Lacković Z (2020) Association of Intranasal and Neurogenic Dural Inflammation in Experimental Acute Rhinosinusitis. Front. Pharmacol. 11:586037. doi: 10.3389/fphar.2020.586037

Background: Nasal cavity and sinus disorders, such as allergic rhinitis, rhinosinusitis, or certain anatomical defects, are often associated with transient or ongoing headaches. On the other hand, migraine headache patients often exhibit pain referral over the area of nasal sinuses and typical nasal autonomic symptoms involving congestion and rhinorrhea. Mechanism for convergence of nasal or sinus disorders and headaches is unknown. Herein, we examined the association of sino-nasal inflammatory pain with common preclinical indicators of trigeminovascular system activation such as dural neurogenic inflammation (DNI) and neuronal activation in brainstem nociceptive nuclei.

Methods: Nasal and paranasal cavity inflammation and pain was induced by formalin (2.5%/10 μl) or capsaicin (0.1%/10 μl) instillation at the border of maxillary sinus and nasal cavity in rats. Quantification of inflammation of nasal mucosa and DNI was performed by spectrophotometric measurement of Evans blue - plasma protein complex extravasation. Pain behavior was quantified by rat grimace scale (RGS). Nociceptive neuronal activation in caudal part of spinal trigeminal nucleus (TNC) was assessed by c-Fos protein immunohistochemistry.

Results: Capsaicin and formalin administered into rat nasal cavity increased plasma protein extravasation in the nasal mucosa and dura mater. Intensity of plasma protein extravasation in nasal mucosa correlated with extravasation in dura. Similarly, facial pain intensity correlated with nociceptive neuronal c-Fos activation in the TNC.

Conclusion: Present data show that inflammatory stimuli in deep nasal and paranasal structures provoke distant intracranial changes related to trigeminovascular system activation. We hypothesize that this phenomenon could explain overlapping symptoms and comorbidity of nasal/paranasal inflammatory disorders with migraine.

Keywords: facial pain expressions, headache, neurogenic inflammation, cFos protein, rhinosinusitis

INTRODUCTION

Transient headache is a common symptom of different sino-nasal disorders, which is usually resolved by successful treatment of the underlying condition. Nasal and sinus inflammatory conditions, some anatomic abnormalities such as septal spine, bullous nasal turbinate and intranasal contact points have been found to be associated with migraine (Lee et al., 2017). Sino-nasal disorders, such as sinusitis, allergic rhinitis, and mixed rhinitis, could be associated with higher prevalence of migraine and other headaches (Ku et al., 2006; Martin et al., 2014; Wang et al., 2016). Migraine patients may have more intranasal contact points between opposing mucosal surfaces (Ferrero et al., 2014) and their operative removal leads to migraine improvement in some patients. Ongoing headache associated with pain referral above the area of sinuses and accompanied by autonomic symptoms in the sino-nasal area such as nasal congestion, rhinorrhea, and lacrimation has been previously referred to as "sinus headache". However, according to current third edition of International Headache Society Classification criteria (ICHD-3), this term is outdated since it encompasses both primary headaches such as migraine (which may be presenting with nasal symptoms), and secondary headache attributed to disorders of the nose or sinuses. In absence of typical inflammatory findings, many patients previously diagnosed by themselves or by the physician with "sinus headache" are eventually diagnosed with migraine (Schreiber et al., 2004; Eross et al., 2007), and treatable with antimigraine drugs (Patel et al., 2013). Also, in animal models, various stimuli used to model migraine (mechanical or electrical sagittal sinus stimulation, chemical stimulation of meninges) (Mitsikostas and Sanchez del Rio, 2001) and nasal inflammation induce c-Fos expression in the caudal part of spinal trigeminal nucleus (TNC) (Anton et al., 1991). Overall, the role of nasal pathology in the pathogenesis of migraine remains controversial.

In present study, we assessed the possibility that painful inflammatory stimuli in the sino-nasal area are associated with neurogenic inflammation of cranial meninges and neuronal activation of second order nociceptive sensory neurons, the markers of trigeminovascular system activation.

MATERIALS AND METHODS

Animals

Male Wistar rats 2 to 3 months old and weighing 280 to 400 g, bred at the Department of Pharmacology at the Faculty of Medicine of the University of Zagreb, kept at 12-h light/dark cycle with free access to food and water were used in all experiments. The experiments were planned and conducted in accordance with European Union Directive (2010/63/EU) and International Association for the Study of Pain (Zimmermann, 1983). The experiments were approved by Ethical Committees of University of Zagreb School of Medicine and Croatian Ministry of Agriculture (permission no. EP 03-2/2015).

Chemicals

Formalin (formaldehyde mass concentration 36%) (T.T.T., Sveta Nedjelja, Croatia) was diluted with saline (0.9% sodium chloride solution) to the 2.5% concentration required for intranasal instillation. The concentration of formalin used was based on 2.5% concentration usually employed in the orofacial formalin test.

Capsaicin (Sigma Aldrich, St. Louis, MO, USA) was first diluted with ethanol to the mass concentration of 20% and kept at −20°C until further use. For the animal treatment, the solution was further diluted to 0.1% capsaicin concentration in 0.9% physiological saline. The concentration of capsaicin used was based on concentrations and doses previously used for subcutaneous stimulation of the rat hind paw (Bach-Rojecky and Lacković, 2005; Bach-Rojecky et al., 2008; Arreola-Peralta et al., 2018) and rat or mouse whisker pad (Pelissier et al., 2002; Rossi et al., 2016).

Animal Treatment

The animals were treated intranasally with formalin or capsaicin 30 min after 40 mg/kg Evans blue intravenous administration *via* the tail vein (for timeline see **Figure 1A**). Upon administration of Evans blue and irritants, the rats were briefly anesthetized with isoflurane inhalation (Forane, Baxter, Deerfield, IL, USA, 5% induction). Rats were taken out of the induction chamber, and prior to awaking, the volume of 10 µl was instilled by a plastic tubing (outer diameter 0.6 mm) coupled to Hamilton syringe (Hamilton 705 LT 50 µl, Hamilton Company, Reno, Nevada, USA), which was advanced approximately 1.5 cm through the nostril into the nasal cavity without significant resistance (for site of instillation see **Figure 1B**). The period needed for rat recovery from isoflurane anesthesia allowed enough time for instillation. Volume of 10 µl was employed based on the micro-computer tomography-calculated volume of maxillary sinus (Phillips et al., 2009). In preliminary experiments in saline-perfused animals, 10-µl methylene-blue injection induced ipsilateral localized coloration of the nasal mucosa near the entrance of the maxillary sinus (not shown).

Quantification of Pain by Rat Grimace Scale

Twelve rats were used for determining the relationship between painful behavior assessed by rat grimace scale (RGS) (Sotocinal et al., 2011), and the neuronal activation in the primary trigeminal nociceptive nucleus, the TNC. The rats were divided in three experimental groups: non-treated (three animals), intranasally treated with saline (four animals), and the pain group intranasally treated with formalin (five animals). The number of animals used was determined according to previous studies (Matak et al., 2014; Lacković et al., 2016). In order to administer formalin, the animals were briefly restrained since we observed lack of behavioral response in animals subjected to inhalational anesthesia. In conscious animals, using a thin plastic tube coupled to Hamilton syringe was not appropriate due to duration of the procedure. Thus, to enable a quicker delivery, here we employed a flexible electrophoretic gel loading tip (tip

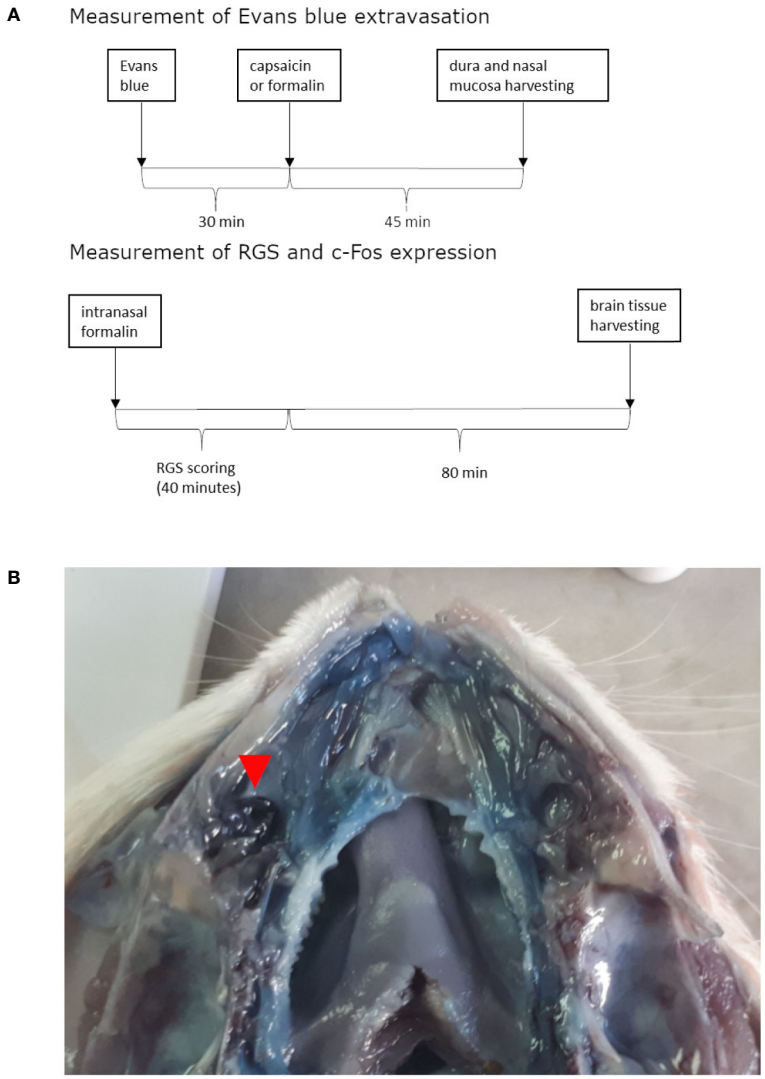

FIGURE 1 | Timeline of experiments **(A)** and site of irritant instillation (in this case formalin) shown on opened nasal cavity (septum was removed) of rat injected with Evans blue and perfused with saline **(B)**. Formalin instillation site is situated near the entrance to the paranasal sinus and is marked with the red arrow. Near it marked Evans blue extravasation can be observed when comparing to contralateral side.

diameter = 0.5 mm) coupled to a 10–100 µl Eppendorf pipette. Immediately following the 10-µl formalin instillation, the animals were put into transparent plastic cages for observation (for timeline of experiment see **Figure 1A**). For RGS scoring, the rat faces were captured with a digital camera in 3-min intervals for 39 min after formalin instillation. Three-minute intervals were chosen based on original description of the method where one photograph from each 3-min interval was chosen for scoring (Sotocinal et al., 2011). Rat facial expression was scored as previously described (Sotocinal et al., 2011). In brief, four action units related to whisker positioning, disappearance of the nose bulging and cheek crease, orbital tightening, and distinct ear shape and positioning, were analyzed. To each of this action units, score of 0, 1 (moderate), or 2 (severe) was assigned and the total sum of scores calculated. The experimenter who scored the individual images was blinded to the animal treatment.

Neuronal c-Fos Activation

Of 12 RGS-scored rats, 10 were used for immunohistochemical analysis (2 non-treated, 4 saline treated, 4 formalin treated). Survival time between the intranasal instillation of formalin and the perfusion for immunohistochemistry was 2 h, as previously used in the orofacial formalin-evoked c-Fos expression (Matak et al., 2014). Animals were deeply anesthetized with 70 mg/kg ketamine (Richter Pharma AG, Wels, Austria) and 7 mg/kg xylazine (Alfasan, Woerder, Netherlands), thoracotomized and transcardially perfused with 500-ml saline and 250-ml fixating agent (4% paraformaldehyde in phosphate buffered saline

(PBS)). After craniotomy, brains were collected and stored in 15% sucrose in fixating agent until tissue sank, followed by 30% sucrose in PBS for 24 h. Then, the tissue was taken out of sucrose, and frozen (-80°C). Caudal brainstem area containing TNC was embedded in O.C.T. compound (Tissue-Tek, Sakura Finetek, Japan) and cut to 30-µm coronal sections in the cryostat. Immunohistochemical staining for c-Fos was performed as described previously (Matak et al., 2014). In brief, representative slices of TNC were placed into the free-floating wells containing PBS and 0.25% Triton X-100 (Sigma-Aldrich, St. Louis, MO, USA) (PBST) and further rinsed with fresh PBST (3 × 5 min). To block the non-specific immunoreactivity, samples were incubated in 10% normal goat serum (Sigma-Aldrich, St. Louis, MO, USA) in PBST for 60 min. Then, the slices were incubated overnight at room temperature with the primary c-Fos antibody (sc-52, Santa Cruz, Dallas, TX, USA) (1:500 in PBST + 1% NGS). Next day, after rinsing 3 times with PBST, slices were incubated with a fluorescently labelled Alexa Fluor 488-labeled secondary antibody (Invitrogen, Carlsbad, CA, USA) for 2 h in the dark at room temperature. After 3 rinses with PBST, slices were mounted on slides, and covered with anti-fading coverslip agent (Fluoromount, Sigma-Aldrich, St. Louis, MO, USA). Sections were photographed by fluorescent microscope (Olympus BX-51, Olympus, Tokyo, Japan) with digital camera (Olympus DP-70, Olympus, Tokyo, Japan). Images were obtained in RGB color format, and grey images of separated green channel were further used to count the c-Fos-positive neuronal profiles, by employing associated software (cellSens Dimension, Olympus, Tokyo, Japan). The counting was performed by a blinded observer based on fixed threshold intensity parameters and defined minimal size of the objects. In tissue cuts, the number of objects was counted in the left-ipsilateral and right-contralateral side within observable borders of the TNC. Average number of c-Fos-expressing neuronal profiles was calculated based on four slices analyzed per single animal.

Quantification of Dural and Nasal Inflammation

Nineteen rats that were used for experiment determining relationship between nasal and dural inflammation were administered Evans' blue into tail vein and were divided into three experimental groups, each group intranasally received saline (six animals), capsaicin (six animals), or formalin (seven animals). The number of animals was determined according to previous work done by our group regarding dural Evans blue extravasation (Filipović et al., 2014) and was in accordance with simple sample size calculation for animal studies (Charan and Biswas, 2013). Forty-five minutes after intranasal injection, animals were deeply anesthetized with 70 mg/kg ketamine (Richter Pharma AG, Wels, Austria) and 7 mg/kg xylazine (Alfasan, Woerder, Netherlands), thoracotomized and transcardially perfused with 500-ml saline. After craniotomy, dura mater and nasal mucosa were harvested. To obtain the supratentorial dura primarily innervated by the trigeminal nerve, the dura mater was carefully separated from the skull base and neurocranium. Samples were weighed and incubated in 2-ml formamide (Honeywell, Muskegon, Michigan, USA) for 48 h on 37°C. The absorbances of formamide extracts of Evans blue were measured by spectrophotometer (Iskra, Ljubljana, Slovenia) set to 620 nm wavelength. Evans blue concentration in the tissue (ng/mg) was calculated based on the calibration curve and tissue weight.

Statistical Analysis of Results

Results are presented as mean ± SEM and analyzed by one-way analysis of variance (ANOVA) followed by Newman Keuls *post hoc* test ($p < 0.05$ considered significant). Pearson's correlation coefficient (r) and linear regression were used for the correlation analysis of variables ($p < 0.05$ considered significant).

RESULTS

Pain Assessment by RGS Score

After intranasal administration of formalin, the rats showed observable changes in the facial appearance suggestive of pain (**Figure 2A**), evident as increased total sum of RGS scores during 39 min after the formalin treatment (**Figure 2B**). Animals treated with saline did not show increased sum of RGS compared to non-treated rats.

The c-Fos Expression and Its Association With RGS Score

Animals treated with formalin had higher number of c-Fos-expressing neuronal profiles in the TNC compared to control (no treatment group) or saline (**Figure 3A**). Increased c-Fos expression was observed bilaterally after unilateral nasal formalin instillation. The intensity of c-Fos staining (**Figure 3A**, not quantified directly), and the number of c-Fos-expressing neurons (**Figure 3B**) was lower in the contralateral TNC. Average number of c-Fos positive cells per slice of TNC was 8 in non-treated animals which is similar to number in saline-treated animals.

In individual animals, there was a significant correlation between the sum of RGS scores following instillation of saline or formalin and the number of c-Fos positive cells in the ipsilateral TNC (**Figure 3C**). Similarly, there was a significant correlation of sum of RGS scores with number of c-Fos-expressing cells in the contralateral TNC (Pearson's correlation coefficient $r = 0.8164$; $p = 0.004$) or the total number of c-Fos-expressing cells in bilateral TNC (Pearson's $r = 0.8295$; $p = 0.003$) (results not shown).

Inflammation of the Nasal Mucosa Is Associated With Dural Neurogenic Inflammation

There was a significantly increased tissue content of Evans blue in the nasal mucosa in the animals treated with intranasal capsaicin and formalin, indicative of increased plasma protein extravasation in comparison to saline treatment (**Figure 4A**). Extravasation of Evans blue was similarly elevated in the dura

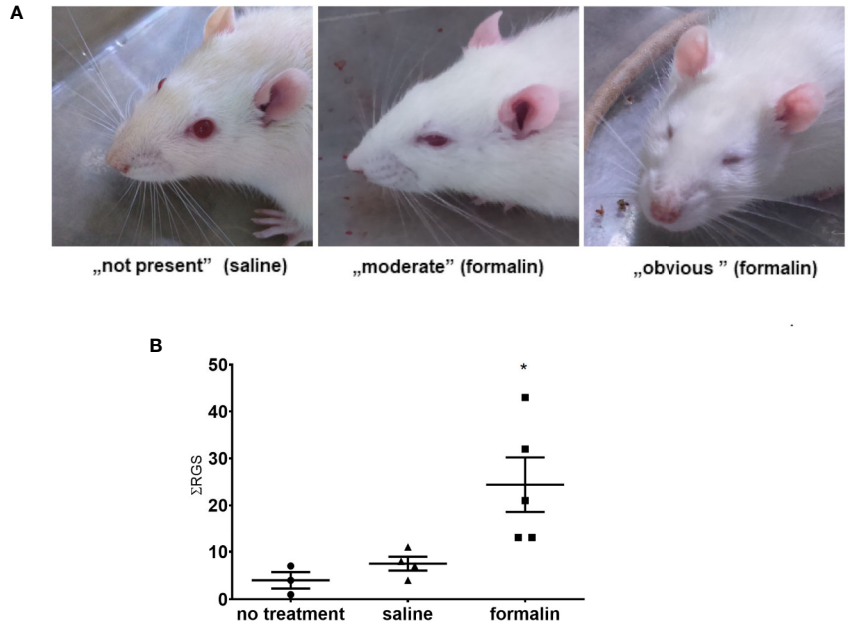

FIGURE 2 | Stimulation of nasal mucosa with 2.5% formalin induces painful grimacing in rats. **(A)** The rat faces showing, from left to right, normal appearance (saline-treated animal), and different severity of painful facial expression in formalin-treated animals (moderate to obvious). In the images, left to right, orbital tightening is the best visible action with following rat grimace scale (RGS) scores ascribable to them: 0, 1, 2. **(B)** Animals treated with formalin had higher sum of total RGS scores (ΣRGS) assessed every 3 min during the 39 min period after intranasal treatment with formalin, compared to saline or no treatment (3–5 animals per group, mean ± SEM, * $p < 0.05$ in comparison to non-treated or saline-treated group, one-way ANOVA followed by Newman Keuls *post hoc* test).

mater of rats treated with formalin or capsaicin relative to the control group treated with saline (**Figure 4B**) and shown to be significantly correlated with the Evans blue extravasation in nasal mucosa (**Figure 4C**). While harvesting dura, we did not observe any differences in Evans blue extravasation in dura on the side of irritant instillation compared to the contralateral side.

DISCUSSION

Formalin-Induced Pain in the Sino-Nasal Area

Here, we observed that low dose formalin instillation into the deeper part of nasal cavity situated at the border of maxillary sinus induces nociceptive behavior, quantified behaviorally by RGS (**Figure 2**). Quantification of pain-related facial expression by RGS is a relatively new method for assessing experimental pain in rats, introduced in 2011 as an adaptation of mouse grimace scale (Sotocinal et al., 2011). Up to now, it has successfully been employed for postsurgical (Kawano et al., 2014; Waite et al., 2015), orthodontic (Liao et al., 2014), neuropathic (Akintola et al., 2017; Philips et al., 2017), and inflammatory pain (Asgar et al., 2015). Herein, we attempted to use additional methods of pain assessment, by measuring the duration of facial wiping and facial mechanical thresholds by Von Frey filaments. After formalin stimulation, we observed that only some of the animals exhibited sequences of facial wiping similar to the ones exerted in orofacial formalin test, which proved unreliable for pain assessment (results not shown). In addition, the animals did not exhibit alteration in cutaneous mechanical thresholds assessed with Von Frey filaments, suggestive of the lack of mechanical allodynia. This could be due to the site of irritant stimulation located deeply into the nasal cavity near the entrance into the maxillary sinus. Stimulation of deep orofacial structures, protected by bone mass, did not lead to pericranial allodynia or wiping behavior characteristic of experimental pain in more superficial pericranial structures. This suggests that, in the orofacial area, RGS scoring could be a method of choice when measurement of spontaneous rubbing behavior or mechanically-evoked pain response is unreliable/not present.

Association of RGS With Brain c-Fos Activation

TNC is a relay nucleus for transduction of cranial pain, and its neurons express c-Fos following the acute noxious stimulation in the trigeminal innervation area (Hathaway et al., 1995), including the nasal mucosa (Anton et al., 1991). Up to now, the c-Fos expression in the TNC after irritant stimulation of the nasal mucosa by mustard oil (Anton and Peppel, 1991) and capsaicin (Plevkova et al., 2010) was shown to occur in anesthetized animals, i.e., without the behavioral assessment of pain. The c-Fos expression in the TNC combined with behavioral data was previously used in other nociceptive assays such as orofacial formalin test (Matak et al., 2014) and found to be in line with the behavioral effect of different pharmacological analgesic treatments.

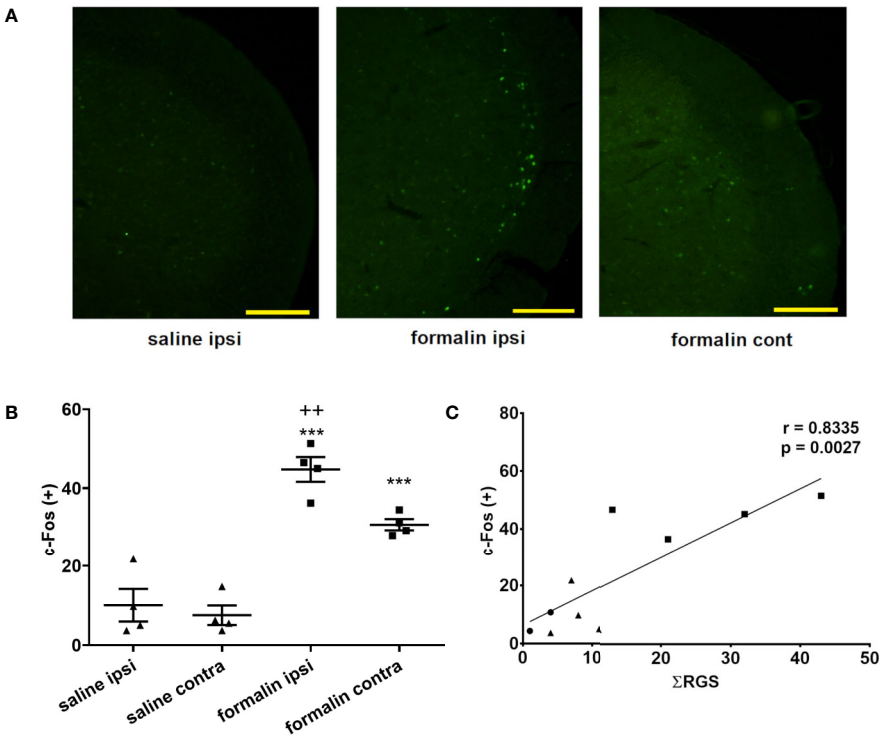

FIGURE 3 | Intranasal formalin (2.5%, 10 µl) induces bilateral neuronal activation in the caudal part of spinal trigeminal nucleus (TNC), which correlates with painful facial grimacing behavior. **(A)** Neuronal activation was quantified by c-Fos immunohistochemistry, and subsequent automatic quantification of the number of c-Fos-expressing [c-Fos (+)] neuronal profiles in ipsilateral (ipsi) and contralateral (cont) TNC. **(B)** The images and quantification are representative of 4 slices per animal, 4 animals per treatment group. Scale bar = 200 µm. Data are represented as mean ± SEM. ***$p < 0.001$ compared to saline ipsilaterally or contralaterally, $^{++}p < 0.01$ compared to formalin contralaterally, ANOVA followed by Newman Keuls *post hoc* test). **(C)** The painful facial grimacing assessed by rat grimace scale total score, measured every 3-min intervals during 39-min observation period (**Σ** RGS) is significantly correlated with the number of c-Fos positive cells in the ipsilateral TNC (circle, no treatment; square, saline; triangle, formalin; r, Pearson's correlation coefficient).

Interestingly, we found that unilateral stimulation of nasal cavity and sinuses leads to bilateral activation of c-Fos in the TNC (**Figure 3**). In contrast to that, unilateral whisker pad stimulation in orofacial formalin test evokes unilateral c-Fos expression (Matak et al., 2014). Both sites of inflammatory stimulation (whisker pad formalin injection and unilateral nasal instillation) are very close to the medial line which represents the border between the innervation areas of left and right trigeminal nerves (Panneton et al., 2006). In present study, preliminary testing of the injection method with methylene blue dye do not support possible spread of the injected volume far from the instillation site, or a contralateral inflammation (**Figure 1B**). Thus, the reason for bilateral occurrence of c-Fos after unilateral nasal stimulation might be other than the direct stimulation of contralateral structures.

So far, the validation of RGS with biomarkers of pain has been scarce. In a model of orthodontic pain, RGS score was shown to be correlated to calcitonin gene-related peptide (CGRP) (Long et al., 2015), however, not with acid sensing ion channel 3 (ASIC3) periodontal expression (Gao et al., 2016). Correlation of RGS score with the neuronal activation in TNC (**Figure 3C**) further adds to validity of RGS as reliable method for pain assessment.

Nociceptive Stimuli in Sino-Nasal Area Induce Dural Neurogenic Inflammation

In present experiments, we found that inflammatory stimulation of nasal mucosa by either formalin or capsaicin induces plasma protein extravasation in the cranial dura (**Figure 4**). Present results indicate a link between painful stimuli in the nasal/paranasal area, and the activation of dural afferents leading to dural neurogenic inflammation (DNI), which is commonly associated with headache.

Previous observations suggested that various types of irritation of the nasal mucosa lead to increased meningeal blood flow in anesthetized animals. Based on the investigation of umbellulone, a known headache trigger from shrub/tree plant *Umbellularia californica*, it was proposed that environmental irritants might either diffuse and directly activate meningeal afferents, or activate reflex pathways by stimulation of trigeminal endings in the nasal mucosa (Nassini et al., 2012; Kunkler et al., 2014). In present experiments, instillation of formalin or capsaicin unilaterally into the border between maxillary sinus and nasal cavity induces unilateral, localized inflammation, which correlated with the intensity of DNI. Thus, our findings are more in line with indirect activation of meningeal afferents by stimulation of a more limited number of sensory endings situated in the nasal/

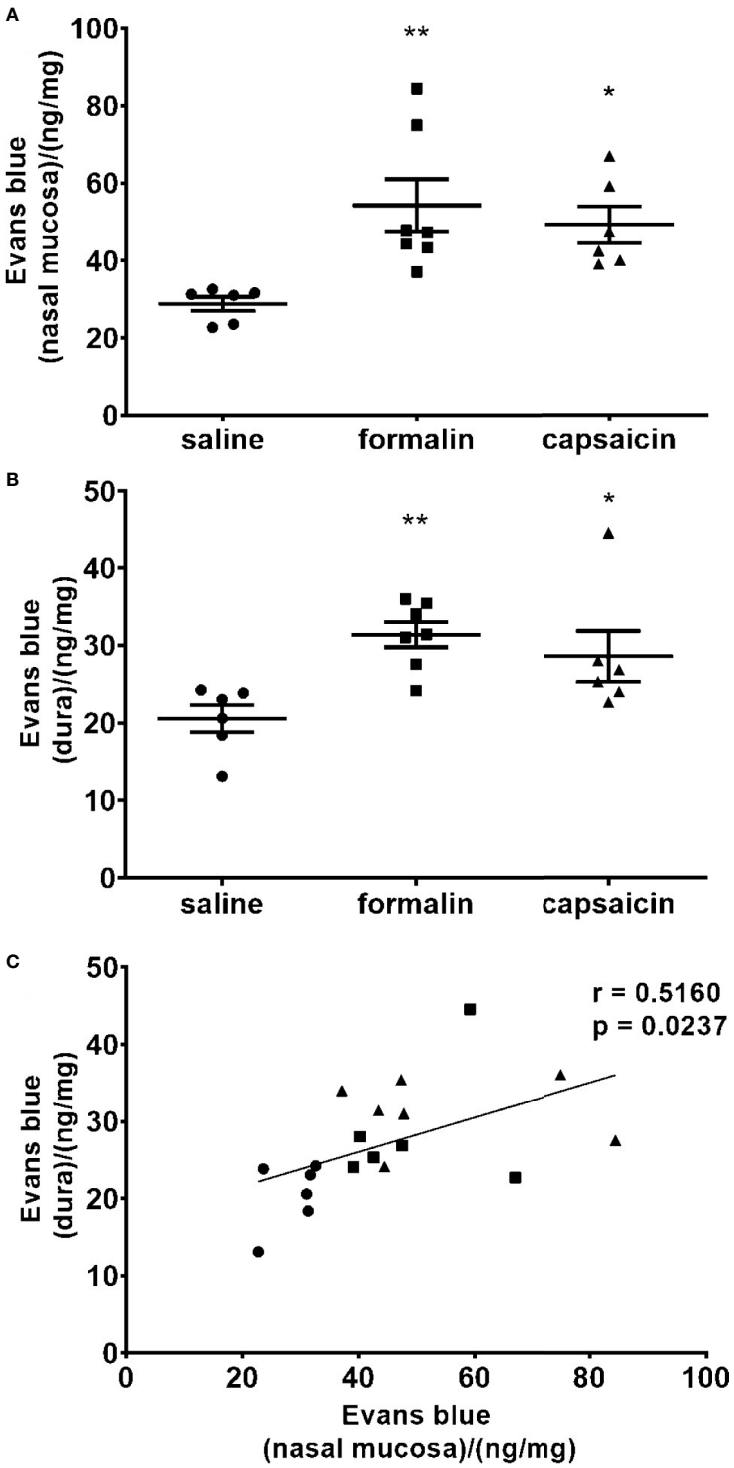

FIGURE 4 | Local stimulation of the deep nasal mucosa by formalin (2.5%) or capsaicin (0.1%) induce plasma protein extravasation in the nasal mucosa and cranial dura mater. The inflammation was quantified by spectrophotometric measurement of formamide extracts of Evans blue dye (ng of the dye per mg of tissue in the nasal mucosa **(A)** and dura mater **(B)**. Mean ± SEM, 6–8 animals per group, *$p < 0.05$, **$p < 0.01$ vs. saline-treated group (one-way ANOVA followed by Newman Keuls *post hoc* test). Intensity of the inflammation in nasal mucosa correlated with the intensity of inflammation in cranial dura. **(C)** Individual animal values are plotted showing extravasation in the nasal mucosa (horizontal axis) and dura (vertical axis) for all experimental groups together (circle, saline; square, formalin; triangle, capsaicin; r, Pearson's correlation coefficient).

paranasal area, rather than the direct diffusion of irritants into the cranial meninges. One of the possible mechanisms for activation of meningeal afferents after stimulation of nasal mucosa might be the axonal reflex, since dura and nasal cavity share sensory innervation from common maxillary and ophthalmic branches of the trigeminal nerve, such as the ethmoidal nerve (Panneton et al., 2006; Poussel et al., 2012). Other mechanism could be the intraganglionic cross-communication between nearby primary sensory neurons which project to the intranasal structures and neurons which innervate the meninges (Kunkler et al., 2014). Third mechanism involving the cross-sensitization of second order sensory neurons within the TNC might also be involved. Neurons that conduct dural pain sensation relay to the same secondary neurons in the TNC as the neurons that conduct the pain sensation from the nasal cavity (Ellrich et al., 1999; Messlinger and Ellrich, 2001). The facts that we did not observe any gross differences in Evans blue extravasation in dura on the side of irritant instillation compared to the contralateral side and that previous models of infraorbital nerve constriction and formalin injection in vibrissal pad have shown similar Evans blue extravasation in dura ipsilateral to the injury and contralateral dura (Filipović et al., 2012) support cross-sensitization at the level of brainstem since brainstem is most likely site where signal could propagate to the side contralateral to the injury. Mentioned mutually non-exclusive mechanisms of convergence of sensory input could be responsible for increased incidence of primary headache in patients suffering from nasal and sinus conditions. Regardless of the level of convergence, activated dural nerves release neuropeptides (CGRP, VIP, substance P, neurokinin A, and PACAP-38) into dura which then cause neurogenic inflammation, vasodilation and increased vessel permeability (Vécsei et al., 2014).

Recently, we found that different types of experimental pain in trigeminal region induce DNI: chemically induced pain (formalin), neuropathic pain (infraorbital nerve constriction), inflammatory pain (CFA-evoked inflammation of temporomandibular joint) (Filipović et al., 2012; Filipović et al., 2014; Lacković et al., 2016). Neuropathic pain outside of cranial area (evoked by constriction or partial transection of sciatic nerve) did not result in DNI of cranial or spinal meninges (Filipović et al., 2014). In cranial meninges, the DNI was attenuated by anti-migraine drugs such as botulinum neurotoxin type A (BoNT/A) and sumatriptan (Filipović et al., 2012; Lacković et al., 2016). In addition, we found a reduction of CGRP expression in the cranial dura by pericranially injected BoNT/A as well as the colocalization of enzymatic products of BoNT/A and CGRP (Lacković et al., 2016). The involvement of CGRP is also suggested by observed efficacy of 5-HT1B/D agonist sumatriptan in reducing both pain and DNI (Lacković et al., 2016). These observations suggest that DNI is not associated only with migraine pathophysiology, but rather a non-specific event related to different types of pain in the trigeminal region.

Results presented here show that acute inflammation in the deep nasal area can induce trigeminovascular changes associated with headache. Understandably, bearing in mind the chronic nature of migraine and different disorders of nasal and sinus cavity, present findings derived by employing an acute stimulation model cannot be interpreted as a direct explanation for the possible pathophysiological link. However, the findings point to a possibility that long-term inflammation in the nasal/sinus area may induce more chronic changes leading to facilitated activation of the trigeminovascular system. It remains to be further investigated whether, in turn, the phenomenon of coupling of nasal inflammation with trigeminovascular activation is involved in observed comorbidities of acute or chronic paranasal and sinus disorders and headache.

CONCLUSION

Present results suggest that acute nasal inflammatory stimulation correlates with painful nociceptive neuronal activation and neurogenic inflammation of cranial meninges, suggesting possible link between the painful disorders of nasal/paranasal craniofacial area and headaches.

DATA AVAILABILITY STATEMENT

The raw data supporting the conclusions of this article will be made available by the authors, without undue reservation.

ETHICS STATEMENT

The animal study was reviewed and approved by Ethical Committees of University of Zagreb School of Medicine and Croatian Ministry of Agriculture (permission no. EP 03-2/2015).

AUTHOR CONTRIBUTIONS

ZL conceptualized experiments. IM and LL planned and performed the experiments. LL and IM analyzed data. All authors contributed to the article and approved the submitted version.

FUNDING

This work was supported by Croatian Science Foundation (Project ID: IP-2014-09-4503) and University of Zagreb Support project.

ACKNOWLEDGMENTS

We wish to thank Božica Hržan for technical assistance during the experiments.

REFERENCES

Akintola, T., Raver, C., Studlack, P., Uddin, O., Masri, R., and Keller, A. (2017). The grimace scale reliably assesses chronic painin a rodent model of trigeminal neuropathic pain. *Neurobiol. Pain* 2 (October), 13–17. doi: 10.1016/j.ynpai.2017.10.001

Anton, F., and Peppel, P. (1991). Central projections of trigeminal primaryafferents innervating the nasal mucosa: A horseradish peroxidase study in the rat. *Neuroscience* 41 (2–3), 617–628. doi: 10.1016/0306-4522(91)90354-Q

Anton, F., Herdegen, T., Peppel, P., and Leah, J. D. (1991). c-FOS-like immunoreactivity in rat brainstemneurons following noxious chemical stimulation of the nasal mucosa. *Neuroscience* 41 (2–3), 629–641. doi: 10.1016/0306-4522(91)90355-R

Arreola-Peralta, L. D., Altamirano-Reyna, F., Galindo-González, D. M., Solis-Anguiano, J. G., Lacivita, E., Leopoldo, M., et al. (2018). Potentiation of capsaicin-induced neurogenic inflammation by 5-HT7 receptors in the rat hind paw: Involvement of calcitonin gen-related peptide. *Peptides* 105 (April), 1–6. doi: 10.1016/j.peptides.2018.05.002

Asgar, J., Zhang, Y., Saloman, J. L., Wang, S., Chung, M.-K., and Ro, J. Y. (2015). The role of TRPA1 in muscle pain and mechanicalhypersensitivity under inflammatory conditions in rats. *Neuroscience* 310, 206–215. doi: 10.1016/j.neuroscience.2015.09.042

Bach-Rojecky, L., and Lacković, Z. (2005). Antinociceptive effect of botulinum toxin type A in rat model of Carrageenan and Capsaicin induced pain. *Croat. Med. J.* 46 (2), 201–208.

Bach-Rojecky, L., Dominis, M., and Lacković, Z. (2008). Lack of anti-inflammatory effect of botulinumtoxin type A in experimental models of inflammation. *Fundam. Clin. Pharmacol.* 22 (5), 503–509. doi: 10.1111/j.1472-8206.2008.00615.x

Charan, J., and Biswas, T. (2013). How to calculate sample size for different studydesigns in medical research? *Indian J. Psychol. Med.*35 (2), 121–126. doi: 10.4103/0253-7176.116232

Ellrich, J., Andersen, O. K., Messlinger, K., and Arendt-Nielsen, L. (1999). Convergence of meningeal and facial afferentsonto trigeminal brainstem neurons: An electrophysiological study in rat and man. *Pain* 82 (3), 229–237. doi: 10.1016/S0304-3959(99)00063-9

Eross, E., Dodick, D., and Eross, M. (2007). The sinus, allergy and migraine study (SAMS). *Headache* 47 (2),213–224. doi: 10.1111/j.1526-4610.2006.00688.x

Ferrero, V., Allais, G., Rolando, S., Pozzo, T., Allais, R., and Benedetto, C. (2014). Endonasal mucosal contact points in chronicmigraine. *Neurol. Sci.* 35 (SUPPL. 1), 83–87. doi: 10.1007/s10072-014-1749-x

Filipović, B., Matak, I., Bach-Rojecky, L., and Lacković, Z. (2012). Central action of peripherally applied botulinumtoxin type a on pain and dural protein extravasation in rat model of trigeminal neuropathy. *PloS One* 7 (1), 1–8. doi: 10.1371/journal.pone.0029803

Filipović, B., Matak, I., and Lacković, Z. (2014). Dural neurogenic inflammation induced byneuropathic pain is specific to cranial region. *J. Neural Transm.* 121 (5), 555–563. doi: 10.1007/s00702-013-1144-4

Gao, M., Long, H., Ma, W., Liao, L., Yang, X., Zhou, Y., et al. (2016). The role of periodontal ASIC3 in orofacial paininduced by experimental tooth movement in rats. *Eur. J. Orthod.* 38 (6), 577–583. doi: 10.1093/ejo/cjv082

Hathaway, C. B., Hu, J. W., and Bereiter, D. A. (1995). Distribution of fos-like immunoreactivity in thecaudal brainstem of the rat following noxious chemical stimulation of the temporomandibular joint. *J. Comp. Neurol.* 356 (3), 444–456. doi: 10.1002/cne.903560311

Kawano, T., Takahashi, T., Iwata, H., Morikawa, A., Imori, S., Waki, S., et al. (2014). Effects of ketoprofen for prevention of postoperative cognitive dysfunction in aged rats. *J. Anesth.* 28 (6), 932–936. doi: 10.1007/s00540-014-1821-y

Ku, M., Silverman, B., Prifti, N., Ying, W., Persaud, Y., and Schneider, A. (2006). Prevalence of migraine headaches in patientswith allergic rhinitis. *Ann. Allergy Asthma Immunol.* 97 (2), 226–230. doi: 10.1016/S1081-1206(10)60018-X

Kunkler, P. E., Ballard, C. J., Pellman, J. J., Zhang, L. J., Oxford, G. S., and Hurley, J. H. (2014). Intraganglionic signaling as a novelnasal-meningeal pathway for TRPA1-dependent trigeminovascular activation by inhaled environmental irritants. *PloS One* 9 (7), 1–10. doi: 10.1371/journal.pone.0103086

Lacković, Z., Filipović, B., Matak, I., and Helyes, Z. (2016). Activity of botulinum toxin type A in cranialdura: implications for treatment of migraine and other headaches. *Br. J. Pharmacol.* 173 (2), 279–291. doi: 10.1111/bph.13366

Lee, M., Erickson, C., and Guyuron, B. (2017). Intranasal pathology in the migraine surgerypopulation: incidence, patterns, and predictors of surgical success. *Plast. Reconstr. Surg.* 139 (1), 184–189. doi: 10.1097/PRS.0000000000002888

Liao, L., Long, H., Zhang, L., Chen, H., Zhou, Y., Ye, N., et al. (2014). Evaluation of pain in rats through facialexpression following experimental tooth movement. *Eur. J. Oral. Sci.* 122 (2), 121–124. doi: 10.1111/eos.12110

Long, H., Liao, L., Gao, M., Ma, W., Zhou, Y., Jian, F., et al. (2015). Periodontal CGRP contributes to orofacial painfollowing experimental tooth movement in rats. *Neuropeptides* 52, 31–37. doi: 10.1016/j.npep.2015.06.006

Martin, V. T., Fanning, K. M., Serrano, D., Buse, D. C., Reed, M. L., Bernstein, J. A., et al. (2014). Chronic rhinitis and its association withheadache frequency and disability in persons with migraine: Results of the American Migraine Prevalence and Prevention (AMPP) Study. *Cephalalgia* 34 (5), 336–348. doi: 10.1177/0333102413512031

Matak, I., Rossetto, O., and Lacković, Z. (2014). Botulinum toxin type A selectivity for certaintypes of pain is associated with capsaicin-sensitive neurons. *Pain* 155 (8), 1516–1526. doi: 10.1016/j.pain.2014.04.027

Messlinger, K., and Ellrich, J. (2001). Meningeal nociception: Electrophysiologicalstudies related to headache and referred pain. *Microsc. Res. Tech.* 53 (2), 129–137. doi: 10.1002/jemt.1077

Mitsikostas, D. D., and Sanchez del Rio, M. (2001). Receptor systems mediating c-fos expressionwithin trigeminal nucleus caudalis in animal models of migraine. *Brain Res. Rev.* 35 (1), 20–35. doi: 10.1016/S0165-0173(00)00048-5

Nassini, R., Materazzi, S., Vriens, J., Prenen, J., Benemei, S., De Siena, G., et al. (2012). The "headache tree" via umbelluloneand TRPA1 activates the trigeminovascular system. *Brain* 135 (2), 376–390. doi: 10.1093/brain/awr272

Panneton, W. M., Gan, Q., and Juric, R. (2006). Brainstem projections from recipient zones ofthe anterior ethmoidal nerve in the medullary dorsal horn. *Neuroscience* 141 (2), 889–906. doi: 10.1016/j.neuroscience.2006.04.055

Patel, Z. M., Kennedy, D. W., Setzen, M., Poetker, D. M., and Delgaudio, J. M. (2013). "Sinus headache": Rhinogenicheadache or migraine? An evidence-based guide to diagnosis and treatment. *Int. Forum Allergy Rhinol.* 3 (3), 221–230. doi: 10.1002/alr.21095

Pelissier, T., Pajot, J., and Dallel, R. (2002). The orofacial capsaicin test in rats: Effects ofdifferent capsaicin concentrations and morphine. *Pain* 96 (1–2), 81–87. doi: 10.1016/S0304-3959(01)00432-8

Philips, B. H., Weisshaar, C. L., and Winkelstein, B. A. (2017). Use of the rat grimace scale to evaluate neuropathic pain in a model of cervical radiculopathy. *Comp. Med.* 67 (1), 34–42.

Phillips, J. E., Ji, L., Rivelli, M. A., Chapman, R. W., and Corboz, M. R. (2009). Three-dimensional analysis of rodent paranasal sinus cavities from X-ray computed tomography (CT) scans. *Can. J. Vet. Res.* 73 (3), 205–211.

Plevkova, J., Poliacek, I., Antosiewicz, J., Adamkov, M., Jakus, J., Svirlochova, K., et al. (2010). Intranasal TRPV1 agonist capsaicin challengeand its effect on c-fos expression in the guinea pig brainstem. *Respir. Physiol. Neurobiol.* 173 (1), 11–15. doi: 10.1016/j.resp.2010.05.015

Poussel, M., Varechova, S., Demoulin, B., Chalon, B., Schweitzer, C., Marchal, F., et al. (2012). Nasal stimulation by water down-regulates coughin anesthetized rabbits. *Respir. Physiol. Neurobiol.* 183 (1), 20–25. doi: 10.1016/j.resp.2012.05.021

Rossi, H. L., Broadhurst, K. A., Luu, A. S., Lara, O., Kothari, S. D., Mohapatra, D. P., et al. (2016). Abnormal trigeminal sensory processing in obesemice Heather. *Pain* 157 (1), 235–246. doi: 10.1097/j.pain.0000000000000355

Schreiber, C. P., Hutchinson, S., Webster, C. J., Ames, M., Richardson, M. S., and Powers, C. (2004). Prevalence of migraine in patients with ahistory of self-reported or physician-diagnosed "sinus" headache. *Arch. Intern. Med.* 164 (16), 1769. doi: 10.1001/archinte.164.16.1769

Sotocinal, S. G., Sorge, R. E., Zaloum, A., Tuttle, A. H., Martin, L. J., Wieskopf, J. S., et al. (2011). The Rat Grimace Scale: A partially automatedmethod for quantifying pain in the laboratory rat via facial expressions. *Mol. Pain* 7 (1), 55. doi: 10.1186/1744-8069-7-55

Vécsei, L., Tuka, B., and Tajti, J. (2014). Role of PACAP in migraineheadaches. *Brain* 137 (3), 650–651. doi: 10.1093/brain/awu014

Waite, M. E., Tomkovich, A., Quinn, T. L., Schumann, A. P., Dewberry, L. S., Totsch, S. K., et al. (2015). Efficacy of Common Analgesics for Postsurgical Pain in Rats. *J. Am. Assoc. Lab. Anim. Sci.* 54 (4), 420–425.

Wang, I. C., Tsai, J. D., Lin, C. L., Shen, T. C., Li, T. C., and Wei, C. C. (2016). Allergic rhinitis and associated risk ofmigraine among children: A nationwide population-based cohort study. *Int. Forum Allergy Rhinol.* 6 (3), 322–327. doi: 10.1002/alr.21654

Zimmermann, M. (1983). Ethical guidelines for investigations of experimental pain in conscious animals. *Pain* 16 (2), 109–110. doi: 10.1016/0304-3959(83)90201-4

Conflict of Interest: The authors declare that the research was conducted in the absence of any commercial or financial relationships that could be construed as a potential conflict of interest.

frontiers in Pharmacology

ORIGINAL RESEARCH
published: 26 November 2020
doi: 10.3389/fphar.2020.584184

Upregulation of Nucleotide-Binding Oligomerization Domain-, LRR- and Pyrin Domain-Containing Protein 3 in Motoneurons Following Peripheral Nerve Injury in Mice

*Bernát Nógrádi[1,2†], Ádám Nyúl-Tóth[1,3†], Mihály Kozma[1,4], Kinga Molnár[1,4], Roland Patai[1], László Siklós[1], Imola Wilhelm[1,5] and István A. Krizbai[1,5]**

[1]Institute of Biophysics, Biological Research Centre, Szeged, Hungary, [2]Foundation for the Future of Biomedical Sciences in Szeged, Szeged Scientists Academy, Szeged, Hungary, [3]Department of Biochemistry and Molecular Biology, Vascular Cognitive Impairment and Neurodegeneration Program, Reynolds Oklahoma Center on Aging/Oklahoma Center for Geroscience, University of Oklahoma Health Sciences Center, Oklahoma City, OK, United States, [4]Theoretical Medicine Doctoral School, University of Szeged, Szeged, Hungary, [5]Institute of Life Sciences, Vasile Goldiş Western University of Arad, Arad, Romania

Neuronal injuries are accompanied by release and accumulation of damage-associated molecules, which in turn may contribute to activation of the immune system. Since a wide range of danger signals (including endogenous ones) are detected by the nucleotide-binding oligomerization domain-, LRR- and pyrin domain-containing protein 3 (NLRP3) pattern recognition receptor, we hypothesized that NLRP3 may become activated in response to motor neuron injury. Here we show that peripheral injury of the oculomotor and the hypoglossal nerves results in upregulation of NLRP3 in corresponding motor nuclei in the brainstem of mice. Although basal expression of NLRP3 was observed in microglia, astroglia and neurons as well, its upregulation and co-localization with apoptosis-associated speck-like protein containing a caspase activation and recruitment domain, suggesting inflammasome activation, was only detected in neurons. Consequently, increased production of active pro-inflammatory cytokines interleukin-1β and interleukin-18 were detected after hypoglossal nerve axotomy. Injury-sensitive hypoglossal neurons responded with a more pronounced NLRP3 upregulation than injury-resistant motor neurons of the oculomotor nucleus. We further demonstrated that the mitochondrial protector diazoxide was able to reduce NLRP3 upregulation in a post-operative treatment paradigm. Our results indicate that NLRP3 is activated in motoneurons following acute nerve injury. Blockade of NLRP3 activation might contribute to the previously observed anti-inflammatory and neuroprotective effects of diazoxide.

Keywords: acute nerve injury, motor neuron, neuroinflammation, inflammasome, nucleotide-binding oligomerization domain-, LRR- and pyrin domain-containing protein 3, diazoxide

OPEN ACCESS

Edited by:
Gerard Bannenberg, Global Organization for EPA and DHA Omega-3s (GOED), United States

Reviewed by:
Robert W. Keane, University of Miami, United States
Sowmya Yelamanchili, University of Nebraska Medical Center, United States
Claudia Espinosa-Garcia, Emory University, United States

****Correspondence:***
István A. Krizbai
krizbai.istvan@brc.hu

†These authors share first authorship.

Specialty section:
This article was submitted to Inflammation Pharmacology, a section of the journal Frontiers in Pharmacology

Received: *16 July 2020*
Accepted: *21 October 2020*
Published: *26 November 2020*

Citation:
Nógrádi B, Nyúl-Tóth Á, Kozma M, Molnár K, Patai R, Siklós L, Wilhelm I and Krizbai IA (2020) Upregulation of Nucleotide-Binding Oligomerization Domain-, LRR- and Pyrin Domain-Containing Protein 3 in Motoneurons Following Peripheral Nerve Injury in Mice. Front. Pharmacol. 11:584184. doi: 10.3389/fphar.2020.584184

INTRODUCTION

Finely tuned interaction between the nervous and the immune systems and different inflammatory processes play a pivotal role in the consequences of neuronal injury. The innate immune system-mediated inflammation can act both as detrimental (reviewed in Labzin et al., 2018; Schwartz et al., 2016) or beneficial player after insult to the central nervous system (CNS) (Raposo et al., 2014), thus may influence the fate of affected neurons after the lesion. Sensing of potentially dangerous molecular structures by the innate immune system relies on pattern recognition receptors (PRRs), whose activation can lead to the induction of inflammatory processes. PRRs are mainly expressed in immune cells; however, cellular components of the CNS, including neurons, have also been demonstrated to express PRRs.

Ligand recognition by several members of the nucleotide-binding oligomerization domain (NOD)-like receptor (NLR) family leads to activation of a multiprotein complex, the inflammasome, which recruits and activates caspase-1 through the adaptor molecule apoptosis-associated speck-like protein containing a CARD (ASC) to proteolytically maturate interleukin-1 beta (IL-1β) and IL-18 (IL-18). The most important NLRs in this respect are NOD, leucine rich repeat and pyrin domain containing (NLRP) 1, nucleotide-binding oligomerization domain NOD-, LRR- and pyrin domain-containing protein 3 (NLRP3), and NLR family caspase activation and recruitment domain (CARD)-containing domain (NLRC) 4. In addition, absent in melanoma 2 (AIM2) can also be part of inflammasomes (Latz et al., 2013). Despite an acknowledged role of inflammation in a large number of CNS disorders, only a few inflammasomes have been characterized so far in the CNS. These include NLRP3, NLRP1 and NLRC4 inflammasomes in microglia and astrocytes (Abulafia et al., 2008; Halle et al., 2008; Hanamsagar et al., 2011; Liu et al., 2013; Freeman et al., 2017) and NLRP2 inflammasome in astrocytes (Minkiewicz et al., 2013). In neurons, initially NLRP1 (Abulafia et al., 2008; de Rivero Vaccari et al., 2008) and AIM2 (Adamczak et al., 2014) inflammasomes were described to be activated in response to different stimuli. In addition, neurons can also express NLRP3 (von Herrmann et al., 2018) to initiate inflammasome formation (Panicker et al., 2020), which is by far the most investigated inflammasome in the CNS. Nowadays it is clear that NLRP3 plays an active role in the pathomechanism of a wide variety of neurological diseases and aging (Latz et al., 2018; Mészáros et al., 2020; Heneka et al., 2013), especially in microglia. Much less is known about regulation of NLRP3 in neurons in response to acute injury.

In humans, peripheral nerve injuries usually occur in traumatic accidents and often lead to complications, such as chronic pain and motor or sensory loss of function (Althagafi and Nadi 2020). In mice, axotomy is a well-documented and standardized method to induce motoneuronal injury (e.g., Koliatsos and Price 1996). Axonal lesions lead to retrograde changes in neurons, activation of glial cells and inflammatory reactions, including extensive microgliosis (Rotterman and Alvarez 2020). Our goal was to determine whether NLRP3-mediated processes could occur in response to peripheral nerve axotomy. Oculomotor and hypoglossal neurons were selected for our experiments because of the difference in the neuronal vulnerability and in the inflammatory response to injury (Obál et al., 2006; Nógrádi et al., 2020).

Mitochondrial dysfunction is a key component and regulator of NLRP3-mediated inflammasome activation (Liu et al., 2018). Furthermore, activated NLRP3 may translocate to mitochondria-associated endoplasmic reticulum membranes, which provide a platform for NLRP3 inflammasome assembly. On the other hand, NLRP3 activators induce mitochondrial damage, while NLRP3 directly interacts with molecules released from injured mitochondria, like cardiolipin, mitochondrial DNA and reactive oxygen species (Elliott et al., 2018; Zhong et al., 2018). Therefore, possible effect of diazoxide (7-chloro-3-methyl-4H-1λ6,2,4-benzothiadiazine 1,1-dioxide), a mitochondrial K^+_{ATP} channel opener and neuroprotective agent, on inflammasome activation was assessed as well.

MATERIAL AND METHODS

Ethical Considerations

All efforts were made to minimize animal suffering throughout the experiments, thus multiple surgeries were avoided. All experiments were carried out in accordance with the institutional guidelines for the use and care of the experimental animals and governmental law for animal protection. The experimental protocols and the animal care were approved by the institutional care and the Regional Animal Health and Food Control Station of Csongrád-Csanád County (permit number: XVI./767/2018 and 03876/0014/2006) and carried out in accordance with the national law (XXVIII. chapter IV. paragraph 31) which conforms to the international laws and policies (EEC Council Directive 86/609, OJL 358 1 DEC. 12, 1987; NIH Guide for the Care and Use of Laboratory Animals, United States National Research Council, revised 1996).

Experimental Animals and Surgical Procedures

Balb/c non-transgenic mice (mean body weight of 22 ± 5 g) were housed in the conventional animal facility of the Biological Research Center (Szeged, Hungary) for the period of the experiments. Examinations were performed on 33 young adult (8–15 week old) male mice, housed in plastic cages (three animals per cage at most) in a thermoneutral (23 ± 2°C) room under a 12 h light:dark cycle, with access to regular rodent chow and water *ad libitum*.

To avoid multiple surgical procedures on individual animals, mice were assigned either to eye enucleation (target deprivation) or hypoglossal nerve axotomy. A total of 30 mice were used for immunohistochemistry (IHC) quantification. From these animals, 10 served as non-operated controls (n = 5 for the oculomotor nucleus, n = 5 for the hypoglossal nucleus) and 20

animals underwent either eye enucleation [n = 5 (non-treated)] or hypoglossal nerve axotomy [n = 15 (n = 5 non-treated, n = 5 diazoxide-treated, n = 5 dimethyl sulfoxide/(DMSO)-treated)]. For western blot (WB) evaluation of IL-1β and IL-18 pro-inflammatory cytokines, surgical unilateral axotomy of the hypoglossal nerve was conducted on three animals. Surgical interventions were performed under deep and reversible anesthesia with Avertin (tribromoethanol, Sigma-Aldrich; 240 mg/kg body weight in a 0.5 ml volume), administered intraperitoneally. For target deprivation of the oculomotor nerve, animals were enucleated, the right eyeball, remaining extraocular muscles and lacrimal gland were removed carefully from the orbit. In case of hypoglossal axotomy, 1 cm long midline incision was made below the hyoid bone, the right cranial nerve XII. was carefully prepared and a 2–3 mm nerve segment was dissected to prevent regeneration.

For diazoxide treatment, 0.25 mg/ml diazoxide (Sigma-Aldrich) was dissolved in 10 mg/ml DMSO (Sigma-Aldrich) in distilled water in a 0.1 ml volume and was administered by intraperitoneal injection (1 mg/kg bodyweight). DMSO-treatment was used as vehicle control (10 mg/ml DMSO dissolved in distilled water, administered intraperitoneally). Animals received the first dose 3 h after the axotomy, then on the first, second and third postoperative days (every 24 h, altogether four doses). On the fourth postoperative day, animals were sacrificed, thus received no treatment. Axotomized, non-treated mice received no treatment. All animals were allowed to survive for 4 days. In each case, the non-operated side of the motor nucleus served as an internal control to determine the difference in NLRP3 (IHC) or IL-1β (WB) expression.

Immunohistochemistry and Immunofluorescence Staining Procedures

Under irreversible anesthesia with Avertin, mice were transcardially perfused with 10 mM phosphate buffered saline (PBS; pH 7.4) followed by 4% paraformaldehyde (Sigma-Aldrich) in 10 mM PBS (pH 7.4). The entire brain was exposed and removed, then fixed further overnight in the same fixative at 4°C. After the fixation protocol, samples were cryoprotected in 30% sucrose (Sigma-Aldrich) dissolved in 10 mM PBS, for at least 1 day at 4°C. Series of consecutive coronal sections of 30 µm thickness were cut throughout the whole anatomical regions of interests with a microtome (Reichert-Jung, Leica Biosystems), collected in 10 mM PBS individually in wells of tissue culture plates and stored at 4°C until processed for staining.

IHC stainings were performed on 30 µm thick free-floating sections. For the quantitative assessment of the changes in NLRP3, diaminobenzidine tetrahydrochloride (DAB)-based IHC was used. In both examined motor nuclei, sections (n = 8/each animal) were selected with respect to the anatomical boundaries. Sections were rinsed (three changes, 5 min each), then 50% methanol (VWR Chemicals) in 10 mM PBS was applied for tissue permeabilization for 30 min at −20°C. Samples were rinsed again in 10 mM PBS, then the non-specific staining was blocked in two steps: 0.6% hydrogen peroxide in 10 mM PBS containing 0.2% Triton X-100 (Sigma-Aldrich) (TPBS) was used first for 30 min to block the endogenous peroxidase activity. After sections were rinsed (three changes, 5 min), the second blocking step was applied with 2% normal rabbit serum (Vector Laboratories) in 10 mM TPBS for 1 h. This was followed by overnight incubation at 4°C with the polyclonal goat primary antibody against NLRP3 diluted in 10 mM TPBS with 2% normal rabbit serum. After washing in 10 mM PBS (three changes, 5 min), sections were incubated at room temperature in a biotinylated rabbit-anti-goat secondary antibody diluted in 10 mM TPBS with 2% normal rabbit serum for 1 h. Next, all the sections were rinsed in 10 mM PBS (three changes, 5 min each), incubated in avidin-biotin complex (Vector Laboratories) diluted to 1:800 in PBS for 1 h at room temperature. After washing in 10 mM PBS, the reactions were visualized by incubation in 0.5% DAB (Sigma-Aldrich) with 1.5% $NiCl_2$ in 10 mM PBS for 15 min. Finally, sections were washed in 10 mM PBS (three changes, 5 min each), mounted on silane-coated glass slides, covered with Entellan (Merck Millipore) and visualized under a brightfield microscope (Eclipse 80i, Nikon). Brightness and contrast were adjusted as needed. To qualitatively evaluate changes in the level of the inflammasome component ASC, the IHC procedure was carried out as previously described, with the difference that serum-specific blocking was performed with 2% normal goat serum (Jackson Immunoresearch).

Immunofluorescence (IF) staining protocols were also performed on 30 µm thick free-floating sections. First, selected sections were rinsed, then 50% methanol was applied, as previously described. Sections were rinsed again (three changes, 5 min each), then a blocking step was used with 2% normal donkey serum (Jackson Immunoresearch) in 10 mM TPBS for 1 h. Primary antibody cocktails were applied for overnight incubation at 4°C. The next day, sections were rinsed (three changes, 5 min each) and secondary antibody cocktails were used for 1 h. Both the primary and secondary cocktails were diluted in 10 mM TPBS with 2% normal donkey serum. Primary and secondary antibody cocktails varied in each double or triple immunofluorescent staining procedure and are detailed in **Table 1**. Finally, sections were washed in 10 mM PBS (three changes, 5 min each) and, where indicated, Hoechst 33342 (B2261, Sigma-Aldrich) staining was applied (diluted to 1 µg/ml in 10 mM PBS) to visualize cell nuclei. Sections were mounted on silane-coated glass slides, covered with Fluoromount-G (0100-01, Southern Biotechnology Associates) mounting medium. Secondary antibody staining controls have been carried out for each of the applied secondary antibodies to exclude the interference of any associated unspecific staining.

Confocal and Super-Resolution Microscopy

Immunofluorescence co-staining was examined with confocal and super-resolution microscopy (STED) (stimulated emission depletion) microscopy. Lower resolution imaging was performed on a Leica SP5 Laser Scanning Microscope (Leica Microsystems), while super-resolution images were obtained with a STEDYCON (Abberior Instruments) STED instrument connected to a ZEISS Axio Observer Z1 inverted microscope. From raw images, confocal z-stacks were prepared with LAS X viewer and FIJI

TABLE 1 | Antibodies used for IHC, IF and WB.

Stainings	Primary antibodies	Secondary antibodies
NLRP3 (IHC)	Polyclonal goat against **NLRP3**, 1:500 (GTX88190, GeneTex)	Biotinylated rabbit anti-goat IgG antibody (H + L), 1:800 (BA-5000, Vector Laboratories)
ASC (IHC)	Monoclonal mouse against **ASC**, 1:400 (sc-271054, Santa Cruz Biotechnology)	Biotinylated goat anti-mouse IgG antibody (H + L), 1:800 (BA-5000, Vector Laboratories)
NLRP3, NeuN (IF) and hoechst	Anti-**NLRP3**, 1:400	Alexa Fluor® 488 cross-adsorbed donkey anti-goat IgG, 1:500 (A-11055, Thermo Fisher Scientific)
	Polyclonal mouse against **NeuN**, 1:500 (MAB377, Millipore)	Cy™5 AffiniPure donkey anti-mouse IgG (H + L), 1:500 (715–175-150, Jackson Immunoresearch)
NLRP3, ChAT (IF) and hoechst	Anti-**NLRP3**, 1:400	Cy™3 AffiniPure donkey anti-goat IgG (H + L), 1:500 (705–165-003, Jackson Immunoresearch)
	Polyclonal rabbit against **ChAT**, 1:250 (GTX113164, GeneTex)	Alexa Fluor® 488 AffiniPure donkey anti-rabbit IgG (H + L), 1:500 (711–545-152, Jackson Immunoresearch)
NLRP3, GFAP (IF) and hoechst	Anti-**NLRP3**, 1:400	Alexa Fluor® 488 donkey anti-goat IgG (H + L), 1:500
	Polyclonal rabbit against **GFAP**, 1:500 (ab7260, Abcam)	Alexa Fluor® 546 highly cross-adsorbed donkey anti-rabbit IgG (H + L), 1:500 (A-10040, Thermo Fisher Scientific)
NLRP3, IBA1 (IF) and hoechst	Polyclonal goat against **NLRP3**, 1:400 (GTX88190, GeneTex)	Alexa Fluor® 488 donkey anti-goat IgG (H + L), 1:500
	Polyclonal rabbit against **IBA1**, 1:500 (019–19,741, Wako)	Alexa Fluor® 546 donkey anti-rabbit IgG, 1:500
NLRP3 and AQP4 (IF)	anti-**NLRP3**, 1:400	Cy™3 donkey anti-goat IgG (H + L), 1:500
	Polyclonal rabbit against **AQP4**, 1:100, (sc-390488, Santa Cruz Biotechnology)	Alexa Fluor® 647 AffiniPure donkey anti-rabbit IgG (H + L), 1:500 (711-605-152, Jackson Immunoresearch)
NLRP3, GFAP and ASC (IF)	Anti-**NLRP3**, 1:400	Alexa Fluor® 488 cross-adsorbed donkey anti-goat IgG, 1:500 (A-11055, Thermo Fisher Scientific)
	Anti-**GFAP**, 1:500	Alexa Fluor® 546 donkey anti-rabbit IgG, 1:500
	Anti-**ASC**, 1:100	Cy™5 donkey anti-mouse IgG, 1:500
IL-1β (WB)	Polyclonal goat against **IL-1β**, 1:500 (AF-401-NA, R&D Systems)	HRP-conjugated rabbit anti-goat IgG (H + L), 1:4,000 (A5420, Sigma-Aldrich)
IL-18 (WB)	Polyclonal rabbit against **IL-18**, 1:500 (5180R-100, BioVision Incorporated)	HRP-conjugated goat anti-rabbit IgG (H + L), 1:4,000 (111–035-003, Jackson Immunoresearch)
β-actin (WB)	Monoclonal mouse against **β-actin**, 1:10,000 (A5441, Sigma-Aldrich)	HRP-conjugated goat anti-mouse IgG (H + L), 1:4,000 (115–035-003, Jackson Immunoresearch)

NLRP3, nucleotide-binding oligomerization domain-, LRR- and pyrin domain-containing protein 3; ASC, apoptosis-associated speck-like protein containing a caspase activation and recruitment domain; IF, immunofluorescence; IHC, immunohistochemistry; WB, western blot; IL-1β; interleukin-1 beta; IL-18, interleukin-18; GFAP, glial fibrillary acidic protein.

(ImageJ 1.51n engine) software. Some color images are presented in false color, in order to simplify visualization of certain stainings by presenting the same target proteins in uniform colors throughout different images. Brightness and contrast were adjusted as needed.

Quantitative Evaluation of Light Microscopy Immunohistochemistry Staining

Quantitative assessment of NLRP3 expression was carried out with the use of the DAB-based IHC technique, as this method provides photostability, in contrast to IF. Selection of sections for staining and evaluation was performed following a systematic regime. Anatomical boundaries of the nuclei were considered and eight sections were stained for quantification in each nucleus, in a way that after a section was selected, the consecutive section was excluded, to cover more of the anatomical region along the rostrocaudal axis of the brainstem. The contralateral (control) side of the samples was marked with a small incision during the sectioning, thus the injured and control sides could be clearly distinguished during the evaluation. After staining the series of the sections, a standardized digital image recording (in a Nikon Eclipse 80i microscope equipped with a 2,560 × 1,920 pixel resolution MicroPublisher 5.0 RTV charge-coupled device camera, QImaging) was conducted on all sections at ×10 magnification, thus both the operated and contralateral (control) sides of the nucleus were recorded on the same image. As the first step of the image analysis protocol, a consistent background subtraction algorithm was applied, based on internal controls (contralateral side) in each section, to determine the significantly stained profiles in identical regions at both the operated and contralateral sides of the nuclei. This was performed by using an interactive macro developed in our laboratory (Nógrádi et al., 2020) for the Image-Pro Plus image analysis software (Media Cybernetics).This resulted in an automated, unbiased evaluation procedure, since the algorithm determined the stained profile values with the same background subtraction for both the injured and contralateral sides on each section. As the significantly stained partial profile areas were determined at both sides of the brainstem, the data were expressed as a percentage, and the algebraic differences between the operated and the contralateral sides were determined. These numbers were averaged for the stained sections, to arrive at a single number characterizing the net change in the area covered by the significant immunoreaction induced by the axotomy in each animal.

To quantify the ratio of neurons in which the translocation of the target protein from the cell nuclei to the cytoplasm could be observed, a cell-counting procedure was carried out. From the non-treated axotomized group (hypoglossal axotomy), sections

were selected from the hypoglossal nucleus of each animal (n = 5 animals). Neuronal cells were recognized based on their size and the anatomical boundaries. In each of the sections, NLRP3 positive neurons were counted based on the localization of the staining. If NLRP3 was only present in the neuronal nucleus, the expression was counted as "nuclear NLRP3." If NLRP3 staining was clearly present in the cytoplasm, the expression was counted as "cytoplasmic NLRP3." When NLRP3 was clearly present in both the cytoplasm and nucleus, cells were sorted in the "cytoplasmic NLRP3" group, since the nuclear NLRP3 expression was recognized as the basal expression and the cytoplasmic presence of NLRP3 indicated translocation. Neurons were only counted if a well-described point of reference (cell nucleus) could be recognized in the section. Neurons were counted on both the operated and the control side. The ratio of translocation was determined for each side of each section and was averaged.

Sample Preparation, Methanol-Chloroform Precipitation and Western Blot

Under irreversible anesthesia with Avertin, mice were transcardially perfused with 10 mM PBS. The entire brain was exposed, removed and placed in 10 mM PBS, then dissected in the following manner: first, the brain was coronally sliced at approximately −6 mm from Bregma (at the *medulla oblongata* – *pons* transition), then at -7.5 mm from Bregma (at the appearance of the *decussatio pyramidum*). Next, the cerebellum was carefully dissected and removed from the sample. From the remaining sample, 1 mm wide lateral segments were sliced and removed along the sagittal plane on both sides. From the ventral part of the *medulla oblongata*, a 0.5 mm wide segment was cut and removed horizontally. Finally, the sample was sliced along the mid-sagittal axis and the two sides (injured and control sides) were separated and placed into sample holders.

Snap-freezing in liquid nitrogen was performed immediately after tissue dissection, then samples were processed in a Potter-Elvehjem homogenizer with a PTFE pestle in 10 mM PBS. Samples were grinded on ice until they were completely homogeneous. The homogenizer was thoroughly washed multiple times with distilled water between samples. Samples were centrifuged twice at 6,000 × g for 8 min at 4°C to remove debris. An equal volume of methanol and 1/4 volume of chloroform were added. Samples were vortexed, incubated for 5 min on ice, and centrifuged at 13,000 × g for 5 min at 4°C. After phase separation, aqueous phase was removed, and protein samples were washed with ice-cold methanol. Samples were vortexed and centrifuged again, supernatants were discarded, and protein pellets were air-dried. Pellets were reconstituted in 2× Laemmli buffer and heated up to 95°C for 5 min. Protein concentration was determined by using bicinchoninic acid assay (Thermo Fisher Scientific).

Samples were electrophoresed using standard denaturing SDS/PAGE and blotted on polyvinylidene difluoride membranes (0.2 µm pore size; Bio-Rad). After blocking with 3% bovine serum albumin (BSA) in Tris-buffered saline with 0.1% Tween-20 (TBS-T), membranes were incubated with primary antibodies (**Table 1**) overnight at 4°C. Blots were washed in TBS-T three times for 10 min, incubated for 1 h in horseradish peroxidase-conjugated secondary antibodies (**Table 1**) diluted in TBS-T, and then washed again in TBS-T. Immunoreaction was visualized with Clarity Chemiluminescence Substrate (Bio-Rad) in a ChemiDoc MP System (Bio-Rad). Densitometry analysis was performed with the Image lab software, version 5.2 (Bio-Rad).

Statistical Analysis of the Data

Student's t-test was applied to evaluate the differences in NLRP3 translocation from the nucleus to the cytoplasm and the WB quantification of the active IL-1β and IL-18 levels in the axotomized and control sides. Differences among the means of NLRP3 immunostaining was assessed by one-way ANOVA with Fisher LSD (least significant difference) post-hoc test. All statistical analysis was performed with R (version 3.6.2; R Foundation for Statistical Computing) and RStudio integrated development environment (RStudio). All data are represented as mean ± SEM. In order to determine the number of animals needed (sample size: n = 5 for IHC and n = 3 for WB), power analysis was carried out with G × Power (Faul et al., 2009).

RESULTS

Expression of Nucleotide-Binding Oligomerization Domain-, LRR- and Pyrin Domain-Containing Protein 3 in Motor Neurons in Response to Target Deprivation in the Oculomotor Nucleus and Axotomy in the Hypoglossal Nucleus

First, we assessed NLRP3 expression in the brainstem of animals exposed to axotomy. According to literature data, in traumatic brain injury (TBI), the level of inflammasome proteins (NLRP3, ASC, caspase-1) starts to increase 6 h after injury and peaked at 3 and 7 days (Liu et al., 2013). Furthermore, our previous experiments demonstrated that microglial activation and morphological changes, which might correlate with the inflammatory peak (Fernández-Arjona et al., 2019), show highest intensity at 4 and 7 days following nerve axotomy (Paizs et al., 2017; Nógrádi et al., 2020). Thus, in our experiments, all animals were allowed to survive for 4 days until the peak immune/inflammatory reaction was observed.

Under control (i.e., non-operated) conditions, there was a faint basal NLRP3 staining in both sides of the oculomotor and hypoglossal nuclei in mouse brain sections. Target deprivation in the case of the oculomotor nucleus led to a significant increase in the NLRP3 staining which was absent in the contralateral side serving as an internal control (**Figure 1A**). Similar changes were visible in the hypoglossal nucleus after the transection of the hypoglossal nerve; however, the reaction was more intense (**Figure 1A**). Quantitative analysis revealed that increase in NLRP3 was significant in both the oculomotor nucleus (8.04 ± 1.98 vs. 2.66 ± 0.34%; injured *vs.* non-operated; $p < 0.05$) and

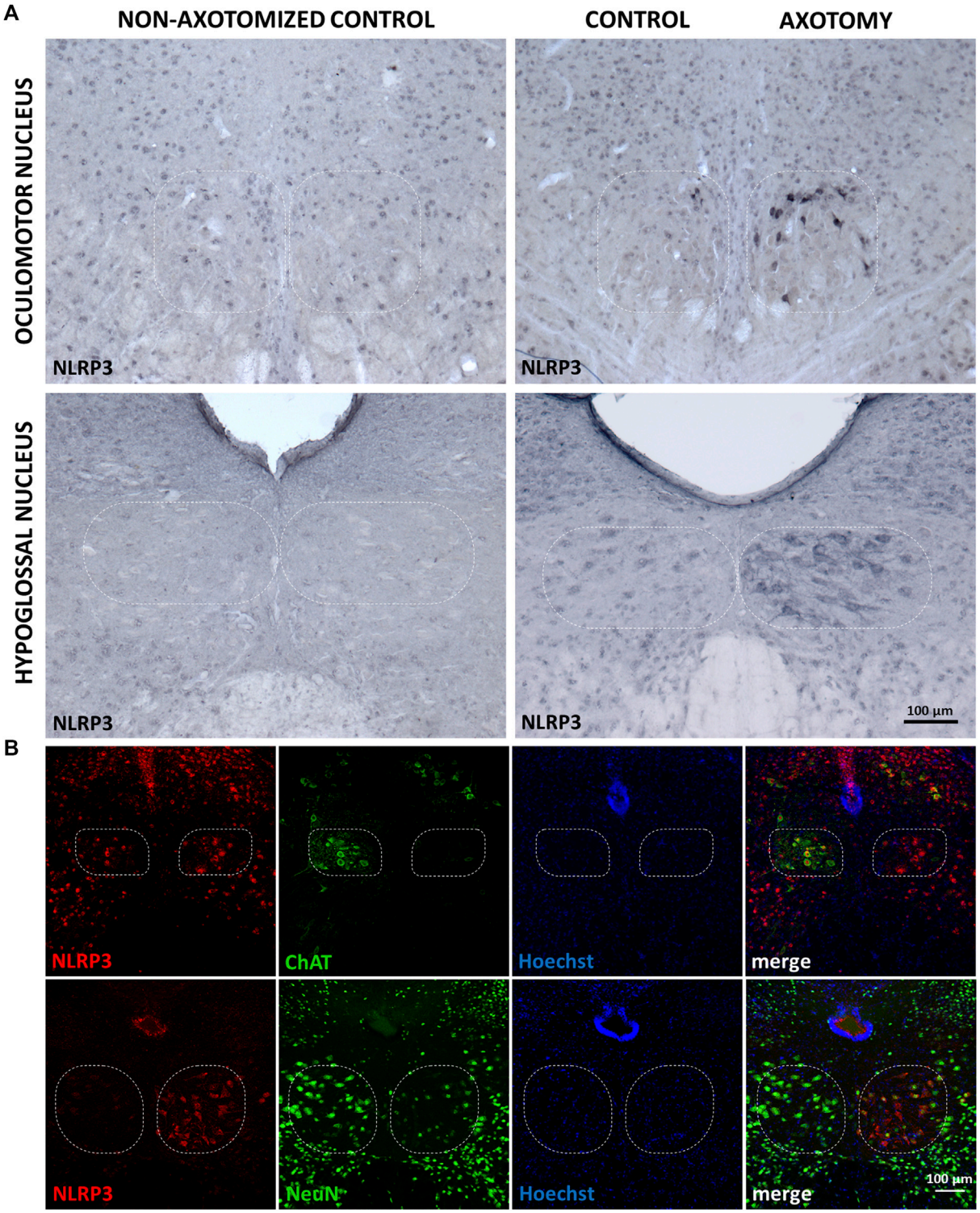

FIGURE 1 | Nucleotide-binding oligomerization domain-, LRR- and pyrin domain-containing protein 3 (NLRP3) protein expression in motor neurons of the oculomotor and hypoglossal nuclei after specific nerve axotomy. **(A)** Representative immunohistochemistry stainings of NLRP3 protein on Balb/c mouse brain sections from the anatomical region of the oculomotor **(top panel)** and the hypoglossal **(bottom panel)** nuclei (scale: 100 µm). Corresponding brain nerves were axotomized. **(B)** Representative fluorescence immunostaining images of NLRP3, neuronal nuclei **(top panel)** and choline acetyltransferase **(bottom panel)** proteins on Balb/c mouse brain sections from the anatomical region of hypoglossal nucleus after corresponding brain nerve axotomy (scale: 100 µm). Nuclei were counterstained with Hoechst 33342.

the hypoglossal nucleus (27.25 ± 4.87 vs.1.13 ± 0.51%; $p < 0.0005$) after the nerve transection, when compared to the non-operated controls. Furthermore, NLRP3 increase was significantly lower in the oculomotor nucleus compared to the hypoglossal nucleus following axotomy (8.04 ± 1.98 vs. 27.25 ± 4.87%; injured oculomotor nucleus vs. injured hypoglossal nucleus; $p < 0.0005$).

Morphology of the staining suggested that the majority of the NLRP3-positive cells were neurons. Therefore, we performed co-stainings with neuronal nuclei (NeuN) and choline acetyltransferase (ChAT) markers (**Figure 1B**). We chose the hypoglossal nucleus because more intense reaction could be observed compared to the oculomotor nucleus, following axotomy. NeuN staining decreased in the affected nucleus compared to its contralateral counterpart reflecting a nucleus-specific neuronal response to target deprivation, as described by others (McPhail et al., 2004; Obál et al., 2006). As anticipated, a significant number of NLRP3-positive cells were NeuN positive as well (**Figure 1B**), indicating neuronal upregulation of NLRP3 in response to target deprivation. ChAT staining almost completely overlapped with NLRP3 staining, indicating that indeed motoneurons expressed NLRP3 (**Figure 1B**). However, at the side of the lesion, ChAT staining, similarly to NeuN staining, decreased due to the disturbance in the neuronal homeostasis (Lams et al., 1988).

In order to identify further cell types that might respond with the upregulation of NLRP3 to peripheral nerve injury, we performed co-staining with ionized calcium-binding adapter molecule 1 (**Figure 2A**), a microglial marker, and glial fibrillary acidic protein (GFAP) (**Figure 2B**), an astroglial marker. Importantly, the majority of the microglia were not stained with the NLRP3 antibody, only a few microglial cells were NLRP3 positive. Similarly, NLRP3 was upregulated only in a small fraction of astrocytes, and astrocytic endfeet were largely excluded as demonstrated by the co-staining with the endfeet marker aquaporin-4 (AQP4) (**Figure 2C**).

Subcellular Redistribution of Nucleotide-Binding Oligomerization Domain-, LRR- and Pyrin Domain-Containing Protein 3 and Co-localization With Inflammasome Component Apoptosis-Associated Speck-Like Protein Containing a Caspase Activation and Recruitment Domain

Under control conditions, a significant part of NLRP3 staining could be seen in the nuclei of neurons. In response to the transection of the hypoglossal nerve, the staining appeared mainly in the cytoplasm, in parallel with weakening of the nuclear staining (**Figure 3A**). In order to visualize the changes more accurately and quantitatively, we performed IHC stainings which confirmed our observations obtained with fluorescence staining (**Figure 3B**). Quantitative analysis revealed that the ratio of neurons showing cytoplasmic NLRP3 was significantly higher on the injured side of the hypoglossal nucleus following axotomy (82.24 ± 5.38 vs. 1.95 ± 1.33%; injured side vs. contralateral side; $p < 0.0005$) (**Figure 3C**).

Activation of inflammasomes involves formation of a multiprotein complex, which includes binding of NLRP3 with the adaptor molecule ASC. Therefore, we performed co-localization analysis with the two proteins, and for a better resolution, we used STED microscopy. Similarly to NLRP3, ASC was also upregulated after nerve transection in the hypoglossal nucleus (**Figure 4A**). Staining performed with NLRP3 and ASC significantly overlapped mainly in neurons (**Figure 4B**). Interestingly, the co-localization could be observed in the nuclei as well (**Figure 4C**). Although NLRP3 could be detected in GFAP-positive cells as well, there was almost no co-localization with ASC (**Figure 4C**). We could not detect any co-localization of NLRP3 and ASC in microglial cells either (data not shown).

Nucleotide-Binding Oligomerization Domain-, LRR- and Pyrin Domain-Containing Protein 3 Inflammasome Activation, Interleukin-1 Beta and Interleukin-18 Activation

To examine NLRP3 inflammasome activation, the protein levels of active IL-1β and IL-18, the main pro-inflammatory cytokines of the inflammasome pathway, were quantified with WB. These changes were evaluated in the hypoglossal nucleus following axotomy of the hypoglossal nerve, since more intense NLRP3 upregulation was observed here compared to the oculomotor nucleus. Axotomy resulted in a 1.507-fold increase of pro- IL-1β levels ($p < 0.0005$), indicative of the priming phenomenon. In addition, we observed a 1.873-fold increase of the active IL-1β protein levels in the operated hypoglossal nucleus compared to the control side ($p < 0.05$) (**Figures 4D,E**). Similarly, a 1.893-fold increase was observed in the active IL-18 levels after axotomy ($p < 0.05$) (**Figures 4D,F**).

Inhibition of Nucleotide-Binding Oligomerization Domain-, LRR- And Pyrin Domain-Containing Protein 3 Upregulation by Diazoxide

In order to investigate the role of mitochondrial injury in axotomy-induced NLRP3 upregulation, we treated experimental animals post-surgery for 4 days with diazoxide, an agent with proven neuroprotective effects, able to preserve mitochondrial function (Teshima et al., 2003). Diazoxide diminished the increase in NLRP3 expression observed in the non-treated group following axotomy in the hypoglossal nucleus, compared to the vehicle control (DMSO), as represented by NLRP3 staining (**Figure 5A**) and quantitative analysis (8.49 ± 2.84 vs. 28.49 ± 5.98%; injured + diazoxide vs. injured + vehicle; $p < 0.0005$) (**Figure 5B**). DMSO did not have any significant effect on axotomy-induced NLRP3 upregulation (**Figure 5A,B**).

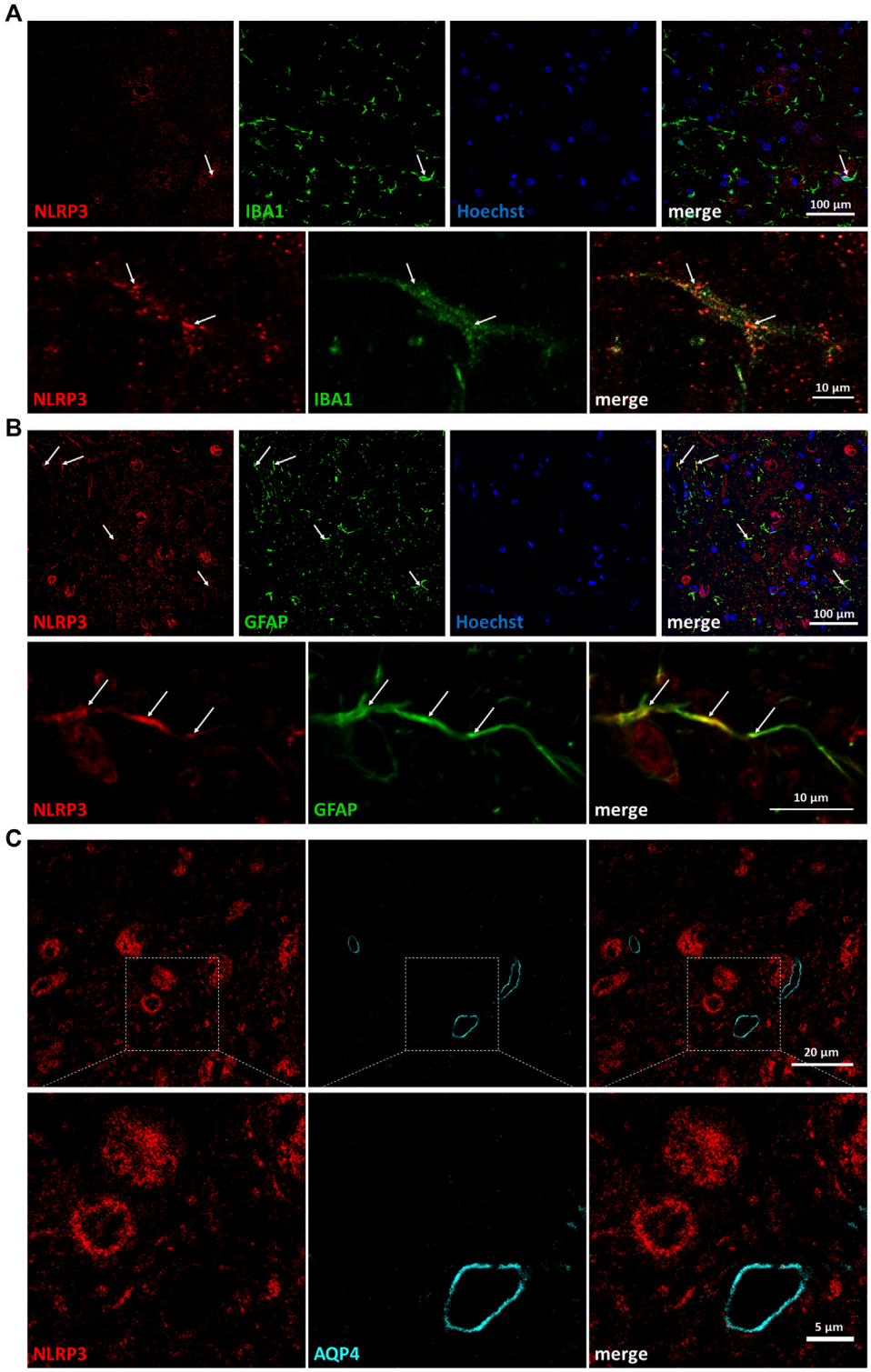

FIGURE 2 | Partial co-localization of nucleotide-binding oligomerization domain-, LRR- and pyrin domain-containing protein 3 (NLRP3) with glial marker proteins but not with microvessels on the injured side. **(A)** Representative confocal super-resolution microscopy (STED) images from fluorescent immunostaining of NLRP3 and ionized calcium-binding adapter molecule 1 proteins on Balb/c mouse brain sections from the anatomical region of the hypoglossal nucleus after corresponding brain nerve axotomy. Nuclei were counterstained with Hoechst 33342. Top panels: lower magnification (scale: 100 µm); bottom panels: high magnification (scale: 10 µm). **(B)** Representative confocal STED images from fluorescent immunostaining of NLRP3 and glial fibrillary acidic protein proteins on Balb/c mouse brain sections from the anatomical region of the hypoglossal nucleus after similar brain nerve axotomy. Nuclei were counterstained with Hoechst 33342. Top panels: lower magnification (scale: 100 µm); bottom panels: high magnification (scale: 10 µm). **(C)** Representative confocal STED images from fluorescent immunostaining of NLRP3 and aquaporin-4 proteins on Balb/c mouse brain sections from the anatomical region of the hypoglossal nucleus after similar brain nerve axotomy. Top panels: lower magnification (scale: 20 µm); bottom panels: high magnification (scale: 5 µm). Arrows indicate co-localization of signals.

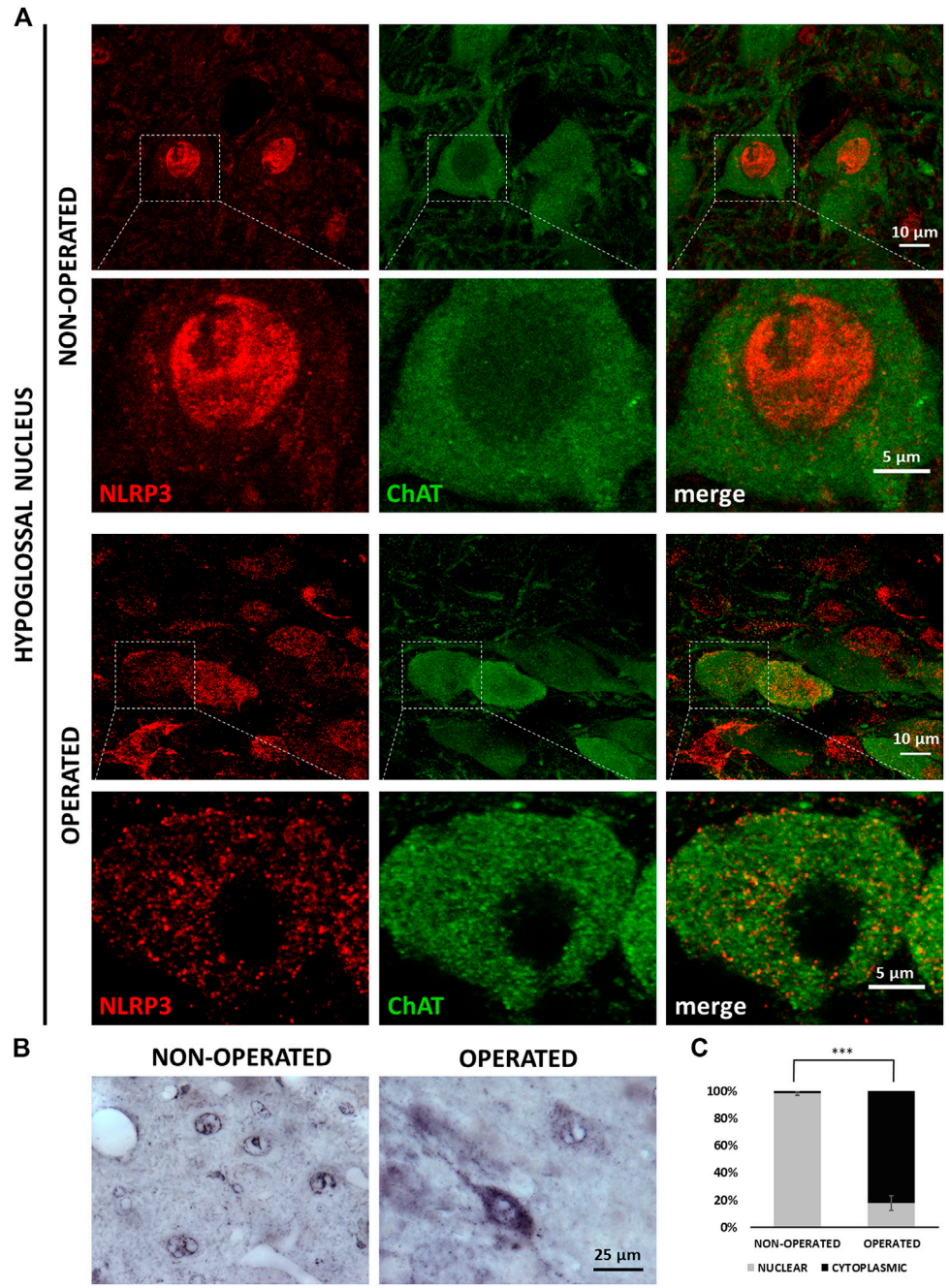

FIGURE 3 | NLRP3 translocation from neuronal cell nuclei into the cytoplasm in response to XII. nerve axotomy. **(A)** Representative super-resolution microscopy [nucleotide-binding oligomerization domain-, LRR- and pyrin domain-containing protein 3 (NLRP3)] and confocal (ChAT) images on Balb/c mouse brain sections from the anatomical region of the hypoglossal nucleus from the non-operated and operated side after hypoglossal nerve axotomy. Top panels (on both the non-operated and operated sides): lower magnification (scale: 10 µm); bottom panels: high magnification (scale: 5 µm). **(B)** Representative immunohistochemistry staining images of NLRP3 protein on Balb/c mouse brain sections from the anatomical region of the hypoglossal nucleus, from the non-operated (left panel) and operated (right panel) sides after equivalent nerve axotomy (scale: 25 µm). **(C)** Quantification of intracellular distribution of NRLP3 staining in neurons from non-operated and operated sides of the hypoglossal nucleus. The graph shows average % ± SEM of neurons in which NLRP3 localized in the nucleus or the cytoplasm (n = 5 animals/group, *** = $p < 0.0005$).

DISCUSSION

Elaborate crosstalk between the nervous and the immune systems modulates a considerable number of pathological processes in the brain. Accumulating evidence suggests that interaction between damaged neurons and the immune system, especially the innate immune system, is pivotal in determining the outcome of neurological disorders (Trakhtenberg and Goldberg, 2011).

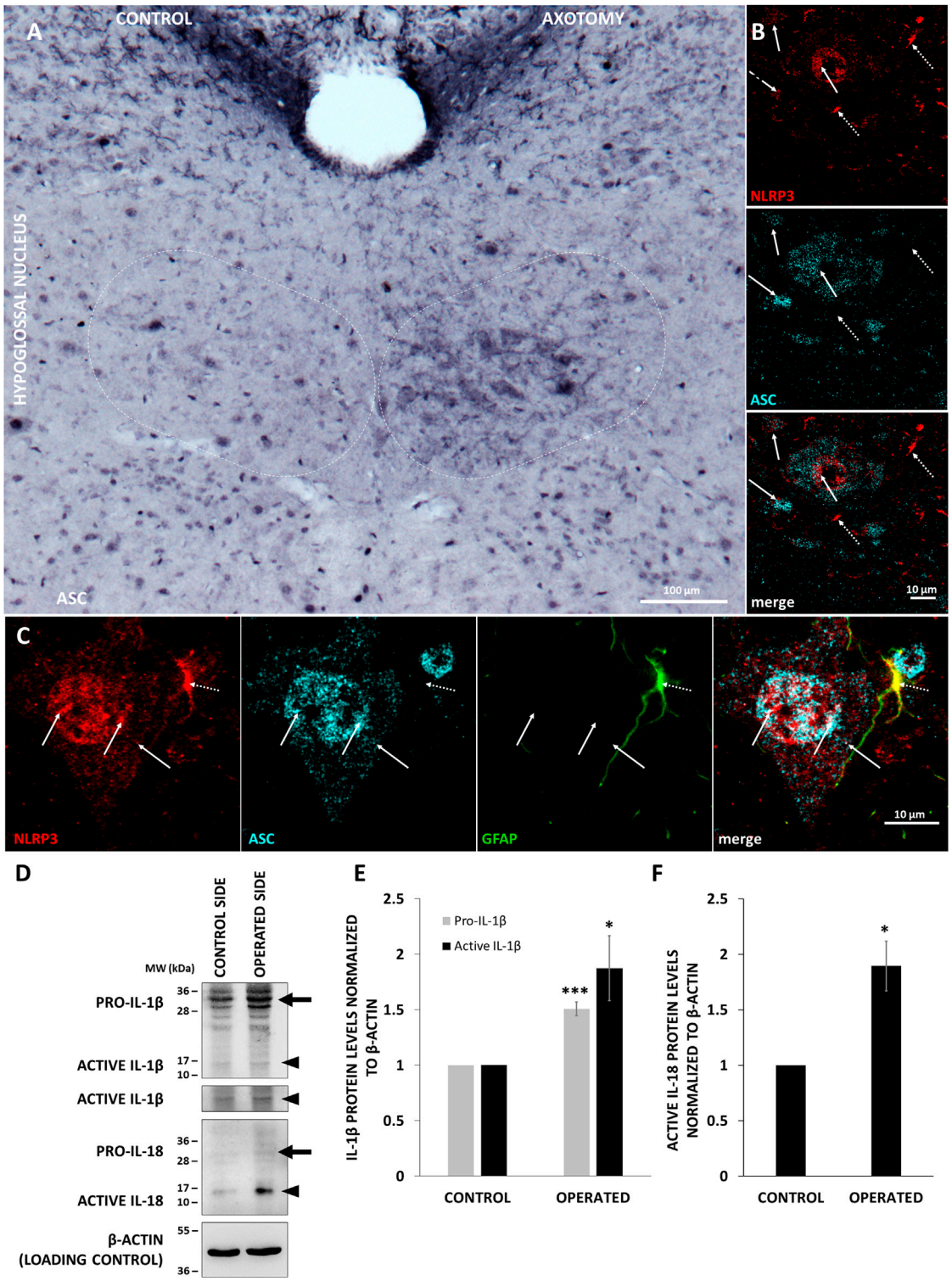

FIGURE 4 | Co-localization of inflammasome components and production of active interleukin-1 beta (IL-1β) and IL-18 (IL-18) in the XII. nucleus. **A)** Representative immunohistochemistry staining images of apoptosis-associated speck-like protein containing a caspase activation and recruitment domain (ASC) protein on Balb/c mouse brain sections from the anatomical region of the hypoglossal nucleus after corresponding brain nerve axotomy (scale: 100 µm). **(B)** Representative confocal [nucleotide-binding oligomerization domain-, LRR- and pyrin domain-containing protein 3 (NLRP3)] and super-resolution microscopy (STED) (ASC) images on Balb/c mouse brain sections from the anatomical region of the hypoglossal nucleus after hypoglossal nerve axotomy (scale: 10 µm). Solid arrows indicate the co-localization of NLRP3 and ASC. Dashed arrows indicate NLRP3 without co-localization with ASC. **(C)** Representative confocal [NLRP3 and glial fibrillary acidic protein (GFAP)] and STED (ASC) images on Balb/c mouse brain sections from the anatomical region of the hypoglossal nucleus after corresponding brain nerve axotomy (scale:

(Continued)

FIGURE 4 | 10 μm). Solid arrows indicate co-localization of NLRP3 and ASC in the nucleus and cytoplasm of the cells. Dashed arrow indicates co-localization of NLRP3 with GFAP, but not with ASC. **(D)** Representative western blot images of IL-1β and IL-18 proteins in of the hypoglossal nuclei after unilateral axotomy of corresponding brain nerve. Arrows indicate pro-forms, arrowheads show active cytokines. **(E)** Quantification of pro- and active IL-1β expression based on the western blot analysis of the hypoglossal nuclei in n = 3 animals. The graph shows values normalized to β-actin levels and to control side (average ± SEM,* = $p < 0.05$; *** = $p < 0.0005$). **(F)** Quantification of active IL-18 expression based on the western blot analysis of the hypoglossal nuclei in n = 3 animals. The graph shows values normalized to β-actin levels and to control side (average % ± SEM, * = $p < 0.05$).

Here we demonstrate that after acute lesion, motor neurons respond with upregulation of NLRP3, an important PRR and inflammasome component. NLRP3 upregulation and inflammasome activation have been largely acknowledged phenomena in CNS diseases (reviewed in Voet et al., 2019); however, microglia, the innate immune cells of the brain, have primarily been considered as resident cells involved in immunological processes of the CNS. Interestingly, in our model, motor neurons proved to initiate NLRP3 activation, while microglia were much less involved, despite their unequivocal role in the pathomechanism of neuronal injury-induced inflammation. Indeed, other NLRs not tested here, like NLRP1 or AIM2, may also become upregulated in microglia or neurons as well in response to axonal injury.

Although our finding that NLRP3 was highly upregulated in neurons was somehow unexpected, neuronal NLRP3 upregulation and inflammasome activation has already been detected in a few pathological conditions. For example, ischemic stroke was shown to activate both NLRP1 and NLRP3 inflammasomes in neurons through nuclear factor kappa-light-chain-enhancer of activated B cells (NF-κB)- and mitogen-activated protein kinase-dependent mechanisms (Fann et al., 2018). NLRP3 can be a mediator of inflammatory pain as well: chemical stimulation of the dura activated NLRP3 inflammasomes mainly in C-type neurons in the trigeminal ganglion (Chen et al., 2014). Furthermore, in the SOD1 (G93A) transgenic mice model of amyotrophic lateral sclerosis (ALS), NLRP3 activation was predominantly detected in degenerating neurons of the anterodorsal thalamic nucleus (Debye et al., 2016). Other studies also suggested activation of NLRP3 in neurons in injury and sterile inflammation (Chen et al., 2019; Voet et al., 2019). Nevertheless, in TBI, a mechanical injury model, NLRP3 upregulation was approximately similar in neurons, astrocytes and microglia (Liu et al., 2013), while in spinal cord contusion injury, NLRP3 was primarily found in microglia and neurons (Zendedel et al., 2015). However, to our best knowledge, inflammasome activation in the CNS after peripheral nerve injury has been unknown so far.

In our previous study, we have demonstrated that following acute nerve axotomy, microglia become activated to a different extent in the different motor nuclei of the brain, depending on the susceptibility of the respective nucleus to injury in chronic stress conditions (Nógrádi et al., 2020). For example, in the oculomotor nucleus, that is known to be resistant to degeneration in ALS, microglial activation was weaker than in the hypoglossal nucleus (Nógrádi et al., 2020), which is classically used as a model region of motoneuronal neurodegeneration in the CNS (reviewed in Nijssen et al., 2017). However, our current results indicate that microglial activation does not necessarily lead to inflammasome activation. This might have functional consequences, since specific microglia depletion had no influence on neuronal degeneration and axon regeneration in another acute nerve injury model (Hilla et al., 2017). On the other hand, the extent of microglial activation correlated with the level of motoneuronal NLRP3 upregulation in the two examined nuclei. Reduced NLRP3 upregulation after axotomy in the oculomotor nucleus compared to the hypoglossal nucleus might be coupled to the improved ionic buffering capacity of oculomotor neurons, especially to their ability to control calcium accumulation in mitochondria (Obál et al., 2006).

Under control conditions, we observed a strong NLRP3 staining in the cell nuclei. In response to nerve injury, NLRP3 was not only upregulated, but also translocated to the cytoplasm of motoneurons. Increased production of active IL-1β and IL-18 on the side of the injury suggests activation of inflammasomes, since cleavage of these cytokines is one of the best readout parameters of inflammasome activity (Broz and Dixit 2016; He et al., 2016; Zheng et al., 2020). Although the classical site of assembly of inflammasomes is the cytoplasm, a recent study revealed that six out of the 20 examined NLRs were detected in the nucleus as well. These include NLRP1, NLRP3, NLRP5, NLRP6, NLR family acidic transactivating domain (NLRA) and NLRC5 (Wang et al., 2016). Although we could clearly detect translocation of NLRP3 from the nucleus to the cytoplasm after nerve injury, a faint NLRP3 signal could still be detected in the nucleus, co-localized with ASC. Importantly, in certain cases, inflammasomes can be activated in the nucleus as well. Nuclear activation of interferon gamma-inducible protein 16 (IFI16) inflammasome could be detected during Kaposi sarcoma-associated herpesvirus infection in endothelial cells (Kerur et al., 2011). In the nucleus, activated caspase-1 may have other substrates than pro-IL-1β and pro-IL-18, e.g., sirtuin-1. Besides participating in the formation of inflammasomes, nuclear NLRs may have other functions as well, e.g., NLRP3 is a transcriptional regulator in T helper type 2 cells and a repressor of regulatory T cell differentiation (Bruchard et al., 2015; Park et al., 2020). It is not known yet, whether beyond serving as a receptor in inflammasomes, NLRP3 has any regulatory functions in neurons.

Several therapeutic approaches have proved that inhibition of the NLRP3 pathway could successfully prevent or slow down neuronal loss in neurodegenerative disorders (Zhou et al., 2016; Dempsey et al., 2017; Gordon et al., 2018). Based on this, reduction of NLRP3 activation seems to be a promising point

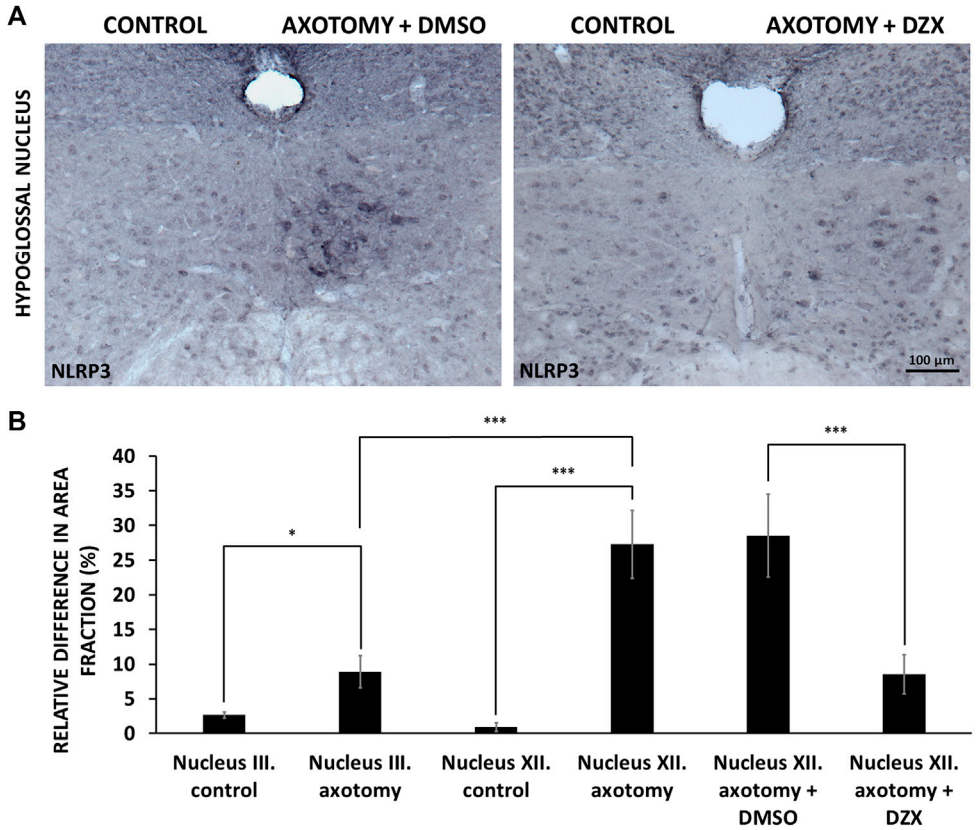

FIGURE 5 | Effect of diazoxide on nucleotide-binding oligomerization domain-, LRR- and pyrin domain-containing protein 3 (NLRP3) protein expression in hypoglossal nucleus. **(A)** Representative immunohistochemical staining images of NLRP3 protein on Balb/c mouse brain sections from the anatomical region of the hypoglossal nucleus after axotomy and treatment with either vehicle [dimethyl sulfoxide (DMSO)] or diazoxide (DZX) each day for 4 days after surgery (scale: 100 µm). **(B)** Quantitative analysis of NLRP3 protein expression in the oculomotor (n = 4) and in the hypoglossal (n = 4) nuclei after corresponding nerve axotomy. Hypoglossal nerve axotomized mice were treated with either vehicle (DMSO; n = 3) or diazoxide (n = 4) each day for 4 days after surgery. Graph represents the relative difference in the staining area fraction (average % ± SEM) of the operated side compared to the non-operated side of the nuclei (* = $p < 0.05$; *** = $p < 0.0005$).

of intervention in acute injury conditions as well. Diazoxide, an activator of the mitochondrial ATP-dependent K^+ channel, which readily crosses the blood-brain barrier, is known to reduce mitochondrial dysfunction (Domoki et al., 2004) and to protect neurons during ischemia/reperfusion injury (Lei et al., 2018). Opening of mitochondrial K^+_{ATP} channels results also in activation of anti-apoptotic mechanisms in neurons (Liu et al., 2002).

Diazoxide could also block microglial activation and reduce mitochondrial swelling in neurons following nerve axotomy in our previous experiments (Nógrádi et al., 2020). Interestingly, such effect on microglial mitochondrial morphology was not observed. Furthermore, diazoxide could reduce NLRP3 activation during cerebral ischemia/reperfusion injury through protecting mitochondria (Zhe et al., 2018; Gong et al., 2018). Indeed, mitochondrial dysfunction has a pivotal role in initiation and activation of the NLRP3 inflammasome (Liu et al., 2018), thus the ability of diazoxide to reduce neuronal mitochondrial injury could be a major pathway in dampening NLRP3 upregulation following acute nerve injury.

In our acute nerve injury model, diazoxide was able to block NLRP3 increase in a post-surgery treatment paradigm. As the neuroprotective effect of diazoxide has already been established (Lei et al., 2018), our results raise the point whether blockade of NLRP3 increase might act as a contributing factor to the neuroprotective properties of diazoxide in acute nerve injury. Also, as diazoxide could dampen the axotomy-induced microgliosis, it is possible that this effect, at least in part, could be mediated through the reduction of mitochondrial injury and NLRP3 activation. Therefore, our observation further strengthens the significance of the anti-inflammatory properties of diazoxide from a therapeutic point of view.

DATA AVAILABILITY STATEMENT

The original contributions presented in the study are included in the article/supplementary material, further inquiries can be directed to the corresponding author.

ETHICS STATEMENT

The animal study was reviewed and approved by Regional Animal Health and Food Control Station of Csongrád County.

AUTHOR CONTRIBUTIONS

BN, ÁN-T, and IAK designed research study; BN, ÁN-T, MK, KM, and RP performed research; RP, LS, IW, and IAK analyzed the data; LS and IAK supervised research; BN, ÁN-T, IW, and IAK drafted the manuscript; all authors approved final version.

FUNDING

This work was partially supported by the NKFIH (National Research, Development and Innovation Office) through the GINOP-2.3.2-15-2016-00001, GINOP-2.3.2-15-2016-00034, GINOP-2.3.2-15-2016-00020, FK-124114, K-135425, and K-135475 programs; the ÚNKP-19-2-SZTE-92, ÚNKP-20-2-SZTE-68, and ÚNKP-20-4-SZTE-138 New National Excellence Program of the Ministry for Innovation and Technology of Hungary; the NTP-NFTÖ-20-B-0192 National Talent Program of the Hungarian Ministry of Human Capacities and the Szeged Scientists Academy under the sponsorship of the Hungarian Ministry of Human Capacities (EMMI:11136-2/2019/FIRFIN). Support of UEFISCDI (Executive Agency for Higher Education, Research, Development and Innovation Funding; project code: PN-III-P1-1.1-TE-2019-1302) is also acknowledged.

REFERENCES

Abulafia, D. P., de Rivero Vaccari, J. P., Lozano, J. D., Lotocki, G., Keane, R. W., and Dietrich, W. D. (2008). Inhibition of the inflammasome complex reduces the inflammatory response after thromboembolic stroke in mice. *J. Cerebr. Blood Flow Metabol.* 29, 534–544. doi:10.1038/jcbfm.2008.143

Adamczak, S. E., de Rivero Vaccari, J. P., Dale, G., Brand, F. J., 3rd, Nonner, D., Bullock, M., et al. (2014). Pyroptotic neuronal cell death mediated by the AIM2 inflammasome. *J. Cerebr. Blood Flow Metabol.* 34, 621–629. doi:10.1038/jcbfm.2013.236

Althagafi, A., and Nadi, M. (2020). *Acute nerve injury*. Treasure Island, FL: StatPearls Publishing.

Broz, P., and Dixit, V. M. (2016). Inflammasomes: mechanism of assembly, regulation and signalling. *Nat. Rev. Immunol.* 16, 407–420. doi:10.1038/nri.2016.58

Bruchard, M., Rebé, C., Derangère, V., Togbé, D., Ryffel, B., Boidot, R., et al. (2015). The receptor NLRP3 is a transcriptional regulator of TH2 differentiation. *Nat. Immunol.* 16, 859–870. doi:10.1038/ni.3202

Chen, L., Li, X., Huang, L., Wu, Q., Chen, L., and Wan, Q. (2014). Chemical stimulation of the intracranial dura activates NALP3 inflammasome in trigeminal ganglia neurons. *Brain Res.* 1566, 1–11. doi:10.1016/j.brainres.2014.04.019

Chen, Y., Meng, J., Bi, F., Li, H., Chang, C., Ji, C., et al. (2019). NEK7 regulates NLRP3 inflammasome activation and neuroinflammation post-traumatic brain injury. *Front. Mol. Neurosci.* 12, 247. doi:10.3389/fnmol.2019.00247

Debye, B., Schmülling, L., Zhou, L., Rune, G., Beyer, C., and Johann, S. (2016). Neurodegeneration and NLRP3 expression in the anterior thalamus of SOD1(G93A) ALS mice. *Brain Pathol.* 28, 14–27. doi:10.1111/bpa.12467

Dempsey, C., Rubio Araiz, A., Bryson, K. J., Finucane, O., Larkin, C., Mills, E. L., et al. (2017). Inhibiting the NLRP3 inflammasome with MCC950 promotes non-phlogistic clearance of amyloid-β and cognitive function in APP/PS1 mice. *Brain Behav. Immun.* 61, 306–316. doi:10.1016/j.bbi.2016.12.014

de Rivero Vaccari, J. P., Lotocki, G., Marcillo, A. E., Dietrich, W. D., and Keane, R. W. (2008). A molecular platform in neurons regulates inflammation after spinal cord injury. *J. Neurosci.* 28, 3404–3414. doi:10.1523/jneurosci.0157-08.2008

Domoki, F., Bari, F., Nagy, K., Busija, D. W., and Siklós, L. (2004). Diazoxide prevents mitochondrial swelling and Ca 2+ accumulation in CA1 pyramidal cells after cerebral ischemia in newborn pigs. *Brain Res.* 1019, 97–104. doi:10.1016/j.brainres.2004.05.088

Elliott, E. I., Miller, A. N., Banoth, B., Iyer, S. S., Stotland, A., Weiss, J. P., et al. (2018). Cutting edge: mitochondrial assembly of the NLRP3 inflammasome complex is initiated at priming. *J. Immunol.* 200, 3047–3052. doi:10.4049/jimmunol.1701723

Fann, D. Y.-W., Lim, Y.-A., Cheng, Y.-L., Lok, K.-Z., Chunduri, P., Baik, S.-H., et al. (2018). Evidence that NF-κB and MAPK signaling promotes NLRP inflammasome activation in neurons following ischemic stroke. *Mol. Neurobiol.* 55, 1082–1096. doi:10.1007/s12035-017-0394-9

Faul, F., Erdfelder, E., Buchner, A., and Lang, A.-G. (2009). Statistical power analyses using G*Power 3.1: tests for correlation and regression analyses. *Behav. Res. Methods* 41, 1149–1160. doi:10.3758/brm.41.4.1149

Fernández-Arjona, M. D. M., Grondona, J. M., Fernández-Llebrez, P., and López-Ávalos, M. D. (2019). Microglial morphometric parameters correlate with the expression level of IL-1β, and allow identifying different activated morphotypes. *Front. Cell. Neurosci.* 13, 472. doi:10.3389/fncel.2019.00472

Freeman, L., Guo, H., David, C. N., Brickey, W. J., Jha, S., and Ting, J. P.-Y. (2017). NLR members NLRC4 and NLRP3 mediate sterile inflammasome activation in microglia and astrocytes. *J. Exp. Med.* 214, 1351–1370. doi:10.1084/jem.20150237

Gong, Z., Pan, J., Shen, Q., Li, M., and Peng, Y. (2018). Mitochondrial dysfunction induces NLRP3 inflammasome activation during cerebral ischemia/reperfusion injury. *J. Neuroinflammation* 15, 242. doi:10.1186/s12974-018-1282-6

Gordon, R., Albornoz, E. A., Christie, D. C., Langley, M. R., Kumar, V., Mantovani, S., et al. (2018). Inflammasome inhibition prevents α-synuclein pathology and dopaminergic neurodegeneration in mice. *Sci. Transl. Med.* 10, eaah4066. doi:10.1126/scitranslmed.aah4066

Hanamsagar, R., Torres, V., and Kielian, T. (2011). Inflammasome activation and IL-1β/IL-18 processing are influenced by distinct pathways in microglia. *J. Neurochem.* 119, 736–748. doi:10.1111/j.1471-4159.2011.07481.x

Halle, A., Hornung, V., Petzold, G. C., Stewart, C. R., Monks, B. G., Reinheckel, T., et al. (2008) The NALP3 inflammasome is involved in the innate immune response to amyloid-β. *Nat. Immunol.* 9, 857–865. doi:10.1038/ni.1636

He, Y., Hara, H., and Núñez, G. (2016). Mechanism and regulation of NLRP3 inflammasome activation. *Trends Biochem. Sci.* 41, 1012–1021. doi:10.1016/j.tibs.2016.09.002

Heneka, M. T., Kummer, M. P., Stutz, A., Delekate, A., Schwartz, S., Vieira-Saecker, A., et al. (2013). NLRP3 is activated in Alzheimer's disease and contributes to pathology in APP/PS1 mice. *Nature* 493, 674–678. doi:10.1038/nature11729

Hilla, A. M., Diekmann, H., and Fischer, D. (2017). Microglia are irrelevant for neuronal degeneration and axon regeneration after acute injury. *J. Neurosci.* 37, 6113–6124. doi:10.1523/jneurosci.0584-17.2017

Kerur, N., Veettil, M. V., Sharma-Walia, N., Bottero, V., Sadagopan, S., Otageri, P., et al. (2011). IFI16 acts as a nuclear pathogen sensor to induce the inflammasome in response to Kaposi sarcoma-associated herpesvirus infection. *Cell Host Microbe* 9, 363–375. doi:10.1016/j.chom.2011.04.008

Koliatsos, V. E., and Price, D. L. (1996). Axotomy as an experimental model of neuronal injury and cell death. *Brain Pathol.* 6, 447–465. doi:10.1111/j.1750-3639.1996.tb00875.x

Labzin, L. I., Heneka, M. T., and Latz, E. (2018). Innate immunity and neurodegeneration. *Annu. Rev. Med.* 69, 437–449. doi:10.1146/annurev-med-050715-104343

Lams, B. E., Isacson, O., and Sofroniew, M. V. (1988). Loss of transmitter-associated enzyme staining following axotomy does not indicate death of brainstem cholinergic neurons. *Brain Res.* 475, 401–406. doi:10.1016/0006-8993(88)90635-x

Latz, E., and Duewell, P. (2018). NLRP3 inflammasome activation in inflammaging. *Semin. Immunol.* 40, 61–73. doi:10.1016/j.smim.2018.09.001

Latz, E., Xiao, T. S., and Stutz, A. (2013). Activation and regulation of the inflammasomes. *Nat. Rev. Immunol.* 13, 397–411. doi:10.1038/nri3452

Lei, X., Lei, L., Zhang, Z., and Cheng, Y. (2018). Diazoxide inhibits of ER stress-mediated apoptosis during oxygen-glucose deprivation *in vitro* and cerebral ischemia-reperfusion *in vivo*. *Mol. Med. Rep.* 17, 8039–8046. doi:10.3892/mmr.2018.8925

Liu, D., Lu, C., Wan, R., Auyeung, W. W., and Mattson, M. P. (2002). Activation of mitochondrial ATP-dependent potassium channels protects neurons against ischemia-induced death by a mechanism involving suppression of bax translocation and cytochrome c release. *J. Cerebr. Blood Flow Metabol.* 22, 431–443. doi:10.1097/00004647-200204000-00007

Liu, H.-D., Li, W., Chen, Z.-R., Hu, Y.-C., Zhang, D.-D., Shen, W., et al. (2013). Expression of the NLRP3 inflammasome in cerebral cortex after traumatic brain injury in a rat model. *Neurochem. Res.* 38, 2072–2083. doi:10.1007/s11064-013-1115-z

Liu, Q., Zhang, D., Hu, D., Zhou, X., and Zhou, Y. (2018). The role of mitochondria in NLRP3 inflammasome activation. *Mol. Immunol.* 103, 115–124. doi:10.1016/j.molimm.2018.09.010

McPhail, L. T., McBride, C. B., McGraw, J., Steeves, J. D., and Tetzlaff, W. (2004). Axotomy abolishes NeuN expression in facial but not rubrospinal neurons. *Exp. Neurol.* 185, 182–190. doi:10.1016/j.expneurol.2003.10.001

Mészáros, Á., Molnár, K., Nógrádi, B., Hernádi, Z., Nyúl-Tóth, Á., Wilhelm, I., et al. (2020). Neurovascular inflammaging in health and disease. *Cells* 9, 1614. doi:10.3390/cells9071614

Minkiewicz, J., de Rivero Vaccari, J. P., and Keane, R. W. (2013). Human astrocytes express a novel NLRP2 inflammasome. *Glia* 61, 1113–1121. doi:10.1002/glia.22499

Nijssen, J., Comley, L. H., and Hedlund, E. (2017). Motor neuron vulnerability and resistance in amyotrophic lateral sclerosis. *Acta Neuropathol.* 133, 863–885. doi:10.1007/s00401-017-1708-8

Nógrádi, B., Meszlényi, V., Patai, R., Polgár, T. F., Spisák, K., Kristóf, R., et al. (2020). Diazoxide blocks or reduces microgliosis when applied prior or subsequent to motor neuron injury in mice. *Brain Res.* 1741 146875. doi:10.1016/j.brainres.2020.146875

Obál, I., Engelhardt, J. I., and Siklós, L. (2006). Axotomy induces contrasting changes in calcium and calcium-binding proteins in oculomotor and hypoglossal nuclei of Balb/c mice. *J. Comp. Neurol.* 499, 17–32. doi:10.1002/cne.21041

Paizs, M., Patai, R., Engelhardt, J. I., Katarova, Z., Obál, I., and Siklós, L. (2017). Axotomy leads to reduced calcium increase and earlier termination of CCL2 release in spinal motoneurons with upregulated parvalbumin followed by decreased neighboring microglial activation. *CNS Neurol. Disord. Drug Targets* 16, 356–367. doi:10.2174/1871527315666161223130409

Panicker, N., Kam, T.-I., Neifert, S., Hinkle, J., Mao, X., Karuppagounder, S., et al. (2020) NLRP3 inflammasome activation in dopamine neurons contributes to neurodegeneration in Parkinson's disease. *FASEB. J.* 34, 1. doi:10.1096/fasebj.2020.34.s1.01881

Park, S.-H., Ham, S., Lee, A., Möller, A., and Kim, S. T. (2020). NLRP3 negatively regulates treg differentiation through Kpna2-mediated nuclear translocation. *J. Biol. Chem.* 294, 17951–17961. doi:10.1074/jbc.RA119.010545

Raposo, C., and Schwartz, M. (2014). Glial scar and immune cell involvement in tissue remodeling and repair following acute CNS injuries. *Glia* 62, 1895–1904. doi:10.1002/glia.22676

Rotterman, M. T., and Alvarez, J. F. (2020). Microglia dynamics and interactions with motoneurons axotomized after nerve injuries revealed by two-photon imaging. *Sci. Rep.* 10, 8648. doi:10.1038/s41598-020-65363-9

Schwartz, M., and Deczkowska, A. (2016). Neurological disease as a failure of brain-immune crosstalk: the multiple faces of neuroinflammation. *Trends Immunol.* 37, 668–679. doi:10.1016/j.it.2016.08.001

Teshima, Y., Akao, M., Li, R. A., Chong, T. H., Baumgartner, W. A., Johnston, M. V., et al. (2003). Mitochondrial ATP-sensitive potassium channel activation protects cerebellar granule neurons from apoptosis induced by oxidative stress. *Stroke* 34, 1796–1802. doi:10.1161/01.str.0000077017.60947.ae

Trakhtenberg, E. F., and Goldberg, J. L. (2011). Neuroimmune communication. *Science* 334, 47–48. doi:10.1126/science.1213099

Voet, S., Srinivasan, S., Lamkanfi, M., and van Loo, G. (2019). Inflammasomes in neuroinflammatory and neurodegenerative diseases. *EMBO Mol. Med.* 11, e10248. doi:10.15252/emmm.201810248

von Herrmann, K. M., Salas, L. A., Martinez, E. M., Young, A. L., Howard, J. M., Feldman, M. S., et al. (2018). NLRP3 expression in mesencephalic neurons and characterization of a rare NLRP3 polymorphism associated with decreased risk of Parkinson's disease. *NPJ Parkinsons Dis.* 4, 24. doi:10.1038/s41531-018-0061-5

Wang, L., Fu, H., Nanayakkara, G., Li, Y., Shao, Y., Johnson, C., et al. (2016) Novel extracellular and nuclear caspase-1 and inflammasomes propagate inflammation and regulate gene expression: a comprehensive database mining study. *J. Hematol. Oncol.* 9, 122. doi:10.1186/s13045-016-0351-5

Zendedel, A., Johann, S., Mehrabi, S., Joghataei, M.-T., Hassanzadeh, G., Kipp, M., et al. (2015). Activation and regulation of NLRP3 inflammasome by intrathecal application of SDF-1a in a spinal cord injury model. *Mol. Neurobiol.* 53, 3063–3075. doi:10.1007/s12035-015-9203-5

Zheng, D., Liwinski, T., and Elinav, E. (2020). Inflammasome activation and regulation: toward a better understanding of complex mechanisms. *Cell Discov.* 6, 36. doi:10.1038/s41421-020-0167-x

Zhong, Z., Liang, S., Sanchez-Lopez, E., He, F., Shalapour, S., Lin, X.-j., et al. (2018). New mitochondrial DNA synthesis enables NLRP3 inflammasome activation. *Nature* 560, 198–203. doi:10.1038/s41586-018-0372-z

Zhou, Y., Lu, M., Du, R. H., Qiao, C., Jiang, C. Y., Zhang, K. Z., et al. (2016) MicroRNA-7 targets NOD-like receptor protein 3 inflammasome to modulate neuroinflammation in the pathogenesis of Parkinson's disease. *Mol. Neurodegener.* 11, 28. doi:10.1186/s13024-016-0094-3

Conflict of Interest: The authors declare that the research was conducted in the absence of any commercial or financial relationships that could be construed as a potential conflict of interest.

frontiers in Pharmacology

ORIGINAL RESEARCH
published: 26 November 2020
doi: 10.3389/fphar.2020.601344

Largely Accelerated Arterial Aging in Rheumatoid Arthritis Is Associated With Inflammatory Activity and Smoking in the Early Stage of the Disease

Nikolett Mong[1], Zoltan Tarjanyi[2], Laszlo Tothfalusi[3], Andrea Bartykowszki[2], Aniko Ilona Nagy[2], Anett Szekely[1], David Becker[2], Pal Maurovich-Horvat[4,5], Bela Merkely[2†] and Gyorgy Nagy[1,6,7†]*

[1] Polyclinic of Hospitaller Brothers of St. John of God, Budapest, Hungary, [2] Heart and Vascular Center, Semmelweis University, Budapest, Hungary, [3] Department of Pharmacodynamics, Semmelweis University, Budapest, Hungary, [4] MTA-SE Cardiovascular Imaging Research Group, Heart and Vascular Center, Semmelweis University, Budapest, Hungary, [5] Department of Radiology, Medical Imaging Centre, Semmelweis University, Budapest, Hungary, [6] Department of Rheumatology and Clinical Immunology, Semmelweis University, Budapest, Hungary, [7] Department of Genetics, Cell- and Immunobiology, Semmelweis University, Budapest, Hungary

OPEN ACCESS

Edited by:
Zsuzsanna Helyes, University of Pécs, Hungary

Reviewed by:
Ladislav Šenolt, Institute of Rheumatology, Prague, Czechia
Thomas Pap, Institut für Experimentelle Muskuloskelettale Medizin (IEMM), Germany

***Correspondence:**
Zoltan Tarjanyi
zoltan.tarjanyi.dr@gmail.com

†These authors have contributed equally to this work and share senior authorship

Specialty section:
This article was submitted to Inflammation Pharmacology, a section of the journal Frontiers in Pharmacology

Received: *31 August 2020*
Accepted: *07 October 2020*
Published: *26 November 2020*

Citation:
Mong N, Tarjanyi Z, Tothfalusi L, Bartykowszki A, Nagy AI, Szekely A, Becker D, Maurovich-Horvat P, Merkely B and Nagy G (2020) Largely Accelerated Arterial Aging in Rheumatoid Arthritis Is Associated With Inflammatory Activity and Smoking in the Early Stage of the Disease. Front. Pharmacol. 11:601344. doi: 10.3389/fphar.2020.601344

Background: Rheumatoid arthritis (RA) patients have a shorter life expectancy than the general population primarily due to cardiovascular comorbidities.

Objectives: To characterize arterial aging in RA.

Patients and Methods: Coronary calcium score (CCS) were available from 112 RA patients; out of these patients, follow-up CCS were measured for 54 randomly selected individuals. Control CCS were obtained from the MESA database (includes 6,000 < participants); arterial age was calculated from CCS.

Results: RA patients were significantly older (10.45 ± 18.45 years, $p < 0.001$) in terms of the arterial age than the age-, gender-, and race-matched controls. The proportion of RA patients who had zero CCS was significantly less ($p < 0.01$) than that of those in the MESA reference group. Each disease year contributed an extra 0.395 years ($p < 0.01$) on the top of the normal aging process. However, the rate of the accelerated aging is not uniform, in the first years of the disease it is apparently faster. Smoking ($p < 0.05$), previous cardiovascular events ($p < 0.05$), and high blood pressure ($p < 0.05$) had additional significant effect on the aging process. In the follow-up study, inflammatory disease activity (CRP > 5 mg/L, $p < 0.05$) especially in smokers and shorter than 10 years of disease duration ($p = 0.05$) had the largest impact.

Conclusion: Arterial aging is faster in RA patients than in control subjects, particularly in the first 10 years of the disease. Inflammation, previous cardiovascular events, and smoking are additional contributing factors to the intensified coronary atherosclerosis progression. These data support that optimal control of inflammation is essential to attenuate the cardiovascular risk in RA.

Keywords: rheumatoid arthritis, coronary calcium score, arterial aging, inflammatory activity, smoking-adverse effects

INTRODUCTION

Rheumatoid arthritis (RA) is a heterogeneous autoimmune condition; it affects 0.5–1% of the population and is associated with disability and systemic complications (Turesson et al., 2006; Prete et al., 2011; Das and Padhan, 2017). Both genetic and environmental factors have a central role in the pathogenesis of the disease, and cigarette smoke is the strongest known environmental factor (McInnes and Schett, 2007; Baka et al., 2009; McInnes and Schett, 2011). In RA, ongoing inflammation leads to cartilage destruction, bone erosions, and subsequent joint deformities. Although the current treatment strategy, principally the widespread use of biological therapies, improved the outcome of the disease, the mortality rate is still considerably higher among patients with RA than among healthy persons and systemic complications, especially cardiovascular (CV) risk due to RA, and represent a significant challenge (Liu et al., 2017; Nagy et al., 2018). Although biologicals have a beneficial effect on the CV risk in RA, TNF and IL6 inhibitors often increase the total cholesterol and triglyceride levels (Roubille et al., 2015; Gabay et al., 2016; Giles et al., 2019). In addition to the traditional cardiovascular risk factors (hypertension, diabetes, smoking, hyperlipidemia, alcohol, and physical inactivity), the effect of chronic inflammation on cardiovascular mortality is a rapidly developing field of interest (Ormseth et al., 2015). Elevated CRP level is considered as a cardiovascular risk factor (Yousuf et al., 2013; Fonseca and Izar, 2016). It is noteworthy that the risk of acute myocardial infarction (AMI) in RA is similar to the risk of AMI in diabetes mellitus (Nurmohamed et al., 2015). Coronary artery disease in RA appears more often in multivessel form (Karpouzas et al., 2014). In RA, the inflammation is associated with the presence of high-risk plaques (Aubry et al., 2007; Karpouzas et al., 2014). Coronary calcium score (CCS) is a well-established diagnostic marker showing calcium deposits in coronary arteries. It is known to be influenced by several factors including age, gender, race (Greenland et al., 2018), smoking (Shaw et al., 2006), high CRP levels (defined as higher than 5 mg/L), cardiovascular disease, high blood pressure, and diabetes, although the connection between diabetes and CCS is controversial (Raggi et al., 2004; Giles et al., 2009). The CCS assessment is a noninvasive method that has a great value in cardiovascular risk stratification, showing a significant association with the medium- or long-term occurrence of major cardiovascular events (O'Rourke et al., 2000; Neves et al., 2017). The prevalence of coronary artery calcium (CAC) increases with age, ranging from 5% in a middle-aged cohort to more than 50% in an elderly cohort (McClelland et al., 2006). A meta-analysis including asymptomatic individuals indicated that those with coronary artery calcification above the median have an 8.7-fold increased risk of future coronary events (O'Malley et al., 2000). In addition, there are data indicating that progression in CCS is associated with higher risk of myocardial infarction (Raggi et al., 2000; Raggi et al., 2003), and coronary artery calcification adds information to the prediction of overall mortality (Shaw et al., 2003). It has been proposed that CAC can be used to estimate the arterial age in adults. Although the increased cardiovascular risk is widely accepted in RA, the risk factors associated with the chronic autoimmune disease are less clear. The traditional cardiovascular risk scores underestimate the real cardiovascular risk in RA (Crowson et al., 2012; Kawai et al., 2015; Wahlin et al., 2019). CCS is better in CV risk stratification in RA than in combinations of the traditional CV risk factors (Korley et al., 2017; Karpouzas et al., 2020). Here, we investigated the baseline and follow-up CCS of RA patients and studied its progression over time. Our present result underscores the impact of inflammation on the CV risk in RA, especially in the first ten years of the disease.

PATIENTS AND METHODS

Patients and Controls

All RA patients were recruited in the rheumatology outpatient department of the Semmelweis University (Polyclinic of Hospitaller Brothers of St. John of God, Budapest, Hungary). Patients ≥ 18 years of age and diagnosed with RA (n = 112) according to the 2010 American College of Rheumatology/European League Against Rheumatism classification criteria (Aletaha et al., 2010) were enrolled. Exclusion criteria included concomitant autoimmune disease, except Sjögren's syndrome, malignant diseases, chronic infections with or without fever, and known psychiatric disease. The demographic data and the clinical parameters of the patients are summarized in **Tables 1**, **2**. Hypertension, diabetes mellitus, and hyperlipidemia were evaluated based on the standard criteria; smoking history was recorded (smoker/nonsmoker). Disease activity was evaluated by using the 28-joint counts and erythrocyte sedimentation rate–based (disease activity score/DAS28) score at each visit. Medications were recorded including glucocorticoids, NSAIDs, conventional and targeted disease-modifying antirheumatic drugs (DMARDs), and statins. Both national and institutional ethics committees approved the study, and informed consent was obtained from each individual [approval number: IF 567-4-2016]. This work was carried out in accordance with the Helsinki Declaration.

Control population: the Multi-Ethnic Study of Atherosclerosis (MESA) database was used as control. MESA is a prospective cohort study with an aim to investigate predictors of cardiovascular risk factors; coronary artery scan was performed in 6,814 participants without apparent cardiovascular problems. We refer to this population as "healthy" population or "MESA" population (Blaha et al., 2016). Age-, gender-, and race-matched control data were generated by using the online CCS calculator (https://www.mesa-nhlbi.org/Calcium/input.aspx). Based on demographic data and the measured CCS, the online calculator provided the estimated probability of having higher than zero calcium, and the 25th, 50th (median), 75th, and 90th CCS percentiles of in a "healthy" (i.e., without apparent cardiovascular disease) population. Using these percentiles and inverse quantile transformation, we simulated 100 age-, gender-, and race-adjusted CCS for each patient in our study. In this way, the

TABLE 1 | Patient characteristics, categorical variables. dm: diabetes (Type I: 3, Type II: 14), bp_ high: high blood pressure, esr_high: for males: ESR > 15 if age is less than 50 years and 20 if age is above 50 years. For females: 20 if age < 50 years and 30 above 50 years. CRP above 5/mg/L.

Variable	No	Yes	Total	Percent %
Female	18	94	112	83.9
Smoking	61	49	110	44.55
DM	95	17	112	15.18
CVevent	95	17	112	15.18
HT	42	70	112	62.50
RF positivity	36	76	112	83.04
aCCP positivity	46	66	112	60.71
high ESR	87	25	112	22.32
CRP 5	71	41	112	36.61
Biological therapy	52	60	112	53.57

TABLE 2 | Patient characteristics, continuous variables. The arteries are approximately 10 years older in RA than in the matched control group. Disdur: disease duration, CCS: coronary calcium score, CRP: C-reactive protein, artAge: calculated arterial age using Eq. 1, artAge_dif: arterial age difference from the median of the race-, sex-, and age-matched control population.

Variable	*N*	Mean	SD	Min	Max	Median
Age	112	63.00	11.40	35.00	84.00	64
Disdur	112	12.09	10.20	0.50	58.00	10
CCS	112	253.25	488.30	0.00	3,379.00	45
HDL	109	1.64	0.42	0.82	3.66	1.62
Chol	111	5.48	1.11	3.40	8.50	5.5
Hba1c	110	5.67	0.75	4.40	9.40	5.6
CRP	112	7.08	12.89	0.06	79.00	3.6
DAS	112	3.16	1.36	0.57	6.63	2.91
artAge	112	62.22	19.86	39.10	98.01	66.96
artAge_dif	112	10.45	18.53	35.35	52.56	6.35

control population consisted of 100 age-, gender-, and race-matched subjects from the MESA database for each RA patient, altogether 11,200 subjects.

Measurement of Coronary Calcium Score

All RA participants underwent non–contrast-enhanced, prospectively ECG-triggered scan of the heart using a 256-slice multidetector CT (Brilliance iCT 256; Philips Healthcare, Best, The Netherlands) at the Heart and Vascular Center of Semmelweis University. Images were acquired in cranio-caudal direction during a single breath hold in inspiration, at 78% of the R-R interval, with a slice thickness of 2.0 mm. The following acquisition parameters were used: 128 × 0.625 mm detector collimation, 270 ms gantry rotation time, 120 kV tube voltage, and 30 mA s tube current. The quantification of CAC was performed on the axial images on a per-patient and per-vessel basis using a semi-automatic software (Heartbeat-CS, Philips Healthcare, Best, The Netherlands). CCS were computed by the standard calcium scoring algorithm of Agatston (Agatston et al., 1990). Follow-up CCS measurement was performed for 54 patients.

Determination of the Arterial Age and Arterial Age Difference (artAge_dif)

Arterial age is an easy to understand intuitive concept; it shows the apparent age of arteries using healthy population as a reference. Therefore, to help the clinical interpretation of the results, CCS were transformed into "arterial age" using the formula of McClelland et al. (2009):

$$\text{arterial age} = 39.1 + 7.25 \log(\text{CCS} + 1). \quad (1)$$

To facilitate the statistical inference, we introduced an additional variable called artAge_dif. The variable artAge_dif measures difference between the observed and the control arterial ages. For each patient, there were 100 age-, gender-, and race-matched controls, and we obtained artAge_dif by subtracting the median of the corresponding controls from each observed value.

Statistical Analysis

Stata version 15 (StataCorp LP, College Station, TX) was used for statistical analysis and R (R Core Team, 2017) with several additional packages such as ggplot2 (Wickham, 2016) for additional programming tasks and visualization. The difference between the measured and MESA control population values was tested using the one-sample alternative of the tests; that is, we assumed that simulated control population is not different from the "true" population. Percentages of subjects having nonzero CCS in the observed and computer-predicted populations were compared with exact binomial test. The effect of factors that may influence CCS was studied by graphical analysis followed by univariate testing and multivariate linear regression modeling. Due to highly nonnormal distribution of the data, we gave preference to nonparametric methods such as rank-based tests or we took advantage of the "robust" option available for many procedures in Stata. To illuminate the trends, we fitted locally weighted polynomial regression commonly known as LOWESS. Descriptive summaries such as proportion, means, and standard deviation (SD) are provided for all clinically relevant baseline variables, and statistical significance level was set to $p < 0.05$, two-tailed.

RESULTS

Accelerated Arterial Aging in Rheumatoid Arthritis

CCS were measured in 112 RA patients; control CCS were obtained from the MESA database. **Figure 1** upper panel compares the two arterial age distributions. Both histograms can be split into two parts. There is one single outstanding bar

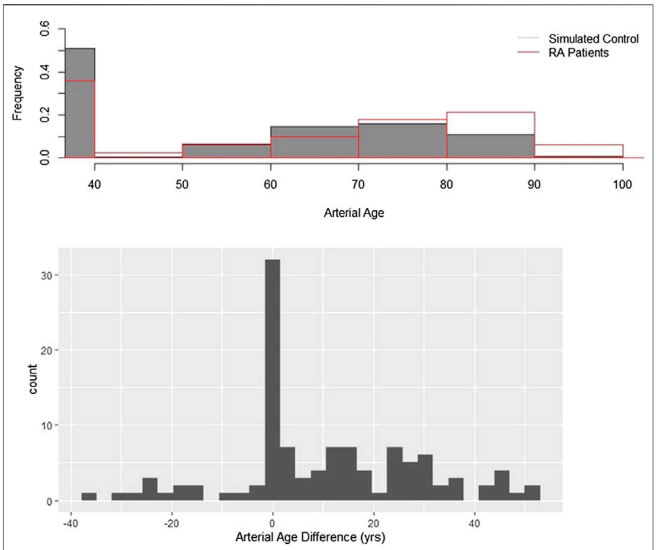

FIGURE 1 | Arterial age in rheumatoid arthritis. Upper panel: Arterial age, converted from the observed and age-, gender-, and race-adjusted simulated coronary calcium scores. The figure shows the resulting distributions of the observed and simulated data. The shaded bars are the simulated control subjects, and the transparent bars with red contours represent the observed values. Lower panel: Arterial age distributions of patients with RA and the control populations are different. artAge_dif is the difference between the observed and the median of the control arterial ages. If there is no difference between RA patients and control subjects, then the histogram of artAge_dif must be symmetric around zero. Using Wilcoxon signed test, we showed that this null hypothesis is unlikely ($p < 0.001$).

which represents subjects with zero CCS, and the arterial age of these subjects is by definition exactly 39.1. A characteristic feature of both curves a rightly skewed distorted bell-shape kind of part ranging from 39.1 up to hundred. These parts correspond to subjects having higher than zero CCS. Although the general features are similar, there are noteworthy differences between the two histograms. Smaller percentage of RA patients have zero CCS, and compared to controls, the center of the histogram is shifted to right, toward older ages. These visual impressions were confirmed by the statistical analysis. The CCS calculator gave the probability for each patient having higher than zero calcium. The average of these predicted probabilities was 0.517, while the found ratio is 0.642. The difference between the groups is highly significant ($p = 0.008$).

The assumption that arteries are older in RA compared to the matched controls was further tested with the help of variable artAge_dif, which is the difference of the observed value from the median of the controls. Statistical theory suggests that if there is no difference between the MESA and RA populations, then the distribution of artAge_dif has symmetric distribution around zero. **Figure 1** lower panel shows that the difference distribution is not symmetric but clearly right skewed with a median of 6.34 years. This difference from the expected zero is highly significant ($z = 5.51$, $p < 0.0001$). Because artAge_dif has right skewed distribution (**Figure 1** lower panel), the mean difference is higher than the median. As **Table 2** shows, the mean difference is 10.45 (SD: 18.45) years, which means that the arteries of the RA patients in average are 10.45 years older than those of their MESA counterparts' ($p < 0.001$).

Correlation of Inflammatory Markers With Clinical Measures

As expected, the inflammatory markers (CRP and ESR) strongly correlated with each other and with the clinical disease activity (DAS28), data not shown. The correlation between artAge_dif and the disease duration is also significant ($r = 0.22$, $p < 0.05$).

Comorbidities, Autoantibodies (Anti-Cyclic Citrullinated Peptide/Rheumatoid Factor), Smoking, and the Arterial Age

Figure 2 displays the dependence of artAge_dif on categorical covariates. The differences between nonsmokers/smokers, patients without and with cardiovascular events, and patients with normal and high blood pressure were significant ($p = 0.016$, 0.029, and 0.023, respectively). By contrast, neither the presence of rheumatoid factor (RF), anti-cyclic citrullinated peptide (aCCP), nor diabetes proved to be predictive. We also checked if the previous statistical conclusions remain valid if we exclude diabetic patients' data from the analysis. Seventeen patients (15.1%, **Table 1**) had diabetes. Excluding these individuals, 64.3% of the remaining patients had CCS above zero. This ratio is still significantly higher than the age- and gender-matched MESA control (49.4%, $p = 0.004$). The same is true for the difference from the matched medians (6.12 years, $p < 0.001$).

The Effect of Cardiovascular Disease on the Coronary Calcium Score

Existing cardiovascular disease or history of cardiovascular events is associated with higher CCS (Lehker and Mukherjee, 2020). Subjects with existing cardiovascular condition were excluded from the MESA study, while 17 patients in our RA study group (15.18%, **Table 1**) had preexisting cardiovascular conditions. Therefore, the question arises to what extent the observed differences are due to the cardiovascular events. To answer this question, we split the RA study group into four subpopulations using the criteria that a patient had a zero CCS or the CCS was above it and that a patient had or had not previous cardiovascular disease. In the left panel of **Supplementary Figure S1**, proportions of patients with zero CCS are compared. Both RA subgroups are significantly different from their corresponding matched samples although the difference is much more pronounced in patients with previous cardiovascular disease (**Supplementary Figure S1**) ($p = 0.023$ and $p = 0.005$ respectively). Such difference between the two RA patient subgroups is not seen in the right panel of **Supplementary**

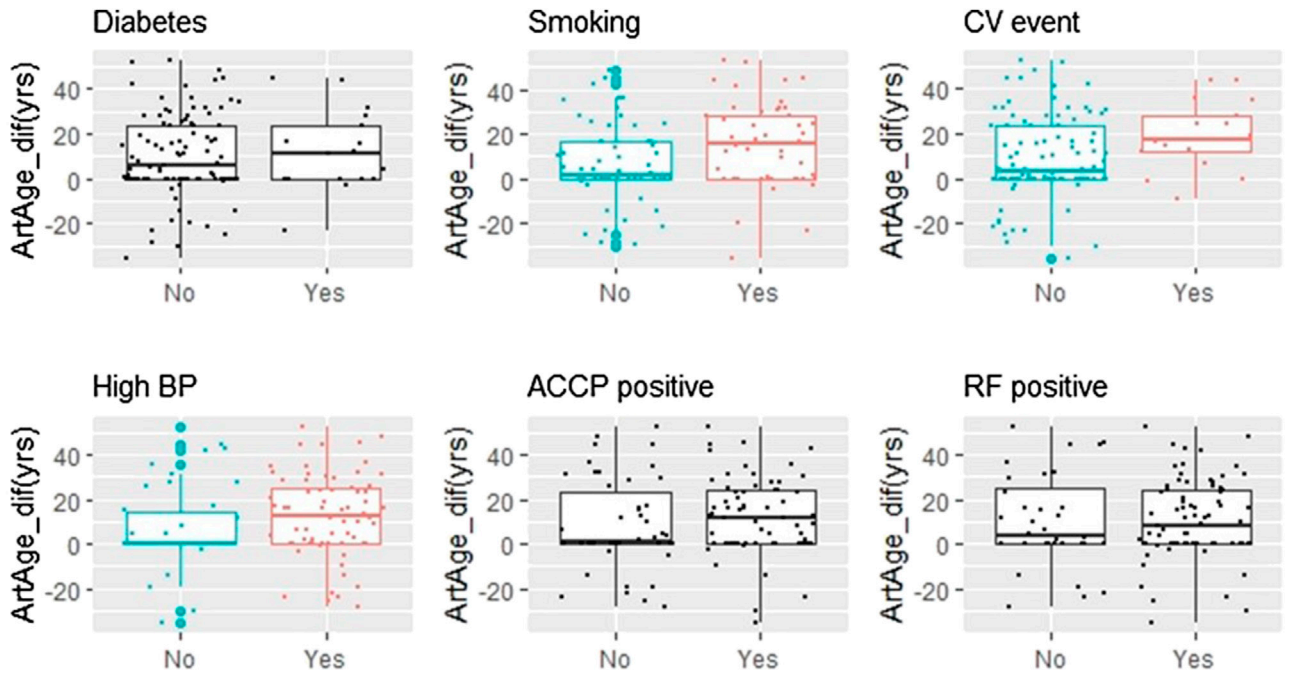

FIGURE 2 | Smoking, CV events, and hypertension are associated with increased Artage_dif. Six binary variables were screened for potential effect on artAge_dif. The arterial age is increased significantly in patients who are smokers, have history of cardiovascular disease (CV event), or who are taking antihypertensive medicines (high BP). The corresponding *p* values (Kruskall–Wallis test): 0.016 (smoking), 0.029 (CV event), and 0.023 (high BP). Plots where the variable effects were significant are colored, while where the effect was not significant are in black (ACCP, anti-cyclic citrullinated peptides antibody; RF, rheumatoid factor).

Figure S1, and the medians of the matched arterial age differences are practically the same (16.7 and 18.1 years) for patients without and with cardiovascular disease. Both of them are significantly different from the expected zero ($p < 0.001$). These data suggest that the effect of RA on the CCS is mostly due to the accelerated progression rate. Cardiovascular disease is an additional risk factor because patients with cardiovascular disease have accelerated conversion rates from being CCS negative to CCS positive. The rate of conversion is significantly higher not only to control ($p = 0.005$) but also compared to RA patients without cardiovascular disease ($p = 0.012$).

Arterial Aging Is More Accelerated in the First 10 Years of the Disease

The analysis presented above suggests that the rate of the calcium build-up process in the control and RA populations is markedly different. Indeed, the time from the onset of the disease (disdur) was the only variable which showed significant correlation with the arterial age acceleration (data not shown). However, as the left panel of **Figure 3** shows, the aging process is not constant. It increases monotonically ($r_s = 0.249$, $p = 0.008$), but the fitted nonparametric regression line (span = 0.9) suggests that the increase is faster in the first 10 years. Nevertheless, to get a numerical estimate of the arterial aging relative to the control, we fitted linear regression between disdur and artAge_dif. The fitted regression line is displayed in the right panel of **Figure 3**. The slope of the regression line is 0.395 (95% CI 0.10–0.68), significantly different from zero ($t = 2.74$, $p = 0.007$). The meaning of this 0.395 is that difference from the control increases by 0.395 years in every year of the disease; thereafter, in average, every year with RA contributes 0.395 extra arterial years.

Progression Rate Estimation Using Follow-Up Data

Fifty-four patients had a follow-up CCS measurement. **Supplementary Table S1** summarizes the DAS, CRP, and ESR values at the time of the two measurements. Generally, there is strong correlation between these values (data not shown). The average time between the CCS scans was 1.28 ± 0.35 years. The annual arterial aging rate was calculated by dividing the difference between the second and first arterial age measurements with the length of the time interval between the two measurements. The least-square estimates with the corresponding 95% confidence intervals are shown in the left panel of **Figure 4**. The estimated aging rate is 1.44 (95% CI 0.77–2.11), which is in good agreement with the previous regression estimate. Nevertheless, from the further analysis, we excluded two subjects who converted during the observation period (i.e., their first CCS was zero and the second above zero, with estimated aging of 8.1 and 12.8 years, respectively), because from a statistical viewpoint, they were gross outliers. Without these two values, the rate estimate was

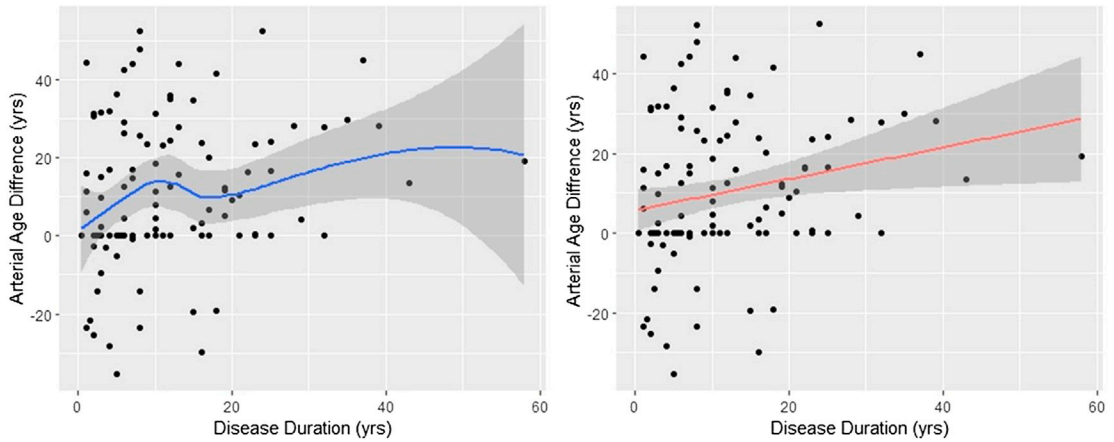

FIGURE 3 | Arterial age difference depends on the disease duration. The effect of disease duration on the arterial age difference between RA patients and controls is shown. The smoothed curve in the left figure was obtained with Lowess. On the right figure, the red line represents the fitted regression line. The slope of the regression line (slope = 0.395, $t = 2.74$, $p = 0.007$) is the yearly divergence rate from the control. In both cases, the shaded areas around the lines are the 95% confidence intervals. The arterial aging is approximately 40% accelerated.

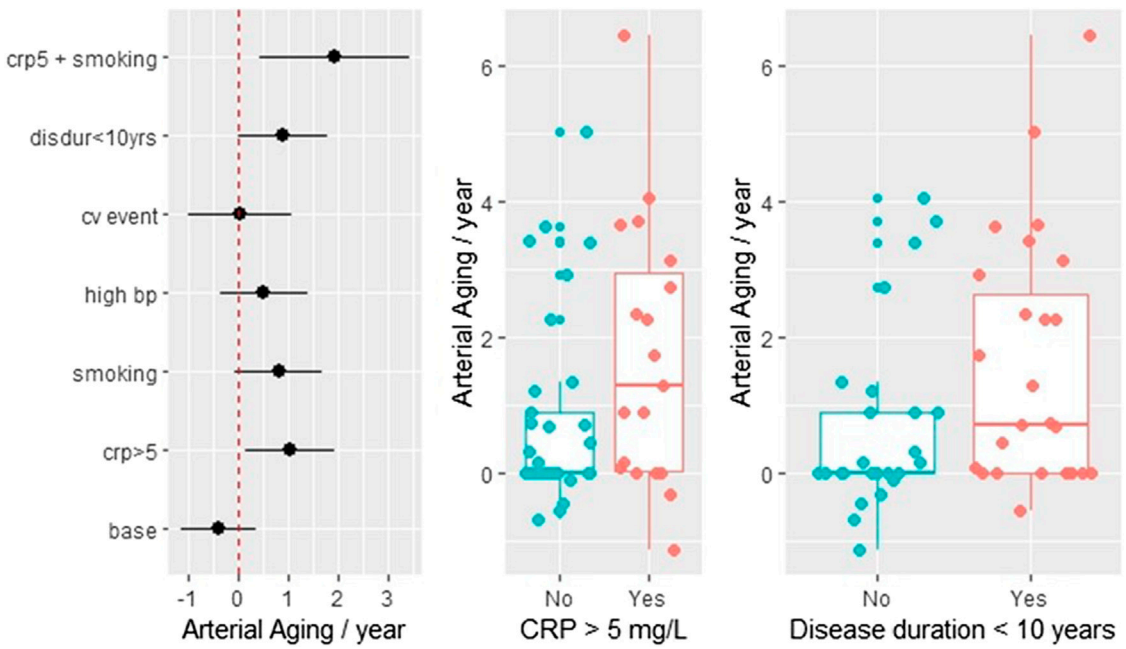

FIGURE 4 | Follow-up data: the effect of inflammation, CV diseases, smoking, and RA disease duration on the arterial aging. The arterial aging rate was calculated by dividing the difference of the two consecutive arterial age estimates with the time interval between the two measurements. The left panel shows least-square estimates of five risk factors on the rate: smoking, disease duration ≤10 years (disdur < 10), history of cardiovascular disease (cvevent), CRP 5 > 5 mg/L, and concomitant antihypertensive drug taking (bp_high). When the 95% confidence intervals do not cross zero the effects are significant, which is true only for crp5 ($p = 0.024$) and disdur < 10 ($p = 0.05$). In the absence of any risk factors (which includes that the disease started more 10 years ago), the aging rate is close to zero (base). The combined effect of two risk factors such as CRP and smoking shown in the figure is an estimated marginal effect. The two boxplots illustrate the effect of crp5 and disdur < 10.

1.09 + 0.22, still highly different from zero ($p < 0.001$, $t = 4.78$). Additional regression analysis showed that the aging process is significantly faster in patients who had elevated CRP (>5 mg/L) level ($p = 0.024$) and in case the time since diagnosis is less than 10 years ($p = 0.05$). The least-square approach allowed us to investigate the combined effect of two or more risk factors.

Figure 4 demonstrates that in smokers with elevated CRP levels, the arterial aging rate is doubled. The additionally computed nonparametric test confirmed the significance of the elevated CRP ($p = 0.0494$). The middle and the right panels of **Figure 4** further demonstrate the effect of CRP and disease duration <10 years on the arterial aging.

Effect of Medications on the Coronary Calcium Score

From the fifty-four patients in the follow-up study, thirty-one received biological therapy (twenty-seven patients anti-TNF-alpha, four patients non–anti–TNF-alpha bDMARDs) and twenty-three csDMARD therapy only. The yearly arterial aging progression rate in the follow-up group in patients receiving bDMARD therapy was numerically lower (1.16 ± 0.35) than that in patients receiving csDMARDs (1.73 ± 058); the difference (0.57 ± 0.67) was not significant (t = −0.85, p = 0.389).

DISCUSSION

Primarily due to cardiovascular comorbidities, patients with RA die significantly earlier (Nurmohamed et al., 2015; Nagy et al., 2018), and the risk of sudden cardiac death is doubled in RA compared to the general population (Maradit-Kremers et al., 2005; Naranjo et al., 2008; Karpouzas et al., 2014; Jagpal and Navarro-Millan, 2018). Due to the accelerated cardiovascular risk, the precise risk evaluation is essential. Our present data confirm and extend previous observations regarding the increased cardiovascular risk in RA. Here, we show for the first time the profound effect of RA on the arterial age, compared to the MESA population. Older arterial age was associated with smoking, previous cardiovascular events, and hypertension. The follow-up substudy was self-controlled and highlighted the importance of other additional factors. Ongoing inflammation (CRP > 5 mg/L), especially in smokers, and shorter disease duration (<10 years) accelerated arterial aging according to our follow-up data. Therefore, the increased cardiovascular risk due to RA increases with the disease years, but the augmentation is not linear, and in the first 10 years of the disease, the arterial aging is apparently more pronounced.

Inflammation plays a central role in the pathogenesis of atherosclerosis; elevated levels of C-reactive protein (CRP), interleukin-6, and N-terminal pro-hormone B-type natriuretic peptide (NTproBNP) correlate closely with cardiac events (Sabatine et al., 2004). Epidemiological studies suggested that chronic inflammation is associated with higher cardiovascular risk. In addition, inflammation is a recognized risk factor of AMI in RA (Meissner et al., 2016). A number of inflammatory mediators have been widely studied, both as surrogate biomarkers and as causal agents, in the pathophysiological network of atherogenesis and plaque vulnerability (Libby et al., 2002). Moreover, it was suggested that inflammatory processes and cytokines are similar in RA and in atherosclerotic vascular diseases (Plein et al., 2020). Low disease activity is associated with decreased risk of CVE in RA (Arts et al., 2017).

In patients with RA, inflammatory markers, disease severity, and RF positivity were found to be associated with the risk of atherosclerosis (Sattar et al., 2003). ACPA and RF are both unfavorable prognostic factors in RA; in accordance with our present data, both autoantibodies are independent of the accelerated arterial aging in RA (Berendsen et al., 2017).

The age is an independent risk factor for cardiovascular diseases; nevertheless, often the atherosclerotic disease burden is discordant with a patient's chronological age. Calcium is a general component of the atherosclerotic plaque, but not that of the normal vessel wall (O'Rourke et al., 2000). Because of this structural difference, calcium is an accurate index of atherosclerotic disease burden and a useful tool to estimate the risk of cardiovascular adverse outcomes (Raggi et al., 2000; Kondos et al., 2003). Previous studies showed the importance of age-specific CCS percentiles to predict the occurrence of a cardiovascular event in patients with a similar risk profile (Wong et al., 2002). CCS is a widely accepted marker of coronary atherosclerosis. In the MESA population, a doubling of the CCS increased the probability of a coronary event by 25% in a 3.8-year follow-up period. Importantly, this predictive value was relatively stable across different ethnic groups (Detrano et al., 2008). Similar to our present data, RA severity was associated with the greater prevalence of coronary artery calcification than the MESA population (Giles et al., 2009). The Framingham risk score includes age, gender, total and HDL cholesterol, blood pressure, diabetes, and smoking. However, long-standing patients with RA had higher Framingham risk scores than patients with early disease or control subjects. Furthermore, long-standing inflammation represents additional cardiovascular risk (Chung et al., 2006). Moreover, the presence of CAC has been shown in early RA as well (Logstrup et al., 2017). The lack of diabetes effect in our study was somewhat surprising because it is generally presumed that the CCS is independently associated with incident coronary heart disease in diabetes (Malik et al., 2017). Framingham risk based on arterial age is more predictive of short-term incident coronary events than Framingham risk based on the observed age (McClelland et al., 2009).

According to recently published data, coronary artery calcification increases with higher total prednisone dose; by contrast, methotrexate and other csDMARDs do not influence coronary plaque progression (Karpouzas et al., 2020). Furthermore, DMARD and TNF-α antagonists are associated with reduced risk of myocardial infarction, stroke, and cardiovascular death (Micha et al., 2011; Westlake et al., 2011).

We could demonstrate neither positive nor negative effect of the applied drug therapy on the arterial aging process. It was somewhat surprising that anti-inflammatory drug therapy did not have a clear effect on the arterial aging process, in our present study. This could be explained by the relatively low number of patients and the limited period covered in the follow-up study. By contrast, in a recent study, another cardiovascular marker, vascular stiffness, significantly and consistently improved in RA patients, treated with biological or conventional synthetic DMARD therapy. RA has profound impact on the vasculature; already at time of the diagnosis, early RA patients have reduced vascular distensibility (Plein et al., 2020). Impaired endothelial function, a key event in the progression of atherosclerosis, was observed in RA. In addition to synovial lesions inflammation leads to vessel wall involvement as well. It was reported that endothelial dysfunction can be improved during anti–TNF-alpha therapy (Hürlimann et al., 2002). However, the limited study power prohibits to draw any definite conclusions regarding the

effect of statins and targeted therapies on arterial aging. There are other limitations of our work as well: most of our patients had moderate disease activity, and untreated patients with early disease were not included in this study.

CONCLUSION

RA significantly accelerates arterial aging; additionally to other risk factors, inflammation might be the pathophysiological link between RA and the increased calcification process. Further large-scale studies are needed to investigate the potential clinical benefit of CCS measurement in RA patients with risk factors for ischemic coronary heart disease.

DATA AVAILABILITY STATEMENT

The raw data supporting the conclusions of this article will be made available by the authors, without undue reservation.

ETHICS STATEMENT

The studies involving human participants were reviewed and approved by both national and institutional ethics committees. IF 567-4-2016. The patients/participants provided their written informed consent to participate in this study.

AUTHOR CONTRIBUTIONS

NM performed design of the study, data collection, first draft of the manuscript, and data interpretation; ZT performed design of the study, data collection, and data interpretation; LT performed statistical analysis; AB, AS, and AIN performed data collection; DB and PMH performed data interpretation; and BM and GN performed design of the study, manuscript preparation, and data analysis. All authors have approved the submitted version. All authors have agreed both to be personally accountable for the author's own contributions and to ensure that questions related to the accuracy or integrity of any part of the work, even ones in which the author was not personally involved, are appropriately investigated, resolved, and the resolution documented in the literature.

FUNDING

This publication was supported by the National Research, Development, and Innovation Office of Hungary (NVKP_16-1-2016-0017 National Heart Program) and by Hungarian Scientific Research Fund Grant K 131479. The authors are grateful for the investigators, the staff, and the participants of the MESA study. AI Nagy was supported by the János Bolyai Scholarship of the Hungarian Academy of Sciences.Thematic Excellence Programme (2020-4.1.1.-TKP2020) of the Ministry for Innovation and Technology in Hungary, within the framework of the Therapeutic Development and Bioimaging programmes of the Semmelweis University.

ACKNOWLEDGMENTS

We are grateful for the outstanding work of Zsófia Tarcza, ultrasound technician.

SUPPLEMENTARY MATERIAL

The Supplementary Material for this article can be found online at: https://www.frontiersin.org/articles/10.3389/fphar.2020.601344/full#supplementary-material

REFERENCES

Agatston, A. S., Janowitz, W. R., Hildner, F. J., Zusmer, N. R., Viamonte, M., and Detrano, R. (1990). Quantification of coronary artery calcium using ultrafast computed tomography. *J. Am. Coll. Cardiol.* 15 (4), 827–832. doi:10.1016/0735-1097(90)90282-t

Aletaha, D., Neogi, T., Silman, A. J., Funovits, J., Felson, D. T., Bingham, C. O., et al. (2010). 2010 rheumatoid arthritis classification criteria: an American College of Rheumatology/European League against Rheumatism collaborative initiative. *Ann. Rheum. Dis.* 69 (9), 1580–1588. doi:10.1136/ard.2010.13846

Arts, E. E., Fransen, J., Den Broeder, A. A., van Riel, P. L. C. M., and Popa, C. D. (2017). Low disease activity (DAS28≤3.2) reduces the risk of first cardiovascular event in rheumatoid arthritis: a time-dependent cox regression analysis in a large cohort study. *Ann. Rheum. Dis.* 76 (10), 1693–1699. doi:10.1136/annrheumdis-2016-210997

Aubry, M. C., Maradit-Kremers, H., Reinalda, M. S., Crowson, C. S., Edwards, W. D., and Gabrieland, S. E. (2007). Differences in atherosclerotic coronary heart disease between subjects with and without rheumatoid arthritis. *J. Rheumatol.* 34 (5), 937–942.

Baka, Z., Buzás, E., and Nagy, G. (2009). Rheumatoid arthritis and smoking: putting the pieces together. *Arthritis Res. Ther.* 11 (4), 238. doi:10.1186/ar2751

Berendsen, M. L. T., van Maaren, M. C., Arts, E. E. A., den Broeder, A. A., Popa, C. D., and Fransen, J. (2017). Anticyclic citrullinated peptide antibodies and rheumatoid factor as risk factors for 10-year cardiovascular morbidity in patients with rheumatoid arthritis: a large inception cohort study. *J. Rheumatol.* 44 (9), 1325–1330. doi:10.3899/jrheum.160670

Blaha, M. J., Cainzos-Achirica, M., Greenland, P., McEvoy, J. W., Blankstein, R., Budoff, M. J., et al. (2016). Role of coronary artery calcium score of zero and other negative risk markers for cardiovascular disease. *Circulation* 133 (9), 849–858. doi:10.1161/circulationaha.115.018524

Chung, C. P., Oeser, A., Avalos, I., Gebretsadik, T., Shintani, A., Raggi, P., et al. (2006). Utility of the Framingham risk score to predict the presence of coronary atherosclerosis in patients with rheumatoid arthritis. *Arthritis Res. Ther.* 8 (6), R186. doi:10.1186/ar2098

Crowson, C. S., Matteson, E. L., Roger, V. L., Therneau, T. M., and Gabriel, S. E. (2012). Usefulness of risk scores to estimate the risk of cardiovascular disease in patients with rheumatoid arthritis. *Am. J. Cardiol.* 110 (3), 420–424. doi:10.1016/j.amjcard.2012.03.044

Das, S., and Padhan, P. (2017). An overview of the extraarticular involvement in rheumatoid arthritis and its management. *J. Pharmacol. Pharmacother.* 8 (3), 81–86. doi:10.4103/jpp.JPP_194_16

Detrano, R., Guerci, A. D., Carr, J. J., Bild, D. E., Burke, G., Folsom, A. R., et al. (2008). Coronary calcium as a predictor of coronary events in four racial or ethnic groups. *N. Engl. J. Med.* 358 (13), 1336–1345. doi:10.1056/nejmoa072100

Fonseca, F. A., and Izar, M. C. (2016). High-sensitivity C-reactive protein and cardiovascular disease across countries and ethnicities. *Clinics* 71 (4), 235–242. doi:10.6061/clinics/2016(04)11

Gabay, C., McInnes, I. B., Kavanaugh, A., Tuckwell, K., Klearman, M., Pulley, J., et al. (2016). Comparison of lipid and lipid-associated cardiovascular risk marker changes after treatment with tocilizumab or adalimumab in patients with rheumatoid arthritis. *Ann. Rheum. Dis.* 75 (10), 1806–1812. doi:10.1136/annrheumdis-2015-207872

Giles, J. T., Szklo, M., Post, W., Petri, M., Blumenthal, R. S., Lam, G., et al. (2009). Coronary arterial calcification in rheumatoid arthritis: comparison with the multi-ethnic study of atherosclerosis. *Arthritis Res. Ther.* 11 (2), R36. doi:10.1186/ar2641

Giles, J. T., Wasko, M. C. M., Chung, C. P., Szklo, M., Blumenthal, R. S., Kao, A., et al. (2019). Exploring the lipid paradox theory in rheumatoid arthritis: associations of low circulating low-density lipoprotein concentration with subclinical coronary atherosclerosis. *Arthritis Rheum.* 71 (9), 1426–1436. doi:10.1002/art.40889

Greenland, P., Blaha, M. J., Budoff, M. J., Erbel, R., and Watson, K. E. (2018). Coronary calcium score and cardiovascular risk. *J. Am. Coll. Cardiol.* 72 (4), 434–447. doi:10.1016/j.jacc.2018.05.027

Hürlimann, D., Forster, A., Noll, G., Enseleit, F., Chenevard, R., Distler, O., et al. (2002). Anti-tumor necrosis factor-alpha treatment improves endothelial function in patients with rheumatoid arthritis. *Circulation* 106 (17), 2184–2187. doi:10.1161/01.cir.0000037521.71373.44

Jagpal, A., and Navarro-Millan, I. (2018). Cardiovascular co-morbidity in patients with rheumatoid arthritis: a narrative review of risk factors, cardiovascular risk assessment and treatment. *BMC Rheumatol* 2, 10. doi:10.1186/s41927-018-0014-y

Karpouzas, G. A., Malpeso, J., Choi, T.-Y., Li, D., Munoz, S., and Budoff, M. J. (2014). Prevalence, extent and composition of coronary plaque in patients with rheumatoid arthritis without symptoms or prior diagnosis of coronary artery disease. *Ann. Rheum. Dis.* 73 (10), 1797–1804. doi:10.1136/annrheumdis-2013-203617

Karpouzas, G. A., Ormseth, S. R., Hernandez, E., and Budoff, M. J. (2020). Impact of cumulative inflammation, cardiac risk factors, and medication exposure on coronary atherosclerosis progression in rheumatoid arthritis. *Arthritis Rheum.* 72 (3), 400–408. doi:10.1002/art.41122

Kawai, V. K., Chung, C. P., Solus, J. F., Oeser, A., Raggi, P., and Stein, C. M. (2015). Brief report: the ability of the 2013 American College of Cardiology/American Heart Association cardiovascular risk score to identify rheumatoid arthritis patients with high coronary artery calcification scores. *Arthritis Rheum.* 67 (2), 381–385. doi:10.1002/art.38944

Kondos, G. T., Hoff, J. A., Sevrukov, A., Daviglus, M. L., Garside, D. B., Devries, S. S., et al. (2003). Electron-beam tomography coronary artery calcium and cardiac events. *Circulation* 107 (20), 2571–2576. doi:10.1161/01.cir.0000068341.61180.55

Korley, F. K., Gatsonis, C., Snyder, B. S., George, R. T., Abd, T., Zimmerman, S. L., et al. (2017). Clinical risk factors alone are inadequate for predicting significant coronary artery disease. *J. Cardiovasc. Comput. Tomogr.* 11 (4), 309–316. doi:10.1016/j.jcct.2017.04.011

Lehker, A., and Mukherjee, D. (2020). Coronary calcium risk score and cardiovascular risk. *Curr. Vasc. Pharmacol.* 18. doi:10.2174/1570161118666200403143518.

Libby, P., Ridker, P. M., and Maseri, A. (2002). Inflammation and atherosclerosis. *Circulation* 105 (9), 1135–1143. doi:10.1161/hc0902.104353

Liu, J.-H., Ng, M.-Y., Cheung, T., Chung, H.-Y., Chen, Y., Zhen, Z., et al. (2017). Ten-year progression of coronary artery, carotid artery, and aortic calcification in patients with rheumatoid arthritis. *Clin. Rheumatol.* 36 (4), 807–816. doi:10.1007/s10067-016-3536-y

Løgstrup, B. B., Masic, D., Laurbjerg, T. B., Blegvad, J., Herly, M., Kristensen, L. D., et al. (2017). Left ventricular function at two-year follow-up in treatment-naive rheumatoid arthritis patients is associated with anti-cyclic citrullinated peptide antibody status: a cohort study. *Scand. J. Rheumatol.* 46 (6), 432–440. doi:10.1080/03009742.2016.1249941

Malik, S., Zhao, Y., Budoff, M., Nasir, K., Blumenthal, R. S., Bertoni, A. G., et al. (2017). Coronary artery calcium score for long-term risk classification in individuals with type 2 diabetes and metabolic syndrome from the multi-ethnic study of atherosclerosis. *JAMA Cardiol.* 2 (12), 1332–1340. doi:10.1001/jamacardio.2017.4191

Maradit-Kremers, H., Nicola, P. J., Crowson, C. S., Ballman, K. V., and Gabriel, S. E. (2005). Cardiovascular death in rheumatoid arthritis: a population-based study. *Arthritis Rheum.* 52 (3), 722–732. doi:10.1002/art.20878

McClelland, R. L., Chung, H., Detrano, R., Post, W., and Kronmal, R. A. (2006). Distribution of coronary artery calcium by race, gender, and age. *Circulation* 113 (1), 30–37. doi:10.1161/circulationaha.105.580696

McClelland, R. L., Nasir, K., Budoff, M., Blumenthal, R. S., and Kronmal, R. A. (2009). Arterial age as a function of coronary artery calcium (from the Multi-Ethnic Study of Atherosclerosis [MESA]). *Am. J. Cardiol.* 103 (1), 59–63. doi:10.1016/j.amjcard.2008.08.031

McInnes, I. B., and Schett, G. (2007). Cytokines in the pathogenesis of rheumatoid arthritis. *Nat. Rev. Immunol.* 7 (6), 429–442. doi:10.1038/nri2094

McInnes, I. B., and Schett, G. (2011). The pathogenesis of rheumatoid arthritis. *N. Engl. J. Med.* 365 (23), 2205–2219. doi:10.1056/nejmra1004965

Meissner, Y., Zink, A., Kekow, J., Rockwitz, K., Liebhaber, A., Zinke, S., et al. (2016). Impact of disease activity and treatment of comorbidities on the risk of myocardial infarction in rheumatoid arthritis. *Arthritis Res. Ther.* 18 (1), 183. doi:10.1186/s13075-016-1077-z

Micha, R., Imamura, F., Wyler von Ballmoos, I.M., Solomon, I.D. H., Hernán, I.M. A., Ridker, I.P. M., et al. (2011). Systematic review and meta-analysis of methotrexate use and risk of cardiovascular disease. *Am. J. Cardiol.* 108 (9), 1362–1370. doi:10.1016/j.amjcard.2011.06.054

Nagy, G., Németh, N., and Buzás, E. I. (2018). Mechanisms of vascular comorbidity in autoimmune diseases. *Curr. Opin. Rheumatol.* 30 (2), 197–206. doi:10.1097/bor.0000000000000483

Naranjo, A., Sokka, T., Descalzo, M. A., Calvo-Alén, J., Hørslev-Petersen, K., et al. (2008). Cardiovascular disease in patients with rheumatoid arthritis: results from the QUEST-RA study. *Arthritis Res. Ther.* 10 (2), R30. doi:10.1186/ar2383

Neves, P. O., Andrade, J., and Monção, H. (2017). Coronary artery calcium score: current status. *Radiol. Bras.* 50 (3), 182–189. doi:10.1590/0100-3984.2015.0235

Nurmohamed, M. T., Heslinga, M., and Kitas, G. D., Cardiovascular comorbidity in rheumatic diseases. *Nat. Rev. Rheumatol.* (2015). 11 (12), 693–704. doi:10.1038/nrrheum.2015.112

O'Malley, P. G., Taylor, A. J., Jackson, J. L., Doherty, T. M., and Detrano, R. C. (2000). Prognostic value of coronary electron-beam computed tomography for coronary heart disease events in asymptomatic populations. *Am. J. Cardiol.* 85 (8), 945–948. doi:10.1016/s0002-9149(99)00906-6

Ormseth, M. J., Chung, C. P., Oeser, A. M., Connelly, M. A., Sokka, T., Raggiand, P., et al. (2015). Utility of a novel inflammatory marker, GlycA, for assessment of rheumatoid arthritis disease activity and coronary atherosclerosis. *Arthritis Res. Ther.* 17, 117. doi:10.1186/s13075-015-0646-x

O'Rourke, R. A., Brundage, B. H., Froelicher, V. F., Greenland, P., Grundy, S. M., Hachamovitch, R., et al. (2000). American College of Cardiology/American Heart Association Expert Consensus document on electron-beam computed tomography for the diagnosis and prognosis of coronary artery disease. *Circulation* 102 (1), 126–140. doi:10.1161/01.cir.102.1.126

Plein, S., Erhayiem, B., Fent, G., Horton, S., Dumitru, R. B., Andrews, J., et al. (2020). Cardiovascular effects of biological versus conventional synthetic disease-modifying antirheumatic drug therapy in treatment-naïve, early rheumatoid arthritis. *Ann. Rheum. Dis.* 79, 1414–1422. doi:10.1136/annrheumdis-2020-217653

Prete, M., Racanelli, V., Digiglio, L., Vacca, A., Dammacco, F., and Perosa, F. (2011). Extra-articular manifestations of rheumatoid arthritis: an update. *Autoimmun. Rev.* 11 (2), 123–131. doi:10.1016/j.autrev.2011.09.001

Raggi, P., Callister, T. Q., Cooil, B., He, Z.-X., Lippolis, N. J., Russo, D. J., et al. (2000). Identification of patients at increased risk of first unheralded acute myocardial infarction by electron-beam computed tomography. *Circulation* 101 (8), 850–855. doi:10.1161/01.cir.101.8.850

Raggi, P., Cooil, B., Shaw, L. J., Aboulhson, J., Takasu, J., Budoff, M., et al. (2003). Progression of coronary calcium on serial electron beam tomographic scanning

is greater in patients with future myocardial infarction. *Am. J. Cardiol.* 92 (7), 827–829. doi:10.1016/s0002-9149(03)00892-0

Raggi, P., Shaw, L. J., Berman, D. S., and Callister, T. Q. (2004). Prognostic value of coronary artery calcium screening in subjects with and without diabetes. *J. Am. Coll. Cardiol.* 43 (9), 1663–1669. doi:10.1016/j.jacc.2003.09.068

R Core Team (2017). *A language and environment for statistical computing*. Vienna, Austria: R Core Team.

Roubille, C., Richer, V., Starnino, T., McCourt, C., McFarlane, A., Fleming, P., et al. (2015). The effects of tumour necrosis factor inhibitors, methotrexate, non-steroidal anti-inflammatory drugs and corticosteroids on cardiovascular events in rheumatoid arthritis, psoriasis and psoriatic arthritis: a systematic review and meta-analysis. *Ann. Rheum. Dis.* 74 (3), 480–489. doi:10.1136/annrheumdis-2014-206624

Sabatine, M. S., Morrow, D. A., de Lemos, J. A., Omland, T., Desai, M. Y., Tanasijevic, M., et al. (2004). Acute changes in circulating natriuretic peptide levels in relation to myocardial ischemia. *J. Am. Coll. Cardiol.* 44 (10), 1988–1995. doi:10.1016/j.jacc.2004.07.057

Sattar, N., McCarey, D. W., Capell, H., and McInnes, I. B. (2003). Explaining how "high-grade" systemic inflammation accelerates vascular risk in rheumatoid arthritis. *Circulation* 108 (24), 2957–2963. doi:10.1161/01.cir.0000099844.31524.05

Shaw, L. J., Raggi, P., Callister, T. Q., and Berman, D. S. (2006). Prognostic value of coronary artery calcium screening in asymptomatic smokers and non-smokers. *Eur. Heart J.* 27 (8), 968–975. doi:10.1093/eurheartj/ehi750

Shaw, L. J., Raggi, P., Schisterman, E., Berman, D. S., and Callister, T. Q. (2003). Prognostic value of cardiac risk factors and coronary artery calcium screening for all-cause mortality. *Radiology* 228 (3), 826–833. doi:10.1148/radiol.2283021006

Turesson, C., McClelland, R. L., Christianson, T. J. H., and Matteson, E. L. (2006). Multiple extra-articular manifestations are associated with poor survival in patients with rheumatoid arthritis. *Ann. Rheum. Dis.* 65 (11), 1533–1534. doi:10.1136/ard.2006.052803

Wahlin, B., Innala, L., Magnusson, S., Möller, B., Smedby, T., Rantapää-Dahlqvist, S., et al. (2019). Performance of the expanded cardiovascular risk prediction score for rheumatoid arthritis is not superior to the ACC/AHA risk calculator. *J. Rheumatol.* 46 (2), 130–137. doi:10.3899/jrheum.171008

Westlake, S. L., Colebatch, A. N., Baird, J., Curzen, N., Kiely, P., Quinn, M., et al. (2011). Tumour necrosis factor antagonists and the risk of cardiovascular disease in patients with rheumatoid arthritis: a systematic literature review. *Rheumatology* 50 (3), 518–531. doi:10.1093/rheumatology/keq316

Wickham, H. (2016). *ggplot2: elegant graphics for data analysis*. Cham, Switzerland: Springer International Publishing AG.

Wong, N. D., Budoff, M. J., Pio, J., and Detrano, R. C. (2002). Coronary calcium and cardiovascular event risk: evaluation by age- and sex-specific quartiles. *Am. Heart J.* 143 (3), 456–459. doi:10.1067/mhj.2002.120409

Yousuf, O., Mohanty, B. D., Martin, S. S., Joshi, P. H., Blaha, M. J., Nasir, K., et al. (2013). High-sensitivity C-reactive protein and cardiovascular disease. *J. Am. Coll. Cardiol.* 62 (5), 397–408. doi:10.1016/j.jacc.2013.05.016

Conflict of Interest: The authors declare that the research was conducted in the absence of any commercial or financial relationships that could be construed as a potential conflict of interest.

GLOSSARY

aCCP: anti-cyclic citrullinated peptide
AMI: acute myocardial infarction
CAC: coronary artery calcium
CCS: coronary calcium scores
CI: confidence interval
CRP: C-reactive protein
CT: computed tomography
CV: cardiovascular
CVE: cardiovascular event
DAS28: disease activity score-28
DMARD: disease-modifying antirheumatic drugs
ECG: electrocardiography
ESR: erythrocyte sedimentation rate
HDL: high-density lipoprotein
IL-6: interleukin-6
LOWESS: locally weighted scatterplot smoothing
MESA: multi-ethnic study of atherosclerosis
NSAID: nonsteroidal anti-inflammatory drug
NTproBNP: N-terminal pro-hormone B-type natriuretic peptide
RA: rheumatoid arthritis
RF: rheumatoid factor
TNF: tumor necrosis factor

frontiers in Pharmacology

ORIGINAL RESEARCH
published: 30 November 2020
doi: 10.3389/fphar.2020.590144

Deletion of Protocadherin Gamma C3 Induces Phenotypic and Functional Changes in Brain Microvascular Endothelial Cells *In Vitro*

*Lydia Gabbert, Christina Dilling, Patrick Meybohm and Malgorzata Burek**

Department of Anaesthesia and Critical Care, University of Würzburg, Würzburg, Germany

Inflammation of the central nervous system (CNS) is associated with diseases such as multiple sclerosis, stroke and neurodegenerative diseases. Compromised integrity of the blood-brain barrier (BBB) and increased migration of immune cells into the CNS are the main characteristics of brain inflammation. Clustered protocadherins (Pcdhs) belong to a large family of cadherin-related molecules. Pcdhs are highly expressed in the CNS in neurons, astrocytes, pericytes and epithelial cells of the choroid plexus and, as we have recently demonstrated, in brain microvascular endothelial cells (BMECs). Knockout of a member of the Pcdh subfamily, PcdhgC3, resulted in significant changes in the barrier integrity of BMECs. Here we characterized the endothelial PcdhgC3 knockout (KO) cells using paracellular permeability measurements, proliferation assay, wound healing assay, inhibition of signaling pathways, oxygen/glucose deprivation (OGD) and a pro-inflammatory cytokine tumor necrosis factor alpha (TNFα) treatment. PcdhgC3 KO showed an increased paracellular permeability, a faster proliferation rate, an altered expression of efflux pumps, transporters, cellular receptors, signaling and inflammatory molecules. Serum starvation led to significantly higher phosphorylation of extracellular signal-regulated kinases (Erk) in KO cells, while no changes in phosphorylated Akt kinase levels were found. PcdhgC3 KO cells migrated faster in the wound healing assay and this migration was significantly inhibited by respective inhibitors of the MAPK-, β-catenin/Wnt-, mTOR- signaling pathways (SL327, XAV939, or Torin 2). PcdhgC3 KO cells responded stronger to OGD and TNFα by significantly higher induction of interleukin 6 mRNA than wild type cells. These results suggest that PcdhgC3 is involved in the regulation of major signaling pathways and the inflammatory response of BMECs.

Keywords: blood-brain barrier, protocadherin gamma C3, inflammation, oxygen/glucose deprivation, stroke, tumor necrosis factor-α, proliferation

OPEN ACCESS

Edited by:
Imola Wilhelm,
Biological Research Centre, Hungary

Reviewed by:
Maria A. Deli,
Biological Research Centre, Hungary
Sergey V. Ryzhov,
Maine Medical Center, United States
Reiner Haseloff,
Leibniz-Institut für Molekulare Pharmakologie (FMP), Germany

****Correspondence:***
Malgorzata Burek
Burek_M@ukw.de

Specialty section:
This article was submitted to Inflammation Pharmacology, a section of the journal Frontiers in Pharmacology

Received: *31 July 2020*
Accepted: *09 November 2020*
Published: *30 November 2020*

Citation:
Gabbert L, Dilling C, Meybohm P and Burek M (2020) Deletion of Protocadherin Gamma C3 Induces Phenotypic and Functional Changes in Brain Microvascular Endothelial Cells In Vitro. *Front. Pharmacol. 11:590144. doi: 10.3389/fphar.2020.590144*

INTRODUCTION

Inflammation is one of the characteristics of CNS disorders. During ischemic stroke, increased levels of pro-inflammatory cytokines are associated with damage to the blood-brain barrier (BBB) (Hotter et al., 2019; Ittner et al., 2020). The BBB is formed by endothelial cells surrounded by pericytes, a basement membrane and astrocytes. Endothelial cells are connected by tight junctions that maintain BBB integrity and regulate paracellular transport from blood to the brain (Abbott, 2013; Wong et al., 2013).

Protocadherins (Pcdhs) with more than 80 members constitute the largest subgroup of the cadherin superfamily, which mediate calcium-dependent cell-cell adhesion. Sano et al. first discovered this large group of cadherin-related molecules with cadherin-like extracellular (EC) but distinct cytoplasmatic domains (Sano et al., 1993; Nollet et al., 2000). While classical cadherins mediate strong cell-cell adhesion, Pcdhs are both adhesive and repulsive (Phillips et al., 2017). Pcdhs can be divided into clustered Pcdhs (α-Pcdhs, β-Pcdhs, γ-Pcdhs) organized in three tandem arrays on mouse chromosome 18 and human chromosome 5, and non-clustered δ-Pcdhs, which are scattered throughout the genome (Weiner and Jontes, 2013). Pcdhs are strongly expressed in the CNS and promote neuronal development and survival. They have been described in astrocytes, pericytes, choroid plexus epithelial cells and in brain microvascular endothelial cells (BMECs) (Garrett et al., 2012; Lobas et al., 2012; Dilling et al., 2017). Pcdhs play a critical role in cell survival (Peek et al., 2017), neuronal differentiation and migration (Weiner and Jontes, 2013), synapse development (Garrett et al., 2012) and dendritic morphogenesis (Suo et al., 2012; Molumby et al., 2017). In addition, they have also been characterized in kidney, lung and colon cells and show effects on both tumor suppressive and progressive functions during malignant cell growth (Okazaki et al., 2002; Dallosso et al., 2009; Zhou et al., 2017).

γ-Pcdh gene clusters contain variable exons which encode the cadherin-like extracellular domains, the transmembrane domain and the variable cytoplasmatic domain. γ-Pcdhs also have three C-like variable exons that are expressed in neurons (Kaneko et al., 2006; Phillips et al., 2017). Mice lacking one of the γ-Pcdh-C3, C4 or C5 isoforms died due to neuronal apoptosis, similar to mice lacking all γ-Pcdhs, suggesting that these C-type-isoforms play a special role in the neuronal survival (Chen et al., 2012; Peek et al., 2017; Miralles et al., 2020).

A member of the Pcdh subfamily, PcdhgC3, is the only isoform that inhibits β-catenin/Wnt- and mTOR-signalling pathways in colorectal cancer, and is a potential tumor suppressor (Dallosso et al., 2012; Mah et al., 2016; Mah and Weiner, 2017). We recently described the expression of γ-Pcdhs in BMECs and showed that the deletion of PcdhgC3 resulted in reduced barrier integrity and changes in gene expression in BMECs (Dilling et al., 2017). Here, we hypothesized that PcdhgC3, similar to cancer cells and neurons, plays a role in multiple signaling pathways in BMECs that lead to functional changes. To investigate this, we used a BMEC PcdhgC3 KO in functional tests such as paracellular permeability measurement, proliferation, wound healing assay, response to signaling pathway inhibitors, oxygen/glucose deprivation (OGD) and TNFα. Our results help to further uncover the role of PcdhgC3 in endothelial cell biology by pointing out its importance for signaling processes at the BBB.

MATERIAL AND METHODS

Chemicals

Stock solutions of the inhibitors SL327 (Mek1/2 inhibitor, 200 nM; Sigma-Aldrich), Torin 2 (mTOR-inhibitor, 25 nM; Sigma-Aldrich) and XAV939 (selective β-catenin/Wnt pathway inhibitor, 20 μM; Sigma-Aldrich), were prepared in DMSO and diluted to the final concentration in cell culture medium. TNFα (Sigma-Aldrich) was dissolved in cell culture medium to a working concentration of 10 nM.

Cell Culture

Mouse brain microvascular endothelial cell line, cerebEND was isolated and immortalized as previously described (Silwedel and Forster, 2006; Burek et al., 2012; Helms et al., 2016). To generate the PcdhgC3 knockout, cerebEND cells were co-transfected with Pcdh2 CRISPR/Cas9 and Pcdh2 HDR vectors (sc-430015 and sc-430015-HDR, Santa Cruz Biotechnology) using Effectene Transfection Reagent (Qiagen). The positive clones were selected with 3 μg/ml puromycin for 4 weeks (Dilling et al., 2017). The cells were grown on gelatin-coated plates in DMEM supplemented with 10% fetal calf serum (FCS). The cells were treated with 10 nM TNFα for 24 h and harvested for qPCR analysis.

Permeability Measurement

Wild type (WT) and PcdhgC3 knockout (KO) cerebEND cells were grown on gelatin-coated transwells (pore size 0.4 μm, Corning) for 6 days. The permeability assay was performed as previously described (Curtaz et al., 2020) using 1 μM fluorescein (376 kDa, Sigma-Aldrich) for 1 h with aliquots taken from the basolateral compartment every 20 min. A parallel assay with cell-free transwells was used to calculate the endothelial permeability coefficient (Pe). The Pe of KO cells was normalized to WT cells.

Proliferation Assay

The proliferation assay was performed using a 5′-bromo-2′-deoxyuridine (BrdU) Cell Proliferation Assay ELISA Kit (Merck) according to the manufacturer's instructions. WT and KO cerebEND cells (5×10^3 cells) suspended in 100 μL culture medium were seeded in gelatin-coated 96-well plate. After the cells attached, the BrdU Label solution was added and the cells were allowed to grow for 24 h. The absorbance was measured using a spectrophotometric plate reader (Tecan) at dual wavelengths of 450 and 540 nm.

In Vitro Stroke Model, Oxygen/Glucose Deprivation

Confluent WT or KO cells were serum-starved for 24 h (1% charcoal stripped FCS). For OGD, the medium was exchanged for glucose-free DMEM and the incubation in a 1% O_2 incubator was carried out for 4 h, as described previously (Burek et al., 2019). Normoxic control cells were only subjected to a complete medium exchange.

Quantitative Polymerase Chain Reaction

Quantitative PCR was performed as previously described (Kaiser et al., 2018). Briefly, total RNA was isolated from cells using the Nucleospin RNA Isolation Kit (Macherey-Nagel) according to the manufacturer's instructions. We used a High Capacity cDNA Revers Transcription Kit (Thermo Fisher Scientific) for cDNA synthesis and TaqMan Fast Advanced Master Mix in StepOnePlus Real-Time PCR System (Thermo Fisher Scientific) for quantitative PCR. Commercially available TaqMan Gene Expression Assays were used (Thermo Fisher Scientific). Calnexin and 18S-RNA were used as endogenous controls. Relative expression was calculated using the comparative Ct method.

Western Blot

Western blot was performed as previously described (Burek et al., 2019; Curtaz et al., 2020). Primary antibodies were diluted in phosphate-buffered saline (PBS) containing 1% bovine serum albumin (BSA). The following primary antibodies were used: rat anti-Bcrp (1:1,000, Abcam #Ab-24114), mouse anti-Glut-1 (1: 200, Millipore #07–1401), rabbit anti-Lrp1 (1:1,000, Abcam #Ab92544), mouse anti-Mrp1 (1:1,000, Millipore #MAB4100), rat anti-Mrp4 (1:1,000, Enzo Life Science #ALX-801–039-C100), mouse anti-Tfrc (Transferrin Receptor, 1:500, Thermo Fisher Scientific #13–6,800), goat anti-RAGE (1:200, Santa Cruz #sc-8230), rabbit anti-PcdhgC3 (1: 10,000 (Frank et al., 2005)), mouse anti-p44/42 MAPK (Erk1/2) (1:2,000, Cell Signaling #9107), rabbit anti-phospho-Erk1/2 (1:2,000, Cell Signaling #4370), rabbit anti-Akt (1:1,000, Cell Signaling #9272) and rabbit anti-phospho Akt (1:1,000, Cell Signaling #4058). After incubation with respective secondary antibodies, images were taken using an Enhanced Chemiluminescence solution and FluorChem FC2 Multi-Imager II (Alpha Innotech). The intensity of the protein bands was estimated using the ImageJ software.

Enzyme-Linked Immunosorbent Assay

The cell culture medium was collected and kept frozen at −80°C until use. Ccl2/Mcp-1 and Ccl5/RANTES Quantikine ELISA Kit (R&D Systems) were performed according to the manufacturer's protocol.

Wound Healing Assay

The wound healing assay was performed as previously described (Blecharz-Lang et al., 2018a). Briefly, cells were seeded on µ-Dish (Ibidi GmbH) and grown to confluence. After 24 h of serum starvation, the cells were left untreated or were treated for 48 h with MAPK-, β-catenin/Wnt-, mTOR-signaling pathway inhibitors (SL327, XAV939, and Torin 2) in triplicates. The wells separating the cells were removed and the dishes were photographed at time 0 h. The cells were allowed to grow in a 500-µm-space for 48 h and were photographed again at 48 h using a Keyence BZ9000 microscope (Keyence). The difference in area covered between 0 and 48 h was calculated and a migration rate was normalized to the control, which was set arbitrarily to 1.

Statistical Analysis

GraphPad Prism 7 (GraphPad Software) was used for statistical analysis. The data are expressed as the mean ± standard deviation. Unpaired *t* test was used to compare two groups while two-way ANOVA with Tukey's multiple comparison test was used to compare WT and KO cells with or without treatment. Statistical significance was assumed at $p < 0.05$ (*).

RESULTS

C-Terminal Truncated Fragment of PcdhgC3 Shows Higher Level in Confluent Brain Microvascular Endothelial Cells

The C-terminus of γ-Pcdhs is cleaved by presenilin and the resulting intracellular fragment can be localized to the nucleus and have potential signaling functions (Haas et al., 2005). Interestingly, the 25 kDa C-terminal truncated fragment of PcdhgC3 is enriched in confluent BMECs and shows significantly lower level in non-confluent BMECs, which is opposite to the full-length protein (**Figures 1A–C**). Confluent BMECs build a tight monolayer. This is accompanied by multiple changes in gene and protein expression and intracellular signal transmission. Pcdhs play a role in contact inhibition of cell proliferation and are potential candidates for tumor suppressors (Okazaki et al., 2002; Yu et al., 2008). The increase in the cleaved PcdhgC3 fragment specifically in confluent BMECs suggests a distinct role for this fragment in processes such as cell proliferation, but the exact mechanisms in BMECs have yet to be investigated.

PcdhgC3 Knockout Cells Show Increased Paracellular Permeability, Proliferation and Changes in Protein and Gene Expression

We measured and compared the proliferation rate of WT and KO cells by BrdU incorporation into newly synthesized DNA (**Figure 2A**). The PcdhgC3 KO cells proliferated 2.46 ± 0.1 fold faster than the WT cells, suggesting the role of PcdhgC3 in endothelial cell proliferation. Increased proliferation leads to more dedifferentiated phenotype and lower barrier properties. We therefore measured the paracellular permeability for fluorescein in WT and KO cells (**Figure 2B**). Consistent with previous results (Dilling et al., 2017), PcdhgC3 KO cells showed an increase in permeability of 45% ± 14.7 compared to WT cells (**Figure 2B**). Next, we tested the effects of PcdhgC3 KO on gene expression of endothelial and BBB markers as well as on genes involved in inflammatory and signaling pathways (**Figure 3**). A comparison of gene expression between WT and KO cells showed increased expression of the efflux pump Abcb1b (P-Glycoprotein, ATP Binding Cassette Subfamily B Member 1) and a significantly reduced Abcb1a (P-Glycoprotein, ATP binding cassette subfamily B member 1a), Abcc1 (Mrp1, Multidrug resistance associated protein 1) and Abcc5 (ATP binding cassette subfamily C member 5) expression (**Figure 3A**). Among the solute carrier transporters analyzed, the Slc9a1 (Nhe1, Cation proton antiporter 1) was significantly increased, while Slc2a1 (Glucose transporter type 1), Slc7a1 (Cat1, Cationic amino acid transporter 1), Slc7a5 (Lat1, L-Type amino acid transporter 1) and Slc16a1 (Mct1, Monocarboxylic acid transporter 1) were downregulated (**Figure 3B**). Among the cellular receptors, PcdhgC3 KO showed increased RAGE (Receptor for Advanced Glycosylation End Products) level and decreased Lrp1 (Low-density lipoprotein receptor-related protein 1) and Tfrc (Transferrin receptor) expression (**Figure 3C**). Transcription factors such as Sox18 (SRY-Box transcription factor 18) and Tgfb1 (Transforming growth factor beta 1) were significantly increased in PcdhgC3 KO (**Figure 3D**). Genes involved in the β-catenin/Wnt-signaling pathway, Axin2 and Ctnnb1 (Catenin Beta 1) were upregulated, similar to genes involved in the Notch-signaling pathway (Dll4, Delta like canonical Notch ligand 4) and the sonic hedgehog signal transduction cascade (Gli1, Gli Family zinc finger 1) (**Figure 3D**). Interestingly, all of the inflammatory mediators

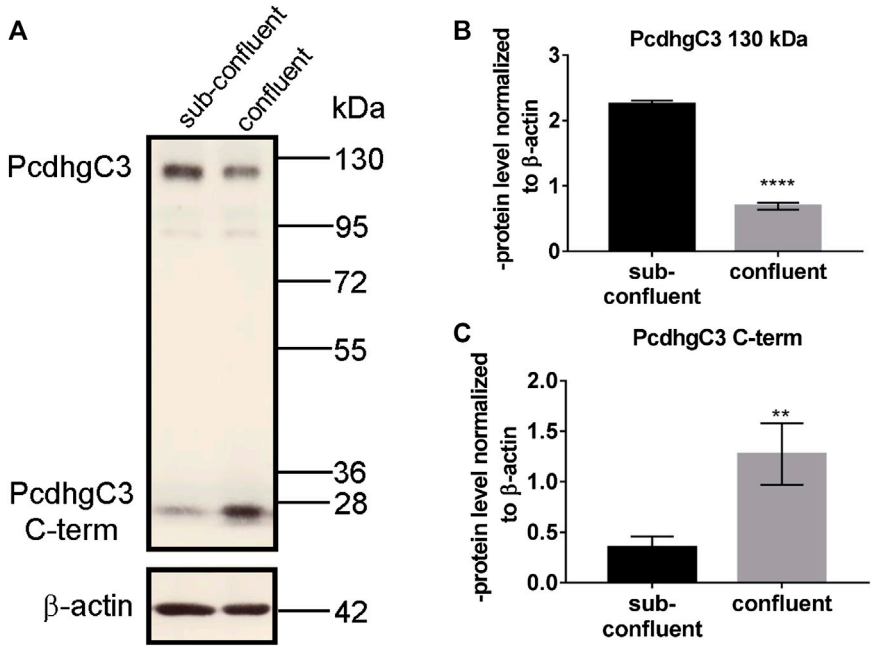

FIGURE 1 | C-terminal fragment of PcdhgC3 accumulates in confluent Brain Microvascular Endothelial Cells. BMECs were seeded on gelatin-coated plates and were grown for 2 or 7 days followed by protein extraction and Western blot. PcdhgC3 protein level was analyzed by Western blot **(A)** and the bands corresponding to the full-length protein (130 kDa) **(B)** and truncated C-terminal fragment of PcdhgC3 (25 kDa) **(C)** were analyzed by densitometry. Data are shown as mean ± standard deviation of three independent experiments. $^{**}p < 0.01$, $^{****}p < 0.0001$.

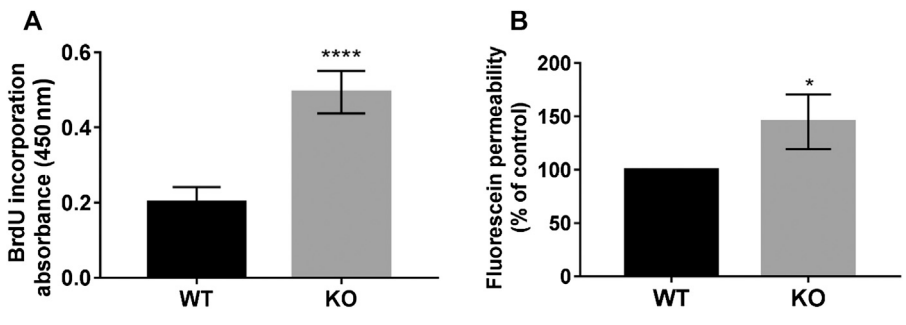

FIGURE 2 | PcdhgC3 knockout cells show increased proliferation and paracellular permeability. **(A)** The proliferation rate of WT and KO cells was measured using BrdU ELISA Kit at 16 h. **(B)** Wild type (WT) and PcdhgC3 knockout (KO) cells were grown in transwells for 6 days followed by measuring the paracellular permeability for fluorescein. Paracellular permeability of KO cells was normalized to WT cells, which was set as 100%. Data are shown as mean ± standard deviation of three independent experiments. $^{*}p < 0.05$, $^{****}p < 0.0001$.

tested, Ccl2 (C-C motif chemokine ligand 2), Ccl5 (C-C motif chemokine ligand 5), Ccl7 (C-C motif chemokine ligand 7), Csf3 (Colony stimulating factor 3), Cxcl10 (C-X-C motif chemokine ligand 10), Tlr4 (Toll like receptor 4) were downregulated in PcdhgC3 KO cells (**Figure 3E**). We analyzed the protein levels of selected transporter and cellular receptors (**Figure 3F**). We detected a significant increase in Lrp1, RAGE, Tfrc and Glut1 proteins. This was opposite to the corresponding mRNA level in KO cells. The Bcrp protein level was significantly downregulated in PcdhgC3 KO cells. Ccl2 and Ccl5 showed a decreased protein level consistently with the mRNA level (**Figure 3G**). Next, we tested the activation of the signaling pathways using antibodies against phosphorylated active kinases Akt and Erk (**Figure 4**). We used the serum starvation of the cells as a trigger for the activation of the signaling pathways. The WT and KO cells were harvested 24 h after serum reduction. Under these conditions, Akt showed no differences between WT and KO cells (**Figure 4A**), while significantly increased phospho-Erk level was detected in PcdhgC3 KO cells, which indicates a strong activation of this signaling pathway (**Figure 4B**).

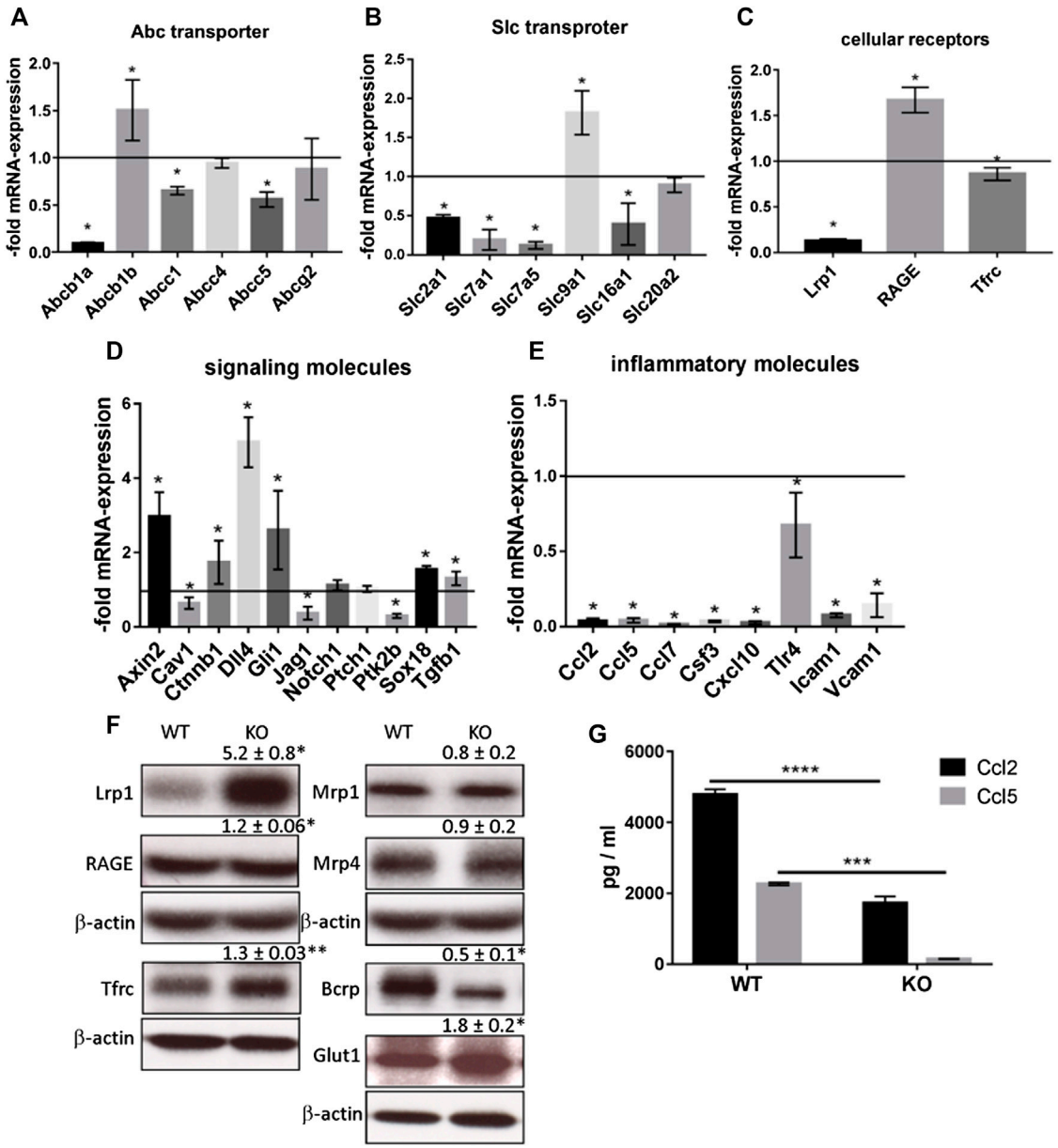

FIGURE 3 | Brain Microvascular Endothelial Cells lacking PcdhgC3 show differential gene and protein expression. Wild type and PcdhgC3 knockout BMECs were grown to confluence, serum-starved for 24 h and harvested for RNA or protein extraction. Target gene expression of Abc transporter **(A)**, Slc transporter **(B)**, cellular receptors **(C)**, signaling molecules **(D)** and inflammatory molecules **(E)**, was normalized to endogenous control and shown as fold over control (wild type cells), which was arbitrarily set as 1 (control level marked in graph). **(F)** Protein expression of selected Abc transporter (Bcrp, Mrp1, Mrp4), Slc transporter (Glut1), cellular receptors (Lrp1, RAGE, Tfrc) was analyzed by Western blot. Protein expression was normalized to β-actin and to WT cells. The densitometry values are given above the corresponding bands. **(G)** Protein levels of Ccl2 and Ccl5 were analyzed by ELISA in cell culture medium of WT and KO cells. Data are shown as mean ± standard deviation of three independent experiments. $^{*}p < 0.05$, $^{**}p < 0.01$, $^{***}p < 0.001$, $^{****}p < 0.0001$. Abbreviations **(A)** Abcb1a: P-Glycoprotein, ATP binding cassette subfamily B member 1A, Abcb1b: P-Glycoprotein, ATP binding cassette subfamily B member 1, Abcc1: Mrp1, Multidrug resistance associated protein 1, Abcc4: Mrp4, Multidrug resistance associated protein 4, Abcc5: ATP binding cassette subfamily C member 5, Abcg2: BCRP, Breast cancer resistance protein **(B)** Slc2a1: Solute carrier family 2 member 1, Glut1, Glucose transporter type 1, Slc7a1: Solute carrier family 7 member 1, Cat1, Cationic amino acid transporter 1, Slc7a5: Solute carrier family 7 member 5, Lat1, L-Type amino acid transporter 1), Slc9a1: Solute carrier family 9 member 1, Nhe1, Cation proton antiporter 1, Slc16a1: Solute carrier family 16 member 1, Mct1, Monocarboxylate transporter 1, Slc20a2: Solute carrier family 20 member 2, Pit2, Phosphate transporter 2 **(C)** Lrp1: Low density lipoprotein receptor-related protein 1, RAGE: Receptor for Advanced Glycosylation End Products, Tfrc: Transferrin receptor **(D)** Cav1: Caveolin 1, Ctnnb1: Catenin beta 1, Dll4: Delta like canonical Notch ligand 4, Gli1: Family zinc finger 1, Jag1: Jagged canonical Notch ligand 1, Notch1: Notch receptor 1, Ptch1: Patched 1, Ptk2b: Protein tyrosine kinase 2 beta, Sox18: SRY-Box transcription factor 18, Tgfb1: Transforming growth factor beta 1 **(E)** Ccl2, 5, 7: C-C motif chemokine ligand 2, 5,7, Csf3: Colony stimulating factor 3, Cxcl10: C-X-C motif chemokine ligand 10, Tlr4: Toll like receptor 4, Icam1: Intercellular adhesion molecule 1, Vcam1: Vascular cell adhesion molecule 1.

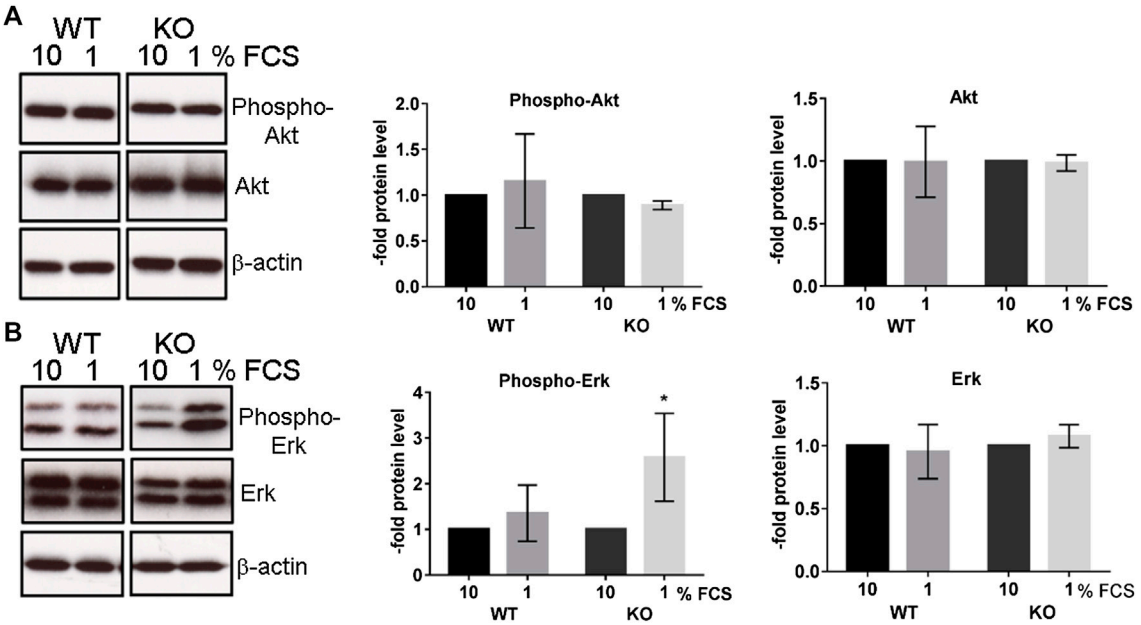

FIGURE 4 | Serum-starved PcdhgC3 knockout cells show higher phosphorylation of extracellular signal-regulated kinases (Erk). Wild type (WT) and PcdhgC3 knockout (KO) BMECs were grown to confluence, serum-starved (1% FCS) or not (10% FCS) for 24 h and harvested for protein extraction and Western blot analysis. **(A)** Phosphorylated (Phospho-Akt) and total Akt **(B)** phosphorylated Erk (Phospho-Erk) and total Erk were detected with specific antibodies. The protein levels were analyzed by densitometry. Data are shown as mean ± standard deviation of three independent experiments. *$p < 0.05$.

Knockout of PcdhgC3 Leads to a Higher Migration Rate of Brain Microvascular Endothelial Cells, Which Is Mediated by MAPK-, β-Catenin/Wnt- and mTOR-Signaling Pathways

The increased activation of Erk in PcdhgC3 KO cells indicates the activation of signaling pathways that are involved in cell proliferation, differentiation, aging and survival (Steelman et al., 2011). We therefore tested the migration rate of WT and KO cells in a wound healing assay (**Figure 5**). KO cells migrated significantly faster than the WT cells (**Figures 5A,B**). This faster migration of KO cells was blocked by MAPK-, β-catenin/Wnt- and mTOR-pathways inhibitors. KO cells treated with inhibitors of the key signaling pathways showed a significantly lower migration rate compared to untreated KO cells (**Figure 5B**).

PcdhgC3 KO Cells Respond Stronger to Oxygen/Glucose Deprivation and to Tumor Necrosis Factor Alpha Treatment

Increased activation of the MAPK-signaling pathway is observed in stroke, Alzheimer's disease and multiple sclerosis. It contributes to decreased BBB integrity and production of pro-inflammatory mediators in the brain (Abbott et al., 2010; Maddahi and Edvinsson, 2010). We tested the response of WT and KO BMECs to OGD treatment. The cells were kept under OGD for 4 h (**Figures 6A,B**). The induction of Vegf in WT and KO cells after 4 h of OGD confirmed our experimental OGD settings, since Vegf is known as a hypoxic marker at the BBB (Zhang et al., 2000). The induction of Vegf was significantly higher in KO cells than in WT cells (**Figure 6A**). OGD treatment resulted in an increased Il6 expression in WT and KO cell and the increase was significantly higher in KO than in WT cells (**Figure 6B**). Next, we tested the response to TNFα treatment of WT and KO cells (**Figures 6C,D**). TNFα treatment led to the induction of Il6 (**Figure 6C**) and Icam1 (**Figure 6D**). The induction of Il6 was higher in KO cells, while the induction of Icam1 was lower in KO cells compared to WT cells. Thus, the deletion of PcdhgC3 alters the inflammatory response of BMECs suggesting a central role of PcdhgC3 in the vascular inflammatory phenotype.

DISCUSSION

The high expression of Pcdhs in BMECs suggests their specific intracellular role in vascular endothelial cells. Here, we further characterized the role of a member of the Pcdh subfamily, PcdhgC3, by showing its involvement in intracellular signaling and the inflammatory response.

The C-terminus of Pcdhs could have a cell surface receptor signaling function regulated by proteolytic events (Haas et al., 2005). We show here that the truncated C-terminus of PcdhgC3 is enriched in confluent BMECs. This is in line with reports showing a tumor suppressor role of Pcdhs, as they play a role in the contact inhibition of cell proliferation (Okazaki et al., 2002; Yu et al., 2008). This fragment could be responsible for signal transduction in confluent BMECs, but the exact regulation

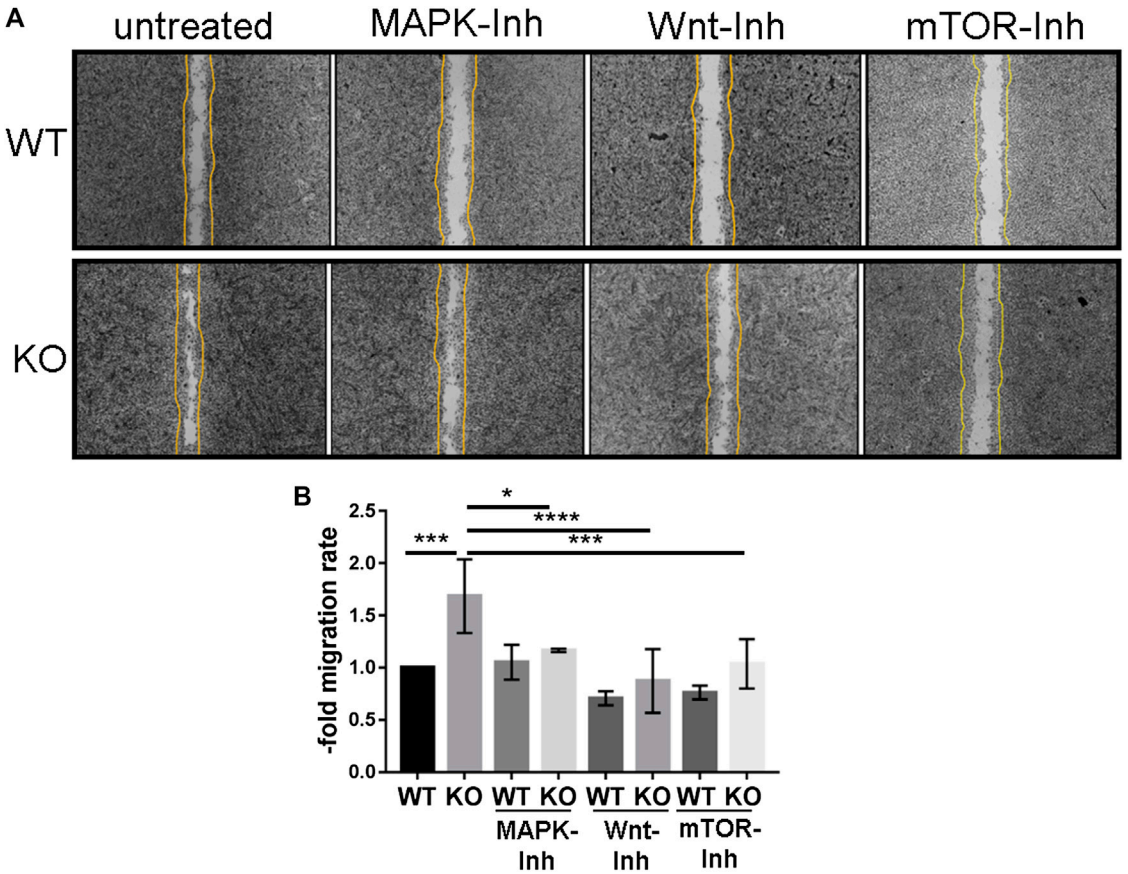

FIGURE 5 | PcdhgC3 knockout Brain Microvascular Endothelial Cells migrate faster in wound healing assay and their migration can be inhibited by specific MAPK-, β-catenin/Wnt- and mTOR-signaling pathway inhibitors. Wild type (WT) and PcdhgC3 knockout (KO) BMECs were seeded on μ-Dish and were grown to confluence. After 24 h serum starvation, the cells were left untreated or were treated with MAPK- (SL327, Mek1/2 inhibitor, 200 nM), Wnt- (XAV939, selective β-catenin/Wnt pathway inhibitor, 20 μM), mTOR- (Torin 2, mTOR-inhibitor, 25 nM) signaling pathways inhibitors (MAPK-Inh, Wnt-Inh, mTOR-Inh). The wells separating the cells were removed and the dishes were photographed at time 0 h. The cells were allowed to grow for 48 h into a 500-μm-space and were photographed again at 48 h. **(A)** The difference in area covered between 0 and 48 h was calculated and a migration rate was normalized to the control, which was arbitrarily set as 1. **(B)** Data are shown as mean ± standard deviation of three independent experiments. $^{*}p < 0.05$, $^{**}p < 0.01$.

mechanism must be determined in further experiments using e.g., specific inhibitors of presenilin or PcdhgC3 mutants and their effect on signaling cascades in BMECs. One of the possible mechanisms could be the interference of PcdhgC3 with VE-cadherin/β-catenin signaling pathway, which has been shown to inhibit endothelial proliferation (Lampugnani et al., 2003). This assumption is strengthened by the observation that PcdhgC3 KO cells have an increased proliferation and a high paracellular permeability compared to WT cells. In addition, we have previously shown that PcdhgC3 KO cells have a lower TEER and a strongly decreased expression of occludin (Dilling et al., 2017). Increased proliferation and permeability of the endothelium are hallmarks of many diseases of the CNS (Daneman, 2012).

The PcdhgC3 KO BMECs showed differences in the expression level of cellular receptors. Changing the expression of cellular receptors could be a useful target for drug delivery to the brain. Drug delivery strategies that use anti-transferrin receptor antibodies have shown increased drug brain penetration in models of neurodegenerative diseases and brain tumors (Lajoie and Shusta, 2015; Wang et al., 2015). Trfc is decreased at mRNA and increased at protein level in KO cells. We observed a significantly increased RAGE mRNA and slightly but significantly increased protein level in KO cells. This receptor for advanced glycation end products plays a role in the transport of molecules such as amyloid-beta peptides through the BBB. The inhibition of RAGE-ligand interaction protects against the accumulation of amyloid-beta peptides in the brain (Deane et al., 2003). PcdhgC3 KO led to changes in the expression of the efflux pumps genes. Most of them were decreased in KO BMECs at mRNA and protein level as shown for Bcrp. Efflux pumps protect the brain from blood-borne substances by pumping them out of endothelial cells. However, many cancer drugs are also substrates of efflux pumps (Lajoie and Shusta, 2015). Glut1 protein and mRNA were inversely regulated in PcdhgC3 KO cells (mRNA was decreased while protein was increased). Increased Glut1 protein level corresponds to increased Vegf level in KO cells (Sanchez-Elsner et al., 2001).

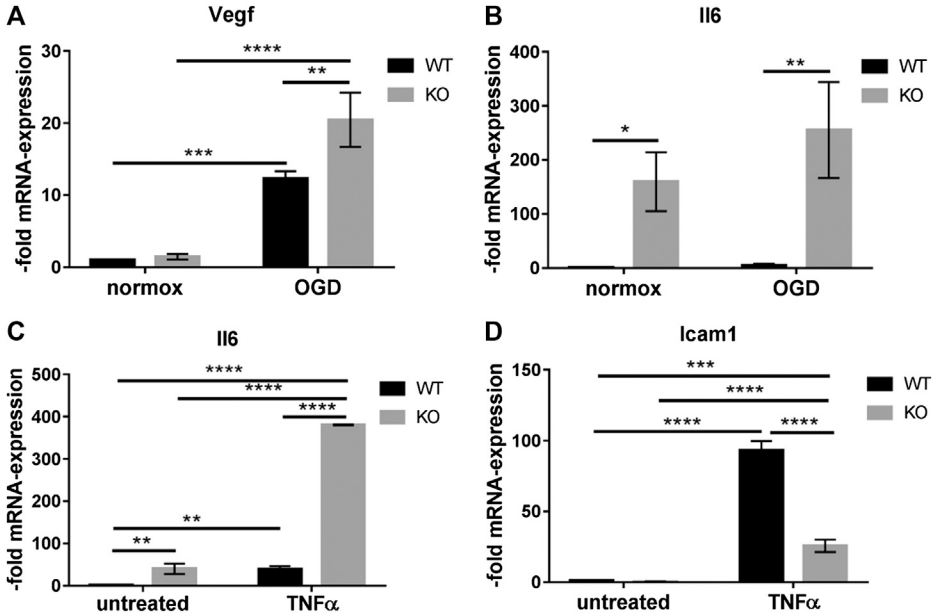

FIGURE 6 | PcdhgC3 knockout Brain Microvascular Endothelial Cells respond stronger to oxygen/glucose deprivation (OGD) conditions and to Tumor Necrosis Factor Alpha treatment. Confluent wild type (WT) and PcdhgC3 knockout (KO) BMECs were subjected to OGD **(A,B)** or TNFα treatment **(C,D)** followed by RNA extraction and qPCR analysis of indicated markers. Target gene expression was normalized to endogenous control and shown as fold over control (untreated WT cells for TNFα and normoxic WT cells for OGD), which was arbitrarily set as 1. Data are shown as mean ± standard deviation of three independent experiments. Icam1, Intracellular adhesion molecule; Il6, Interleukin 6; TNFα, Tumor necrosis factor alpha; Vegf, Vascular endothelia growth factor. $^{*}p < 0.05$, $^{**}p < 0.01$, $^{***}p < 0.001$, $^{****}p < 0.0001$.

We also examined the mRNA expression of various signaling molecules. Dll4, which is involved in Notch signaling, was strongly increased. Based on other studies, the downregulation of Dll4 was accompanied by stimulated endothelial proliferation, migration and sprouting (You et al., 2013). However, our results show otherwise, but we only measured the mRNA expression of Dll4. On the other hand, decreased Dll4 expression correlated with the inhibition of the Src/Akt/β-catenin-signaling pathway in HUVEC (Human Umbilical Vein Endothelial Cells) and the Src/Akt/β-catenin-signaling pathway also directly regulates the Dll4 (Fournier et al., 2020). In addition, the mRNA of Protein tyrosine kinase PYK2 (Ptk2b) is strongly downregulated in PcdhgC3 KO, but it has been shown that this protein positively regulates the MAPK pathway and endothelial cell migration (Lev et al., 1995; Evans et al., 2011). We analyzed several genes involved in the inflammatory response. Most of the genes were downregulated. Ccl2 and -5 were additionally downregulated at the protein level, as shown by ELISA. Ccl2, -5, -7 and Icam1, which are downregulated in PcdhgC3 KO cells show positive correlation with Erk cascade (Dragoni et al., 2017). Since Erk-pathway is upregulated in our case, an opposite regulation of Ccl-2, -5, -7 and Icam1 could be expected. However, we show that due to the deletion of PcdhgC3, other signaling pathways are also deregulated. The effects could be additive and therefore not correlate with the literature. In addition, the activation of Erk in KO cells is not constitutive, as shown by phospho-antibodies, but requires a trigger such as the serum starvation shown here.

In contrast to WT cells, KO cells showed activation of Erk-signaling pathway in response to serum starvation and growth factor reduction. Under normal culture conditions (10% FCS), WT and KO cells do not differ in phosho-Erk level. This indicates that PcdhgC3 may have a protective function in BMECs under stress condition. The increased activity of MAPK-signaling pathway can affect the migration rate of BMECs in wound healing assay. The PcdhgC3 KO cells migrated significantly faster than the WT cells. This increased migration rate was mediated in part by the activity of MAPK-, β-catenin/Wnt- or mTOR-signaling pathways, as demonstrated by the addition of selective inhibitors. Our study is however, limited, since we only analyzed the Erk-activation after 24 h. This activation could be time dependent. Additionally, we can only assume that downstream signaling molecules of the Erk signaling pathway are also activated. The regulation of signaling pathways and the inhibition of cell proliferation has previously been shown in different types of cancer for different Pcdhs (Dallosso et al., 2012; Zhou et al., 2017). The mTOR pathway also plays a role in endothelial cell proliferation. In coronary heart disease as well as in hemangiomas, inhibition of the mTOR pathway blocked abnormal endothelial cell proliferation (Wang et al., 2017; Harari et al., 2018). Endothelial cell proliferation and migration also occurs in the brain during inflammation and hypoxia. Meanwhile, the MAPK-signaling pathway activates pro-inflammatory mediators that contribute to BBB damage in

stroke, traumatic brain injury and dementia (Maddahi and Edvinsson, 2010; Zhu et al., 2018; Griemert et al., 2019). PcdhgC3 KO is more responsive to OGD and to TNFα treatment. PcdhgC3 KO showed a higher basal level and induction of the pro-inflammatory cytokine Il6 and Vegf than the WT cells after OGD and/or TNFα treatment. Also, the Icam1 expression was lower in KO cells and its induction by TNFα was lower than in WT cells. This correlated with the low level of other inflammatory molecules in KO cells, which was shown as evidenced by qPCR and ELISA. BMECs express Il6 and TNFα receptors, secrete Il6 and TNFα and can transmit their intracellular signaling (Coisne and Engelhardt, 2011; Blecharz-Lang et al., 2018b). Expression of Il6 is low in the normal brain and dramatically increases in response to an inflammatory stimulus such as TNFα (Shalaby et al., 1989; Juttler et al., 2002). Elevated level of Il6 could lead to greater damage to neuronal tissue during hypoxic events in the brain. A high Il6 level in PcdhgC3 KO cells corresponds to a high Vegf level and an activated Erk-signaling pathway. Consistent with our results, Il6 has been shown to trigger endothelial cell proliferation by increasing Vegf release and activating Erk-signaling (Yao et al., 2006). Inflammation mediators directly influence junctional proteins of the BBB such as claudin-5 and ZO-1 leading to further functional changes (Burek and Forster, 2009; Ittner et al., 2020).

The phenotypic changes described here are only shown *in vitro* in BMECs without the influence of other cell types present *in vivo* in the brain. This is a major limitation of our study. Nonetheless, we plan to generate endothelial-specific knockout mice of PcdhgC3 in order to investigate the role of PcdhgC3 *in vivo* in brain vascular endothelial cells.

To summarize, our data show that the deletion of only one member of the Pcdh subfamily in BMECs can lead to multiple phenotypic and functional changes. Loss of PcdhgC3 can switch cells from resting barrier type to a more migratory/proliferating and angiogenic type. We provide the first evidence for PcdhgC3-mediated regulation of signaling pathways in BMECs and a changed inflammatory or hypoxia/hypoglycemia response.

DATA AVAILABILITY STATEMENT

The raw data supporting the conclusions of this article will be made available by the authors, without undue reservation, to any qualified researcher.

AUTHOR CONTRIBUTIONS

LG, CD, and MB designed the study, performed and analyzed experiments and drafted the manuscript. PM provided crucial reagents. All authors were involved in critical revision and final approval of the manuscript.

FUNDING

This publication was supported by the Open Access Publication Fund of the University of Wurzburg and institutional funds of the Unviersity Hospital Wurzburg.

ACKNOWLEDGMENTS

We thank Anja Neuhoff and Elisabeth Wilken for their excellent technical assistance.

REFERENCES

Abbott, N. J. (2013). Blood-brain barrier structure and function and the challenges for CNS drug delivery. *J. Inherit. Metab. Dis.* 36, 437–449. doi:10.1007/s10545-013-9608-0.

Abbott, N. J., Patabendige, A. A. K., Dolman, D. E. M., Yusof, S. R., and Begley, D. J. (2010). Structure and function of the blood-brain barrier. *Neurobiol. Dis.* 37, 13–25. doi:10.1016/j.nbd.2009.07.030.

Blecharz-Lang, K. G., Prinz, V., Burek, M., Frey, D., Schenkel, T., Krug, S. M., et al. (2018a). Gelatinolytic activity of autocrine matrix metalloproteinase-9 leads to endothelial de-arrangement in Moyamoya disease. *J. Cereb. Blood Flow Metab.* 38, 1940–1953. doi:10.1177/0271678x18768443.

Blecharz-Lang, K. G., Wagner, J., Fries, A., Nieminen-Kelhä, M., Rösner, J., Schneider, U. C., et al. (2018b). Interleukin 6-mediated endothelial barrier disturbances can Be attenuated by blockade of the IL6 receptor expressed in brain microvascular endothelial cells. *Transl. Stroke Res.* 9, 631–642. doi:10.1007/s12975-018-0614-2.

Burek, M., Salvador, E., and Förster, C. Y. (2012). Generation of an immortalized murine brain microvascular endothelial cell line as an *in vitro* blood brain barrier model. *J. Vis. Exp.*, e4022. doi:10.3791/4022.

Burek, M. and Förster, C. Y. (2009). Cloning and characterization of the murine claudin-5 promoter. *Mol. Cell. Endocrinol.* 298, 19–24. doi:10.1016/j.mce.2008.09.041.

Burek, M., König, A., Lang, M., Fiedler, J., Oerter, S., Roewer, N., et al. (2019). Hypoxia-Induced MicroRNA-212/132 alter blood-brain barrier integrity through inhibition of tight junction-associated proteins in human and mouse brain microvascular endothelial cells. *Transl. Stroke Res.* 10, 672–683. doi:10.1007/s12975-018-0683-2.

Chen, W. V., Alvarez, F. J., Lefebvre, J. L., Friedman, B., Nwakeze, C., Geiman, E., et al. (2012). Functional significance of isoform diversification in the protocadherin gamma gene cluster. *Neuron* 75, 402–409. doi:10.1016/j.neuron.2012.06.039.

Coisne, C., and Engelhardt, B. (2011). Tight junctions in brain barriers during central nervous system inflammation. *Antioxid. Redox Signal.* 15, 1285–1303. doi:10.1089/ars.2011.3929.

Curtaz, C. J., Schmitt, C., Herbert, S. L., Feldheim, J., Schlegel, N., Gosselet, F., et al. (2020). Serum-derived factors of breast cancer patients with brain metastases alter permeability of a human blood-brain barrier model. *Fluids Barriers CNS* 17, 31. doi:10.1186/s12987-020-00192-6.

Dallosso, A. R., Hancock, A. L., Szemes, M., Moorwood, K., Chilukamarri, L., Tsai, H. H., et al. (2009). Frequent long-range epigenetic silencing of protocadherin gene clusters on chromosome 5q31 in Wilms' tumor. *PLoS Genet.* 5, e1000745. doi:10.1371/journal.pgen.1000745.

Dallosso, A. R., Øster, B., Greenhough, A., Thorsen, K., Curry, T. J., Owen, C., et al. (2012). Long-range epigenetic silencing of chromosome 5q31 protocadherins is involved in early and late stages of colorectal tumorigenesis through modulation of oncogenic pathways. *Oncogene* 31, 4409–4419. doi:10.1038/onc.2011.609.

Daneman, R. (2012). The blood-brain barrier in health and disease. *Ann. Neurol.* 72, 648–672. doi:10.1002/ana.23648.

Deane, R., Du Yan, S., Submamaryan, R. K., LaRue, B., Jovanovic, S., Hogg, E., et al. (2003). RAGE mediates amyloid-β peptide transport across the blood-brain barrier and accumulation in brain. *Nat. Med.* 9, 907–913. doi:10.1038/nm890.

Dilling, C., Roewer, N., Förster, C. Y., and Burek, M. (2017). Multiple protocadherins are expressed in brain microvascular endothelial cells and might play a role in tight junction protein regulation. *J. Cereb. Blood Flow Metab.* 37, 3391–3400. doi:10.1177/0271678x16688706.

Dragoni, S., Hudson, N., Kenny, B.-A., Burgoyne, T., McKenzie, J. A., Gill, Y., et al. (2017). Endothelial MAPKs direct ICAM-1 signaling to divergent inflammatory functions. *J. Immunol.* 198, 4074–4085. doi:10.4049/jimmunol.1600823.

Evans, I. M., Yamaji, M., Britton, G., Pellet-Many, C., Lockie, C., Zachary, I. C., et al. (2011). Neuropilin-1 signaling through p130Cas tyrosine phosphorylation is essential for growth factor-dependent migration of glioma and endothelial cells. *Mol. Cell Biol.* 31, 1174–1185. doi:10.1128/mcb.00903-10.

Fournier, P., Viallard, C., Dejda, A., Sapieha, P., Larrivée, B., and Royal, I. (2020). The protein tyrosine phosphatase PTPRJ/DEP-1 contributes to the regulation of the Notch-signaling pathway and sprouting angiogenesis. *Angiogenesis* 23, 145–157. doi:10.1007/s10456-019-09683-z.

Frank, M., Ebert, M., Shan, W., Phillips, G. R., Arndt, K., Colman, D. R., et al. (2005). Differential expression of individual gamma-protocadherins during mouse brain development. *Mol. Cell. Neurosci.* 29, 603–616. doi:10.1016/j.mcn.2005.05.001.

Garrett, A. M., Schreiner, D., Lobas, M. A., and Weiner, J. A. (2012). γ-Protocadherins control cortical dendrite arborization by regulating the activity of a FAK/PKC/MARCKS signaling pathway. *Neuron* 74, 269–276. doi:10.1016/j.neuron.2012.01.028.

Griemert, E. V., Schwarzmaier, S. M., Hummel, R., Gölz, C., Yang, D., Neuhaus, W., et al. (2019). Plasminogen activator inhibitor-1 augments damage by impairing fibrinolysis after traumatic brain injury. *Ann. Neurol.* 85, 667–680. doi:10.1002/ana.25458.

Haas, I. G., Frank, M., Veron, N., and Kemler, R. (2005). Presenilin-dependent processing and nuclear function of -protocadherins. *J. Biol. Chem.* 280, 9313–9319. doi:10.1074/jbc.m412909200.

Harari, E., Guo, L., Smith, S. L., Paek, K. H., Fernandez, R., Sakamoto, A., et al. (2018). Direct targeting of the mTOR (mammalian target of rapamycin) kinase improves endothelial permeability in drug-eluting stents-brief report. *Arterioscler. Thromb. Vasc. Biol.* 38, 2217–2224. doi:10.1161/atvbaha.118.311321.

Helms, H. C., Abbott, N. J., Burek, M., Cecchelli, R., Couraud, P.-O., Deli, M. A., et al. (2016). *In vitro* models of the blood-brain barrier: an overview of commonly used brain endothelial cell culture models and guidelines for their use. *J. Cereb. Blood Flow Metab.* 36, 862–890. doi:10.1177/0271678x16630991.

Hotter, B., Hoffmann, S., Ulm, L., Meisel, C., Fiebach, J. B., and Meisel, A. (2019). IL-6 plasma levels correlate with cerebral perfusion deficits and infarct sizes in stroke patients without associated infections. *Front. Neurol.* 10, 83. doi:10.3389/fneur.2019.00083.

Ittner, C., Burek, M., Stork, S., Nagai, M., and Forster, C. Y. (2020). Increased catecholamine levels and inflammatory mediators alter barrier properties of brain microvascular endothelial cells *in vitro*. *Front. Cardiovasc. Med.* 7, 73. doi:10.3389/fcvm.2020.00073.

Jüttler, E., Tarabin, V., and Schwaninger, M. (2002). Interleukin-6 (IL-6): a possible neuromodulator induced by neuronal activity. *Neuroscientist* 8, 268–275. doi:10.1177/1073858402008003012.

Kaiser, M., Burek, M., Britz, S., Lankamp, F., Ketelhut, S., Kemper, B., et al. (2018). The influence of capsaicin on the integrity of microvascular endothelial cell monolayers. *Int. J. Mol. Sci.* 20 (1), 122. doi:10.3390/ijms20010122.

Kaneko, R., Kato, H., Kawamura, Y., Esumi, S., Hirayama, T., Hirabayashi, T., et al. (2006). Allelic gene regulation ofPcdh-α andPcdh-γ clusters involving both monoallelic and biallelic expression in single purkinje cells. *J. Biol. Chem.* 281, 30551–30560. doi:10.1074/jbc.m605677200.

Lajoie, J. M., and Shusta, E. V. (2015). Targeting receptor-mediated transport for delivery of biologics across the blood-brain barrier. *Annu. Rev. Pharmacol. Toxicol.* 55, 613–631. doi:10.1146/annurev-pharmtox-010814-124852.

Lampugnani, M. G., Zanetti, A., Corada, M., Takahashi, T., Balconi, G., Breviario, F., et al. (2003). Contact inhibition of VEGF-induced proliferation requires vascular endothelial cadherin, β-catenin, and the phosphatase DEP-1/CD148. *J. Cell Biol.* 161, 793–804. doi:10.1083/jcb.200209019.

Lev, S., Moreno, H., Martinez, R., Canoll, P., Peles, E., Musacchio, J. M., et al. (1995). Protein tyrosine kinase PYK2 involved in Ca2+-induced regulation of ion channel and MAP kinase functions. *Nature* 376, 737–745. doi:10.1038/376737a0.

Lobas, M. A., Helsper, L., Vernon, C. G., Schreiner, D., Zhang, Y., Holtzman, M. J., et al. (2012). Molecular heterogeneity in the choroid plexus epithelium: the 22-member γ-protocadherin family is differentially expressed, apically localized, and implicated in CSF regulation. *J. Neurochem.* 120, 913–927. doi:10.1111/j.1471-4159.2011.07587.x.

Maddahi, A., and Edvinsson, L. (2010). Cerebral ischemia induces micro vascular pro-inflammatory cytokine expression via the MEK/ERK pathway. *J. Neuroinflammation* 7, 14. doi:10.1186/1742-2094-7-14.

Mah, K. M., Houston, D. W., and Weiner, J. A. (2016). The gamma-Protocadherin-C3 isoform inhibits canonical Wnt signalling by binding to and stabilizing Axin1 at the membrane. *Sci. Rep.* 6, 31665. doi:10.1038/srep31665.

Mah, K. M., and Weiner, J. A. (2017). Regulation of Wnt signaling by protocadherins. *Semin. Cell Dev. Biol.* 69, 158–171. doi:10.1016/j.semcdb.2017.07.043.

Miralles, C. P., Taylor, M. J., Bear, J., Jr., Fekete, C. D., George, S., Li, Y., et al. (2020). Expression of protocadherin-γ*C4* protein in the rat brain. *J. Comp. Neurol.* 528, 840–864. doi:10.1002/cne.24783.

Molumby, M. J., Anderson, R. M., Newbold, D. J., Koblesky, N. K., Garrett, A. M., Schreiner, D., et al. (2017). γ-Protocadherins interact with neuroligin-1 and negatively regulate dendritic spine morphogenesis. *Cell Rep.* 18, 2702–2714. doi:10.1016/j.celrep.2017.02.060.

Nollet, F., Kools, P., and van Roy, F. (2000). Phylogenetic analysis of the cadherin superfamily allows identification of six major subfamilies besides several solitary members 1 1Edited by M. Yaniv. *J. Mol. Biol.* 299, 551–572. doi:10.1006/jmbi.2000.3777.

Okazaki, N., Takahashi, N., Kojima, S., Masuho, Y., and Koga, H. (2002). Protocadherin LKC, a new candidate for a tumor suppressor of colon and liver cancers, its association with contact inhibition of cell proliferation. *Carcinogenesis* 23, 1139–1148. doi:10.1093/carcin/23.7.1139.

Peek, S. L., Mah, K. M., and Weiner, J. A. (2017). Regulation of neural circuit formation by protocadherins. *Cell. Mol. Life Sci.* 74, 4133–4157. doi:10.1007/s00018-017-2572-3.

Phillips, G. R., LaMassa, N., and Nie, Y. M. (2017). Clustered protocadherin trafficking. *Semin. Cell Dev. Biol.* 69, 131–139. doi:10.1016/j.semcdb.2017.05.001.

Sánchez-Elsner, T., Botella, L. M., Velasco, B., Corbí, A., Attisano, L., and Bernabéu, C. (2001). Synergistic cooperation between hypoxia and transforming growth factor-β pathways on human vascular endothelial growth factor gene expression. *J. Biol. Chem.* 276, 38527–38535. doi:10.1074/jbc.m104536200.

Sano, K., Tanihara, H., Heimark, R. L., Obata, S., Davidson, M., St John, T., et al. (1993). Protocadherins: a large family of cadherin-related molecules in central nervous system. *EMBO J.* 12, 2249–2256. doi:10.1002/j.1460-2075.1993.tb05878.x.

Shalaby, M. R., Waage, A., Aarden, L., and Espevik, T. (1989). Endotoxin, tumor necrosis factor-α and interleukin 1 induce interleukin 6 production *in vivo*. *Clin. Immunol. Immunopathol.* 53, 488–498. doi:10.1016/0090-1229(89)90010-x.

Silwedel, C., and Förster, C. (2006). Differential susceptibility of cerebral and cerebellar murine brain microvascular endothelial cells to loss of barrier properties in response to inflammatory stimuli. *J. Neuroimmunol.* 179, 37–45. doi:10.1016/j.jneuroim.2006.06.019.

Steelman, L. S., Chappell, W. H., Abrams, S. L., Kempf, C. R., Long, J., Laidler, P., et al. (2011). Roles of the Raf/MEK/ERK and PI3K/PTEN/Akt/mTOR pathways in controlling growth and sensitivity to therapy-implications for cancer and aging. *Aging (Albany NY)* 3, 192–222. doi:10.18632/aging.100296.

Suo, L., Lu, H., Ying, G., Capecchi, M. R., and Wu, Q. (2012). Protocadherin clusters and cell adhesion kinase regulate dendrite complexity through Rho GTPase. *J. Mol. Cell Biol.* 4, 362–376. doi:10.1093/jmcb/mjs034.

Wang, S., Meng, Y., Li, C., Qian, M., and Huang, R. (2015). Receptor-mediated drug delivery systems targeting to glioma. *Nanomaterials (Basel)* 6, 3. doi:10.3390/nano6010003.

Wang, Y., Chen, J., Tang, W., Zhang, Y., and Li, X. (2017). Rapamycin inhibits the proliferation of endothelial cells in hemangioma by blocking the mTOR-FABP4 pathway. *Biomed. Pharmacother.* 85, 272–279. doi:10.1016/j.biopha.2016.11.021.

Weiner, J. A., and Jontes, J. D. (2013). Protocadherins, not prototypical: a complex tale of their interactions, expression, and functions. *Front. Mol. Neurosci.* 6, 4. doi:10.3389/fnmol.2013.00004.

Wong, A. D., Ye, M., Levy, A. F., Rothstein, J. D., Bergles, D. E., and Searson, P. C. (2013). The blood-brain barrier: an engineering perspective. *Front. Neuroeng.* 6, 7. doi:10.3389/fneng.2013.00007.

Yao, J. S., Zhai, W., Young, W. L., and Yang, G.-Y. (2006). Interleukin-6 triggers human cerebral endothelial cells proliferation and migration: the role for KDR and MMP-9. *Biochem. Biophys. Res. Commun.* 342, 1396–1404. doi:10.1016/j.bbrc.2006.02.100.

You, C., Erol Sandalcioglu, I., Dammann, P., Felbor, U., Sure, U., and Zhu, Y. (2013). Loss of CCM3 impairs DLL4-Notch signalling: implication in endothelial angiogenesis and in inherited cerebral cavernous malformations. *J. Cell Mol. Med.* 17, 407–418. doi:10.1111/jcmm.12022.

Yu, J. S., Koujak, S., Nagase, S., Li, C.-M., Su, T., Wang, X., et al. (2008). PCDH8, the human homolog of PAPC, is a candidate tumor suppressor of breast cancer. *Oncogene* 27, 4657–4665. doi:10.1038/onc.2008.101.

Zhang, Z. G., Zhang, L., Jiang, Q., Zhang, R., Davies, K., Powers, C., et al. (2000). VEGF enhances angiogenesis and promotes blood-brain barrier leakage in the ischemic brain. *J. Clin. Invest.* 106, 829–838. doi:10.1172/jci9369.

Zhou, X., Updegraff, B. L., Guo, Y., Peyton, M., Girard, L., Larsen, J. E., et al. (2017). PROTOCADHERIN 7 acts through SET and PP2A to potentiate MAPK signaling by EGFR and KRAS during lung tumorigenesis. *Cancer Res.* 77, 187–197. doi:10.1158/0008-5472.can-16-1267-t.

Zhu, H., Dai, R., Zhou, Y., Fu, H., and Meng, Q. (2018). TLR2 ligand Pam3CSK4 regulates MMP-2/9 expression by MAPK/NF-κB signaling pathways in primary brain microvascular endothelial cells. *Neurochem. Res.* 43, 1897–1904. doi:10.1007/s11064-018-2607-7.

Conflict of Interest: The authors declare that the research was conducted in the absence of any commercial or financial relationships that could be construed as a potential conflict of interest.

frontiers in Pharmacology

SYSTEMATIC REVIEW
published: 15 December 2020
doi: 10.3389/fphar.2020.615166

The Protective Role of Immunomodulators on Tissue-Type Plasminogen Activator-Induced Hemorrhagic Transformation in Experimental Stroke: A Systematic Review and Meta-Analysis

Yang Ye[1,2†*], *Yu-Tian Zhu*[3,4†], *Hong-Xuan Tong*[5] *and Jing-Yan Han*[1,2*]

[1]Department of Integration of Chinese and Western Medicine, School of Basic Medical Sciences, Peking University, Beijing, China, [2]Tasly Microcirculation Research Center, Peking University Health Science Center, Beijing, China, [3]Department of Traditional Chinese Medicine, Peking University Third Hospital, Beijing, China, [4]Department of Urology, Peking University Third Hospital, Beijing, China, [5]Institute of Basic Theory for Chinese Medicine, China Academy of Chinese Medical Sciences, Beijing, China

OPEN ACCESS

Edited by:
Zsuzsanna Helyes,
University of Pécs, Hungary

Reviewed by:
Balint Mihaly Eross,
University of Pécs, Hungary
Margit Varjú-Solymár,
University of Pécs, Hungary
Zsolt Molnár,
University of Szeged, Hungary

***Correspondence:**
Jing-Yan Han
hanjingyan@bjmu.edu.cn
Yang Ye
yeyang89@126.com

[†]These authors have contributed equally to this work and share first authorship

Specialty section:
This article was submitted to Inflammation Pharmacology, a section of the journal Frontiers in Pharmacology

Received: 08 October 2020
Accepted: 24 November 2020
Published: 15 December 2020

Citation:
Ye Y, Zhu Y-T, Tong H-X and Han J-Y (2020) The Protective Role of Immunomodulators on Tissue-Type Plasminogen Activator-Induced Hemorrhagic Transformation in Experimental Stroke: A Systematic Review and Meta-Analysis. Front. Pharmacol. 11:615166. doi: 10.3389/fphar.2020.615166

Background: Recanalization with tissue plasminogen activator (tPA) is the only approved agent available for acute ischemic stroke. But delayed treatment of tPA may lead to lethal intracerebral hemorrhagic transformation (HT). Numerous studies have reported that immunomodulators have good efficacy on tPA-induced HT in ischemic stroke models. The benefits of immunomodulators on tPA-associated HT are not clearly defined. Here, we sought to conduct a systematic review and meta-analysis of preclinical studies to further evaluate the efficacy of immunomodulators.

Methods: The PubMed, Web of Science, and Scopus electronic databases were searched for studies. Studies that reported the efficacy of immunomodulators on tPA-induced HT in animal models of stroke were included. Animals were divided into two groups: immunomodulators plus tPA (intervention group) or tPA alone (control group). The primary outcome was intracerebral hemorrhage, and the secondary outcomes included infarct volume and neurobehavioral score. Study quality was assessed by the checklist of CAMARADES. We used standardized mean difference (SMD) to assess the impact of interventions. Regression analysis and subgroup analysis were performed to identify potential sources of heterogeneity and evaluate the impact of the study characteristics. The evidence of publication bias was evaluated using trim and fill method and Egger's test.

Results: We identified 22 studies that met our inclusion criteria involving 516 animals and 42 different comparisons. The median quality checklist score was seven of a possible 10 (interquartile range, 6–8). Immunomodulators improved cerebral hemorrhage (1.31 SMD, 1.09–1.52); infarct volume (1.35 SMD, 0.95–1.76), and neurobehavioral outcome (0.9 SMD, 0.67–1.13) in experimental stroke. Regression analysis and subgroup analysis indicated that control of temperature and time of assessment were important factors that influencing the efficacy of immunomodulators.

Conclusion: Our findings suggested that immunomodulators had a favorable effect on tPA-associated intracerebral hemorrhage, cerebral infarction, and neurobehavioral impairments in animal models of ischemic stroke.

Keywords: tissue-type plasminogen activator, stroke, meta-analysis, immunomodulator, hemorrhagic transformation, animal model

INTRODUCTION

Currently, thrombolysis with tissue plasminogen activator (tPA) remains the only approved drug treatment for acute ischemic stroke (Pena et al., 2017). However, tPA must be administered intravenously within 4.5 h of ischemic stroke onset due to the increased risk of hemorrhagic transformation (HT) (Mao et al., 2017). HT is believed as one of the leading causes of death and disability after stroke (Xu et al., 2017). Therefore, it is urgent to decrease the risk of HT caused by delayed tPA treatment.

Evidence indicated that inflammatory injury plays an important role in tPA-induced HT (Li et al., 2018). Blood brain-barrier (BBB) damage is the most critical factor in the pathogenesis of HT. Although the mechanism underlying BBB damage is not fully understood, excessive neuroinflammation is thought to be involved in the process (Sorby-Adams et al., 2017). Therefore, immunomodulation seems like a promising direction of drug development for tPA-associated HT. Substances that regulate the function of the immune system are called immunomodulators. Although it is not yet entirely clear how immunomodulators work, it is hypothesized that immunomodulators act on certain points of the immune activation pathways to regulate inflammatory process. They may act as immunosuppressants by inhibiting the immune response or as immunostimulants by stimulating the immune response. A lot of immunomodulators, such as high-mobility group box 1 (HMGB1) inhibitor (Chen et al., 2020) and regulatory T cells therapy (Mao et al., 2017), have been used to relieve HT induced by tPA thrombolysis in animal studies. Although many immunomodulators have shown protective effects on tPA-associated HT, the efficacy of immunomodulators has not yet been systematically reviewed.

In this study, we presented a systematic review and meta-analysis of data from animal studies testing the efficacy of immunomodulators on tPA-induced HT. We aimed to comprehensively review the protective effects of immunomodulators on intracerebral hemorrhage, infarct size, and neurobehavioral outcome in animal models of tPA-induced HT. The factors that influencing the efficacy of immunomodulators in preclinical studies were also identified. Our results may lead to refinements of animal experiments in this field and hence reduce animal numbers required.

METHODS

Search Strategy

Electronic search was performed in PubMed, Web of Science, and Scopus electronic databases (by July 2020). Studies that reported the efficacy of immunomodulators on tPA-induced HT in animal models of stroke were included. Animals were divided into two groups: immunomodulators plus tPA (intervention group) or tPA alone (control group). The predetermined primary endpoint was intracerebral hemorrhage, and the secondary endpoints included infarct volume and neurobehavioral score. The following search term was constructed to identify animal studies that examined the efficacy of immunomodulators on tPA-induced HT (tPA OR rtPA OR t-PA OR rt-PA OR tissue plasminogen activator OR tissue-plasminogen activator OR alteplase) AND (hemorrhagic transformation OR hemorrhage OR hemorrhage OR bleeding) AND (stroke OR ischemia OR cerebral OR brain). The search strategy is specified in **Supplemental Material**.

Inclusion Criteria

Studies were included if they fulfilled the following criteria: 1) the study reported the efficacy of immunomodulators on tPA-induced HT in animal models of stroke; 2) a control group receiving vehicle or no treatment in animal models of tPA-induced HT was described; 3) intracerebral hemorrhage was quantified as an outcome (including hemoglobin content, hemorrhage volume/area/score, studies that only quantified the incidence of HT were excluded); 4) the number of animals per group was described; 5) studies were published in English. Studies were screened by two independent investigators (YY and YTZ) with discrepancies resolved through discussion.

Data Extraction

We abstracted from studies the publication details (author, year), animal used (sex, species), type of stroke model, intervention used (route, dose, and timing), anesthetic used, tPA administration (dose, timing), and details of the outcome measures. We also extracted the sample size, mean value, and standard deviation for both intervention and control groups. Infarct size was quantified as infarct volume, infarct area, or infarct score. Neurobehavioral outcome was quantified as various neurological scoring system.

If data were only represented graphically, numerical values were extracted using ImageJ software (NIH, Bethesda, MD, United States). When multiple groups were served by a single control group, sample size of the control group was divided by the number of treatment groups (McCann et al., 2014). When outcomes were measured at more than one time point, only data from the latest time point was included. When multiple indicators were used to measure intracerebral hemorrhage, we chose hemoglobin content as our preferred indicator because it is more accurate.

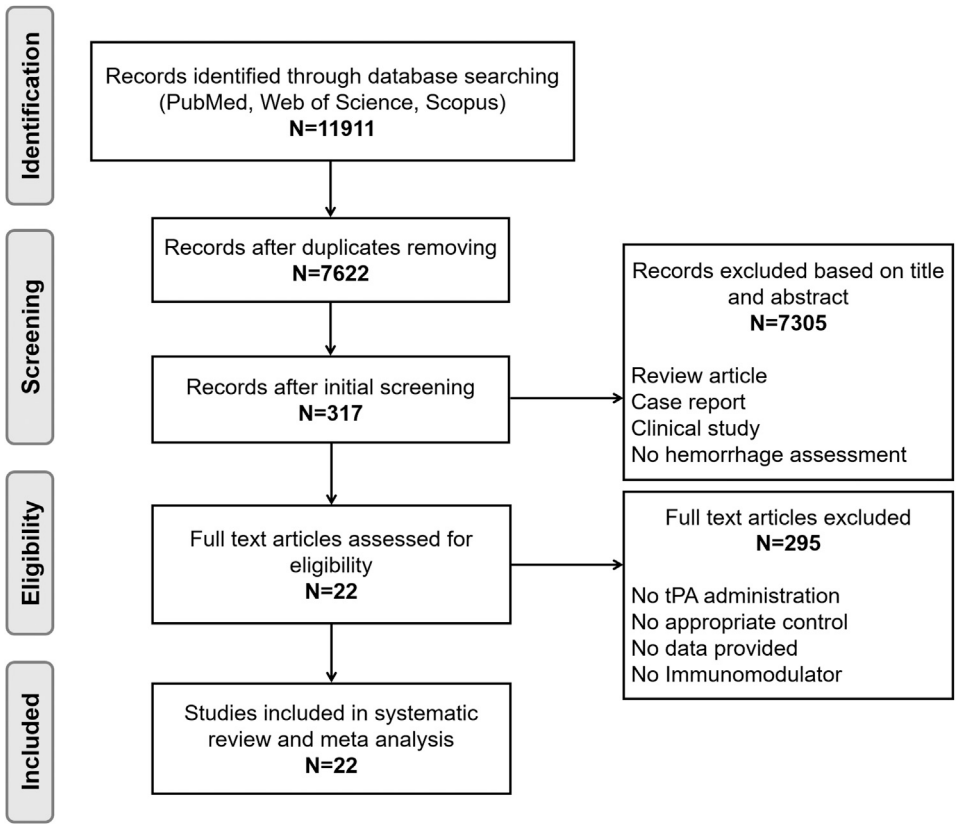

FIGURE 1 | Flow diagram of the study selection process.

Quality Assessment

We assessed the quality of the individual publication using the 10-item checklist of CAMARADES (Collaborative Approach to Meta-Analysis and Review of Animal Data in Experimental Stroke) (Sena et al., 2007) comprising the following: 1) publication in a peer-reviewed journal, 2) control of temperature, 3) random allocation to groups, 4) allocation concealment (blinded induction of ischemia), 5) blinded assessment of outcome, 6) use of an anesthetic without intrinsic neuroprotective activity (ketamine), 7) the use of co-morbid animals, 8) performing a sample size calculation, 9) compliance with animal welfare regulations, and 10) statement of potential conflicts of interest. The PRISMA (Preferred Reporting Items for Systematic Reviews and Meta-Analyses) guidelines (Satapathy et al., 2020) were also followed to perform this systematic review and meta-analysis. The study quality was evaluated independently by two researchers (YY and HXT).

Data Analysis

For each endpoint, we used the standardized mean difference (SMD) effect size to standardize the results to a uniform scale. For intracerebral hemorrhage and neurobehavioral outcome, SMD values were pooled in a weighted mean difference meta-analysis using a fixed-effects model. For infarct size, we combined the comparisons using random-effect meta-analysis. When the pooled SMD effect size (including pooled 95% CI) was greater than 0, it can be defined as an improvement. Heterogeneity across studies was assessed by the Cochran's Q statistic and quantified by the I2 statistic (Yang et al., 2012). We used meta-regression and subgroup analysis to explore the possible source of heterogeneity. We also used meta-regression to evaluate the impact of the study characteristics. Funnel plots, trim and fill method (Pimpin et al., 2019), and Egger's test (Wang et al., 2019) were employed to assess the publication bias. We performed sensitivity analysis to confirm the stability of the results. Statistical analyses were performed using Review Manager 5.3 and STATA 13 software.

RESULTS

Study Characteristics

Our initial search identified 11,911 publications of which 11,889 were excluded, leaving 22 for inclusion in this systematic review and meta-analysis. The review process is detailed in the flow diagram shown in **Figure 1**. The 22 included publications described 42 different comparisons for intracerebral hemorrhage, 22 comparisons for infarct size, and 22 comparisons for neurobehavioral outcome. Study

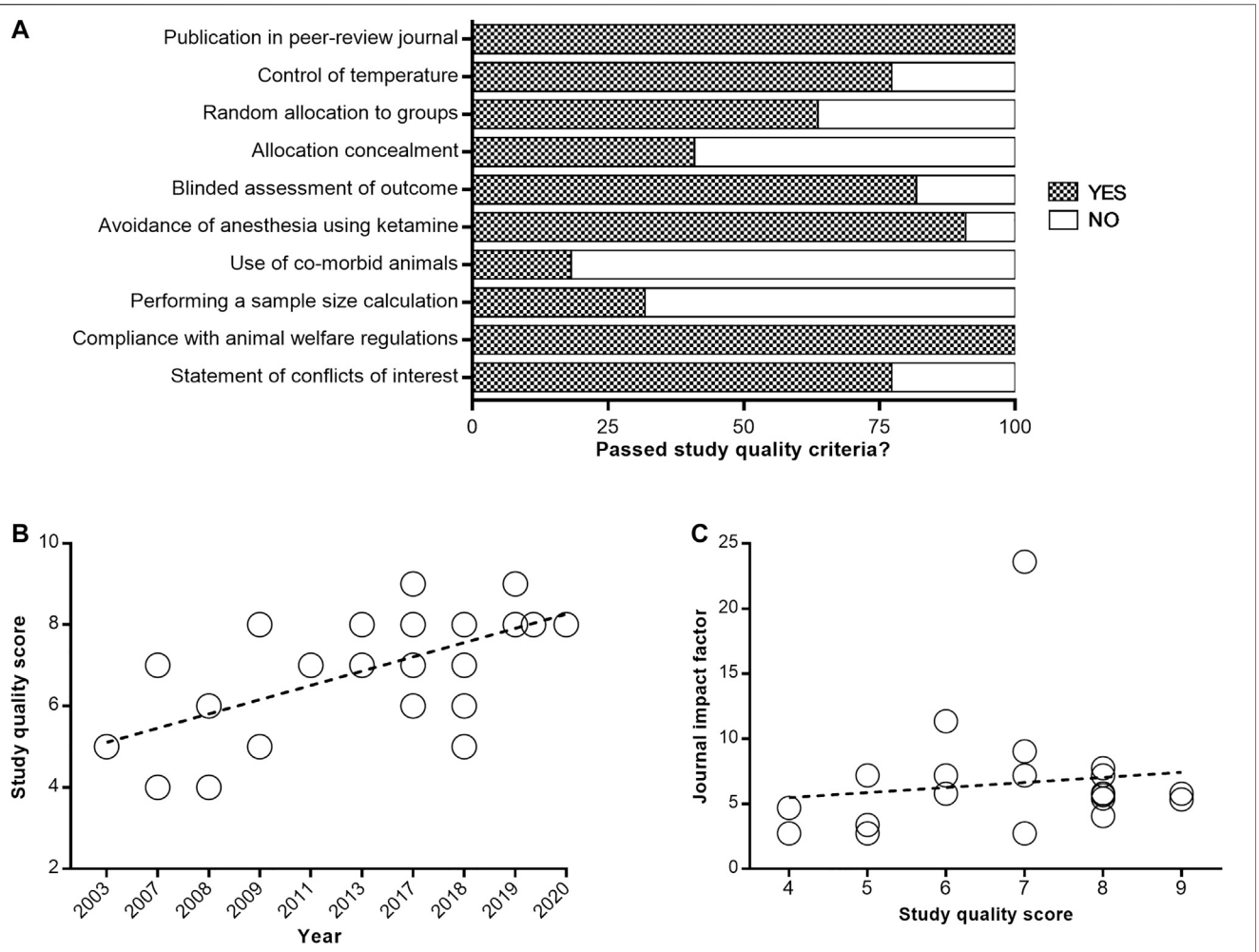

FIGURE 2 | Quality assessment of enrolled studies. Study quality was assessed using the CAMARADES checklist **(A)**. Values are expressed as the percentage of studies reporting each quality indicator. The correlation of study quality with year of publication **(B)** and journal impact factor **(C)**.

characteristics of the included publications are listed in **Supplementary Table S1**.

Study Quality

The median reported study quality score was 7 of a possible 10 (interquartile range, 6–8) for the 22 included papers. All articles were published in peer-reviewed journals (**Figure 2A**). Control of temperature during surgery was documented in 17 of 22 papers (77.3%), and random allocation to groups was described in 14 of 22 papers (63.6%). Allocation concealment was reported in 9 of 22 papers (40.9%), whereas blinded assessment was documented in 18 of 22 papers (81.8%). Anesthesia without using ketamine during surgery was reported in 20 of 22 papers (90.9%), whereas use of co-morbid animals was only described in 4 of 22 studies (18.2%). Performed a sample size calculation was documented in 7 of 22 papers (31.8%), and statement of conflicts of interest was reported in 17 of 22 papers (77.3%). All studies reported compliance with animal welfare regulations. A significant correlation between study quality and year of publication was observed, with fresher papers giving higher quality (R^2 = 77.82%; p = 0.0007; **Figure 2B**). However, no significant correlation was found between study quality and journal impact factor (R^2 = 1.76%; p = 0.5564; **Figure 2C**). The complete study quality score report is included in **Supplemental Material**.

Meta-Analysis

Intracerebral hemorrhage after immunomodulator administration was improved by 1.31 SMD (95% CI, 1.09–1.52; 42 comparisons; 516 animals), with moderate heterogeneity between studies (χ^2 = 61.21; I^2 = 33%; df = 41; p = 0.02; **Figure 3A**; **Supplementary Figure S1**). Infarct size after immunomodulator administration was improved by 1.35 SMD (95% CI, 0.95–1.76; 22 comparisons; 332 animals), with large heterogeneity between studies (χ^2 = 46.96; I^2 = 55%; df = 21; p = 0.001; **Figure 3B**; **Supplementary Figure S2**). Neurobehavioral outcome after immunomodulator administration was improved by 0.9 SMD (95% CI, 0.67–1.13; 22 comparisons; 380 animals), with moderate heterogeneity between studies (χ^2 = 41.28; I^2 = 49%; df = 21; p = 0.005; **Figure 3C**; **Supplementary Figure S3**).

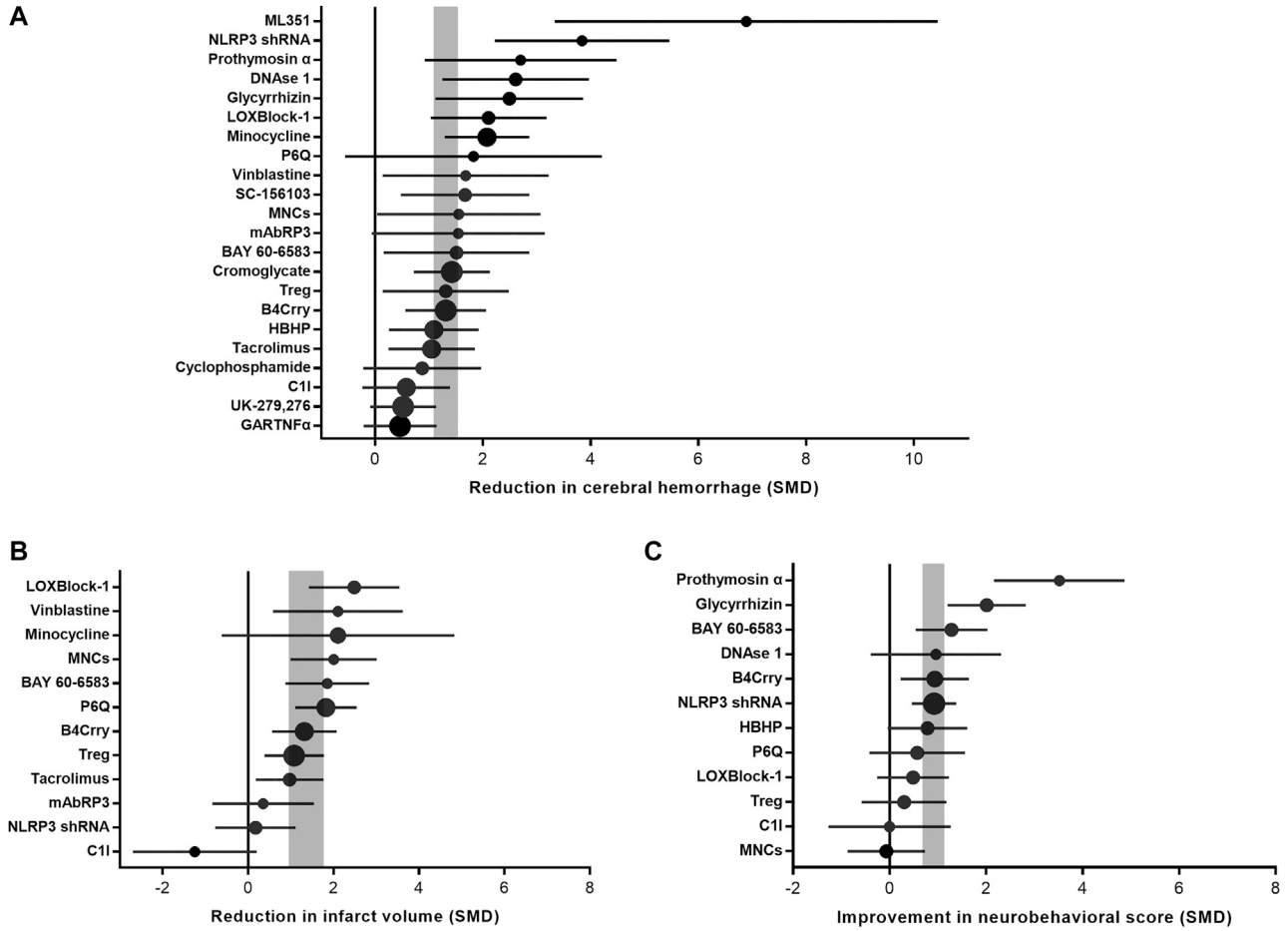

FIGURE 3 | Efficacy of immunomodulators on intracerebral hemorrhage, infarct size, and neurobehavioral score. Forest plots of the effect size in intracerebral hemorrhage **(A)**, infarct size **(B)**, and neurobehavioral score **(C)** calculated using standardized mean differences. Symbol sizes represent the relative number of animals tested for each intervention. The horizontal error bars represent the 95% confidence interval of individual studies. The vertical gray bars represent the 95% confidence interval of the pooled estimate of efficacy.

Meta-Regression and Subgroup Analysis

Meta-regression and subgroup analysis were performed to explore the source of heterogeneity. For studies that measured intracerebral hemorrhage, analysis demonstrated that effect size was significantly greater when the study quality score was lower (adjusted R^2 = 13.23%; p = 0.01; **Figure 4A**). For studies that measured infarct size, there was no significant correlation between study quality and effect size (adjusted R^2 = −6.59%; p = 0.14; **Figure 4B**). However, for studies that measured neurobehavioral outcome, that effect size was significantly greater when the study quality score was higher (adjusted R^2 = 22.03%; p = 0.002; **Figure 4C**).

For intracerebral hemorrhage and neurobehavioral outcome, efficacy were lower in studies that reported control of temperature during surgery (adjusted R^2 = 1.81%; p = 0.002; adjusted R^2 = 65.95%; p = 0.004; **Figure 5A**). Whereas for infarct size, there was no significant correlation between temperature control and effect size (adjusted R^2 = −12.52%; p = 0.61). For studies that measured intracerebral hemorrhage and neurobehavioral outcome, effect size was significantly greater when outcome was assessed within 30 h after stroke onset (adjusted R^2 = −8.78%; p = 0.001; adjusted R^2 = 20.44%; p = 0.03; **Figure 5B**). But for studies that measured infarct size, no significant correlation was found between evaluation time and effect size (adjusted R^2 = 0.82%; p = 0.22).

For intracerebral hemorrhage, effect size was significantly greater when studies used chloral hydrate and pentobarbital as anesthetic (adjusted R^2 = −11.49%; p = 0.004; **Supplementary Figure S4A**). While for infarct size and neurobehavioral outcome, effect size was not significantly changed by anesthetic used (adjusted R^2 = −48.85%; p = 0.22; adjusted R^2 = −74.01%; p = 0.75). For intracerebral hemorrhage and neurobehavioral outcome, no significant correlation was found between route of drug delivery and effect size (adjusted R^2 = −4.66%; p = 0.25; adjusted R^2 = −30.08%; p = 0.31; **Supplementary Figure S4B**). But for infarct size, the route of drug delivery had an effect on effect size (adjusted R^2 = −40.77%; p = 0.0002). For all the three outcomes, neither blinded assessment nor random allocation contributed significantly to the effect size (**Supplementary Figure S5**).

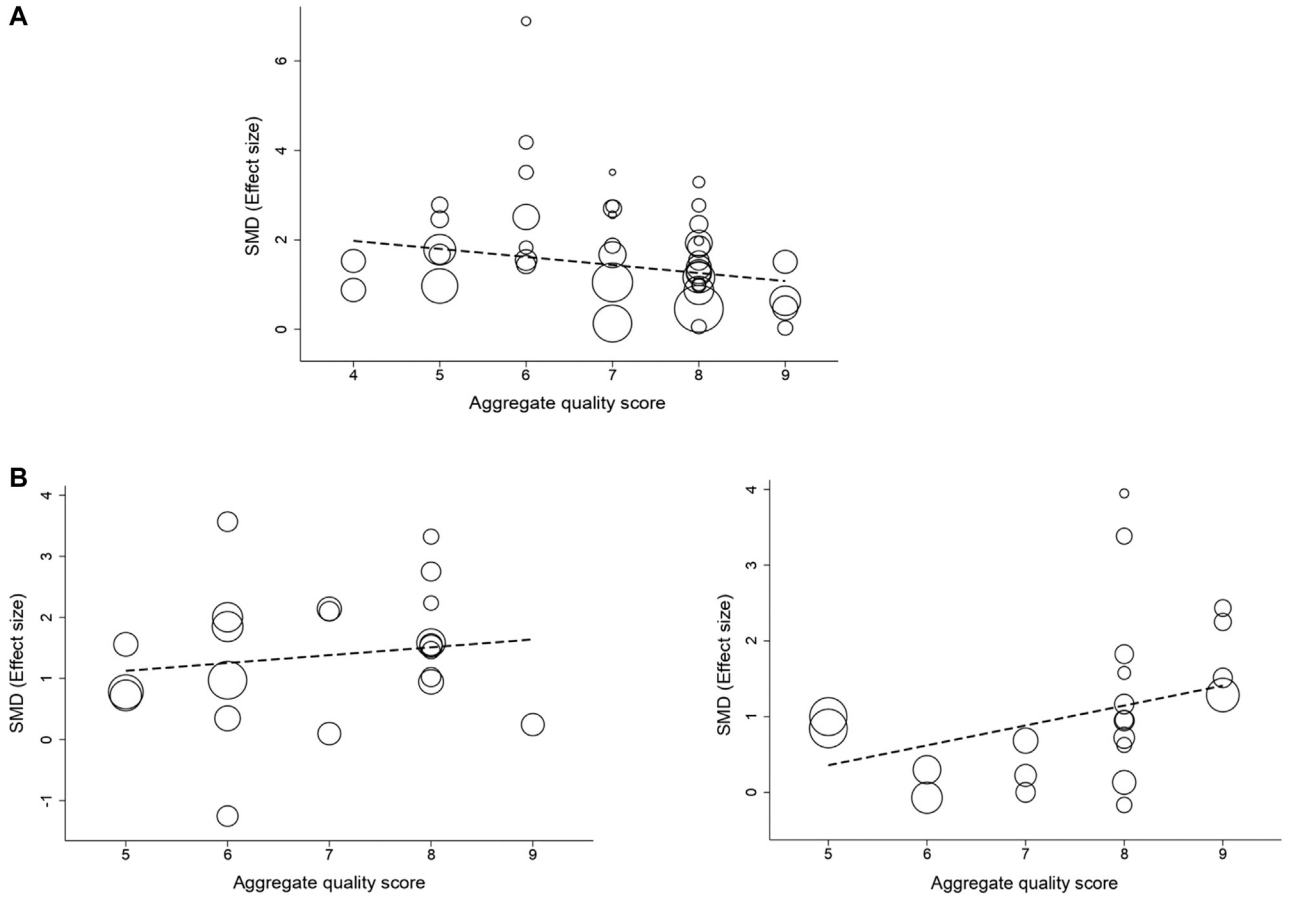

FIGURE 4 | The correlation between study quality score and effect size in intracerebral hemorrhage **(A)**, infarct size **(B)**, and neurobehavioral score **(C)**. The sizes of hollow circles represent the relative number of animals tested for each intervention.

Publication Bias

Potential publication bias was assessed by funnel plots, trim and fill method, and Egger's test. Funnel plots showed obvious asymmetry for intracerebral hemorrhage, and minor asymmetry for infarct size and neurobehavioral outcome (**Figure 6A**). Trim and fill analysis suggested 14 theoretically missing studies with an adjusted reduction in intracerebral hemorrhage of 1.06 SMD (95% CI, 0.86 to 1.26; compared with 1.31 SMD [95% CI, 1.09–1.52]; **Figure 6B**). We also estimate five theoretically missing studies with an adjusted reduction in infarct size of 1.04 SMD (95% CI, 0.62 to 1.47; compared with 1.35 SMD [95% CI, 0.95–1.76]), and four unpublished studies with an adjusted improvement in neurobehavioral outcome of 0.74 SMD (95% CI, 0.52 to 0.96; compared with 0.9 SMD [95% CI, 0.67–1.13]). Egger's regression test indicated significant publication bias for intracerebral hemorrhage ($p < 0.001$; **Figure 6C**). Whereas Egger's regression showed no publication bias for infarct size ($p = 0.194$) and neurobehavioral outcome ($p = 0.068$).

Sensitivity Analysis

Sensitivity analysis was conducted by removing one study at a time to explore whether the results were robust. Results from sensitivity analysis showed that excluding any one study did not affect the results, which demonstrated the stability of our results (**Figure 7**).

DISCUSSION

This study evaluated the preclinical literature reporting administration of immunomodulators for the treatment of tPA-induced HT after ischemic stroke. Twenty-two different studies were finally included in this systematic review and meta-analysis. Our results found that immunomodulators led to a reduction in intracerebral hemorrhage, infarct size, and neurobehavioral outcome in animal models of tPA-induced HT. We also found that study quality, temperature control, and evaluation time of outcome were significant factors affecting the efficacy of immunomodulators.

Inflammation plays a critical role in the BBB damage after ischemic stroke(Li et al., 2018). Administration with tPA after stroke exacerbates inflammatory response through various mechanisms including enhancing leukocyte infiltration (Jin et al., 2019) and activating matrix metalloproteinases

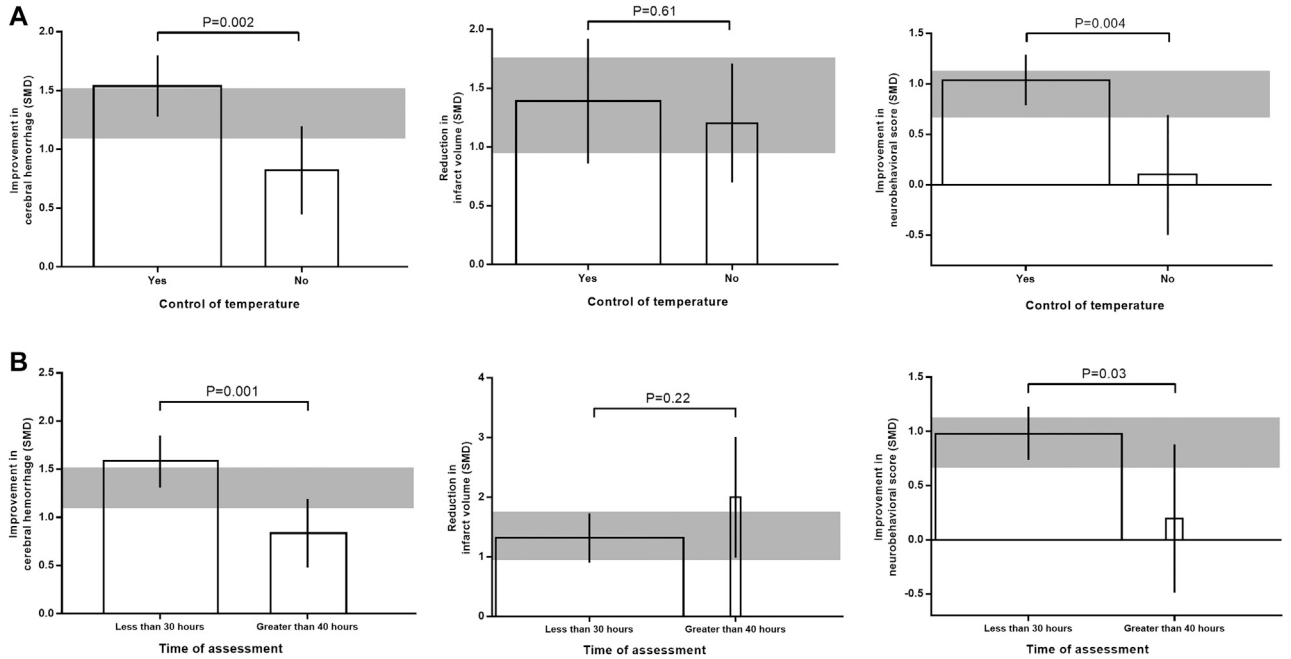

FIGURE 5 | Effects of temperature control **(A)** and time of outcome assessment **(B)** on the efficacy of immunomodulators in intracerebral hemorrhage, infarct size, and neurobehavioral score. The width of each bar represent the relative number of animals in that subgroup. The vertical error bars represent the 95% confidence interval for the individual estimates and the horizontal gray bars represent the 95% confidence interval of the pooled estimate of efficacy.

(MMPs)(Mao et al., 2017). The integrity of BBB was further damaged after tPA treatment, which would eventually lead to lethal intracerebral hemorrhage (Li et al., 2019). Therefore, limiting inflammatory responses may help to reduce the risk of brain hemorrhage and improve the safety of tPA treatment following stroke. Various of immunomodulators have been used in preclinical studies to reduce the risk of hemorrhage induced by tPA treatment. In our analysis, immunomodulators exhibited robust efficacy on tPA-induced intracerebral hemorrhage, cerebral infarction, and neurobehavioral impairments in experimental stroke. Immunomodulators had shown great clinical potential to alleviate cerebral hemorrhage associated with tPA, though relevant clinical trial is lacking.

The study quality overall was high. Only two study received a relatively low score of 4. Some study quality items such as the use of co-morbid animals and sample size calculation were rarely reported. A significant positive correlation was found between study quality and publication year, which was consistent with the previous finding that study quality improved over time (Vahidy et al., 2016). Moreover, there was no significant correlation between study quality and journal impact factor. Paper published in high impact factor journal does not mean it's of high study quality. This was probably because that even high impact factor journals were mostly low-quality in the early days, but even low impact factor journals were mostly high-quality now. Besides, we also found that study quality is one of the important factors that affect the efficacy of immunomodulators. For intracerebral hemorrhage, a significant negative correlation was found between study quality and effect size. Positive outcomes are more likely to happen in low-quality studies, which is consistent with previous findings (Antonic et al., 2013). However, this theory was inapplicable for infarct size and neurobehavioral outcome in our study. Maybe the relative limited sample size can partly account for the results.

Studies that conducted temperature control during surgery was significantly associated with a higher effect size. This may partly because that animals can get better rehabilitation from good operation environment (Xiao et al., 2013). Furthermore, control of temperature was also highly recommend from the perspective of animal ethics. A significant correlation was also observed between time of assessment and effect size. Larger improvements were seen in studies that reported assessment time less than 30 h after stroke onset. This was possibly because that tPA induced pathological damage was still deteriorating after 30 h from the initiation of stroke.

Our analysis showed that there was no significant correlation of effect size with the anesthetic used, route of drug delivery, blinded assessment, and random allocation (see **Supplemental Material**). The effects of sample size calculation, animal model used, time of drug delivery, and animal species were also analyzed (data not shown). They had no significant correlation with the efficacy of immunomodulators.

Evidence from funnel plots and Egger's test showed that obvious asymmetry was observed for intracerebral hemorrhage but only minor asymmetry was found for infarct size and neurobehavioral outcome. After a correction for potential publication bias by using the trim and fill method, the main results for all studies combined were still significant. This

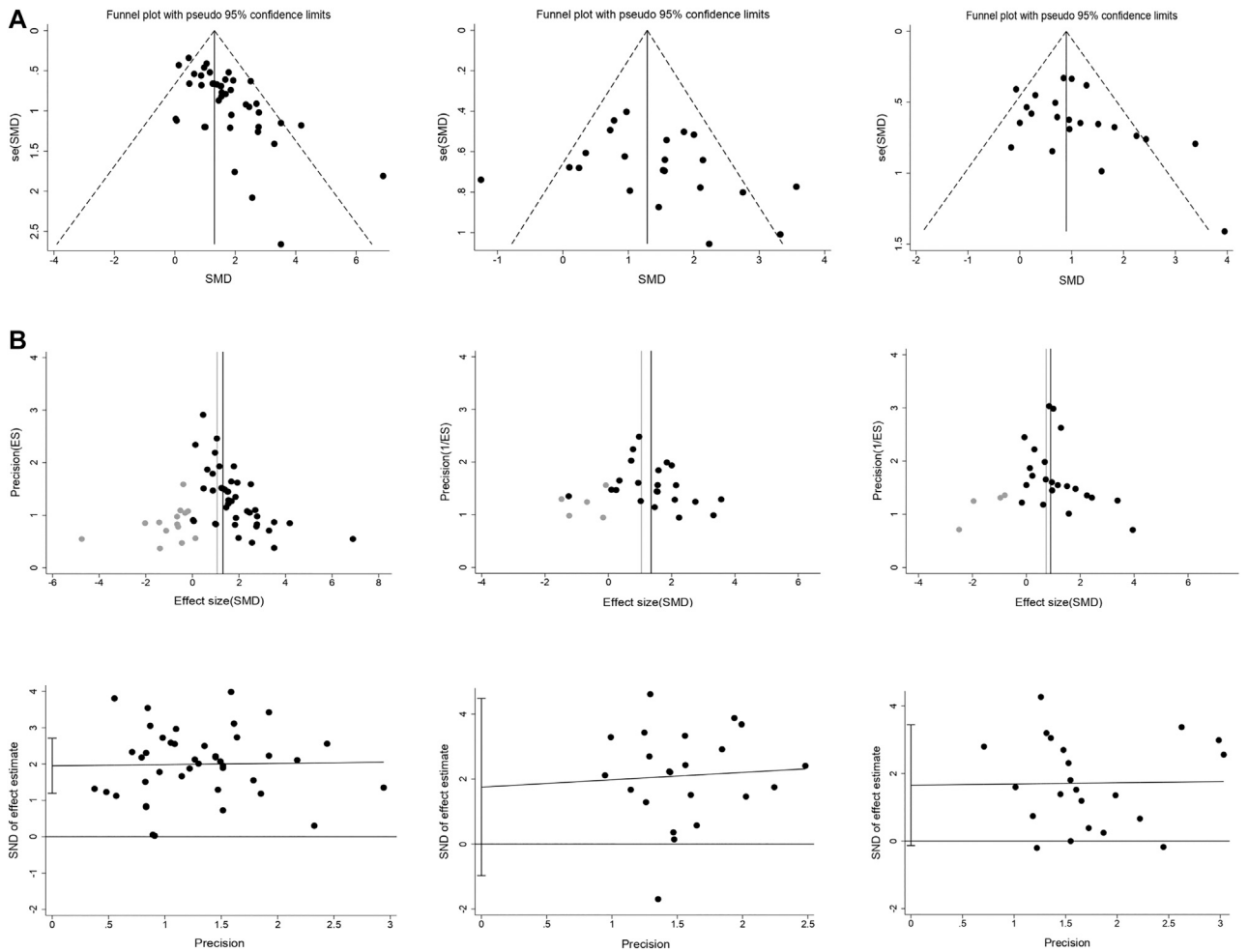

FIGURE 6 | Publication bias assessment. Funnel plots **(A)** for intracerebral hemorrhage, infarct size, and neurobehavioral score showing the publication bias. Trim and fill analysis **(B)** showed the distribution of published study outcomes (black circles) and imputed outcomes (gray circles) in intracerebral hemorrhage, infarct size, and neurobehavioral score. The vertical black lines represent the actual estimate and the gray vertical lines represent the theoretical estimate when publication bias does not exist. Egger's regression **(C)** for intracerebral hemorrhage, infarct size, and neurobehavioral score confirming potential evidence for publication bias. The short vertical lines represent the 95% confidence interval.

suggested that the publication bias observed did not significantly impact this analysis. Sensitivity analysis confirmed that the results of this study were stable.

Although the results of this meta-analysis are very good, the conclusions should be interpreted cautiously given this analysis is based on animal studies. Animal models cannot realistically simulate the pathophysiology involved in patients. Moreover, murine models have markedly different immune systems from humans. So it's hard to translate the results of animal studies into the clinical setting efficiently, conclusions from the present study also need to be treated with caution.

There are several limitations of this study. First, immunomodulator is a general term for a large class of drugs. It's hard to evaluate the efficacy of specific class of immunomodulators due to the lack of sufficient studies. Second, no female animals were used in all the included studies, so it is impossible to assess the efficacy of immunomodulators on female animals. Moreover, only English-language publications were included in this study, which may cause publication bias to some degree.

CONCLUSION

To the best of our knowledge, this is the first systematic review and meta-analysis which has evaluated the efficacy of immunomodulators on tPA-induced HT in animal models. This meta-analysis confirmed that immunomodulators may improve intracerebral hemorrhage, infarct size, and neurobehavioral outcome in animal models of tPA-induced HT. Furthermore, this study also demonstrated some factors such as study quality score, control of temperature during surgery, and evaluation time of outcome may affect the

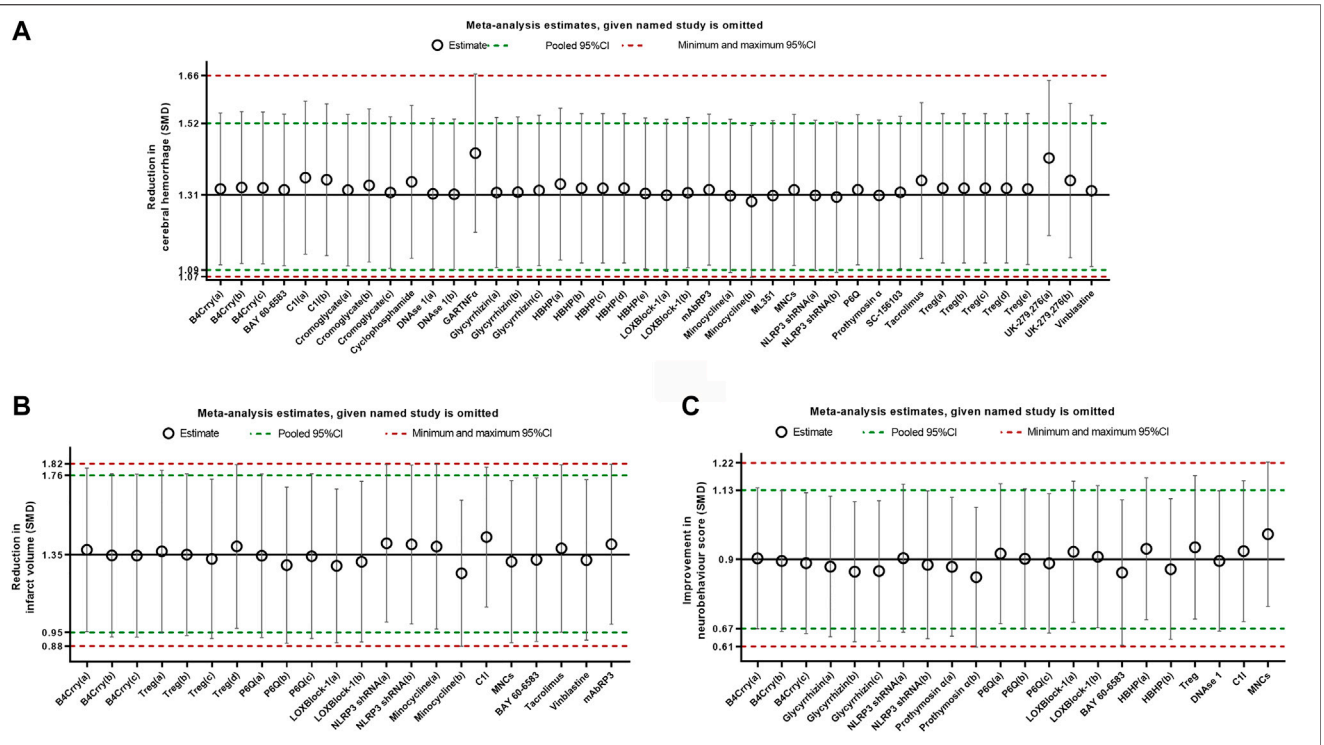

FIGURE 7 | Sensitivity analysis for intracerebral hemorrhage **(A)**, infarct size **(B)**, and neurobehavioral score **(C)** evaluating the robustness of the results. The vertical error bars represent the 95% confidence interval for the individual estimates. The horizontal red bars represent the potentially minimum and maximum 95% confidence interval and the horizontal green bars represent the actual 95% confidence interval of the pooled estimate of efficacy.

efficacy of immunomodulators. The results of this study will be help to refine animal experiments in this field and hence reduce the number of animals used in experiments.

DATA AVAILABILITY STATEMENT

The original contributions presented in the study are included in the article/**Supplemental Material**, further inquiries can be directed to the corresponding authors.

AUTHOR CONTRIBUTIONS

Conception and design: YY and H-XT. Screening of titles and abstracts, full-text data extraction: YY and Y-TZ. Analysis and interpretation of data, drafting the article: YY and J-YH. Critically revising the article: J-YH, Y-TZ, and H-XT. Statistical analysis: YY.

FUNDING

This study was supported by the National Natural Science Foundation of China (Grant No. 81903942) and the China Postdoctoral Science Foundation (Grant No. 2019M650393).

SUPPLEMENTARY MATERIAL

The Supplementary Material for this article can be found online at: https://www.frontiersin.org/articles/10.3389/fphar.2020.615166/full#supplementary-material.

REFERENCES

Alawieh, A. M., Langley, E. F., Feng, W., Spiotta, A. M., and Tomlinson, S. (2020). Complement-dependent synaptic uptake and cognitive decline after stroke and reperfusion therapy. *J. Neurosci.* 40 (20), 4042–4058. doi:10.1523/JNEUROSCI.2462-19.2020

Antonic, A., Sena, E. S., Lees, J. S., Wills, T. E., Skeers, P., Batchelor, P. E., et al. (2013). Stem cell transplantation in traumatic spinal cord injury: a systematic review and meta-analysis of animal studies. *PLoS Biol.* 11 (12), e1001738. doi:10.1371/journal.pbio.1001738

Chen, H., Guan, B., Wang, B., Pu, H., Bai, X., Chen, X., et al. (2020). Glycyrrhizin prevents hemorrhagic transformation and improves neurological outcome in ischemic stroke with delayed thrombolysis through targeting peroxynitrite-mediated HMGB1 signaling. *Transl Stroke Res* 11 (5), 967–982. doi:10.1007/s12975-019-00772-1

Copin, J. C., Merlani, P., Sugawara, T., Chan, P. H., and Gasche, Y. (2008). Delayed matrix metalloproteinases inhibition reduces intracerebral hemorrhage after embolic stroke in rats. *Exp. Neurol.* 213 (1), 196–201. doi:10.1016/j.expneurol.2008.05.022

Fan, X., Lo, E. H., and Wang, X. (2013). Effects of minocycline plus tissue plasminogen activator combination therapy after focal embolic stroke in

type 1 diabetic rats. *Stroke* 44 (3), 745–752. doi:10.1161/STROKEAHA.111.000309

Gautier, S., Ouk, T., Petrault, O., Caron, J., and Bordet, R. (2009). Neutrophils contribute to intracerebral haemorrhages after treatment with recombinant tissue plasminogen activator following cerebral ischaemia. *Br. J. Pharmacol.* 156 (4), 673–679. doi:10.1111/j.1476-5381.2009.00068.x

Guo, Z., Yu, S., Chen, X., Zheng, P., Hu, T., Duan, Z., et al. (2018). Suppression of NLRP3 attenuates hemorrhagic transformation after delayed rtPA treatment in thromboembolic stroke rats: involvement of neutrophil recruitment. *Brain Res. Bull.* 137, 229–240. doi:10.1016/j.brainresbull.2017.12.009

Halder, S. K., Matsunaga, H., and Ueda, H. (2020). Prothymosin alpha and its mimetic hexapeptide improve delayed tissue plasminogen activator-induced brain damage following cerebral ischemia. *J. Neurochem.* 153 (6), 772–789. doi:10.1111/jnc.14858

Jin, R., Xiao, A. Y., Li, J., Wang, M., and Li, G. (2019). PI3Kgamma (phosphoinositide 3-Kinase-gamma) inhibition attenuates tissue-type plasminogen activator-induced brain hemorrhage and improves microvascular patency after embolic stroke. *Hypertension* 73 (1), 206–216. doi:10.1161/HYPERTENSIONAHA.118.12001

Jin, R., Xiao, A. Y., Liu, S., Wang, M., and Li, G. (2018). Taurine reduces tPA (Tissue-Type plasminogen activator)-induced hemorrhage and microvascular thrombosis after embolic stroke in rat. *Stroke* 49 (7), 1708–1718. doi:10.1161/STROKEAHA.118.020747

Karatas, H., Eun Jung, J., Lo, E. H., and Van Leyen, K. (2018). Inhibiting 12/15-lipoxygenase to treat acute stroke in permanent and tPA induced thrombolysis models. *Brain Res.* 1678, 123–128. doi:10.1016/j.brainres.2017.10.024

Lapchak, P. A. (2007). Tumor necrosis factor-alpha is involved in thrombolytic-induced hemorrhage following embolic strokes in rabbits. *Brain Res.* 1167, 123–128. doi:10.1016/j.brainres.2007.06.072

Li, M., Chen, S., Shi, X., Lyu, C., Zhang, Y., Tan, M., et al. (2018). Cell permeable HMGB1-binding heptamer peptide ameliorates neurovascular complications associated with thrombolytic therapy in rats with transient ischemic stroke. *J. Neuroinflammation* 15 (1), 237. doi:10.1186/s12974-018-1267-5

Li, Q., Han, X., Lan, X., Hong, X., Li, Q., Gao, Y., et al. (2017). Inhibition of tPA-induced hemorrhagic transformation involves adenosine A2b receptor activation after cerebral ischemia. *Neurobiol. Dis.* 108, 173–182. doi:10.1016/j.nbd.2017.08.011

Li, Y., Zhu, Z. Y., Lu, B. W., Huang, T. T., Zhang, Y. M., Zhou, N. Y., et al. (2019). Rosiglitazone ameliorates tissue plasminogen activator-induced brain hemorrhage after stroke. *CNS Neurosci. Ther.* 25 (12), 1343–1352. doi:10.1111/cns.13260

Liu, Y., Zheng, Y., Karatas, H., Wang, X., Foerch, C., Lo, E. H., et al. (2017). 12/15-Lipoxygenase inhibition or knockout reduces warfarin-associated hemorrhagic transformation after experimental stroke. *Stroke* 48 (2), 445–451. doi:10.1161/STROKEAHA.116.014790

Maeda, M., Furuichi, Y., Noto, T., Matsuoka, N., Mutoh, S., and Yoneda, Y. (2009). Tacrolimus (FK506) suppresses rt-PA-induced hemorrhagic transformation in a rat thrombotic ischemia stroke model. *Brain Res.* 1254, 99–108. doi:10.1016/j.brainres.2008.11.080

Mao, L., Li, P., Zhu, W., Cai, W., Liu, Z., Wang, Y., et al. (2017). Regulatory T cells ameliorate tissue plasminogen activator-induced brain haemorrhage after stroke. *Brain* 140 (7), 1914–1931. doi:10.1093/brain/awx111

Mccann, S. K., Irvine, C., Mead, G. E., Sena, E. S., Currie, G. L., Egan, K. E., et al. (2014). Efficacy of antidepressants in animal models of ischemic stroke: a systematic review and meta-analysis. *Stroke* 45 (10), 3055–3063. doi:10.1161/STROKEAHA.114.006304

Murata, Y., Rosell, A., Scannevin, R. H., Rhodes, K. J., Wang, X., and Lo, E. H. (2008). Extension of the thrombolytic time window with minocycline in experimental stroke. *Stroke* 39 (12), 3372–3377. doi:10.1161/STROKEAHA.108.514026

Pena, I. D., Borlongan, C., Shen, G., and Davis, W. (2017). Strategies to extend thrombolytic time window for ischemic stroke treatment: an unmet clinical need. *J. Stroke* 19 (1), 50–60. doi:10.5853/jos.2016.01515

Pimpin, L., Kranz, S., Liu, E., Shulkin, M., Karageorgou, D., Miller, V., et al. (2019). Effects of animal protein supplementation of mothers, preterm infants, and term infants on growth outcomes in childhood: a systematic review and meta-analysis of randomized trials. *Am. J. Clin. Nutr.* 110 (2), 410–429. doi:10.1093/ajcn/nqy348

Satapathy, S., Mittal, B. R., and Sood, A. (2020). Visceral metastases as predictors of response and survival outcomes in patients of castration-resistant prostate cancer treated with 177Lu-labeled prostate-specific membrane antigen radioligand therapy: a systematic review and meta-analysis. *Clin. Nucl. Med.* 45 (12), 935–942. doi:10.1097/RLU.0000000000003307

Sena, E., Van Der Worp, H. B., Howells, D., and Macleod, M. (2007). How can we improve the pre-clinical development of drugs for stroke? *Trends Neurosci.* 30 (9), 433–439. doi:10.1016/j.tins.2007.06.009

Sorby-Adams, A. J., Marcoionni, A. M., Dempsey, E. R., Woenig, J. A., and Turner, R. J. (2017). The role of neurogenic inflammation in blood-brain barrier disruption and development of cerebral oedema following acute central nervous system (CNS) injury. *Int. J. Mol. Sci.* 18 (8). doi:10.3390/ijms18081788

Strbian, D., Karjalainen-Lindsberg, M. L., Kovanen, P. T., Tatlisumak, T., and Lindsberg, P. J. (2007). Mast cell stabilization reduces hemorrhage formation and mortality after administration of thrombolytics in experimental ischemic stroke. *Circulation* 116 (4), 411–418. doi:10.1161/CIRCULATIONAHA.106.655423

Tan, Q., Guo, P., Zhou, J., Zhang, J., Zhang, B., Lan, C., et al. (2019). Targeting neutrophil extracellular traps enhanced tPA fibrinolysis for experimental intracerebral hemorrhage. *Transl. Res.* 211, 139–146. doi: doi:10.1016/j.trsl.2019.04.009

Tomasi, S., Sarmientos, P., Giorda, G., Gurewich, V., and Vercelli, A. (2011). Mutant prourokinase with adjunctive C1-inhibitor is an effective and safer alternative to tPA in rat stroke. *PLoS One* 6 (7), e21999. doi:10.1371/journal.pone.0021999

Vahidy, F. S., Rahbar, M. H., Zhu, H., Rowan, P. J., Bambhroliya, A. B., and Savitz, S. I. (2016). Systematic review and meta-analysis of bone marrow-derived mononuclear cells in animal models of ischemic stroke. *Stroke* 47 (6), 1632–1639. doi:10.1161/STROKEAHA.116.012701

Wang, J., Zhang, Z., Li, Y., Xu, Y., Wan, K., and Chen, Y. (2019). Variable and limited predictive value of the European society of cardiology hypertrophic cardiomyopathy sudden-death risk model: a meta-analysis. *Can. J. Cardiol.* 35 (12), 1791–1799. doi:10.1016/j.cjca.2019.05.004

Xiao, H., Run, X., Cao, X., Su, Y., Sun, Z., Tian, C., et al. (2013). Temperature control can abolish anesthesia-induced tau hyperphosphorylation and partly reverse anesthesia-induced cognitive impairment in old mice. *Psychiatr. Clin. Neurosci.* 67 (7), 493–500. doi:10.1111/pcn.12091

Xu, X. H., Gao, T., Zhang, W. J., Tong, L. S., and Gao, F. (2017). Remote diffusion-weighted imaging lesions in intracerebral hemorrhage: characteristics, mechanisms, outcomes, and therapeutic implications. *Front. Neurol.* 8, 678. doi:10.3389/fneur.2017.00678

Yang, B., Li, W., Satani, N., Nghiem, D. M., Xi, X., Aronowski, J., et al. (2018). Protective effects of autologous bone marrow mononuclear cells after administering t-PA in an embolic stroke model. *Transl Stroke Res* 9 (2), 135–145. doi:10.1007/s12975-017-0563-1

Yang, Z. Y., Shen, W. X., Hu, X. F., Zheng, D. Y., Wu, X. Y., Huang, Y. F., et al. (2012). EGFR gene copy number as a predictive biomarker for the treatment of metastatic colorectal cancer with anti-EGFR monoclonal antibodies: a meta-analysis. *J. Hematol. Oncol.* 5, 52. doi:10.1186/1756-8722-5-52

Yigitkanli, K., Pekcec, A., Karatas, H., Pallast, S., Mandeville, E., Joshi, N., et al. (2013). Inhibition of 12/15-lipoxygenase as therapeutic strategy to treat stroke. *Ann. Neurol.* 73 (1), 129–135. doi:10.1002/ana.23734

Zhang, L., Zhang, Z. G., Zhang, R. L., Lu, M., Krams, M., and Chopp, M. (2003). Effects of a selective CD11b/CD18 antagonist and recombinant human tissue plasminogen activator treatment alone and in combination in a rat embolic model of stroke. *Stroke* 34 (7), 1790–1795. doi:10.1161/01.STR.0000077016.55891.2E

Conflict of Interest: The authors declare that the research was conducted in the absence of any commercial or financial relationships that could be construed as a potential conflict of interest.

frontiers in Pharmacology

ORIGINAL RESEARCH
published: 22 January 2021
doi: 10.3389/fphar.2020.607287

Netosis and Inflammasomes in Large Vessel Occlusion Thrombi

*Stephanie H. Chen[1], Xavier O. Scott[2], Yoandy Ferrer Marcelo[1], Vania W. Almeida[1], Patricia L. Blackwelder[4], Dileep R. Yavagal[5], Eric C. Peterson[1], Robert M. Starke[1], W. Dalton Dietrich[1], Robert W. Keane[1,2] and Juan Pablo de Rivero Vaccari[1,3]**

[1]Department of Neurological Surgery and the Miami Project to Cure Paralysis, University of Miami Miller School of Medicine, Miami, FL, United States, [2]Department of Physiology and Biophysics, University of Miami Miller School of Medicine, Miami, FL, United States, [3]Center for Cognitive Neuroscience and Aging University of Miami Miller School of Medicine, Miami, FL, United States, [4]University of Miami Center for Advanced Microscopy (UMCAM) and Department of Chemistry, University of Miami, Coral Gables, FL, United States, [5]Department of Neurology, University of Miami Miller School of Medicine, Miami, FL, United States

The inflammatory response appears to play a critical role in clotting in which neutrophil extracellular traps (NETs) are the major drivers of thrombosis in acute ischemic stroke (AIS). The inflammasome is an innate immune complex involved in the activation of interleukin (IL)-18 and IL-1β through caspase-1, but whether the inflammasome plays a role in NETosis in AIS remains poorly understood. Here we assessed the levels of inflammasome signaling proteins in NETs and their association with clinical and procedural outcomes of mechanical thrombectomy for AIS. Electron microscopy and immunofluorescence indicate the presence of NETs in thrombi of patients with AIS. Moreover, the inflammasome signaling proteins caspase-1 and apoptosis-associated speck-like protein containing a caspase recruitment domain (ASC) were also present in clots associated with the marker of NETosis citrullinated histone ^{3}H (CitH3). Analysis of protein levels by a simple plex assay show that caspase-1, ASC and interleukin (IL)-1β were significantly elevated in clots when compared to plasma of AIS patients and healthy controls, while IL-18 levels were lower. Moreover, multivariate analyses show that IL-1β levels in clots contribute to the number of passes to achieve complete recanalization, and that ASC, caspase-1 and IL-18 are significant contributors to time to recanalization. Thus, inflammasome proteins are elevated in NETs present in thrombi of patients with AIS that contribute to poor outcomes following stroke.

Keywords: inflammation, stroke, inflammasome, thrombus, caspase-1, ASC, neutrophil extracellular traps, NETs

OPEN ACCESS

Edited by:
Imola Wilhelm,
Biological Research Center, Hungary

Reviewed by:
Gabriela Constantin,
University of Verona, Italy
Ádám Nyúl-Tóth,
University of Oklahoma Health Sciences Center, United States

****Correspondence:***
Juan Pablo de Rivero Vaccari
JdeRivero@med.miami.edu

Specialty section:
This article was submitted to Inflammation Pharmacology, a section of the journal Frontiers in Pharmacology

Received: *16 September 2020*
Accepted: *18 December 2020*
Published: *22 January 2021*

Citation:
Chen SH, Scott XO, Ferrer Marcelo Y, Almeida VW, Blackwelder PL, Yavagal DR, Peterson EC, Starke RM, Dietrich WD, Keane RW and de Rivero Vaccari JP (2021) Netosis and Inflammasomes in Large Vessel Occlusion Thrombi. Front. Pharmacol. 11:607287. doi: 10.3389/fphar.2020.607287

INTRODUCTION

Stroke is the leading cause of long-term disability and the second leading cause of death worldwide. Although large vessel occlusion acute ischemic strokes (LVOS) account for approximately 40% of ischemic strokes, they are disproportionately associated with severe disability and mortality (Rennert et al., 2019). Currently, treatment options for LVOS are limited to intravenous alteplase (tPA) within 4.5 h as well as mechanical thrombectomy within 24 h of symptom onset (Powers et al., 2019). While early reperfusion has been shown to improve functional outcomes, many patients are ineligible or lack access to treatment (Fransen et al., 2014; Goyal et al., 2016a; Goyal et al., 2016b; Jadhav et al.,

2018). Moreover, over half of the patients who are treated with endovascular intervention and/or tPA remain severely disabled or deceased at 90 days (Goyal et al., 2016b; Hankey, 2017). While the thrombus is the primary target of stroke treatment, little is known about the composition and pathogenesis following stroke. Previous studies attempted to use computed tomography (CT) and magnetic resonance imaging (MRI) to predict clot density (Niesten et al., 2014; Kim et al., 2015; Jagani et al., 2017). However, a further understanding of the dynamic processes of clot pathology is necessary in order to translate these findings into improved clinical treatment methods.

Cerebral thrombus histopathology reveals common components, including presence of platelets, leukocytes, and red blood cells in diverse histological and quantitative patterns (Brinjikji et al., 2017). The heterogeneity of thrombi composition is thought to be associated with thrombus origin. However, recent studies have detected extensive neutrophil extracellular traps (NETs) throughout all LVOS thrombi (Laridan et al., 2017; Ducroux et al., 2018). NETs are large extracellular web-like structures composed of decondensed chromatin lined with granular and cytosolic proteins (Brinkmann et al., 2004) that are formed in a cell death pathway known as NETosis (Gupta et al., 2010). In addition to acting as a scaffold for platelets and red blood cells, NETs have a pro-inflammatory role that is associated with thrombogenesis in the arterial and venous vasculature (Kimball et al., 2016; Laridan et al., 2019).

The inflammasome is a multiprotein complex comprised of a sensor such as a NOD-like receptor (NLR), the adaptor protein apoptosis-associated speck-like protein containing a caspase-recruitment domain (ASC) and the inflammatory cysteine aspartase caspase-1 (Govindarajan et al., 2020). We have previously shown that the NRLP1 inflammasome is activated following cerebral ischemia in rodents (Abulafia et al., 2009). In addition, numerous studies have reported inflammasome involvement in the pathogenesis of cerebral ischemia (Kastbom et al., 2015; Tong et al., 2015; Gao et al., 2017; Ismael et al., 2018; Yang et al., 2018; Kim et al., 2020). The NLRP1 inflammasome was the first inflammasome reported to play a role in cerebral ischemia (Abulafia et al., 2009). However, inhibition of the NLRP3 inflammasome with intravenous immunoglobulin has been shown to be neuroprotective is an animal model of stroke (Fann et al., 2013), and studies in NLRP3 knockout mice indicate that NLRP3 deletion results in decreased infarct volume, decreased edema and decreased permeability of the blood brain barrier (Yang et al., 2014). Moreover, inflammasome proteins in humans have been shown to be reliable biomarkers of central nervous system (CNS) injury (Adamczak et al., 2012; Kerr et al., 2018b; Perez-Barcena et al., 2020) and disease (Keane et al., 2018; Scott et al., 2020), including stroke (Kerr et al., 2018a). Thus, the inflammasome is an important regulator of the inflammatory innate immune response following stroke.

Here we isolated thrombi and plasma from patients following AIS and performed electron microscopy and immunofluorescent staining to determine the cytoarchitecture of thrombi and the composition of NETs and the inflammasome proteins in clots in this patient population.

TABLE 1 | Baseline characteristics of patients who underwent mechanical thrombectomy.

Patient and procedural characteristics (N = 30)	
Mean age (StdDev)	70 (15)
Male (%)	18 (60%)
Median NIHSS (SEM)	16 (1.1)
IV tPA (%)	14 (46%)
Comorbidities	
Congestive heart failure (%)	3 (10%)
Atrial fibrillation (%)	14 (47%)
Coronary artery disease (%)	10 (33%)
Diabetes mellitus (%)	9 (30%)
Hyperlipidemia (%)	13 (43%)
Hypertension (%)	26 (87%)
Cancer (%)	5 (17%)
Prior stroke (%)	9 (30%)
Smoking (%)	13 (43%)
Substance abuse (%)	4 (13%)
Antiplatelet (%)	4 (13%)
Anticoagulation (%)	6 (20%)
Median mRS pre-MT	0 (0.23)
Median time LKN to recanalization (SEM)	303 min (92)
Mean # passes	1.8 (1.1)
Stentriever (%)	22 (73%)
ADAPT (%)	8 (2.7%)
TICI score	
2B (%)	2 (6.7%)
2C (%)	7 (23%)
3 (%)	21 (70%)
Hemorrhage	
rICH (%)	9 (30%)
sICH (%)	2 (6.7%)
Median mRS @ discharge	4 (0.39)
Death (%)	7 (23%)

tPA, tissue plasminogen activator; mRS, modified ranking score; MT, mechanical thrombectomy; LKN, Last known normal; ADAPT, a direct aspiration first pass technique, TICI: thrombolysis in cerebral infarction; rICH, radiographic intracranial hemorrhage; sIH, symptomatic intracranial hemorrhage.

MATERIAL AND METHODS

Participants

Between November 2018 and November 2019, we conducted a prospective study investigating thrombi retrieved from mechanical thrombectomy procedures in AIS patients admitted to Jackson Memorial Hospital/University of Miami Hospital (**Table 1**). All patients with age ≥18 years old who presented with acute stroke and underwent thrombectomy with retrieval of thrombus material were eligible for the study. Ethics approval was approved by the Institutional Review Board at the University of Miami (IRB 20160699), and informed consent was obtained from all patients included in this study. Patients were excluded if adequate thrombus material could not be obtained or the patient/legal representative refused to participate in the study. Patient demographics, clinical presentation, neurological exam (National Institutes of Health Stroke Scale (NIHSS)), pre-procedural imaging results, intravenous tissue plasminogen activator (IV-tPA) administration, procedural details including number of passes, thrombectomy technique used, recanalization results (Thrombolysis in Cerebral Infarction (TICI) scale, and follow-up data were collected. A total of 30 clots were obtained

from patients undergoing mechanical thrombectomy. Following mechanical thrombectomy, six clots were fixed in 4% paraformaldehyde for histology and the remaining 24 clots were processed for molecular analysis. Healthy control samples were purchased from BioIVT (Hicksville, NY), and they were obtained from donors without any diagnosed disease.

Thrombectomy Procedure

The mechanical thrombectomy procedures were all performed or supervised by board-certified neurointerventional experts under biplane neuroangiography (Artis Q, Siemens Healthcare, Erlangen, Germany). All patients were treated under general anesthesia, per institutional protocol. Site of access and thrombectomy technique were at the discretion of the treating physician. If an aspiration-alone technique was used, a large guide catheter was navigated into the cervical segment of the target vessel, then a microcatheter (0.027″) telescoped through the aspiration catheter (0.068″ or 0.071″) was introduced and navigated just proximal to the clot. With the aspiration pump initiated, the aspiration catheter was brought over the microcatheter to the face of the clot. The microcatheter was then removed for improved aspiration and the aspiration catheter was retracted. Moreover, if a Solumbra technique was used, a guide catheter (balloon guide or 0.088") was brought into the cervical segment of the target vessel, a microcatheter telescoped through an aspiration catheter was introduced and navigated over a microwire past the site of occlusion. The microwire was then removed and the stent retriever was deployed through the microcatheter across the occluded segment. The microcatheter was then removed and aspiration from the aspiration catheter was initiated. The stent retriever was left in place for 5 min to encourage integration of the clot and then slowly retracted under constant aspiration into the guide catheter. Heparin was not administered during mechanical thrombectomy, although non-therapeutic doses of 1,000 IU unfractionated heparin were always added to the 1-L bags of standard 0.9% saline flushes in order to avoid catheter-associated thrombus formation.

Immunofluorescence

For immunohistochemical procedures, six clots were fixed in 4% paraformaldehyde overnight, and then processed for paraffin embedment as described in (de Rivero Vaccari et al., 2009). Sections were then double-stained with primary antibodies rabbit anti-caspase-1 (Cat #06-503-I, EMD Millipore) or rabbit anti-ASC (amino acids 182-195, EMD Millipore) and mouse anti-Citrullinated-Histone H3 (amino acids 1-100, Abcam) followed by fluorescently labeled secondary Alexa Fluor antibodies (488 and 594) raised in goat (Invitrogen). Autofluorescence in sections was quenched using the Vector TrueVIEW Autofluorescence Quenching Kit (Vector Laboratories) according to manufacturer instructions. Sections were imaged using an EVOS FL Auto two Imaging System (ThermoFisher Scientific). Secondary antibodies alone were used as negative controls **(Supplementary Figure 1)**.

Immunoblotting

For immunoblot analysis of NLRP1 and ASC proteins from clots of nine different patients, protein was extracted and resolved as described in (Brand et al., 2015). Briefly, equal amounts of protein lysates (20 μg of total protein) were resolved in 4–20% Criterion TGX Stain-Free precasted gels (Bio-Rad). Protein was then transferred to polyvinylidene difluoride (PVDF) membranes (BioRad) using the Trans Blot Turbo System (BioRad). Membranes were then blocked in blocking buffer with I-Block (Applied Biosystems) diluted in phosphate buffered saline (PBS) and incubated with primary antibodies (1:1000 dilution) rabbit anti-NLRP1 (#NBP1-54899, Novus Biologicals) and rabbit anti-AIM2 (D-14, Santa Cruz) followed by incubation with anti-mouse IgG HRP-linked secondary antibodies (1:1000 dilution, Cell Signaling) and enhanced chemilluminescence using LumiGLO reagent (Cell Signaling). PVDF membranes were imaged using the ChemiDoc Touch Imaging System (BioRad).

Transmission Electron Microscopy (TEM)

Blood clot samples were fixed in 2% glutaraldehyde in 0.05 M phosphate buffer and 100 mM sucrose. Then they were post-fixed overnight in 1% osmium tetroxide in 0.1 M phosphate buffer, followed by dehydration and embedment in a mixture of EM-bed/Araldite (Electron Microscopy Sciences). One μm-thick sections were then stained with Richardson's stain for observation by light microscopy. One hundred ηM sections were then cut on a Leica Ultracut-R ultramicrotome and stained with uranyl acetate and lead citrate. Grids were viewed at 80 kV in a JEOL JEM-1400 transmission electron microscope. Images were captured by an AMT BioSprint digital camera.

Scanning Electron Microscopy (SEM)

For SEM imaging, blood clot samples were fixed in 2% glutaraldehyde in 1X phosphate buffer saline (PBS) (E.M. Sciences,Inc.), post-fixed for 1 h in 1% osmium tetroxide in PBS buffer, rinsed in buffer, dehydrated through a graded series of ethanols, and dried after three changes of Hexamethyldisilazane (HMDS) (E.M.Sciences,Inc.). Samples were then coated with a 20 nm layer of palladium (Pd) in a plasma sputter coater, and imaged in a Philips XL-30 Field Emission SEM.

Simple Plex Assays

Clots were analyzed using a four-plex assay for the protein expression of caspase-1, apoptosis-associated speck-like protein containing a caspase-recruitment domain (ASC), IL-18 and IL-1β (Protein Simple) as described in Brand *et al.* (Brand et al., 2016). Briefly, samples were diluted 50:50 in dilution buffer, and 50 μL were loaded in the respective wells of the cartridge. One ml of washing buffer was loaded in the assigned wells, and the assay was run in the Ella instrument (Protein Simple) using the Simple Plex Runner 3.5.2.20 software. Data were then processed using the Simple Plex Explorer 3.5.2.20, and further analyzed by Prism 8.0 statistical software (GraphPad Prism). Results presented correspond to the mean of samples run in triplicates.

Statistical Analyses

Statistical analyses were carried using Prism 8 (GraphPad Prism) software. Data were tested for normality using the

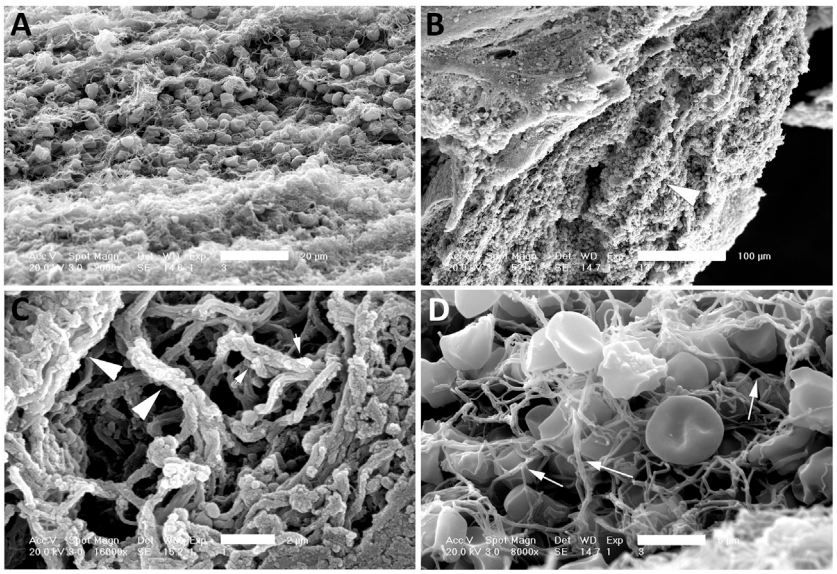

FIGURE 1 | SEM of clots from AIS patients. Clots were processed for SEM indicating the presence of red blood cells **(A and D)**, fibrin (arrow heads, B and C), histones (short arrows, C) and interconnected fibers (arrows, **D)** consistent with the presence of NETs in the clots of these patients. Scale bars: **(A)** 20 μm, **(B)** 100 μm, **(C)** 2 μm, **(D)** 5 μm.

D'Agostino and Pearson omnibus normality test. Comparison between groups for normally distributed data were done using a Kruskal-Wallis test followed by Dunn's multiple comparison test for data that were not normally distributed. p-values of significance were $p < 0.05$. Mean values of inflammatory cytokines in the clot lysate of LVOS patients were compared to plasma levels of stroke patients and healthy controls. In addition, linear and logistic regression using inflammasome protein concentration in the clot of patients and other clinical variables were done using RStudio software Version 1.2.5033 using the following packages: ggplot2, MASS, dplyr, broom, car, regclass and ROCit and with Stata 10.0 (College Station, TX). Factors predictive in univariate analysis ($p < 0.15$) were entered into a multivariate logistic regression analysis. p-values of ≤0.05 were considered statistically significant.

RESULTS

Patients With AIS

A total of 30 clots were retrieved by mechanical thrombectomy from patients presenting with acute large vessel occlusion stroke (**Table 1**). Mean patient age was 70 years old and the majority of patients were male (60%). Median national institutes of health stroke scale (NIHSS) score on presentation was 16, median time from last known well to recanalization was 303 min, all patients had a thrombolysis in cerebral infarction (TICI) score of 2B or greater, 11 patients had a modified ranking scale (mRS) less than three at discharge, and 23% of patients died during the hospitalization (Zaidat et al., 2018).

NETosis Is Present in the Clots of Patients With AIS

Coarse fibrin and activated platelets have been previously described in electron microscopy images of blood clots (Kawasaki et al., 2004). Isolated clots from patients that underwent thrombectomy following ischemic stroke were fixed and processed for electron microscopy procedures. Processed sections of clots from three different patients were analyzed by SEM (**Figure 1**) and TEM (**Figure 2**). A series of images were collected and the most representative images are presented in **Figures 1** and **2**. Accordingly, clots presented deformed red blood cells (**Figures 1A and 1D**), neutrophils (asterisk, 1D), interconnecting fibers (arrows, **Figure 1D**), fibrin (arrow heads, **Figures 1B and 1C**) and histones (short arrows, **Figure 1C**) that are consistent with the presence of neutrophil extracellular trap (NET) fibers. In addition, transmission electron microscopy analysis of the clots (**Figure 2**) indicate the presence of granulocytes (arrows, **Figures 2A and 2D**), red blood cells (asterisk, **Figures 2B and 2D**) and dying neutrophils (arrow heads, **Figure 2C**). Thus, these findings indicate that NETs are present in the clots of patients with LVOS in addition to neutrophils, deformed red blood cells, platelets, and fibrin.

Inflammasome Proteins Are Present in NETs of Patients With AIS

Inflammasome signaling in neutrophils has been previously associated with the formation of NETs and NETosis activation (Chen et al., 2018). To determine if inflammasome proteins are present in NETs present in the clots of patients with AIS, we stained immunohistochemical sections with antibodies against

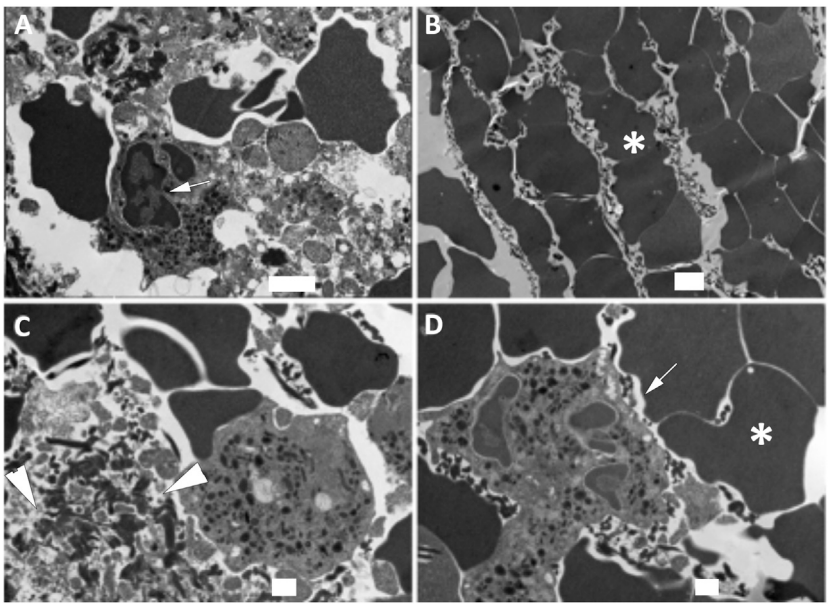

FIGURE 2 | TEM of clots from AIS patients. Clots were processed for TEM indicating the presence of granulocytes (arrows, **A and D)**, red blood cells (asterisk, **B and D)**, dying neutrophils (arrow heads, C) consistent with the presence of NETs in the clots of these patients. Scale bars: **(A)** 2 μm, **(B)** 2 μm, **(C)** 1 μm, **(D)** 1 μm.

the inflammasome signaling proteins caspase-1 and ASC, as well as citrullinated histone-3 (Cit-^{3}H), a marker of NETs. (Hirose et al., 2014). **Figure 3** shows that caspase-1 (green) and ASC (red) immunoreactivity were present in structures positive for CitH3, indicating that the inflammasome proteins caspase-1 and ASC are present in NETs within the clots of patients with AIS.

Inflammasome Signaling Proteins Are Elevated in the Clots of Patients With AIS

Inflammasome proteins have been previously shown to be elevated in the serum and extracellular vesicles of patients with stroke (Kerr et al., 2018a). To determine if inflammasome signaling proteins were elevated in the clots of patients with stroke, we obtained protein lysates from the clots of patients with AIS and analyzed the protein levels of caspase-1, ASC, IL-1β and IL-18 compared them to the plasma of stroke patients (plasma) and healthy controls (control). Caspase-1 (Mean values = thrombi: 191 pg/ml, plasma: 3.26 pg/ml, healthy control: 2.09 pg/ml) (**Figure 4A**), ASC (Mean values = thrombi: 5,039 pg/ml, plasma: 386.9 pg/ml, healthy control: 243.5 pg/ml) (**Figure 4B**) and IL-1β (Mean values = thrombi: 39.82 pg/ml, plasma: 0.92 pg/ml, healthy control: 0.68 pg/ml) (**Figure 4C**) were elevated in the clot when compared to plasma in AIS and healthy controls; whereas IL-18 protein levels were lower in the clot than in the plasma of healthy controls and AIS patients (Mean values = thrombi: 53.31 pg/ml, plasma: 201 pg/ml, healthy control: 200.2 pg/ml) (**Figure 4D**). Importantly, the levels of caspase-1, IL-1β and IL-18 measured were total protein values and do not differentiate between the pro-forms and the cleaved forms of these proteins. Taken together, these findings indicate that acute inflammasome signaling protein expression is higher in the clots of AIS patients consistent with higher levels of IL-1β.

NLRP1 and AIM2 Are Present in the Clots of Patients With AIS

In rodents, the NLRP1 inflammasome has been previously shown to contribute to the innate immune inflammatory following thromboembolic stroke (Abulafia et al., 2009). To determine which NLR sensor molecules were present in the clot of patients with stroke, we immunoblotted samples for NOD-like receptor protein-1 (NLRP1) and Absent in Melanoma-2 (AIM2); two receptors that form protein-protein interactions with caspase-1 and ASC to form an inflammasome complex. Accordingly, NLRP1 and AIM2 were present in the clots of nine patients with stroke (**Figure 5**). Interestingly, patient eight differed in its expression of NLRP1 *vs.* AIM2, in which NLRP1 showed laddering of the protein (Levinsohn et al., 2012), that may indicate cleavage of NLRP1 or post-translational modifications during inflammasome activation of this sensor molecule that do not occur in activation of AIM2 in the clot of the same patient.

IL-1β and TICI Score Contribute to the Number of Passes to Achieve Recanalization

The number of passes needed to achieve complete recanalization is known to correlate with better outcomes after stroke, so that the less passes needed, the better the outcomes (Zaidat et al., 2018). Here we developed a logistic regression model using inflammasome protein levels to explain the influence of

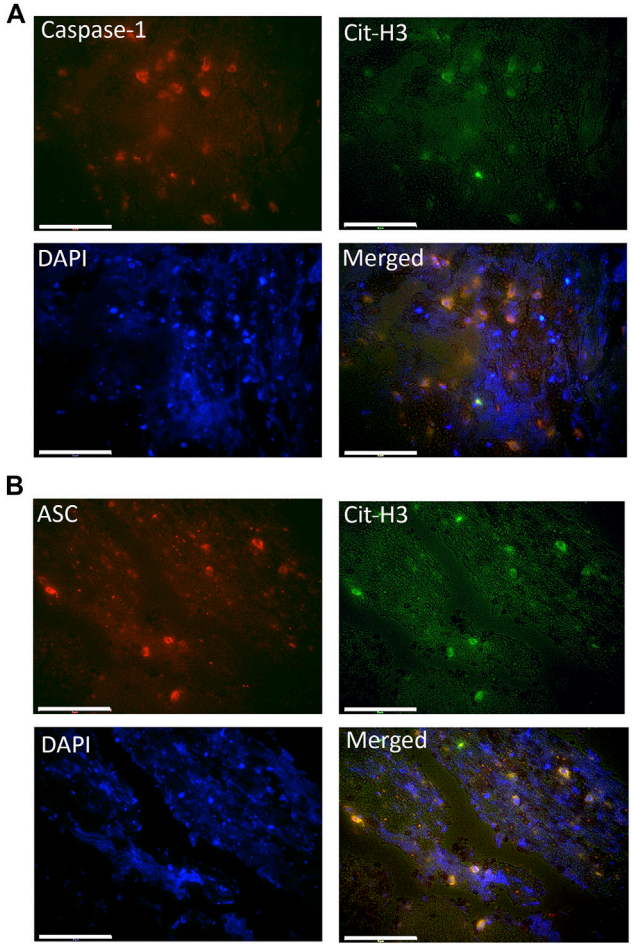

FIGURE 3 | Caspase-1 and ASC are present within citrullinated-H3 structures. Fluorescent images of the clots of patients that were double-stained for Cit-H3 (green) and **(A)** caspase-1 (red) or **(B)** ASC (red). Caspase-1 and ASC positive cells were also immunorective for Cit-H3 (yellow) and nuclei were stained with DAPI (blue). Magnification: 60X. Scale bar: 75 μm.

inflammasome proteins in clots to the number of passes. Our data indicate that IL-1β positively contributes (p = 0.049) to the number of passes whereas the TICI score, as expected, negatively contributes (p = 0.016) to the number of passes (**Table 2**). Thus, in regards to the number of passes and inflammasome signaling proteins, as IL-1β protein levels in the clot increase, so do the odds of increasing the number of passes to achieve complete recanalization as well.

Inflammasome Proteins Affect the Last Known Normal (LKN) Time to Recanalization

Recanalization is a main determinant of patient outcomes (Yeo et al., 2013). Here we fit a linear regression model to explain what factors contribute to the LKN time to recanalization using the protein levels of ASC, caspase-1, IL-18 and IL-1β as well as tissue plasminogen activator (TPA), Body Mass Index (BMI), Coronary artery disease (CAD) and whether patients had diabetes or not (**Table 3**). The model indicates that in the clots, caspase-1 (p = 0.016) and IL-18 (p = 0.043), CAD (p = 0.004) and DM (p = 0.037) positively contributed to the LKN time to recanalization, whereas ASC (p = 0.041) presented a negative correlation to the LKN time to recanalization outcome. Together, based on the adjusted R-squared, this model explained 41% of the LKN time to recanalization.

DISCUSSION

Inflammatory mechanisms initiate clotting, decrease natural anticoagulant activity, and impair the fibrinolytic system (Levi et al., 2004). Recent studies have shown that NETosis plays a role in thrombosis in stroke, suggesting that NETs play a critical role in inflammatory and thrombotic disorders (Ducroux et al., 2018). Our earlier study found elevated levels of inflammasome proteins in serum of stroke patients (Kerr et al., 2018a). Here we extend these observations and show that inflammasome proteins are present in cerebral stroke thrombi that localize with NETs (**Figure 6**). These findings are consistent with previous studies that show that inflammasome activation is critical for NETosis (Westerterp et al., 2018). Thus, it appears that inflammasome activation contributes to the pathophysiology of cerebral stroke thrombi that associate with NETs and that the level of inflammasome proteins is predictive of outcome.

Neutrophils are key cells of the immune system capable of phagocytosis, degranulation and release of NETs (Papayannopoulos, 2018). NETs are extracellular structures comprised of cytosolic and granule proteins intertwined with scaffolds of chromatin that has been decondensed (Brinkmann et al., 2004). NETs become extracellular by the cell death process of NETosis (Fuchs et al., 2007). NETs have been shown to form in vein occlusive events such as deep vein thrombosis and maybe associated with the hypoxia that induces NETosis (Brill et al., 2011; Etulain et al., 2015).

NETs quantity and content is correlated with endovascular thrombectomy procedure length as well as number of passes required to remove the clot (Ducroux et al., 2018). However, the pathogenesis of activation of NET formation in cerebral thrombi remains unknown. In mouse models of atherosclerosis, cholesterol crystals induce inflammation by activating macrophage and neutrophil inflammasomes (Warnatsch et al., 2015). Inflammasomes are cytoplasmic multiprotein complexes containing caspase-1, the adaptor protein ASC and an NLR or ALR sensor molecule (e.g., NLRP1, AIM2). Inflammasomes process the pro-inflammatory cytokines IL-1β and IL-18 into their active forms (de Rivero Vaccari et al., 2014; de Rivero Vaccari et al., 2016). In neutrophils, activated caspase-1 or caspase-11 cleave gasdermin-D (GSDM-D), which leads to pyroptosis and NETosis (Chen et al., 2018; Chen et al., 2020). Moreover, NETs are downstream of neutrophil inflammasome activation (Chen et al., 2018; Sollberger et al., 2018; Westerterp et al., 2018).

The AIM2 inflammasome in the CNS is activated by double stranded DNA (dsDNA) (Adamczak et al., 2014), and dsDNA is

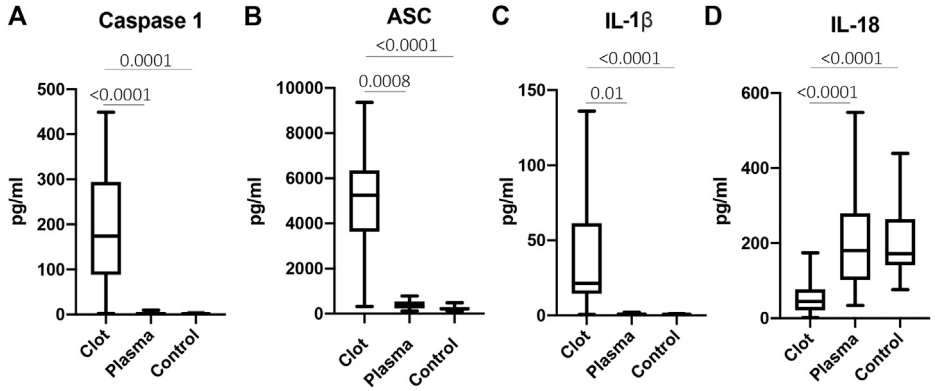

FIGURE 4 | Inflammasome signaling proteins are elevated in the clots of patients with stroke. Protein levels in pg/ml of caspase-1 **(A)**, ASC **(B)**, IL-1β **(C)** and IL-18 **(D)** in the clots of patients with AIS as well as plasma of stroke patients (plasma) and from healthy controls (control). Caspase-1: N = 26 clot, N = 13 plasma stroke patients, N = 39 plasma healthy control; ASC: N = 26 clot, N = 11 plasma stroke patients, N = 8 plasma healthy control; IL-1β: N = 19 clot, N = 5 plasma stroke patients, N = 15 plasma healthy control; IL-18: N = 25 clot, N = 15 plasma stroke patients, N = 39 plasma healthy control a. Box and whiskers are shown for the 5th and 95th percentile. *p*-value of significance <0.05. All groups were compared by a Kruskall-Wallis test followed by Dunn's multiple comparison test.

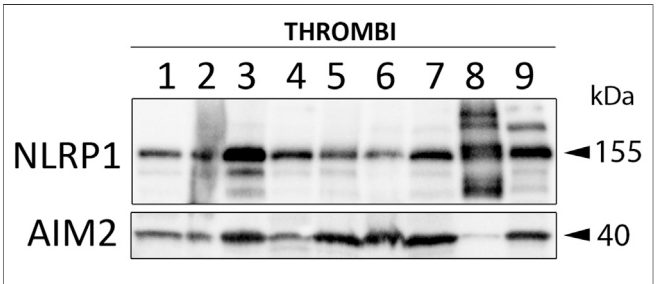

FIGURE 5 | NLRP1 and AIM2 are expressed in the clots of patients with AIS. Immunoblot analysis of clots from nine AIS patients that were blotted for NLRP1 and AIM2.

TABLE 2 | Logistic regression output of factors influencing number of passes.

Factors influencing Number of Passes			
	Estimate	**Std. Error**	***p*-Value**
IL-18	0.045	0.030	0.131
IL-1β	0.019	0.010	0.049*
TICI	–5.353	2.221	0.016*
Smoking	–0.951	0.835	0.255

*TICI, Thrombolysis in Cerebral Infarction. *p < 0.05.*

TABLE 3 | Linear regression output for factors affecting LKN time to recanalization.

Factors Influencing LKN Time to Recanalization (min)			
	Estimate	**Std. Error**	***p*-Value**
ASC	–0.195	0.087	0.041*
Caspase-1	3.872	1.429	0.016*
IL-18	1.777	0.805	0.043*
IL-1β	1.904	1.094	0.102
TPA	–145.342	208.956	0.497
BMI	–31.165	15.832	0.068
CAD	888.713	264.213	0.004*
DM	601.35	263.286	0.037*

*tPA, tissue plasminogen activator; BMI, body mass index; CAD, Coronary artery disease; DM, Diabetes Mellitus. *p < 0.05.*

present in NETs associated with atherosclerotic lesions. These findings suggest that NETs are capable of activating inflammasomes. In addition, our findings show that AIM2 is present in thrombi of patients with AIS. Moreover, previous findings also indicate that inflammasomes can also promote NET formation in a process that relies of caspase-11 and gasdermin-D cleavage (Chen et al., 2018; Sollberger et al., 2018). Furthermore, NETs have been shown to activate NLRP3 inflammasome (Kahlenberg et al., 2013). However, in this study we were unable to detect by immunoblotting procedures NLRP3 in thrombi (data not shown). However, NLRP1 and AIM2 were readily identified in clots using the same methodologies (Abulafia et al., 2009). Unlike other NLRs, such as NLRP3, NLRP1 is cleaved as part of its activation process (Levinsohn et al., 2012). Interestingly, immunoblots of a thrombus from one patient (patient 8) showed NLRP1 laddering, indicating NLRP1 cleavage or post-translational modifications. However, that same patient showed very low levels of AIM2, another inflammasome complex involved in inflammation and pyroptosis (Adamczak et al., 2014). Although beyond the scope of this project, it is possible that AIM2 is the active inflammasome in the clots of the other patients, and in patient 8, the inflammasome that was activated was the NLPR1 inflammasome instead, which would explain the lack of cleaved NLRP1 products in the clots of the other patients. Moreover, another possibility is that multiple inflammasomes may be activated in the same clots, thus producing an even more heightened innate immune response since clots from other patients such as patient three had more cleavage fragments of NLRP1 as well as higher expression of AIM2 than in other patients e.g., patient 6 (for NLRP1) or patient 4 (for AIM2).

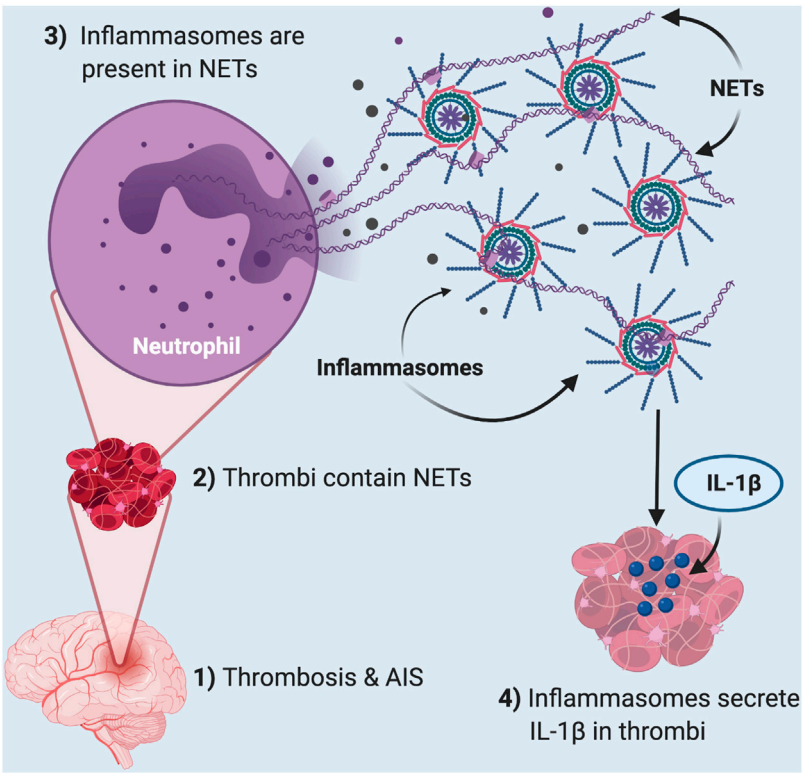

FIGURE 6 | Thrombosis in acute ischemic stroke induces inflammasome activation in NETs present in clots. In AIS (1), thrombi (2) contain neutrophil extracellular traps (NETs) that contain inflammasomes (3). These inflammasomes are responsible for the released IL-1β in the thrombi of these patients (4).

Future studies are needed to determine the role of different NLRs and AIM-2 like receptors (ALRs) in the clots of stroke patients.

Our findings show that IL-1β is significantly elevated in cerebral thrombi in contrast to the plasma of stroke patients and healthy controls. IL-1β has a fundamental role in inflammation and coagulation (Wada et al., 1991; Danton and Dietrich, 2003). Previous studies have found that IL-1β contributes to slow progressive chronic conditions such as atherosclerosis, diabetes, osteoarthritis and acute ischemic processes, including myocardial infarction and stroke (Gabay et al., 2010; Kerr et al., 2018a). In particular, IL-1β down-regulates thrombomodulin and impairs protein C activity, thus acting as a procoagulant. Furthermore, platelets express IL-1-R1 receptor and the presence of its ligand, IL1β, results in platelet hyperactivation and clumping (Bester and Pretorius, 2016). Consistent with the hyperinflammatory response in the clot are our findings of neutrophil composition and deformed red blood cells within the clot as shown by electron microscopy. Thus, inflammasome activation in cerebral thrombi may lead to further clot propagation and stabilization, and hinder breakdown by the body's natural anticoagulant processes.

In contrast, IL-18 was significantly decreased in cerebral thrombi as compared to plasma of healthy controls. IL-18 is an important immunoregulatory cytokine that is involved in the production of IFN-γ and T cell polarization as well as increasing cell adhesion molecules, nitric oxide synthesis, and chemokine induction (Dinarello et al., 2013). However, unlike IL-1β, precursor IL-18 is constitutively expressed by whole blood cells and epithelial cells (Dinarello et al., 2013), and may explain our finding that patients had lower levels of IL-18 in cerebral thrombi as compared to plasma. It is also possible that in the clot there is compensatory mechanism in which as IL-1β levels increase, the levels of IL-18 decrease in order to modulate the exacerbated inflammatory response present at the clot site.

High resolution SEM and TEM showed that NETs are structures comprised of stretches of globular proteins. These proteins are released into the extracellular matrix by activated or dying neutrophils as a result of damage or infection (Kessenbrock et al., 2009). A key protein involved in NETosis is CitH3, characteristic of decondensed chromatin structures and hypercitrullination of histone H3 by peptidylarginine deiminase 4 (PAD4) (Fuchs et al., 2007). In support of this observation, we found CitH3 within clot structures, which contained the inflammasome proteins caspase-1 and ASC, indicating heightened inflammasome activation in NETosis in thrombi following AIS.

The activation of IL-1β and other proinflammatory cytokines recruit myeloid cells to the vascular endothelium to initiate remodeling and perpetuate inflammation (Duewell et al., 2010). In more advanced stages of the disease, cytokines destabilize atherosclerotic plaques by promoting apoptosis and matrix degradation. In patients with carotid plaques, elevated

levels of IL-1β, IL-6, IL-8, IL-12 p70, IFN-γ, TNF and caspase-3 are significantly higher in rupture-prone post bifurcation segments of the plaque, suggesting a prominent inflammatory role in creating cerebral emboli (Caparosa et al., 2019). Thus, inflammasome activation may influence NETs and coagulation at the site of cerebrovascular occlusion, thus affecting thrombectomy outcomes, inflammasome activation may also be a product of emboli formation.

Importantly, NETs in thrombi may act as molecular filters for a variety of proteins, including inflammasome proteins. However, whether those proteins are catalytically active or capable of carrying out other roles in the inflammasome pathway is presently under investigation in our laboratory. Future studies are needed to analyze the role of inflammasome activation in neutrophils isolated from thrombi of AIS on the cell mediated processes of NETosis and pyroptosis. It is also critical to establish how these processes affect the inflammatory milieu in the thrombus microenvironment and in the systemic inflammatory response after cerebral ischemia. However, we have previously shown secreted inflammasome proteins caspase-1, ASC, IL-1β and IL-18 correlate with poorer outcomes in a variety of diseases or conditions of the nervous system and periphery, suggesting that these secreted inflammasome proteins are functional in inflammasome signaling (Kerr et al., 2018a; Kerr et al., 2018b; Keane et al., 2018; Forouzandeh et al., 2020; Perez-Barcena et al., 2020; Scott et al., 2020), suggesting an important role in disease- or trauma-related inflammatory pathological processes.

Our study is limited by the small number of samples as well as the significant heterogeneity that exists between patients and providers. There is not a standardized mechanical thrombectomy technique and both tools and technique remain at the discretion of the provider. Furthermore, there is a selection bias wherein clot samples are only available in patients who had at least partial success in clot removal. Thus, there are very few patients in the cohort where at least partial successful recanalization was not achieved. Additionally, there is selection bias for techniques wherein the clot could be preserved such as stentriever as opposed to aspiration alone. Nonetheless, our regression analyses indicate that inflammasome proteins in thrombi from AIS patients were associated with a greater number of thrombectomy passes in order to achieve complete recanalization, which is consistent with a longer time to achieve reperfusion and poorer outcomes in AIS patients. While, clot properties such as size, density, and strength were not obtained for this study, future studies are necessary to assess the association of inflammasome concentration with physical clot properties.

Taken together, our results provide evidence for inflammasome activation and NETosis in cerebral thrombi as well as a significant role of inflammasome proteins in contributing to poorer outcomes in patients after stroke. Therefore, an improved mechanistic understanding of the role of inflammasomes in NETosis will help in the development of therapies to treat thrombotic and inflammatory disorders, including stroke.

DATA AVAILABILITY STATEMENT

The raw data supporting the conclusions of this article will be made available by the authors, without undue reservation.

AUTHORS CONTRIBUTIONS

SC, XS, YM, VA, PB, DY, EP, RS, and JdR performed the experiments. SC, DY, EP, RS, WD, RK, and JdR contributed to the study design. SC, XS, YM, VA, and PB contributed to data acquisition and analysis. JdR also contributed to data acquisition and analysis. All authors contributed to preparation of the manuscript.

FUNDING

This research received grant funding from the Robert J. Dempsey Cerebrovascular Research Award to SC and JdR, an R01 grant from the NIH/NINDS to RK and JdR (R01NS113969-01) and a James and Ester King Biomedical Research Program grant from the State of Florida (7JK03) to WD. RS research is supported by the NREF, Joe Niekro Foundation, Brain Aneurysm Foundation, Bee Foundation, and by the NIH (R01NS111119-01A1) and (UL1TR002736, KL2TR002737) through the Miami Clinical and Translational Science Institute, from the National Center for Advancing Translational Sciences and the National Institute on Minority Health and Health Disparities. Its contents are solely the responsibility of the authors and do not necessarily represent the official views of the NIH.

ACKNOWLEDGMENTS

Figure 6 was made with BioRender.

SUPPLEMENTARY MATERIAL

The Supplementary Material for this article can be found online at: https://www.frontiersin.org/articles/10.3389/fphar.2020.607287/full#supplementary-material.

REFERENCES

Abulafia, D. P., De Rivero Vaccari, J. P., Lozano, J. D., Lotocki, G., Keane, R. W., and Dietrich, W. D. (2009). Inhibition of the inflammasome complex reduces the inflammatory response after thromboembolic stroke in mice. *J. Cerebr. Blood Flow Metabol.* 29, 534–544. doi:10.1038/jcbfm.2008.143

Adamczak, S., Dale, G., De Rivero Vaccari, J. P., Bullock, M. R., Dietrich, W. D., and Keane, R. W. (2012). Inflammasome proteins in cerebrospinal fluid of brain-injured patients as biomarkers of functional outcome: clinical article. *J. Neurosurg.* 117, 1119–1125. doi:10.3171/2012.9.JNS12815

Adamczak, S. E., De Rivero Vaccari, J. P., Dale, G., Brand, F. J., 3rd, Nonner, D., Bullock, M. R., et al. (2014). Pyroptotic neuronal cell death mediated by the AIM2 inflammasome. *J. Cerebr. Blood Flow Metabol.* 34, 621–629. doi:10.1038/jcbfm.2013.236

Bester, J., and Pretorius, E. (2016). Effects of IL-1β, IL-6 and IL-8 on erythrocytes, platelets and clot viscoelasticity. *Sci. Rep.* 6, 32188. doi:10.1038/srep32188

Brand, F. J., 3rd, De Rivero Vaccari, J. C., Mejias, N. H., Alonso, O. F., and De Rivero Vaccari, J. P. (2015). RIG-I contributes to the innate immune response after cerebral ischemia. *J. Inflamm.* 12, 52. doi:10.1186/s12950-015-0101-4

Brand, F. J., 3rd, Forouzandeh, M., Kaur, H., Travascio, F., and De Rivero Vaccari, J. P. (2016). Acidification changes affect the inflammasome in human nucleus pulposus cells. *J. Inflamm.* 13, 29. doi:10.1186/s12950-016-0137-0

Brill, A., Fuchs, T. A., Chauhan, A. K., Yang, J. J., De Meyer, S. F., Köllnberger, M., et al. (2011). von Willebrand factor-mediated platelet adhesion is critical for deep vein thrombosis in mouse models. *Blood.* 117, 1400–1407. doi:10.1182/blood-2010-05-287623

Brinjikji, W., Duffy, S., Burrows, A., Hacke, W., Liebeskind, D., Majoie, C. B. L. M., et al. (2017). Correlation of imaging and histopathology of thrombi in acute ischemic stroke with etiology and outcome: a systematic review. *J. Neurointerventional Surg.* 9, 529–534. doi:10.1136/neurintsurg-2016-012391

Brinkmann, V., Reichard, U., Goosmann, C., Fauler, B., Uhlemann, Y., Weiss, D. S., et al. (2004). Neutrophil extracellular traps kill bacteria. *Science.* 303, 1532–1535. doi:10.1126/science.1092385

Caparosa, E. M., Sedgewick, A. J., Zenonos, G., Zhao, Y., Carlisle, D. L., Stefaneanu, L., et al. (2019). Regional molecular signature of the symptomatic atherosclerotic carotid plaque. *Neurosurgery.* 85, E284–E293. doi:10.1093/neuros/nyy470

Chen, K. W., Demarco, B., and Broz, P. (2020). Beyond inflammasomes: emerging function of gasdermins during apoptosis and NETosis. *EMBO J.* 39, e103397. doi:10.15252/embj.2019103397

Chen, K. W., Monteleone, M., Boucher, D., Sollberger, G., Ramnath, D., Condon, N. D., et al. (2018). Noncanonical inflammasome signaling elicits gasdermin D-dependent neutrophil extracellular traps. *Sci Immunol.* 3. doi:10.1126/sciimmunol.aar6676

Danton, G. H., and Dietrich, W. D. (2003). Inflammatory mechanisms after ischemia and stroke. *J. Neuropathol. Exp. Neurol.* 62, 127–136. doi:10.1093/jnen/62.2.127

De Rivero Vaccari, J. P., Dietrich, W. D., and Keane, R. W. (2014). Activation and regulation of cellular inflammasomes: gaps in our knowledge for central nervous system injury. *J. Cerebr. Blood Flow Metabol.* 34, 369–375. doi:10.1038/jcbfm.2013.227

De Rivero Vaccari, J. P., Dietrich, W. D., and Keane, R. W. (2016). Therapeutics targeting the inflammasome after central nervous system injury. *Transl. Res.* 167, 35–45. doi:10.1016/j.trsl.2015.05.003

De Rivero Vaccari, J. P., Lotocki, G., Alonso, O. F., Bramlett, H. M., Dietrich, W. D., and Keane, R. W. (2009). Therapeutic neutralization of the NLRP1 inflammasome reduces the innate immune response and improves histopathology after traumatic brain injury. *J. Cerebr. Blood Flow Metabol.* 29, 1251–1261. doi:10.1038/jcbfm.2009.46

Dinarello, C. A., Novick, D., Kim, S., and Kaplanski, G. (2013). Interleukin-18 and IL-18 binding protein. *Front. Immunol.* 4, 289. doi:10.3389/fimmu.2013.00289

Ducroux, C., Di Meglio, L., Loyau, S., Delbosc, S., Boisseau, W., Deschildre, C., et al. (2018). Thrombus neutrophil extracellular traps content impair tPA-induced thrombolysis in acute ischemic stroke. *Stroke.* 49, 754–757. doi:10.1161/STROKEAHA.117.019896

Duewell, P., Kono, H., Rayner, K. J., Sirois, C. M., Vladimer, G., Bauernfeind, F. G., et al. (2010). NLRP3 inflammasomes are required for atherogenesis and activated by cholesterol crystals. *Nature.* 464, 1357–1361. doi:10.1038/nature08938

Etulain, J., Martinod, K., Wong, S. L., Cifuni, S. M., Schattner, M., and Wagner, D. D. (2015). P-selectin promotes neutrophil extracellular trap formation in mice. *Blood.* 126, 242–246. doi:10.1182/blood-2015-01-624023

Fann, D. Y., Lee, S. Y., Manzanero, S., Tang, S. C., Gelderblom, M., Chunduri, P., et al. (2013). Intravenous immunoglobulin suppresses NLRP1 and NLRP3 inflammasome-mediated neuronal death in ischemic stroke. *Cell Death Dis.* 4, e790. doi:10.1038/cddis.2013.326

Forouzandeh, M., Besen, J., Keane, R. W., and De Rivero Vaccari, J. P. (2020). The inflammasome signaling proteins ASC and IL-18 as biomarkers of psoriasis. *Front. Pharmacol.* 11, 1238. doi:10.3389/fphar.2020.01238

Fransen, P. S., Beumer, D., Berkhemer, O. A., Van Den Berg, L. A., Lingsma, H., Van Der Lugt, A., et al. (2014). MR CLEAN, a multicenter randomized clinical trial of endovascular treatment for acute ischemic stroke in The The Netherlands: study protocol for a randomized controlled trial. *Trials.* 15, 343. doi:10.1186/1745-6215-15-343

Fuchs, T. A., Abed, U., Goosmann, C., Hurwitz, R., Schulze, I., Wahn, V., et al. (2007). Novel cell death program leads to neutrophil extracellular traps. *J. Cell Biol.* 176, 231–241. doi:10.1083/jcb.200606027

Gabay, C., Lamacchia, C., and Palmer, G. (2010). IL-1 pathways in inflammation and human diseases. *Nat. Rev. Rheumatol.* 6, 232–241. doi:10.1038/nrrheum.2010.4

Gao, L., Dong, Q., Song, Z., Shen, F., Shi, J., and Li, Y. (2017). NLRP3 inflammasome: a promising target in ischemic stroke. *Inflamm. Res.* 66, 17–24. doi:10.1007/s00011-016-0981-7

Govindarajan, V., De Rivero Vaccari, J. P., and Keane, R. W. (2020). Role of inflammasomes in multiple sclerosis and their potential as therapeutic targets. *J. Neuroinflammation.* 17, 260. doi:10.1186/s12974-020-01944-9

Goyal, M., Menon, B. K., Van Zwam, W. H., Dippel, D. W., Mitchell, P. J., Demchuk, A. M., et al. (2016a). Endovascular thrombectomy after large-vessel ischaemic stroke: a meta-analysis of individual patient data from five randomised trials. *Lancet.* 387, 1723–1731. doi:10.1016/S0140-6736(16)00163-X

Goyal, M., Yu, A. Y., Menon, B. K., Dippel, D. W., Hacke, W., Davis, S. M., et al. (2016b). Endovascular therapy in acute ischemic stroke: challenges and transition from trials to bedside. *Stroke.* 47, 548–553. doi:10.1161/STROKEAHA.115.011426

Gupta, A. K., Joshi, M. B., Philippova, M., Erne, P., Hasler, P., Hahn, S., et al. (2010). Activated endothelial cells induce neutrophil extracellular traps and are susceptible to NETosis-mediated cell death. *FEBS Lett.* 584, 3193–3197. doi:10.1016/j.febslet.2010.06.006

Hankey, G. J. (2017). Stroke. *Lancet.* 389, 641–654. doi:10.1016/S0140-6736(16)30962-X

Hirose, T., Hamaguchi, S., Matsumoto, N., Irisawa, T., Seki, M., Tasaki, O., et al. (2014). Presence of neutrophil extracellular traps and citrullinated histone H3 in the bloodstream of critically ill patients. *PloS One.* 9, e111755. doi:10.1371/journal.pone.0111755

Ismael, S., Zhao, L., Nasoohi, S., and Ishrat, T. (2018). Inhibition of the NLRP3-inflammasome as a potential approach for neuroprotection after stroke. *Sci. Rep.* 8, 5971. doi:10.1038/s41598-018-24350-x

Jadhav, A. P., Desai, S. M., Kenmuir, C. L., Rocha, M., Starr, M. T., Molyneaux, B. J., et al. (2018). Eligibility for endovascular trial enrollment in the 6- to 24-hour time window: analysis of a single comprehensive stroke center. *Stroke.* 49, 1015–1017. doi:10.1161/STROKEAHA.117.020273

Jagani, M., Kallmes, D. F., and Brinjikji, W. (2017). Correlation between clot density and recanalization success or stroke etiology in acute ischemic stroke patients. *Intervent Neuroradiol.* 23, 274–278. doi:10.1177/1591019917694478

Kahlenberg, J. M., Carmona-Rivera, C., Smith, C. K., and Kaplan, M. J. (2013). Neutrophil extracellular trap-associated protein activation of the NLRP3 inflammasome is enhanced in lupus macrophages. *J. Immunol.* 190, 1217–1226. doi:10.4049/jimmunol.1202388

Kastbom, A., Ärlestig, L., and Rantapää-Dahlqvist, S. (2015). Genetic variants of the NLRP3 inflammasome are associated with stroke in patients with rheumatoid arthritis. *J. Rheumatol.* 42, 1740–1745. doi:10.3899/jrheum.141529

Kawasaki, J., Katori, N., Kodaka, M., Miyao, H., and Tanaka, K. A. (2004). Electron microscopic evaluations of clot morphology during thrombelastography. *Anesth. Analg.* 99, 1440–1444. doi:10.1213/01.ANE.0000134805.30532.59

Keane, R. W., Dietrich, W. D., and De Rivero Vaccari, J. P. (2018). Inflammasome proteins as biomarkers of multiple sclerosis. *Front. Neurol.* 9, 135. doi:10.3389/fneur.2018.00135

Kerr, N., García-Contreras, M., Abbassi, S., Mejias, N. H., Desousa, B. R., Ricordi, C., et al. (2018a). Inflammasome proteins in serum and serum-derived extracellular vesicles as biomarkers of stroke. *Front. Mol. Neurosci.* 11, 309. doi:10.3389/fnmol.2018.00309

Kerr, N., Lee, S. W., Perez-Barcena, J., Crespi, C., Ibañez, J., Bullock, M. R., et al. (2018b). Inflammasome proteins as biomarkers of traumatic brain injury. *PloS One.* 13, e0210128. doi:10.1371/journal.pone.0210128

Kessenbrock, K., Krumbholz, M., Schönermarck, U., Back, W., Gross, W. L., Werb, Z., et al. (2009). Netting neutrophils in autoimmune small-vessel vasculitis. *Nat. Med.* 15, 623–625. doi:10.1038/nm.1959

Kim, H., Seo, J. S., Lee, S. Y., Ha, K. T., Choi, B. T., Shin, Y. I., et al. (2020). AIM2 inflammasome contributes to brain injury and chronic post-stroke cognitive impairment in mice. *Brain Behav. Immun.* 87, 765–776. doi:10.1016/j.bbi.2020.03.011

Kim, S. K., Yoon, W., Kim, T. S., Kim, H. S., Heo, T. W., and Park, M. S. (2015). Histologic analysis of retrieved clots in acute ischemic stroke: correlation with stroke etiology and gradient-echo MRI. *AJNR Am J Neuroradiol.* 36, 1756–1762. doi:10.3174/ajnr.A4402

Kimball, A. S., Obi, A. T., Diaz, J. A., and Henke, P. K. (2016). The emerging role of NETs in venous thrombosis and immunothrombosis. *Front. Immunol.* 7, 236. doi:10.3389/fimmu.2016.00236

Laridan, E., Denorme, F., Desender, L., François, O., Andersson, T., Deckmyn, H., et al. (2017). Neutrophil extracellular traps in ischemic stroke thrombi. *Ann. Neurol.* 82, 223–232. doi:10.1002/ana.24993

Laridan, E., Martinod, K., and De Meyer, S. F. (2019). Neutrophil extracellular traps in arterial and venous thrombosis. *Semin. Thromb. Hemost.* 45, 86–93. doi:10.1055/s-0038-1677040

Levi, M., Van Der Poll, T., and Büller, H. R. (2004). Bidirectional relation between inflammation and coagulation. *Circulation.* 109, 2698–2704. doi:10.1161/01.CIR.0000131660.51520.9A

Levinsohn, J. L., Newman, Z. L., Hellmich, K. A., Fattah, R., Getz, M. A., Liu, S., et al. (2012). Anthrax lethal factor cleavage of Nlrp1 is required for activation of the inflammasome. *PLoS Pathog.* 8, e1002638. doi:10.1371/journal.ppat.1002638

Niesten, J. M., Van Der Schaaf, I. C., Van Dam, L., Vink, A., Vos, J. A., Schonewille, W. J., et al. (2014). Histopathologic composition of cerebral thrombi of acute stroke patients is correlated with stroke subtype and thrombus attenuation. *PloS One.* 9, e88882. doi:10.1371/journal.pone.0088882

Papayannopoulos, V. (2018). Neutrophil extracellular traps in immunity and disease. *Nat. Rev. Immunol.* 18, 134–147. doi:10.1038/nri.2017.105

Pérez-Bárcena, J., Crespí, C., Frontera, G., Llompart-Pou, J. A., Salazar, O., Goliney, V., et al. (2020). Levels of caspase-1 in cerebrospinal fluid of patients with traumatic brain injury: correlation with intracranial pressure and outcome. *J. Neurosurg.* 1, 1–6. doi:10.3171/2020.2.JNS193079

Powers, W. J., Rabinstein, A. A., Ackerson, T., Adeoye, O. M., Bambakidis, N. C., Becker, K., et al. (2019). Guidelines for the early management of patients with acute ischemic stroke: 2019 update to the 2018 guidelines for the early management of acute ischemic stroke: a guideline for Healthcare professionals from the American heart association/American stroke association. *Stroke.* 50, e344–e418. doi:10.1161/STR.0000000000000211

Rennert, R. C., Wali, A. R., Steinberg, J. A., Santiago-Dieppa, D. R., Olson, S. E., Pannell, J. S., et al. (2019). Epidemiology, natural history, and clinical presentation of large vessel ischemic stroke. *Neurosurgery.* 85, S4–S8. doi:10.1093/neuros/nyz042

Scott, X. O., Stephens, M. E., Desir, M. C., Dietrich, W. D., Keane, R. W., and De Rivero Vaccari, J. P. (2020). The inflammasome adaptor protein ASC in mild cognitive impairment and alzheimer's disease. *Int. J. Mol. Sci.* 21, 4674. doi:10.3390/ijms21134674

Sollberger, G., Choidas, A., Burn, G. L., Habenberger, P., Di Lucrezia, R., Kordes, S., et al. (2018). Gasdermin D plays a vital role in the generation of neutrophil extracellular traps. *Sci. Immunol.* 3, eaar6689. doi:10.1126/sciimmunol.aar6689

Tong, Y., Ding, Z. H., Zhan, F. X., Cai, L., Yin, X., Ling, J. L., et al. (2015). The NLRP3 inflammasome and stroke. *Int. J. Clin. Exp. Med.* 8, 4787–4794.

Wada, H., Tamaki, S., Tanigawa, M., Takagi, M., Mori, Y., Deguchi, A., et al. (1991). Plasma level of IL-1 beta in disseminated intravascular coagulation. *Thromb. Haemostasis.* 65, 364–368.

Warnatsch, A., Ioannou, M., Wang, Q., and Papayannopoulos, V. (2015). Inflammation. Neutrophil extracellular traps license macrophages for cytokine production in atherosclerosis. *Science.* 349, 316–320. doi:10.1126/science.aaa8064

Westerterp, M., Fotakis, P., Ouimet, M., Bochem, A. E., Zhang, H., Molusky, M. M., et al. (2018). Cholesterol efflux pathways suppress inflammasome activation, NETosis, and atherogenesis. *Circulation.* 138, 898–912. doi:10.1161/CIRCULATIONAHA.117.032636

Yang, F., Wang, Z., Wei, X., Han, H., Meng, X., Zhang, Y., et al. (2014). NLRP3 deficiency ameliorates neurovascular damage in experimental ischemic stroke. *J. Cerebr. Blood Flow Metabol.* 34, 660–667. doi:10.1038/jcbfm.2013.242

Yang, S. J., Shao, G. F., Chen, J. L., and Gong, J. (2018). The NLRP3 inflammasome: an important driver of neuroinflammation in hemorrhagic stroke. *Cell. Mol. Neurobiol.* 38, 595–603. doi:10.1007/s10571-017-0526-9

Yeo, L. L., Paliwal, P., Teoh, H. L., Seet, R. C., Chan, B. P., Liang, S., et al. (2013). Timing of recanalization after intravenous thrombolysis and functional outcomes after acute ischemic stroke. *JAMA Neurol.* 70, 353–358. doi:10.1001/2013.jamaneurol.547

Zaidat, O. O., Castonguay, A. C., Linfante, I., Gupta, R., Martin, C. O., Holloway, W. E., et al. (2018). First pass effect: a new measure for stroke thrombectomy devices. *Stroke.* 49, 660–666. doi:10.1161/STROKEAHA.117.020315

Conflict of Interest: JdR, RK and WD are co-founders and managing members of InflamaCORE, LLC and have patents on inflammasome proteins as biomarkers of injury and disease as well as on targeting inflammasome proteins for therapeutic purposes. JdR, RK and WD are scientific advisory board members of ZyVersa Therapeutics. EP is a consultant for Stryker Neurovascular, Penumbra, Medtronic Neurovascular and Cerenovus, as well as a stockholder for RIST Neurovascular. DY is a consultant for Medtronic Neurovascular, Cerenovus, Rapid Medical and Neuralanalytics. RS has consulting and teaching agreements with Penumbra, Abbott, Medtronic, InNeuroCo and Cerenovus.

The remaining authors declare that the research was conducted in the absence of any commercial or financial relationships that could be construed as a potential conflict of interest.

frontiers in Pharmacology

ORIGINAL RESEARCH
published: 27 January 2021
doi: 10.3389/fphar.2020.601887

In Silico, *In Vitro* and *In Vivo* Pharmacodynamic Characterization of Novel Analgesic Drug Candidate Somatostatin SST_4 Receptor Agonists

Boglárka Kántás[1,2†], Éva Szőke[1,2,3†], Rita Börzsei[4], Péter Bánhegyi[5], Junaid Asghar[6], Lina Hudhud[1,2], Anita Steib[1,2], Ágnes Hunyady[1,2], Ádám Horváth[1,2], Angéla Kecskés[1,2], Éva Borbély[1,2], Csaba Hetényi[1,2], Gábor Pethő[1,4], Erika Pintér[1,2,3,7†] and Zsuzsanna Helyes[1,2,3,7†]*

[1]Department of Pharmacology and Pharmacotherapy, Medical School, University of Pécs, Pécs, Hungary, [2]János Szentágothai Research Center and Center for Neuroscience, University of Pécs, Pécs, Hungary, [3]PharmInVivo Ltd., Pécs, Hungary, [4]Department of Pharmacology, Faculty of Pharmacy, University of Pécs, Pécs, Hungary, [5]Avicor Ltd., Budapest, Hungary, [6]Gomal Centre of Pharmaceutical Sciences, Gomal University, Khyber Pakhtoonkhwa, Pakistan, [7]Algonist Biotechnolgies GmbH, Vienna, Austria

Background: Somatostatin released from the capsaicin-sensitive sensory nerves mediates analgesic and anti-inflammatory effects via its receptor subtype 4 (SST_4) without influencing endocrine functions. Therefore, SST_4 is considered to be a novel target for drug development in pain, especially chronic neuropathy which is a great unmet medical need.

Purpose and Experimental Approach: Here, we examined the *in silico* binding, SST_4-linked G protein activation and β-arrestin activation on stable SST_4 expressing cells and the effects of our novel pyrrolo-pyrimidine molecules (20, 100, 500, 1,000, 2,000 $\mu g \cdot kg^{-1}$) on partial sciatic nerve ligation-induced traumatic mononeuropathic pain model in mice.

Key Results: The novel compounds bind to the high affinity binding site of SST_4 the receptor and activate the G protein. However, unlike the reference SST_4 agonists NNC 26-9100 and J-2156, they do not induce β-arrestin activation responsible for receptor desensitization and internalization upon chronic use. They exert 65–80% maximal anti-hyperalgesic effects in the neuropathy model 1 h after a single oral administration of 100–500 $\mu g \cdot kg^{-1}$ doses.

Conclusion and Implications: The novel orally active compounds show potent and effective SST_4 receptor agonism *in vitro* and *in vivo*. All four novel ligands proved to be full agonists based on G protein activation, but failed to recruit β-arrestin. Based on their potent antinociceptive effect in the neuropathic pain model following a single oral administration, they are promising candidates for drug development.

Abbreviations: EF1, elongation factor 1; $hsstr_4$, human somatostatin receptor subtype 4; NMRI, naval medical research institute; IRES, internal ribosomal entry site; RLUs, relative luminescence units; RMSD, root mean square deviation; SST_1-SST_5, somatostatin receptor subtypes 1–5; TM3, transmembrane domain 3; Tris–EGTA, tris-ethylene glycol bis(2-aminoethyl)tetraacetic acid.

OPEN ACCESS

Edited by:
Galina Sud'ina, Lomonosov Moscow State University, Russia

Reviewed by:
Alejandro Ibáñez-Costa, Maimonides Biomedical Research Institute of Cordoba, Spain
Maree Therese Smith, The University of Queensland, Australia

***Correspondence:**
Zsuzsanna Helyes
zsuzsanna.helyes@aok.pte.hu
[†]These authors have contributed equally to this work

Specialty section:
This article was submitted to Inflammation Pharmacology, a section of the journal Frontiers in Pharmacology

Received: *01 September 2020*
Accepted: *30 November 2020*
Published: *27 January 2021*

Citation:
Kántás B, Szőke É, Börzsei R, Bánhegyi P, Asghar J, Hudhud L, Steib A, Hunyady Á, Horváth Á, Kecskés A, Borbély É, Hetényi C, Pethő G, Pintér E and Helyes Z (2021) In Silico, In Vitro and In Vivo Pharmacodynamic Characterization of Novel Analgesic Drug Candidate Somatostatin SST_4 Receptor Agonists. Front. Pharmacol. 11:601887. doi: 10.3389/fphar.2020.601887

Keywords: neuropathic pain, drug discovery, G protein coupled receptor, somatostatin, somatostatin receptor subtype 4, molecular, modeling

INTRODUCTION

Targeting somatostatin receptors as novel analgesic and anti-inflammatory drug developmental approaches has emerged after our team discovered that somatostatin was released from the activated capsaicin-sensitive peptidergic sensory nerve endings into the systemic circulation which leads to anti-inflammatory and anti-hyperalgesic actions at distant parts of the body (Pintér et al., 2006; Szolcsanyi et al., 2011; Pintér et al., 2014; Schuelert et al., 2015; Shenoy et al., 2018; Hernández et al., 2020; Kuo et al., 2020). These effects were mimicked by a synthetic heptapeptide agonist, TT-232, acting on the somatostatin receptors subtype 4 and 1 (SST_4 and SST_1) located on both primary sensory neurons and immune cells (Pintér et al., 2002; Helyes et al., 2004; Szolcsányi et al., 2004). J-2156, a highly selective and efficacious non-peptide SST_4 receptor agonist inhibited nocifensive behavior in the second phase of the formalin test, adjuvant-evoked chronic inflammatory mechanical allodynia, and sciatic nerve ligation-induced neuropathic mechanical hyperalgesia (Sándor et al., 2006). Furthermore, J-2156 decreased neuropeptide release from the peripheral terminals of peptidergic sensory neurones, as well as neurogenic and non-neurogenic acute inflammatory processes and adjuvant-induced chronic arthritic changes (Helyes et al., 2006; Elekes et al., 2008). In accordance with the above findings, in SST_4 receptor knockout mice acute and chronic inflammatory as well as neuropathic hyperalgesia were more severe than in wild types (Helyes et al., 2009). In addition to the peripheral nervous system, the SST_4 receptor is present in several central nervous system regions involved in the regulation in pain, such as the spinal cord, hippocampus and amygdala (Schreff et al., 2000; Selmer et al., 2000a; Selmer et al., 2000b). All these data provide strong proof of concept that small molecule non-peptide SST_4 receptor agonists are promising drug candidates for novel analgesic development. Furthermore, it is also important, that SST_4 does not mediate endocrine actions of somatostatin.

Based on these data, SST_4 agonists have recently become the focus of interest and development pipeline of several pharmaceutical companies for the treatment of chronic pain with one compound being tested in phase 1 clinical trial (Lilly, 2020; Stevens et al., 2020). We synthesized and patented novel pyrrolo-pyrimidine molecules (Compound 1, Compound 2, Compound 3, Compound 4) (see details in the Supplementary Materials) (Szolcsányi et al., 2019), and in the present paper we characterize their *in silico* binding, *in vitro* receptor activation and *in vivo* anti-hyperalgesic effects after single oral administration.

METHODS

In Silico Modeling Studies

Preparation of Ligand and Target Structures

Five ligand structures were built in Maestro (Schrödinger, 2017). The semi-empirical quantum chemistry program package MOPAC (Stewart, 2016) was used to minimize the raw structures with a PM7 parametrization (Stewart, 2013). The gradient norm was set to 0.001. Force calculations were applied on the energy minimized structures and the force constant matrices were positive definite. The energy-minimized structures were forwarded to docking calculations. The structure of SST_4 receptor was created by homology modeling using the active form of adrenergic β2-receptor (PDB code: 3p0g) as template. The sequence alignment was performed as in the model constructed and described by Liu and co-workers (Liu et al., 2012). Five homology models generated by Modeller program package (Stewart, 2016) were ranked related to their Discrete Optimized Protein Energy score (DOPE score) value. The first ranked model was energy-minimized and equilibrated by GROMACS 5.0.2 (Abraham et al., 2015) as described in the previous study (Liu et al., 2012). The energy-minimized receptor structure was used as a target in the docking calculations.

Docking

Docking of all ligands was performed by AutoDock 4.2.6 (Morris et al., 2009) focused on the extracellular region of the SST_4 target. In order to reduce false positive conformations, the transmembrane and intracellular target regions were not included in the docking search. Gasteiger-Marsilli partial charges were assigned to both the ligand and target atoms in AutoDock Tools (Morris et al., 2009), and united atom representation was applied for non-polar moieties. Flexibility was allowed at all active torsions of the ligand, but the target was treated rigidly. The grid maps were prepared by AutoGrid 4. The number of grid points was determined by **Eq. 1**, where L_{max} is the length of the longest ligand structure and x is the number of grid points.

$$L_{max} + 5 = 0.375x. \quad (1)$$

The docking box was centered on the extracellular region of SST_4 including 66 × 66 × 66 grid points at a 0.375 Å spacing. Lamarckian genetic algorithm was used for global search. After 10 docking runs, ligand conformations were ranked according to the corresponding calculated interaction energy values and subsequently clustered using a root mean square deviation (RMSD) tolerance of 3.5 Å between cluster members. Rank 1 was analyzed and selected as representative structure for each ligand.

G Protein Activation Assay

Membrane fractions prepared from Chinese hamster ovary (CHO) cells stably expressing the SST_4 receptor (in Tris-Ethylene glycol bis(2-aminoethyl)tetraacetic acid (Tris–EGTA) buffer (50 mM Tris–HCl, 1 mM EGTA, 3 mM $MgCl_2$, 100 mM NaCl, pH 7.4, 10 μg of protein/sample) were used for the investigations. The SSTR4 coding sequence was cloned into a

pWPTS-derived lentiviral transfer vector containing an internal ribosomal entry site (IRES) and the green fluorescent protein (GFP) gene. The SSTR4-IRES-GFP construct was driven by the EF1 promoter. HEK293 cells were used to produce the lentiviral particles, by cotransfecting the cells with the SST4 receptor coding "transfer," pMD.G "helper" and R8.91 "packaging" vectors. The culture media of HEK293 cells containing the lentiviral particles were transferred to the CHO-K1 cells. The virus particles stably transfected the CHO cells creating the stable SSTR4 expressing CHO cell line, which was used in the further experiments. Cell culture media containing the virus particles were transferred onto CHO-K1 cells. These fractions were incubated for 60 min at 30°C in the buffer containing 0.05 nM guanosine triphosphate (GTP), labeled on the gamma phosphate group with ^{35}S ([^{35}S]GTPγS) and increasing concentrations (0.1 nM–10 μM) of test compounds. 30 μM guanosine diphosphate (GDP) was added in a final volume of 500 μl. We determined the non-specific binding in the presence of 10 μM unlabelled GTPγS and total binding in the absence of test compounds. At the end of the experiment we filtered the samples through Whatman GF/B glass fiber filters using 48-well Slot Blot Manifold from Cleaver Scientific. Filters were washed with ice-cold 50 mM Tris–HCl buffer (pH 7.4) and radioactivity was measured in a β-counter (PerkinElmer Inc., Waltham, MA, United States). Test compound-induced G protein activation was given as percentage of the specific [^{35}S] GTPγS binding detected in the absence of agonists (Markovics et al., 2012).

β-Arrestin Activation Assay

In the PathHunter™ Enzyme Fragment complementation assay (DiscoverX, Fremont, CA), pCMV Mammalian cloning vector is used to drive the CHO-K1 SSTR4 cell lines to express both GPCR fused to a small enzyme donor fragment ProLink (PK), and β-Arrestin tagged with Enzyme Acceptor fragment. Upon stimulation of GPCR, β-arrestin binds to the prolink leading to the complementation of the enzyme fragments. The signal is then detected by adding the chemiluminescent reagent.

β-arrestin2 CHO-K1 SSTR4 cells were plated at a density of 20,000 cells/well in white 96 well plates and incubated overnight at 37°C. Cells were then loaded with a range of SST_4 receptor agonists' concentrations (10^{-12}–10^{-5} M) in the assay media for 90 min at 37°C. Determinations were made in duplicates. The detection reagents were added and the incubation continued at room temperature for 60 min. The agonist mediated β-arrestin 2 interaction was determined using the detection reagents according to the manufacturer's instructions. Chemiluminescence indicated as relative luminescence units (RLUs) was measured on EnSpire Alpha Plate Reader (Perkin Elmer).

Animals and Ethics

Male NMRI (named after the U.S. Naval Medical Research Institute) mice (8–12-week-old, 35–40 g weight) were used in the pain experiments. They have the highest nociceptive threshold among all mouse strains (Leo et al., 2008). Partial sciatic nerve ligation is a well-known, widely used, reproducible method to induce neuropathic pain in mice, characterized by significant allodynia and hyperalgesia, mimicking human neuropathic pain (Malmberg and Basbaum, 1998; Shields et al., 2003). We performed the first series of behavioral experiments with NMRI mice. Since we observed that the individual results show significant differences within each group including the control group, we used male C57Bl/6 mice (12–16-week-old, 25–30 g weight) for this purpose to be comparable with previous behavioral studies (Scheich et al., 2016; Scheich et al., 2017).

Mice were bred in the Laboratory Animal House of the Department of Pharmacology and Pharmacotherapy of the University of Pécs, kept in standard plastic cages at 24–25°C, under a 12–12 h light–dark cycle and provided with standard rodent chow and water *ad libitum*.

The study was designed and conducted according to European legislation (Directive 2010/63/EU) and Hungarian Government regulation (40/2013., II. 14.) on the protection of animals used for scientific purposes. The project was approved by the Animal Welfare Committee of the University of Pécs and the National Scientific Ethical Committee on Animal Experimentation of Hungary and licensed by the Government Office of Baranya County (license No. BA1/35/55-50/2017). We made all efforts to minimize the number and suffering of the animals used in this study. The group size in our experiments was chosen based upon free available power analysis program (Power and Sample Size.com, 2020) and our previous experiences using similar experimental protocols. The minimal required number for sufficient statistical power was 7. After the experiments, mice were sacrificed by cervical dislocation.

Measurement of the Mechanonociceptive Threshold of the Hindpaw and Partial Sciatic Nerve Ligation-Induced Neuropathic Pain Model of the Mouse

To measure the mechanical threshold of both hindpaws, mice were placed individually in small cages with a framed metal mesh floor. The mechanonociceptive thresholds of the mouse hindpaw were determined with the Dynamic Plantar Aesthesiometer (Ugo Basile Dynamic Plantar Aesthesiometer 37400; Comerio, Italy). This electronic von Frey device applied pressure to the plantar surface of the hindpaw with a blunt-end needle which continuously rose for 4 s until 10 g force. The force at which a paw withdrawal response occurred is registered by the equipment and it was taken as the mechanonociceptive threshold. Paw withdrawal automatically turned off the stimulus.

After conditioning, three control mechanonociceptive hindpaw threshold measurements were performed on three consecutive days. Mice were then anesthetized by the combination of ketamine (100 mg·kg^{-1}, i.p.) and xylazine (10 mg·kg^{-1}, i.p.) and placed under a dissection microscope. The right sciatic nerve was isolated from the surrounding connective tissues at a proximal site and the dorsal 1/3–1/2 of the nerve was tightly ligated with only one 8–0 silk suture in order to induce traumatic sensory mononeuropathy (Seltzer et al., 1990). The surgery was performed under aseptic conditions,

including sterile gloves, mask and sterile instruments. The animals were placed on a heating plate after the operation and monitored until complete awakening. The mechanonociceptive threshold of the plantar surface of the hindpaws was measured again on the seventh postoperative day in order to detect the development of the neuropathic pain-like state mechanical hyperalgesia in response to the nerve ligation expressed as percentage decrease compared to the mean three initial (pre-surgery) control values. Animals that failed to show at least 20% hyperalgesia were excluded from the experiment (107 out of 358 animals; 70% success rate of the operation), since they did not have obvious neuropathic pain. Subsequently, the test compounds or the vehicle methylcellulose were applied orally (in a volume of 20 ml·kg^{-1} body weight) and threshold measurements were repeated 60 min later in order to compare mechanical hyperalgesia before and after the treatment. The anti-hyperalgesic effects of the test compounds were expressed in percentage by the following formula: ((hyperalgesia before drug treatment—hyperalgesia after drug treatment)/hyperalgesia before drug treatment) · 100. The intact contralateral paws were also measured for comparison.

The experiment consisted of 15 separate series and the animals were randomized to receive the respective treatment or the vehicle. The experimenter was blinded from the treatment the animals received. The number of animals in the control group was at least four per day to minimize the bias caused by the different experimental days. Therefore, the total number of animals in the different experimental groups ranged from 7 to 19 (see details in the respective figures).

Determination of Anxiety and Spontaneous Locomotor Activity: Elevated Plus Maze (EPM) and Open Field Test (OFT)

Anxiety behavior was examined in the EPM apparatus consisting of two open and two closed arms that are extended from a common central platform. The platform was 60 cm above floor level, the floor and the walls of each arm were plastic and painted gray. Sixty min after oral administration of the vehicle or Compound 2 (500 μg·kg^{-1}), mice were placed in the center of the maze and the time they spent in the open arms during the 5-min experiment was measured (Lister, 1987; Kraeuter et al., 2019a; He et al., 2020). The surface of the maze was cleaned with 70% ethyl alcohol after each test to remove permeated odors from previous animals. There were 10 mice in each group.

Spontaneous locomotor activity and anxiety level was determined in the OFT composed of a plastic box (39 cm × 39 cm × 39 cm) with white floor and gray walls. Sixty min after the oral administration of the vehicle or Compound 2 (500 μg·kg^{-1}), mice were placed individually in the center of the box and were observed for 5 min. The arena was cleaned with 70% ethyl alcohol after each trial to remove permeated odors from previous animals (Kraeuter et al., 2019b; He et al., 2020). Behavioral parameters were recorded and analyzed by EthoVision XT 8.0 (Noldus Information Technology, Wageningen, Netherlands) motion tracking software. The number of the animals are 10 in each group.

Data and Statistical Analysis

Graphs and calculations were made using GraphPad Prism (GraphPad Prism version 8.0.1 for Windows). Curves of both G protein activation and β-arrestin 2 recruitment assays were fit by nonlinear regression using the sigmoidal dose–response equation. In the G protein activation assay we performed three experiments in triplicates. In β-arrestin assay, the experiments were conducted twice. In one experiment there were six different concentrations of each drug, each concentration was tested in duplicates to provide $n = 2$.

Results are expressed as means ± S.E.M. The maximum responses for all compounds in β-arrestin 2 recruitment assay were compared using one-way ANOVA with Dunnett's post hoc test. Data of neuropathic pain model were analyzed by one-way ANOVA Bonferroni's Multiple Comparison Test for comparing the anti-hyperalgesic effects in the different groups. Data of behavioral experiments were compared using Student's unpaired t-test except the number of rearings which were made using the Mann-Whitney U-test. The levels for statistically significant differences were set as $^{*}p < 0.05$, $^{**}p < 0.01$.

Materials

In the SST_4 receptor activation assay all the compounds were dissolved in dimethyl sulfoxide (DMSO). The concentration of the stock solutions was 10 mM, that was diluted with distilled water or assay medium to reach the final concentrations. For the *in vivo* experiments 1 mg of the compounds was suspended thoroughly in 1 ml 1.25% methylcellulose solution dissolved in sterile bidistilled water to get a 1,000 μg·ml^{-1} stock solution freshly every experimental day. Most microsuspensions looked opalescent, they were shaken properly, sonicated, and further diluted with 1.25% methylcellulose to obtain the 1, 5, 25, 50 and 100 μg·ml^{-1} solution for oral administrations (20 ml·kg^{-1} body weight for the 20, 100, 500, 1,000 and 2,000 μg·kg^{-1} dose). The solutions were shaken and sonicated again directly before use. The vehicle was always 1.25% methylcellulose dissolved in sterile bidistilled water.

Tris–HCl (PubChem CID: 93573), EGTA (PubChem CID: 6207), $MgCl_2$ (PubChem CID: 5360315), NaCl (PubChem CID: 5234): Reanal, Budapest, Hungary; GTP (PubChem CID: 135398633) : BioChemica International Inc., Melbourne, FL, United States; GDP (PubChem CID: 135398619), urea (PubChem CID: 1176), acetic acid (PubChem CID: 176): Sigma, St. Louis, MO, United States; dimethyl sulfoxide (DMSO, PubChem CID: 679): Szkarabeusz Ltd., Pécs, Hungary; [^{35}S]GTPγS: Institute of Isotopes, Budapest, Hungary; CHO-K1 cells: European Collection of Authenticated Cell Cultures (ECACC Cat# 85051005, RRID:CVCL_0214), SST_4 receptor-expressing cell line was prepared in our laboratory; methylcellulose (MC; Ph. Eur. V.; PubChem CID: 44263857): Central Pharmacy of the University of Pécs, Pécs, Hungary; $hsstr_4$ cAMP CHO-K1 (RRID:CVCL_KV83) and $hsstr_4$ β-arrestin 2 CHO-K1 cells (RRID:CVCL_KZ14): DiscoverX, Fremont, CA; methylcellulose (MC;Ph.Eur.V.; PubChem CID: 44263857): Central Pharmacy of the University of Pécs, Pécs, Hungary.

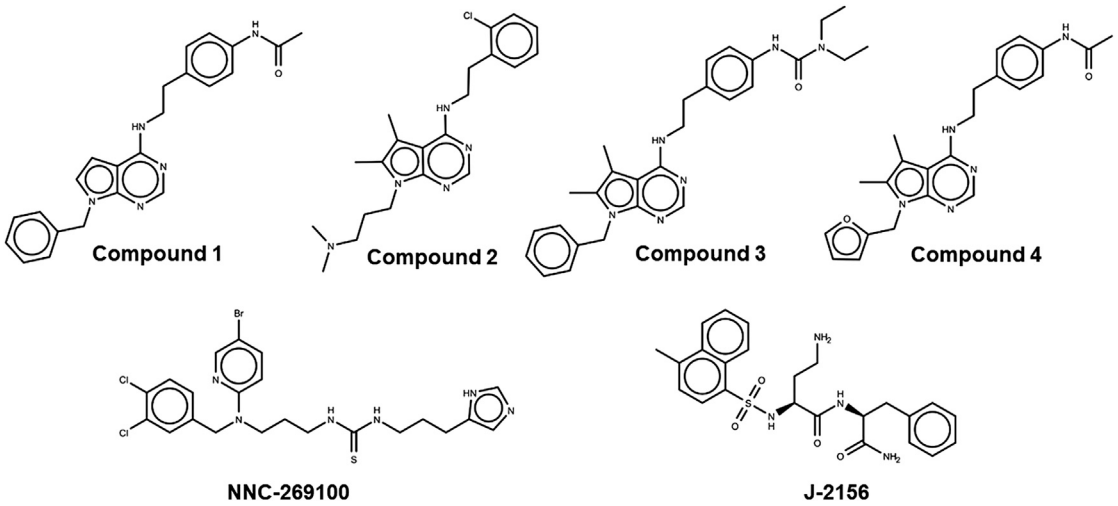

FIGURE 1 | Lewis structures of the tested new pyrrolo-pyrimidine ligands (upper panel) and the high affinity reference molecules (lower panel).

TABLE 1 | Target residues interacting with representative docked ligand structures within 3.5 Å.

	NNC-269100	J2156	Compound 1	Compound 2	Compound 3	Compound 4
Tyr18			x	x	x	
Val67	X		x	x	x	
Ser70	Xx	xx	xx	xx	xx	
Ala71				x		
Trp76	X		x	x	x	
Cys83	Xx	xx	xx		xx	xx
Arg84			x			x
Val86					x	
Leu87	Xx	xx	xx	xx	xx	
Asp90		x		x	x	x
Pro153			x			x
Asn163			x			x
Pro169	xx	xx	xx	xx	xx	xx
Ala170			x			x
Trp171	xx	xx	xx		xx	xx
His258	xx	xx				xx
Val259		x		X		
Ile262	xx	xx	xx	xx	xx	
Tyr265			X			
Fit (%)	82	82	73	73	82	45
E_{inter}	−6.58	−6.58	−8.17	−6.67	−7.97	−7.17

Amino acids interacting with the docked representatives within 3.5 Å are marked with a cross. Gray color shows the amino acids interacting with reference molecules. Double cross indicates amino acids interacting with both reference molecules.

RESULTS

In Silico Modeling and Binding Assay

Two high affinity SST_4 agonist reference compounds NNC-269100 and J-2156 (Liu et al., 1998) were used in the present study. They were shown to bind a region called high affinity binding pocket in previous studies composed of amino acids Tyr18, Val67, Ser70, Ala71, Cys83, Asp90, His258, Val259, Ile262, Leu263. Serial numbering of target residues follows that of the previous study (Liu et al., 2012). Docking of the references and four new Compounds (**Figure 1**) to the SST_4 target was performed as described in Methods. It was found that interaction energy values of the docked representatives of Compounds 1–4 do not show significant differences if compared with the high affinity reference molecules NNC-269100 and J-2156 (**Table 1**) Amino acids interacting with the representative docked ligands are marked with a cross in **Table 1**. Reference molecules have interaction with eleven target (showed with gray color in **Table 1**) residues that are identical (10^{-5} M) more than 60% (showed with double cross in

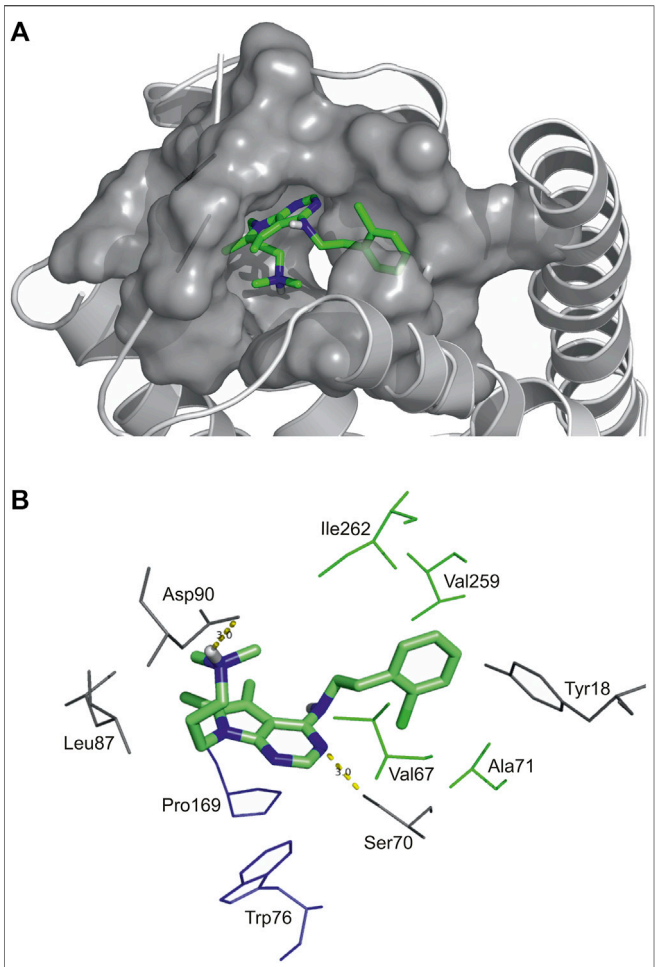

FIGURE 2 | High affinity binding pocket with Compound 2 in SST_4 receptor **(A)**, Binding pattern of Compound 2: hydrophobic pocket composed of Val67, Ala71 in TM2, Val259 and Ile262 in TM7, aromatic-aromatic interactions with Pro169 and Trp76, H-bonds (yellow) with Asp90 and Ser70 **(B)**.

Table 1). Fit % means the ratio of identical interacting residues of the references calculated for each compound. It shows that the ratio of interacting target residues for Compounds 1–3 is similar as that of the reference molecules. However, fit % of Compound 4 is 45%, it has interaction with Asp90, the key amino acid suggested essential role in ligand binding and receptor activation. Analyzes of the residues interacting with the representative docked ligand conformations within 3.5 Å showed that the new compounds maintain the contact with amino acids similarly to reference molecules, likewise to the interaction energy. Thus, reference ligands and new compounds have overlapping binding site on SST_4.

As an example, atomic details of binding of Compound 2 to SST_4 is further shown in a close-up view (**Figure 2**). The chlorobenzyl group of Compound 2 is buried in a hydrophobic pocket formed by Val67, Ala71 in TM2, Val259 and Ile262 in TM7 (TM2/TM7 hydrophobic cavity (Liu et al., 2012). The 7H-pyrrolo[2,3-d] pyrimidine core of molecule has aromatic-aromatic interactions with Pro169 and Trp76 and stabilized by a H-bond with Ser70. Furthermore, there is an ionic interaction between Asp90 on TM3 and tertiary amine group of Compound 2. It is presumed based on site-directed mutagenesis studies that an ionic interaction between Lys9 of endogenous peptide and the conserved aspartic acid on TM3 of all SST receptors has a crucial role in ligand binding and receptor activation (Kaupmann et al., 1995; Nehrung et al., 1995; Ozenberger and Hadcock, 1995; Chen et al., 1999; Liu et al., 2012).

SST_4 Receptor-Coupled G Protein Activation

Based on the *in silico* binding results, the SST_4 receptor activating potential of the new compounds was measured and compared to the reference agonist NNC 26-9100 and J-2156 (Engström et al., 2005). We found concentration-dependent stimulation in the [^{35}S]GTPγS binding assay on SST_4-expressing CHO cells (**Figure 3**.). The EC_{50} values demonstrating the potency of the ligands were, 75 , 28 , 16 and 24 nM for Compound 1, 2, 3 and 4, respectively (n=3 independent experiments with each compound). The maximal activation values over the basal activities of the receptor showing the efficacy of the compounds were 242.7 ± 26%, 213 ± 9%, 220 ± 7% and 228.7 ± 9%, in cases of Compounds 1, 2, 3 and 4, respectively. Thus, all these compounds are potent and effective SST_4 receptor agonists.

Effects of Compounds 1–4 on SST_4 Activation-Related β-Arrestin 2 Recruitment

Subsequently, we investigated the ability of the agonists to mediate β-arrestin two recruitment, measured as an increase in the chemiluminescent signal. The novel ligands displayed no detectable β-arrestin 2 recruitment in the PathHunter assay (testing range: 10^{-12}–10^{-5} M). However, the reference compounds, NNC 26-9100 and J-2156 showed marked β-arrestin 2 recruitment (**Figure 4**).

Anti-Hyperalgesic Effect of Compounds 1–4 in the Partial Sciatic Nerve Ligation-Induced Neuropathy Model

In response to the partial sciatic nerve ligation, 37.3 ± 0.8% mechanical hyperalgesia (drop of the mechanonociceptive threshold) developed on the seventh postoperative day, while the thresholds of the contralateral paws did not change compared to the baseline values. Treatment with the 500 μg·kg^{-1} oral dose of Compound 1, 2, 3 and 4 significantly increased the mechanonociceptive threshold of the treated paw 60 min later showing anti-hyperalgesic effects, while the vehicle had no effect (Compound 1: 52.1 ± 5.4% vs. vehicle: 14.7 ± 6.1%; Compound 2: 54.6 ± 13.6% vs. vehicle: 7.8 ± 8.1%; Compound 3: 57.0 ± 16.1%vs. vehicle: 12.0 ± 7.2%; Compound 4: 57.2 ± 14.6% vs. vehicle: 10.0 ± 7.6%). In case of Compound 2, the 100 μg·kg^{-1} dose also had a significant anti-hyperalgesic effect (Compound 2: 64.4 ± 14.3% vs. vehicle: 7.8 ± 8.1%). Higher doses of the compounds had smaller effects not reaching statistical significance making the dose–response relationship bell-shaped (**Figure 5**.).

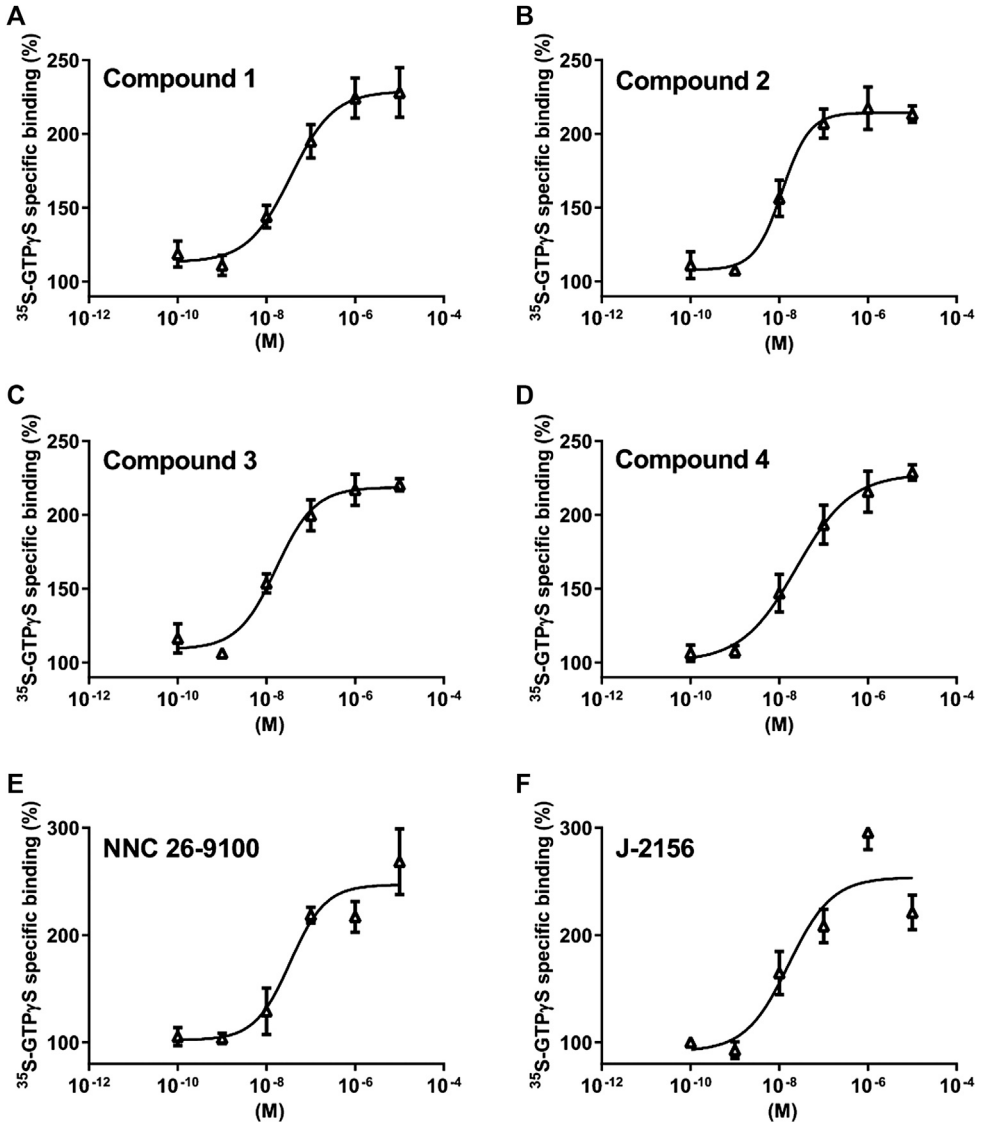

FIGURE 3 | Effect of Compounds 1–4 compared with reference molecules NNC 26-9100 and J-2156 on SST_4 receptor-linked G protein activation. [^{35}S]GTPγS binding induced by the compound in SST_4-expressing CHO cells. The ligand-stimulated [^{35}S]GTPγS binding reflects the GDP–GTP exchange reaction on α subunits of G proteins by receptor agonists. Increasing concentrations of all compounds result in similar concentration-dependent stimulations of [^{35}S]GTPγS binding. Each data point represents the mean ± SEM of n = 3 independent experiments, each performed in triplicates.

Spontaneous Locomotor Activity and Anxiety Level Are Not Influenced by Compound 2

Neither spontaneous locomotor activity nor anxiety-related behaviors in the OFT and the EPM were influenced by Compound 2.

There was no significant difference in the time spent in the open arms of the EPM (Compound 2: 52.8 ± 7.4 s vs. vehicle: 51.0 ± 8.5 s) or in the distant 1/3 of the open arms (Compound 2: 9.1 ± 3.1 s vs. vehicle: 6.2 ± 2.8) between Compound 2- and vehicle-treated mice (**Figure 6**.).

None of the parameters in the OFT, such as the distance moved (Compound 2: 1,798 ± 180.8 cm vs. vehicle: 1,824 ± 130.2 cm), velocity (Compound 2: 6.0 ± 0.6 m/s vs. vehicle: 6.1 ± 0.4 m/s), time spent moving (Compound 2: 56.0 ± 5.2 s vs. vehicle: 56.3 ± 3.7 s), time spent in center zone (Compound 2: 59.8 ± 8.7 s vs. vehicle: 59.5 ± 4.0 s), and number of rearings (Compound 2: 31.1 ± 4.1 vs. vehicle: 30.6 ± 3.2) differed significantly between Compound 2- and vehicle-treated mice (**Figure 7**.).

DISCUSSION

In the present study, four novel ligands designed for agonism at SST_4 somatostatin receptor have been characterized. *In silico*

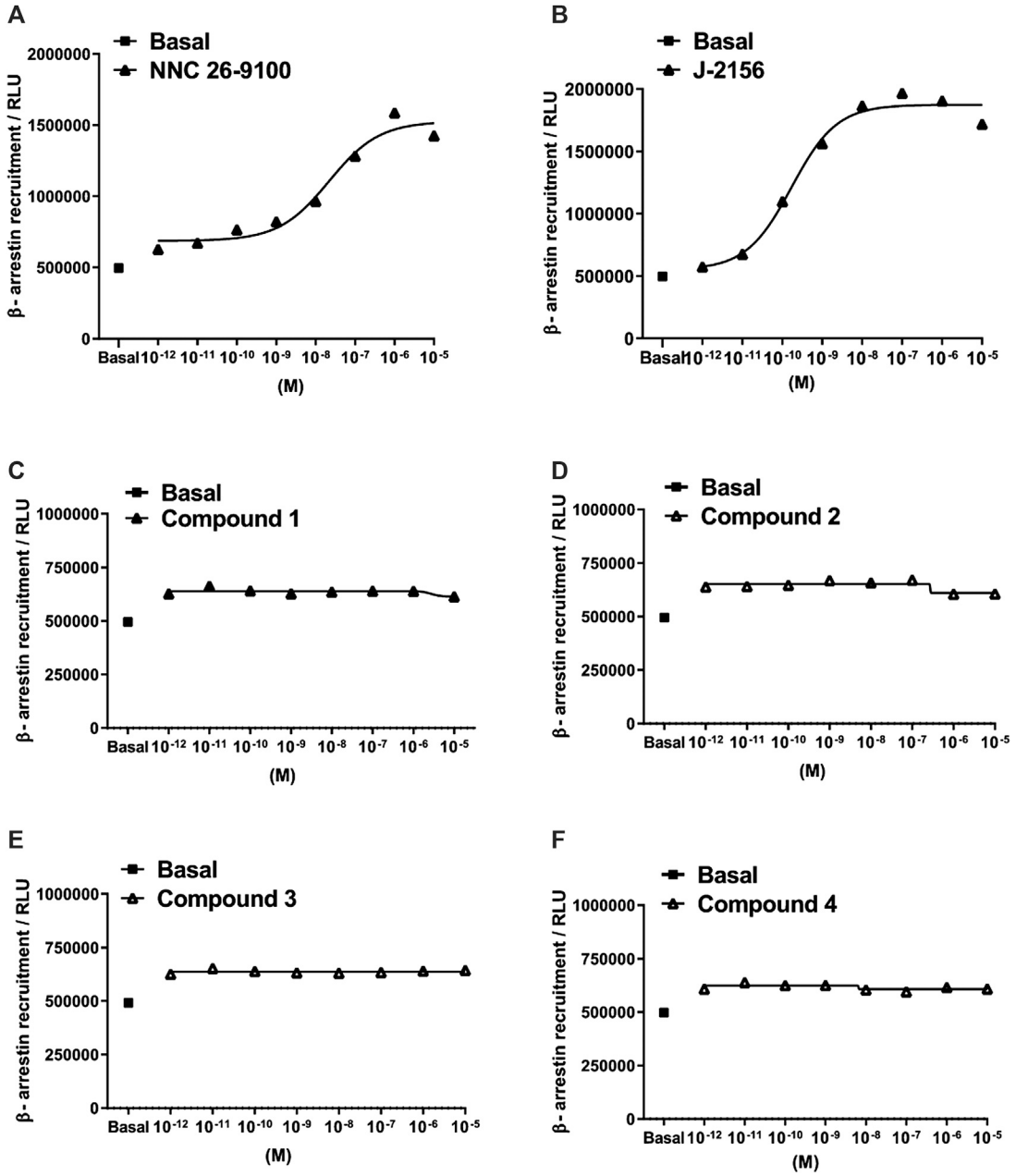

FIGURE 4 | Concentration-response curves of Compounds 1–4 in the β-arrestin 2 recruitment assay. Data represent concentration–response curves of the novel compounds expressed as relative luminescence units (RLU) in comparison to the reference compounds NNC 26-9100 and J-2156. All values are means ± SEM (n = 2 experiments). In each experiment, data points were obtained in duplicates.

modeling studies revealed that Compounds 1–4 interact with the receptor with similar energy and have overlapping binding sites on the SST_4 receptor (Liu et al., 2012) as the reference ligands NNC 26-9100 and J-2156 (**Table 1**). The binding region of J-2156 composed of amino acids Tyr18, Val67, Ser70, Ala71, Cys83, Val259 is overlapped to the binding site called high affinity binding pocket and described by Liu and coworkers (Liu et al., 2012). Docking calculations revealed that Compounds 2–4 maintain the interaction with Asp90 of TM3, as a key residue suggested by previous experimental studies with J-2156 (Kaupmann et al., 1995; Nehrung et al., 1995; Ozenberger and Hadcock, 1995; Chen et al., 1999; Liu et al., 2012). However, neither Compound 1 nor the high affinity reference NNC 26-9100 bind to the conserved aspartic acid. As they have interaction with similar residues in a high percent, our above findings suggest an alternative binding mode for these ligands.

Stimulation of G protein-coupled receptors by agonists regulates multiple downstream pathways through alpha and

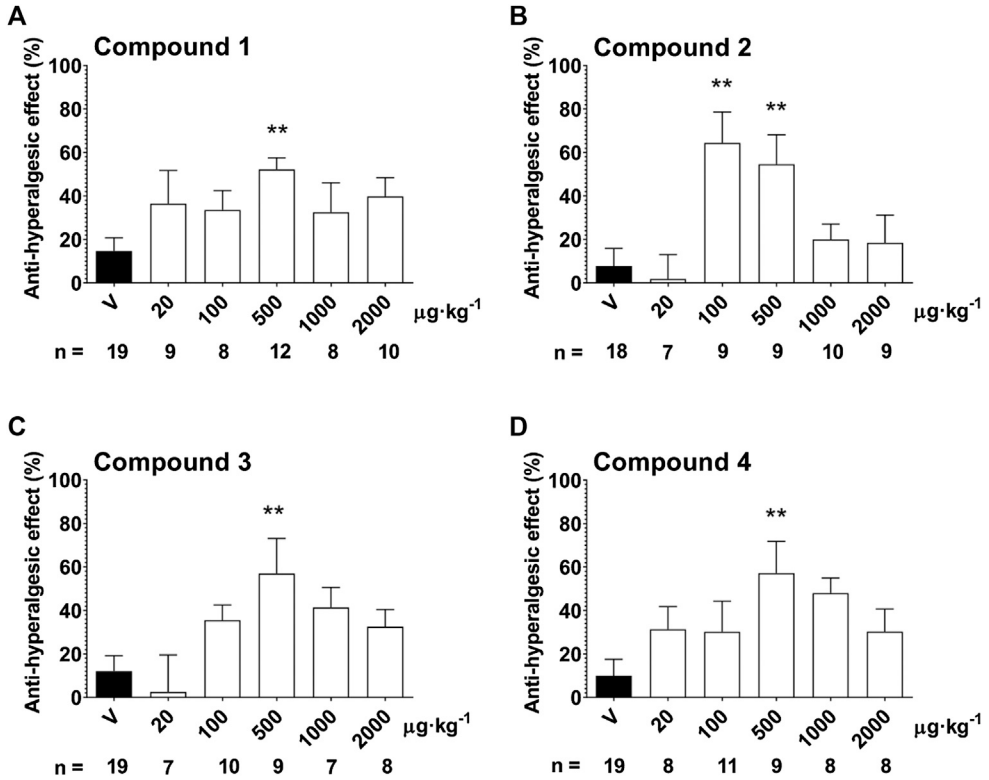

FIGURE 5 | Anti-hyperalgesic effect of a single oral treatment with Compounds 1–4 7 days after partial tight ligation of the sciatic nerve in the mouse. Columns represent anti-hyperalgesic effect 60 min after treatment with the respective test compound compared to pre-treatment control values. Each column represents the mean + S.E.M. of *n*. Data were analyzed with one-way ANOVA Bonferroni's Multiple Comparison Test (*$p < 0.05$, **$p < 0.001$ vs. vehicle control values).

beta–gamma subunits of the various G proteins. In the G protein activation assay performed on SST_4 receptor-expressing CHO cells, all the four novel compounds evoked concentration-dependent increases in [^{35}S]GTPγS binding reflecting the GDP–GTP exchange reaction on the alpha subunit of G protein similarly to the reference agonists NNC 26-9100 and J-2156. As NNC 26-9100 and J-2156 proved to be full agonists of SST_4 in a previous study (Liu et al., 1999) and the maximal achievable activation was comparable with that of the other four investigated compounds, all the novel ligands can be considered as full SST_4 agonists. Based on the EC_{50} values, the novel ligands displayed similar potencies, but Compound 3 was the most potent.

Agonist-evoked activation of heptahelical receptors also stimulates G protein-coupled receptor kinases phosphorylating the activated receptor, thereby allowing attachment of β-arrestin proteins to the receptor. While β-arrestin recruitment/binding physically obstructs the G protein coupling with the receptor, additional mechanisms have been revealed by which β-arrestins ensure efficient blockade of G protein signaling and thus, desensitization of the heptahelical receptors (Shenoy and Lefkowitz, 2011). Although β-arrestins were initially held responsible only for desensitization and down-regulation of these receptors, newer data support the view that they can also initiate several signal transduction mechanisms including e.g. activation of mitogen-activated protein kinase enzymes

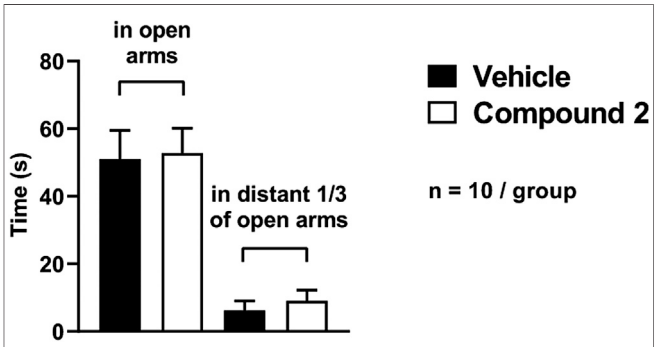

FIGURE 6 | Anxiety-like behavior quantification using EPM. Results are expressed as means ± S.E.M., data were analyzed by Student's unpaired t-test, *n* = 10/group.

(Lefkowitz, 2005). Furthermore, the existence of these two distinct pathways (i.e. G protein-dependent and β-arrestin-mediated) allows for biased agonism (also called stimulus trafficking) meaning that some ligands may act exclusively through either G protein-dependent or β-arrestin-mediated cascade (Rajagopal et al., 2010). In case of the SST_4 receptor, a dissociation of G protein activation and desensitization of a cellular effect with some agonists has been revealed, but the

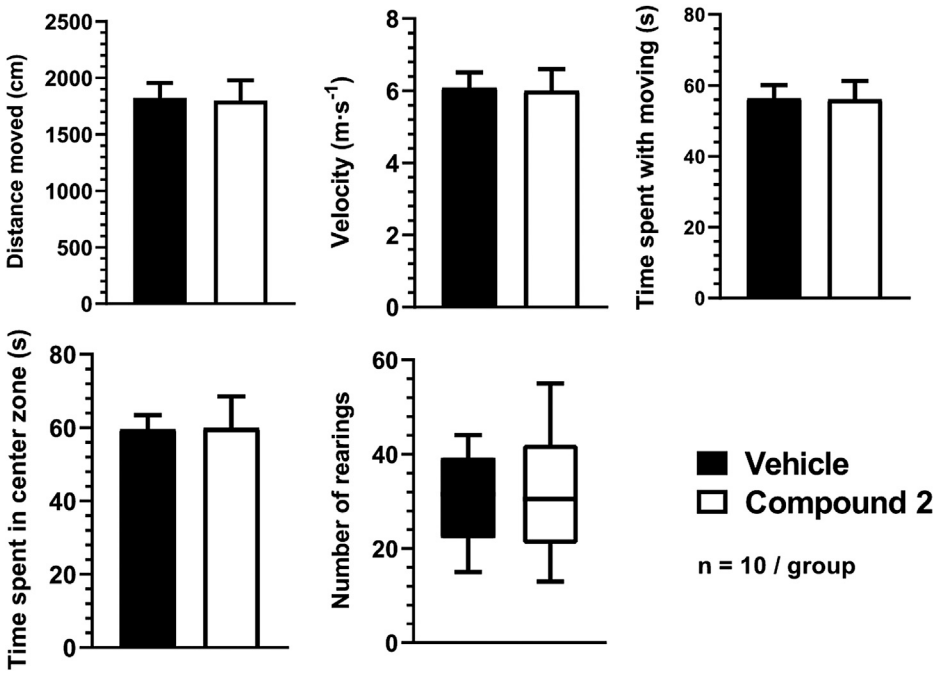

FIGURE 7 | Spontaneous locomotor activity and anxiety-like behavior quantification using OFT. The number of rearings are expressed as the geometric mean with 95% confidence intervals and statistical comparisons were made using the Mann-Whitney U-test. All other data are determined as mean ± S.E.M. and were compared using the Student's unpaired t-test, *n* = 10/group.

possible role of β-arrestins in the latter response has not been demonstrated so far (Smalley et al., 1998; Engström et al., 2006). In addition, both reference compounds showed an association with β-arrestin 2 recruitment. It was a surprising finding that all four novel SST_4 receptor agonists failed to evoke any detectable β-arrestin 2 recruitment. This result can be interpreted as biased agonism with Compounds 1–4 meaning that they initiate G_i protein-mediated receptor activation, but they are unable to recruit β-arrestin. The latter feature may be advantegous if it results in smaller degree of SST_4 desensitization to SST_4 receptor agonists upon repeated administration. However, if β-arrestin-mediated signaling also contributes to some potential therapeutic effects of SST_4 receptor agonists, this biased agonism may reduce some effects mediated by these receptors. Further studies are needed to clarify these issues. It is worth to mention that the SST_{2A} somatostatin receptor, biased agonism has also been demonstrated (Schonbrunn, 2008).

The high *in vitro* efficacy and potency of the novel SST_4 agonists made them suitable for *in vivo* testing of their antinociceptive activity. In the mouse model of traumatic neuropathic pain employing partial sciatic nerve ligation (Seltzer et al., 1990), a decrease of the mechanonociceptive threshold of the hindpaw occurred indicating the development of mechanical hyperalgesia. Following oral administration, all novel compounds were able to increase the mechanonociceptive threshold evoking anti-hyperalgesic effects. Interestingly, no conventional dose–response relationship could be established for these drugs. Bell-shaped dose–response curves could be determined for all compounds with two lower and two higher statistically ineffective doses, while the middle dose ($500\ \mu g \cdot kg^{-1}$) produced a significant anti-hyperalgesic effect. Similar efficacies corresponding to about 50–60% anti-hyperalgesic actions were observed for all drugs. Compound 2 also proved to be more potent than the other three ones as it was already effective at the $100\ \mu g \cdot kg^{-1}$ dose. The (minimal) effective anti-hyperalgesic dose of these novel SST_4 agonists is rather low indicating high *in vivo* potencies of the compounds. The reason for the bell-shaped dose–response relationship is not clear. The SST_4 receptors are present in pain-related brain regions (Kecskés et al., 2020) and also on primary sensory neurons including the peripheral terminals. We showed earlier that SST4 activation by the selective agonist J-2156 inhibits the release of sensory neuropeptides, such as substance P, calcitonin gene related peptide and somatostatin (Helyes et al., 2006). Therefore, the potential inhibitory effect of SST_4 agonists on the release of endogenous inhibitory mediators, such as somatostatin and opioid peptides cannot be excluded and might explain the lack of dose-response relationship or the bell-shaped dose-response curves. The anti-hyperalgesic effect of the compounds is not accompanied by modulated spontaneous locomotor activity and/or anxiety level, as shown by the results obtained with Compound 2, suggesting selective actions on the pain pathway.

We clearly see a significant therapeutic potential in stable, orally active, non-peptide SST_4 agonists. On the basis of the data obtained with the compounds tested in previous work as well as the present studies, these agents appear to possess broad-spectrum antinociceptive activity in models of both inflammatory and neuropathic pain (Kántás et al., 2019). Regarding the mode of action, a similarity with opioid analgesics is apparent: in both cases G_i protein-coupled, typically presynaptically/prejunctionally located receptors are activated. This

may result in—among other actions—reduction of the release of a huge array of proinflammatory and/or pronociceptive mediators from peripheral and central endings of nociceptive primary sensory neurons. This mechanism is in sharp contrast with that of receptor antagonists which can only inhibit the action of the endogenous agonist(s) of the respective receptor. As the SST_4 receptor does not appear to be involved in the myriad of endocrine effects of somatostatin (mediated by SST_2, SST_3 and SST_5 receptors), a good tolerability can be predicted for these agents. A great interest of drug companies is indicated by Lilly's recently announced licensing agreement for CNTX-0290, a SST_4 receptor agonist studied in a phase 1 clinical trial (Lilly, 2020; Stevens et al., 2020).

CONCLUSION

The novel pyrrolo-pyrimidine compounds are effective and potent SST_4 receptor agonists as shown by their *in silico* binding to the high affinity binding site and G protein activation on SST_4-expressing cells, but do not recruit β-arrestin suggesting biased agonism. They inhibit chronic neuropathic mechanical hyperalgesia following a single oral administration of a low dose (500 $\mu g \cdot kg^{-1}$), therefore, they are promising candidates for the development of a completely novel group of analgesic drugs for a huge unmet medical need.

DATA AVAILABILITY STATEMENT

The original contributions presented in the study are included in the article/**Supplementary Material**, further inquiries can be directed to the corresponding author.

ETHICS STATEMENT

The animal study was reviewed and approved by Ethics Committee on Animal Research of Pécs University.

AUTHOR CONTRIBUTIONS

ZH, EP, and EB designed the study, BK, ES, RB, CH, JA, AS, LH, AgH, AdH and AK performed parts of experiments, interpreted the data and performed data analysis and BK, ES, PB, GP, EP, and ZH drafted the manuscript and revised it critically for intellectual content. All authors read and approved the final version of the manuscript before submission.

FUNDING

This work was funded by the Hungarian National Research, Development and Innovation Office (K123836, K134214), 2017-1.2.1-NKP-2017-00002 (NAP-2; Chronic Pain Research Group), EFOP-3.6.1.-16-2016-00004 and GINOP 2.3.2-15-2016-00050 "PEPSYS". EB, ES, CH and AK were supported by the János Bolyai Research Scholarship of the Hungarian Academy of Sciences. We acknowledge the grant of computer time from the Governmental Information Technology Development Agency, Hungary. The University of Pécs is acknowledged for a support by the 17886-4/23018/FEKUTSTRAT excellence grant, and by PTE ÁOK-KA No: 2019/KA-2019-31. CH's work was supported by a grant co-financed by Hungary and the European Union (EFOP-3.6.2-16-2017-00008) and the ÚNKP-20-5 New National Excellence Program of the Ministry for Innovation and Technology. BK's work was supported by ÚNKP-20-3 New National Excellence Program of the Ministry for Innovation and Technology and Gedeon Richter's Talentum Foundation.

ACKNOWLEDGMENTS

The authors thank László Őrfi and Tamás Szűts for the collaboration in the synthesis of the compounds and Dóra Ömböli for expert technical assistance. We dedicate this work to our highly respected dear colleagues, János Szolcsányi and György Kéri, who sadly passed away recently, and whose contributions were essential to the present project.

SUPPLEMENTARY MATERIAL

The Supplementary Material for this article can be found online at: https://www.frontiersin.org/articles/10.3389/fphar.2020.601887/full#supplementary-material.

REFERENCES

Abraham, M. J., Murtola, T., Schulz, R., Páll, S., Smith, J. C., Hess, B., et al. (2015). GROMACS: high performance molecular simulations through multi-level parallelism from laptops to supercomputers. *Software* 1 (2), 19–25. doi:10.1016/j.softx.2015.06.001

Chen, L., Hoeger, C., Rivier, J., Fitzpatrick, V. D., Vandlen, R. L., Tashjian, A. H., et al. (1999). Structural basis for the binding specificity of a $SSTR_1$-selective analog of somatostatin. *Biochem. Biophys. Res. Commun* 258, 689–694. doi:10.1006/bbrc.1999.0699

Elekes, K., Helyes, Z., Kereskai, L., Sándor, K., Pintér, E., Pozsgai, G., et al. (2008). Inhibitory effects of synthetic somatostatin receptor subtype 4 agonists on acute and chronic airway inflammation and hyperreactivity in the mouse. *Eur. J. Pharmacol.* 578, 313–322. doi:10.1016/j.ejphar.2007.09.033

Engström, M., Savola, J.-M., and Wurster, S. (2006). Differential efficacies of somatostatin receptor agonists for G-protein activation and desensitization of somatostatin receptor subtype 4-mediated responses. *J. Pharmacol. Exp. Therapeut*. 316, 1262–1268. doi:10.1124/jpet.105.094128

Engström, M., Tomperi, J., El-Darwish, K., Åhman, M., Savola, J.-M., and Wurster, S. (2005). Superagonism at the human somatostatin receptor subtype 4. *J. Pharmacol. Exp. Therapeut* 312, 332–338. doi:10.1124/jpet.104.075531

He, T., Guo, C., Wang, C., Hu, C., and Chen, H. (2020). Effect of early life stress on anxiety and depressive behaviors in adolescent mice. *Brain Behav.* 10, e01526. doi:10.1002/brb3.1526

Helyes, Z., Pintér, E., Németh, J., Sándor, K., Elekes, K., Szabó, A., et al. (2006). Effects of the somatostatin receptor subtype 4 selective agonist J-2156 on sensory neuropeptide release and inflammatory reactions in rodents. *Br. J. Pharmacol.* 149, 405–415. doi:10.1038/sj.bjp.0706876

Helyes, Z., Pinter, E., Sandor, K., Elekes, K., Bánvölgyi, A., Keszthelyi, D., et al. (2009). Impaired defense mechanism against inflammation, hyperalgesia, and airway hyperreactivity in somatostatin 4 receptor gene-deleted mice. *Proc. Natl. Acad. Sci. U.S.A.* 106, 13088–13093. doi:10.1073/pnas.0900681106

Helyes, Z., Szabó, Á., Németh, J., Jakab, B., Pintér, E., Bánvölgyi, Á., et al. (2004). Antiinflammatory and analgesic effects of somatostatin released from capsaicin-sensitive sensory nerve terminals in a freund's adjuvant-induced chronic arthritis model in the rat: function of somatostatin in chronic inflammation. *Arthritis Rheum.* 50, 1677–1685. doi:10.1002/art.20184

Hernández, C., Arroba, A. I., Bogdanov, P., Ramos, H., Simó-Servat, O., Simó, R., et al. (2020). Effect of topical administration of somatostatin on retinal inflammation and neurodegeneration in an experimental model of diabetes. *J. Clin. Med.* 9, 2579. doi:10.3390/jcm9082579

Kántás, B., Börzsei, R., Szőke, É., Bánhegyi, P., Horváth, Á., Hunyady, Á., et al. (2019). Novel drug-like somatostatin receptor 4 agonists are potential analgesics for neuropathic pain. *Int. J. Mol. Sci* 20, 6245. doi:10.3390/ijms20246245

Kaupmann, K., Bruns, C., Raulf, F., Weber, H. P., Mattes, H., Lübbert, H., et al. (1995). Two amino acids, located in transmembrane domains VI and VII, determine the selectivity of the peptide agonist SMS 201-995 for the $SSTR_2$ somatostatin receptor. *EMBO J.* 14, 727–735. doi:10.1002/j.1460-2075.1995.tb07051.x

Kecskés, A., Pohóczky, K., Kecskés, M., Varga, Z. V., Kormos, V., Szőke, É., et al. (2020). Characterization of neurons expressing the novel analgesic drug target somatostatin receptor 4 in mouse and human brains. *Int. J. Mol. Sci.* 21, 7788. doi:10.3390/ijms21207788

Kraeuter, A-K., Guest, P. C., and Sarnyai, Z. (2019a). "The elevated plus maze test for measuring anxiety-like behavior in rodents," in *Pre-clinical models*. Editor P. C. Guest (New York, NY: Springer New York), 69–74.

Kraeuter, A-K., Guest, P. C., and Sarnyai, Z. (2019b). "The open field test for measuring locomotor activity and anxiety-like behavior," in *Pre-clinical models*. Editor P. C. Guest (New York, NY: Springer New York), 99–103, 1916. doi:10.1007/978-1-4939-8994-2_9

Kuo, A., Lourdesamy, J., Nicholson, J. R., Corradini, L., and Smith, M. T. (2020). Assessment of the anti-hyperalgesic efficacy of J-2156, relative to clinically available analgesic/adjuvant agents in a rat model of mild to moderate chronic mechanical low back pain (LBP). *Clin. Exp. Pharmacol. Physiol* 47 (12), 1912–1922. doi:10.1111/1440-1681.13383

Lefkowitz, R. J. (2005). Transduction of receptor signals by-arrestins. *Science* 308, 512–517. doi:10.1126/science.1109237

Leo, S., Straetemans, R., Dhooge, R., and Meert, T. (2008). Differences in nociceptive behavioral performance between C57BL/6J, 129S6/SvEv, B6 129 F1 and NMRI mice. *Behav. Brain Res.* 190, 233–242. doi:10.1016/j.bbr.2008.03.001

Lilly (2020). Available at: https://centrexion.com/wp-content/uploads/2019/09/NeuPSIG-2019-0290-SAD-Poster-Final-4-29-19.pdf. In: https://www.lilly.com/discovery/pipeline

Lister, R. G. (1987). The use of a plus-maze to measure anxiety in the mouse. *Psychopharmacology (Berl)* 92, 180. doi:10.1007/BF00177912

Liu, S., Crider, A. M., Tang, C., Ho, B., Ankersen, M., and Stidsen, C. E. (1999). 2-pyridylthioureas: novel nonpeptide somatostatin agonists with SST_4 selectivity. *Curr. Pharmaceut. Des.* 5, 255–263. doi:10.1002/chin.199925292

Liu, S., Tang, C., Ho, B., Ankersen, M., Stidsen, C. E., Crider, A. M., et al. (1998). Nonpeptide somatostatin agonists with sst $_4$ selectivity: synthesis and Structure−Activity relationships of thioureas. *J. Med. Chem* 41, 4693–4705. doi:10.1021/jm980118e

Liu, Z., Crider, A. M., Ansbro, D., Hayes, C., and Kontoyianni, M. (2012). A structure-based Approach to understanding somatostatin receptor-4 agonism (SST_4). *J. Chem. Inf. Model* 52, 171–186. doi:10.1021/ci200375j

Malmberg, A. B., and Basbaum, A. I. (1998). Partial sciatic nerve injury in the mouse as a model of neuropathic pain: behavioral and neuroanatomical correlates. *Pain* 76, 215–222. doi:10.1016/S0304-3959(98)00045-1

Markovics, A., Szőke, É., Sándor, K., Börzsei, R., Bagoly, T., Kemény, Á., et al. (2012). Comparison of the anti-inflammatory and anti-nociceptive effects of cortistatin-14 and somatostatin-14 in distinct *in vitro* and *in vivo* model systems. *J. Mol. Neurosci* 46, 40–50. doi:10.1007/s12031-011-9577-4

Morris, G. M., Huey, R., Lindstrom, W., Sanner, M. F., Belew, R. K., Goodsell, D. S., et al. (2009). AutoDock4 and AutoDockTools4: automated docking with selective receptor flexibility. *J. Comput. Chem.* 30, 2785–2791. doi:10.1002/jcc.21256

Nehrung, R. B., Meyerhof, W., and Richter, D. (1995). Aspartic acid residue 124 in the third transmembrane domain of the somatostatin receptor subtype 3 is essential for somatostatin-14 binding. *DNA Cell Biol* 14, 939–944. doi:10.1089/dna.1995.14.939

Ozenberger, B. A., and Hadcock, J. R. (1995). A single amino acid substitution in somatostatin receptor subtype 5 increases affinity for somatostatin-14. *Mol. Pharmacol* 47, 82–87.

Pintér, E., Helyes, Z., Németh, J., Pórszász, R., Pethö, G., Thán, M., et al. (2002). Pharmacological characterisation of the somatostatin analogue TT-232: effects on neurogenic and non-neurogenic inflammation and neuropathic hyperalgesia. *Naunyn-Schmiedeberg's Arch. Pharmacol.* 366, 142–150. doi:10.1007/s00210-002-0563-9

Pintér, E., Helyes, Z., and Szolcsányi, J. (2006). Inhibitory effect of somatostatin on inflammation and nociception. *Pharmacol. Ther.* 112, 440–456. doi:10.1016/j.pharmthera.2006.04.010

Pintér, E., Pozsgai, G., Hajna, Z., Helyes, Z., and Szolcsányi, J. (2014). Neuropeptide receptors as potential drug targets in the treatment of inflammatory conditions: neuropeptide receptors in inflammation. *Br. J. Clin. Pharmacol.* 77, 5–20. doi:10.1111/bcp.12097

Power and Sample Size.com (2020) Overview of power and sample size.com. Calculators [online]. Available at: http://powerandsamplesize.com/Calculators.

Rajagopal, S., Rajagopal, K., and Lefkowitz, R. J. (2010). Teaching old receptors new tricks: biasing seven-transmembrane receptors. *Nat. Rev. Drug Discov.* 9, 373–386. doi:10.1038/nrd3024

Sándor, K., Elekes, K., Szabó, Á., Pintér, E., Engström, M., Wurster, S., et al. (2006). Analgesic effects of the somatostatin SST_4 receptor selective agonist J-2156 in acute and chronic pain models. *Eur. J. Pharmacol.* 539, 71–75. doi:10.1016/j.ejphar.2006.03.082

Scheich, B., Csekő, K., Borbély, É., Ábrahám, I., Csernus, V., Gaszner, B., et al. (2017). Higher susceptibility of somatostatin 4 receptor gene-deleted mice to chronic stress-induced behavioral and neuroendocrine alterations. *Neuroscience* 346, 320–336. doi:10.1016/j.neuroscience.2017.01.039

Scheich, B., Gaszner, B., Kormos, V., László, K., Ádori, C., Borbély, É., et al. (2016). Somatostatin receptor subtype 4 activation is involved in anxiety and depression-like behavior in mouse models. *Neuropharmacology* 101, 204–215. doi:10.1016/j.neuropharm.2015.09.021

Schonbrunn, A. (2008). Selective agonism in somatostatin receptor signaling and regulation. *Mol. Cell. Endocrinol* 286, 35–39. doi:10.1016/j.mce.2007.09.009

Schreff, M., Schulz, S., Händel, M., Keilhoff, G., Braun, H., Pereira, G., et al. (2000). Distribution, targeting, and internalization of the sst $_4$ somatostatin receptor in rat brain. *J. Neurosci.* 20, 3785–3797. doi:10.1523/JNEUROSCI.20-10-03785.2000

Schrödinger (2017). *Schrödinger Release 2017–4*. New York, NY: Maestro, Schrödinger, LLC.

Schuelert, N., Just, S., Kuelzer, R., Corradini, L., Gorham, L. C., Doods, H., et al. (2015). The somatostatin receptor 4 agonist J-2156 reduces mechanosensitivity of peripheral nerve afferents and spinal neurons in an inflammatory pain model. *Eur. J. Pharmacol.* 746, 274–281. doi:10.1016/j.ejphar.2014.11.003

Selmer, I.-S., Schindler, M., Humphrey, P. P. A., and Emson, P. C. (2000a). Immunohistochemical localization of the somatostatin sst4 receptor in rat brain. *Neuroscience* 98, 523–533. doi:10.1016/S0306-4522(00)00147-0

Selmer, I.-S., Schindler, M., Humphrey, P. P. A., Waldvogel, H. J., Faull, R. L., Emson, P. C., et al. (2000b). First localisation of somatostatin sst4 receptor protein in selected human brain areas: an immunohistochemical study. *Brain Res Mol Brain Res.* 82, 114–125. doi:10.1016/S0169-328X(00)00186-8

Seltzer, Z., Dubner, R., and Shir, Y. (1990). A novel behavioral model of neuropathic pain disorders produced in rats by partial sciatic nerve injury. *Pain* 43, 205–218. doi:10.1016/0304-3959(90)91074-S

Shenoy, P. A., Kuo, A., Khan, N., Gorham, L., Nicholson, J. R., Corradini, L., et al. (2018). The somatostatin receptor-4 agonist J-2156 alleviates mechanical hypersensitivity in a rat model of breast cancer induced bone pain. *Front. Pharmacol.* 9, 495. doi:10.3389/fphar.2018.00495

Shenoy, S. K., and Lefkowitz, R. J. (2011). β-arrestin-mediated receptor trafficking and signal transduction. *Trends Pharmacol. Sci* 32, 521–533. doi:10.1016/j.tips.2011.05.002

Shields, S. D., Eckert, W. A., and Basbaum, A. I. (2003). Spared nerve injury model of neuropathic pain in the mouse: a behavioral and anatomic analysis. *J. Pain* 4, 465–470. doi:10.1067/S1526-5900(03)00781-8

Smalley, K. S. M., Feniuk, W., and Humphrey, P. P. A. (1998). Differential agonist activity of somatostatin and L-362855 at human recombinant SST_4 receptors. *Br. J. Pharmacol.* 125, 833–841. doi:10.1038/sj.bjp.0702133

Stevens, R. M., Guedes, K., Kerns, W., Fong, K., Silverman, M. H., Zhou, G., et al. (2020). "Safety and pharmacokinetics of single ascending doses of human somatostatin receptor 4 (hSSTR4) agonist CNTX-0290 in healthy subjects," In: *Medicines in development*. https://www.lilly.com/discovery/pipeline

Stewart, J. J. P. (2013). Optimization of parameters for semiempirical methods VI: more modifications to the NDDO approximations and re-optimization of parameters. *J. Mol. Model.* 19, 1–32. doi:10.1007/s00894-012-1667-x

Stewart, J. J. P. (2016). *MOPAC2016 Stewart computational chemistry*. Colorado Springs, CO: OpenMOPAC. Available at: http://OpenMOPAC.net

Szolcsányi, J., Bölcskei, K., Szabó, Á., Pintér, E., Petho, G., Elekes, K., et al. (2004). Analgesic effect of TT-232, a heptapeptide somatostatin analogue, in acute pain models of the rat and the mouse and in streptozotocin-induced diabetic mechanical allodynia. *Eur. J. Pharmacol.* 498, 103–109. doi:10.1016/j.ejphar.2004.07.085

Szolcsanyi, J., Pinter, E., Helyes, Z., and Petho, G. (2011). Inhibition of the function of TRPV1-expressing nociceptive sensory neurons by somatostatin 4 receptor agonism: echanism and therapeutical Implications. *Curr. Top. Med. Chem.* 11, 2253–2263. doi:10.2174/156802611796904852

Szolcsányi, J., Pintér, E., Helyes, Z., Szőke, É., Wáczek, F., Őrfi, L., et al. (2019). *New agents for treating neurogenic inflammation and neuropathic hyperalgesia related disorders*. US10344032. USA Patent: European Patent: EP3194399.

Conflict of Interest: ZH is the strategic director and shareholder of PharmInVivo Ltd. (Pécs, Hungary) and shareholder of Algonist Biotechnologies Gmbh, (Wien, Austria). EP is the scientific director and shareholder of PharmInVivo Ltd. (Pécs, Hungary) and shareholder of Algonist Biotechnologies Gmbh, (Wien, Austria). ES is also a shareholder of Algonist Biotechnologies Gmbh, (Wien, Austria). PB is the head of R&D at Avicor Ltd.

The remaining authors declare that the research was conducted in the absence of any commercial or financial relationships that could be construed as a potential conflict of interest.

frontiers in Pharmacology

REVIEW
published: 14 April 2021
doi: 10.3389/fphar.2021.610585

Immune Axonal Neuropathies Associated With Systemic Autoimmune Rheumatic Diseases

Delia Tulbă[1,2,3], *Bogdan Ovidiu Popescu*[1,3,4]*, *Emilia Manole*[4] *and Cristian Băicuș*[2,3,5]

[1]Department of Neurology, Colentina Clinical Hospital, Bucharest, Romania, [2]Colentina-Research and Development Center, Colentina Clinical Hospital, Bucharest, Romania, [3]"Carol Davila" University of Medicine and Pharmacy, Bucharest, Romania, [4]Laboratory of Cell Biology, Neurosciences and Experimental Myology, "Victor Babeș" National Institute of Pathology, Bucharest, Romania, [5]Department of Internal Medicine, Colentina Clinical Hospital, Bucharest, Romania

Immune axonal neuropathies are a particular group of immune-mediated neuropathies that occasionally accompany systemic autoimmune rheumatic diseases such as connective tissue dissorders and primary systemic vasculitides. Apart from vasculitis of vasa nervorum, various other mechanisms are involved in their pathogenesis, with possible therapeutic implications. Immune axonal neuropathies have highly heterogeneous clinical presentation and course, ranging from mild chronic distal sensorimotor polyneuropathy to severe subacute mononeuritis multiplex with rapid progression and constitutional symptoms such as fever, malaise, weight loss and night sweats, underpinning a vasculitic process. Sensory neuronopathy (ganglionopathy), small fiber neuropathy (sensory and/or autonomic), axonal variants of Guillain-Barré syndrome and cranial neuropathies have also been reported. In contrast to demyelinating neuropathies, immune axonal neuropathies show absent or reduced nerve amplitudes with normal latencies and conduction velocities on nerve conduction studies. Diagnosis and initiation of treatment are often delayed, leading to accumulating disability. Considering the lack of validated diagnostic criteria and evidence-based treatment protocols for immune axonal neuropathies, this review offers a comprehensive perspective on etiopathogenesis, clinical and paraclinical findings as well as therapy guidance for assisting the clinician in approaching these patients. High quality clinical research is required in order to provide indications and follow up rules for treatment in immune axonal neuropathies related to systemic autoimmune rheumatic diseases.

Keywords: immune axonal neuropathy, vasculitic neuropathy, sensorimotor polyneuropathy, mononeuritis multiplex, connective tissue disease, systemic vasculitis, systemic autoimmune rheumatic disease, small fiber neuropathy

OPEN ACCESS

Edited by:
Éva Szőke,
University of Pécs, Hungary

Reviewed by:
Gurudutt Pendyala,
University of Nebraska Medical Center, United States
Anita Mahadevan,
National Institute of Mental Health and Neurosciences (NIMHANS), Bangalore, India

***Correspondence:**
Bogdan Ovidiu Popescu
bogdan.popescu@umfcd.ro

Specialty section:
This article was submitted to Inflammation Pharmacology, a section of the journal Frontiers in Pharmacology

Received: *26 September 2020*
Accepted: *10 March 2021*
Published: *14 April 2021*

Citation:
Tulbă D, Popescu BO, Manole E and Băicuș C (2021) Immune Axonal Neuropathies Associated With Systemic Autoimmune Rheumatic Diseases. Front. Pharmacol. 12:610585. doi: 10.3389/fphar.2021.610585

INTRODUCTION

Autoimmune diseases are a broad group of conditions characterized by chronic activation of the immune system that eventually leads to tissue inflammation and damage (Doria et al., 2012). In contrast to autoinflammatory disorders entirely mediated by the innate immune system, autoimmune diseases imply dysregulation of both innate and adaptive immunity, yet the injury is mediated by adaptive immune responses (Doria et al., 2012; Firestein et al., n.d.). However, a less restrictive demarcation might be appropriate since conditions such as Behçet's disease (BD) share

both autoimmune and autoinflammatory features, underpinning the possibility of an autoreactivity spectrum that encompasses autoimmune diseases at one end and autoinflammatory diseases at the other (Firestein et al., n.d.).

Autoimmune diseases are classified into organ-specific and systemic conditions, depending on their expansion (Firestein et al., n.d.). In systemic autoimmune disorders, autoreactivity targets ubiquitous self-antigens, leading to autoantibodies and/or T cells that mediate end-organ injury (Firestein et al., n.d.). Since the musculoskeletal system is often targeted, most of them are considered systemic autoimmune rheumatic diseases (SARDs) and include systemic lupus erythematosus (SLE), rheumatoid arthritis (RA), primary Sjögren's syndrome (SS), antiphospholipid syndrome (aPL), systemic sclerosis (SSc), sarcoidosis and systemic vasculitides (Doria et al., 2012; Firestein et al., n.d.; Starshinova et al., 2019). According to the type of the vessels involved, systemic vasculitides are further classified into predominantly large vessel vasculitides (e.g., giant cell arteritis), predominantly medium vessel vasculitides (e.g., polyarteritis nodosa (PAN)) and predominantly small vessel vasculitides (e.g., antineutrophil cytoplasmic antibody (ANCA)-associated vasculitides and cryoglobulinemia) (Jennette et al., 2012). Another classification identifies primary systemic vasculitides (e.g., ANCA-associated vasculitides) and secondary systemic vasculitides that occur in the setting of other SARDs (e.g., lupus vasculitis, rheumatoid vasculitis, sarcoid vasculitis), various infections, drugs, malignancies, inflammatory bowel disease and hypocomplementemic urticarial vasculitis syndrome (Collins et al., 2010; Sampaio et al., 2011; Collins, 2012; Jennette et al., 2012).

Systemic autoimmune rheumatic diseases occasionally involve the nervous system. Moreover, the presence of central or peripheral nervous system dysfunction of unknown cause can assist the diagnosis of SARDs, as pointed out by the classification criteria designed for some of these disorders. For instance, the 2012 SLICC Systemic Lupus Erythematosus Criteria refer to "mononeuritis multiplex, peripheral or cranial neuropathy" as a clinical criterion for lupus (Petri et al., 2012); the 1990 ACR Classification Criteria for Polyarteritis Nodosa (Lightfoot Jr. et al., 1990) or Churg-Strauss Syndrome (Masi et al., 1990) mention "mononeuropathy or polyneuropathy" likewise. However, the inaccurate definition of terms–i.e. "peripheral neuropathy" does not specifically refer to immune axonal neuropathy, which is the main peripheral nervous system involvement in SARDs–reveals the diagnostic limits of these criteria (Collins et al., 2013).

Immune axonal neuropathies are a heterogeneous group of immune-mediated peripheral neuropathies that target the axons, showing absent or reduced nerve amplitudes with normal latencies and conduction velocities on nerve conduction studies, in contrast to demyelinating neuropathies (Bril and Katzberg, 2014). They are linked to various conditions such as SARDs, monoclonal gammopathy, celiac disease, inflammatory bowel disease, paraneoplastic syndromes and infections (Bril and Katzberg, 2014). Vasculitic neuropathies are a distinct group of immune axonal neuropathies that appear in the setting of a vasculitis. Inflammation of vasa nervorum leads to fibrinoid necrosis, with multifocal nerve infarction and accumulating disability (Sampaio et al., 2011). Their recognition is important since they do not usually respond to intravenous (IV) immunoglobulin and require a higher level of immunosuppression straightaway.

We aim to review immune axonal neuropathies associated with SARDs, with a special focus on vasculitic neuropathies encountered in systemic vasculitides, both primary and secondary to other SARDs. We have briefly discussed about BD (and BD-associated neuropathy), which is classified either as SARD or autoinflammatory disorder. We have not included secondary systemic vasculitides (other than SARDs), non-systemic/localized vasculitides (i.e. non-systemic vasculitic neuropathy, localized cutaneous/neuropathic vasculitis), demyelinating neuropathies and neuropathies with other mechanisms (e.g. nerve entrapment). Considering the lack of validated diagnostic criteria and evidence-based treatment protocols, a comprehensive review on etiopathogenesis, clinical and paraclinical findings as well as treatment guidance are offered in order to assist the clinician in approaching the patients with immune axonal neuropathies related to SARDs.

EPIDEMIOLOGY

There is a scarcity of data regarding the incidence and prevalence of immune axonal neuropathies associated with SARDs, but some information can be drawn indirectly from other epidemiological findings. For instance, systemic vasculitides, both primary and secondary, have an annual incidence of 60–140/million (Blaes, 2015) and up to 60–70% of patients with systemic vasculitis develop neuropathy (Gwathmey et al., 2014). Up to 30% of elderly patients with progressive, severe and painful peripheral nervous system involvement might have vasculitic neuropathy (Vrancken and Said, 2013) and 1% of nerve biopsy specimens from patients with cryptogenic neuropathy display vasculitic features (Vrancken and Said, 2013; Blaes, 2015). However, since these findings pertain to the whole group of vasculitides (including non-systemic/localized vasculitides and systemic vasculitides secondary to infections, drugs, malignancies, etc.), it is difficult to obtain accurate and relevant information about vasculitic neuropathies strictly related to SARDs. Moreover, the broad interval of vasculitic neuropathy frequency reported in SARDs patients, ranging from 15 to 70% in RA, 65–80% in eosinophilic granulomatosis with polyangiits (EGPA), 5–50% in granulomatosis with polyangiits (GPA) and 6–75% in microscopic polyangiitis (MPA) reflects the heterogeneity in population and diagnostic means (either clinical or electrophysiological testing) among studies (Snoussi et al., 2019). Epidemiological data about other types of immune axonal neuropathies related to SARDs are even more scarce.

ETIOPATHOGENESIS

The nutrient supply of peripheral nerves is provided by both neuronal cell bodies (which synthesize proteins and transfer them

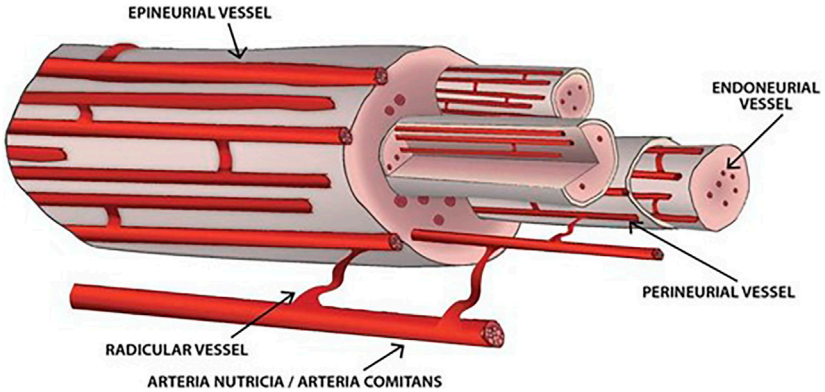

FIGURE 1 | Vasa nervorum. The extrinsic vessels derive from either arteriae nutriciae or arteria comites and branch into radicular vessels. The intrinsic vessels are supplied by radicular vessels, run longitudinally along the nerve and comprise epineurial, perineurial and endoneurial vessels. Various anastomoses between and within each of these structures arise.

down the axons through the microtubules) and blood vessels, the latter being particularly important in nerves with long axons (Ishibe et al., 2011). An impairment at any of these levels might damage the nerve and cause malfunctioning (e.g., ischemia due to vasa nervorum thrombosis/blood flow restriction usually manifests as mononeuritis multiplex, inflammatory damage of axons induces axonal sensorimotor polyneuropathy, inflammatory injury of dorsal root ganglia neurons leads to sensory neuronopathy (ganglionopathy), whereas immunological/metabolic changes elicit small nerve fiber degeneration with subsequent small fiber neuropathy).

Vasa Nervorum Vasculitis

Vasa nervorum (the vasculature of peripheral nerves) (**Figure 1**) are a complex vessel network designed to fulfill the structural and functional metabolic requirements of the nerves and to maintain homeostasis within the endoneurial microenvironment, as part of the blood nerve barrier (which involves the perineurial cellular layers and the endoneurial capillary endothelium) (Mizisin and Weerasuriya, 2011). Vasa nervorum consist of two distinct systems, the extrinsic and intrinsic vessels, with various anastomoses between and within each of them. The extrinsic system (extraneural vasa nervorum) includes regional arteries, either arteriae nutriciae from adjacent large muscular arteries or arteriae comites from musculocutaneous/fascial arteries, that branch into radicular vessels responsible for supplying the intraneural vessels (Boissaud-Cooke et al., 2015). As they insert segmentally into the epineurium, a longitudinal plexus of arterioles takes shape, marking the outer layer of the intrinsic system (intraneural vasa vasorum) (Boissaud-Cooke et al., 2015). While reaching deeper into the epineurium, a further multiplanar branching occurs, generating the terminal arterioles that penetrate the perineurium and cross it mainly obliquely (Boissaud-Cooke et al., 2015). They eventually end up as an intrafascicular endoneurial vascular plexus, running along the longitudinal axis of the nerve, yet with multidirectional branching and anastomoses (Boissaud-Cooke et al., 2015). The endoneurial capillary bed consists of particular capillaries—with large diameter resembling that of postcapillary venules, increased intercapillary distance and tight endothelial junctions with sporadic open interendothelial gaps (Mizisin and Weerasuriya, 2011), outlining the blood nerve interface (Ishibe et al., 2011; Boissaud-Cooke et al., 2015). This intricate structural and functional organization of the vasa nervorum coupled with the low compliance of the perineurium - preventing increases in intrafascicular volume - might explain the vulnerability of peripheral nerves to slight increases in capillary permeability: the endoneurial edema briskly raises the hydrostatic pressure and leads to compression of transperineurial vessels and subsequent reduction in blood flow and ischemia (Mizisin and Weerasuriya, 2011; Boissaud-Cooke et al., 2015).

Systemic vasculitides (either primary or secondary to other SARDs) can affect the vasa nervorum, leading to inflammatory damage of vessel walls and blood flow restriction/thrombosis responsible for nerve ischemia (Sampaio et al., 2011; Collins et al., 2013). Considering the dimensions of the blood vessels in the peripheral nerves (approximately 10–300 μm), it is not surprising that vasculitic neuropathies are mainly confined to medium and small vessel vasculitides (Vrancken and Said, 2013; Naddaf and Dyck, 2015). The inflammation usually occurs in the small arteries and large arterioles of the epineurium and perineurium, as opposed to the non-systemic vasculitic neuropathy that involves the endoneurial microvessels (Collins et al., 2013; Gwathmey et al., 2014). Although the pathogenesis of systemic vasculitides mainly implies a humoral immune response, the vasa nervorum display a cellular immune-mediated reaction with vascular infiltrates of CD4+/helper and CD8+/cytotoxic T cells and antigen-presenting cells (mainly macrophages) in the epineurial vessel walls (Jennette et al., 2012). A pathogenic model centered on T cells with the following sequences has been proposed: autoreactive T cells are recruited to the peripheral nervous system, recognize the antigens presented by macrophages, endothelial cells and Schwann cells, undergo activation by cell adhesion molecules and chemotactic cytokines and ultimately mature into or recruit cytotoxic T cells that mediate the destruction of vessel walls

(Sampaio et al., 2011; Collins et al., 2013). An ongoing inflammatory milieu ensues as the macrophages exhibit upregulation of the inducible costimulator ligand that binds to the highly expressed inducible costimulator (a CD28-like molecule engaged in T-cell activation) on effector memory T cells, hence restimulating activated T cells (Collins et al., 2013). Although of lesser importance, humoral immune mechanisms also contribute to vasa nervorum vasculitis, as indicated by the deposits of immunoglobulin and complement in epineurial vessel walls that imply either *in situ* formation of immune complexes or deposition of circulating ones, with consecutive activation of the complement system and recruitment of phagocytes (Collins et al., 2013). The involvement of ANCA in the pathogenesis of vasculitic neuropathy is doubtful: more than half of the ANCA-negative EGPA patients have peripheral neuropathy, whereas ANCA are rarely detected in the most common vasculitic neuropathy, namely nonsystemic vasculitic neuropathy (Collins et al., 2013). Furthermore, the rich immune complex deposits found in vasculitic neuropathies do not match the pauci-immune states of ANCA-associated vasculitides (Collins et al., 2013) and the prevalence of vasculitic neuropathy is similar in seropositive and seronegative ANCA-associated vasculitides (Collins, 2012).

Immune and Metabolic Abnormalities

Apart from the vasculitis of vasa nervorum that leads to ischemic damage of the axon, various other pathogenic mechanisms have been observed in patients with immune axonal neuropathy related to SARDs, particularly immune/inflammatory abnormalities and metabolic changes (Bril and Katzberg, 2014; Snoussi et al., 2019). In SLE, local inflammatory changes (i.e. increased vascular permeability and cellular trafficking) are mediated by neuropeptides such as substance P, calcitonin gene-related protein, nitric oxide and chemokines (Imam et al., 2019). Inflammatory molecules released from activated immune cells induce peripheral sensitization and hyperalgesia by targeting sensory neurons (Imam et al., 2019). Additionally, a direct autoantibody-induced aggression is supposedly pathogenic (Mizisin and Weerasuriya, 2011). Antiphospholipid antibodies are linked to severe neural lesions (Snoussi et al., 2019) and are thought to induce ischemic damage by thrombosis of vasa nervorum (Imam et al., 2019) or vasculitis (Santos et al., 2010; Fleetwood et al., 2018). Antigenic determinants of the myelin phospholipids might be targets for anticardiolipin antibodies, leading to demyelinating neuropathies, as suggested by Santos et al. (Santos et al., 2010). Moreover, it has been hypothesized that anticardiolipin antibodies elicit an immune response by binding to nodal axonal epitopes, which might be responsible for the axonal variants of Guillain-Barré syndrome (GBS) reported in SLE patients (Santiago-Casas et al., 2013). In SS, small fiber neuropathy is probably the result of immune-mediated disruption of small unmyelinated or thinly myelinated fibers by inflammatory perivascular infiltrates, with elevated local proinflammatory cytokines such as IL-6, IL-8, TNF-α and IL-1β (Hoeijmakers et al., 2012; Bril and Katzberg, 2014), whereas sensory neuronopathy (ganglionopathy) occurs in the setting of direct inflammatory damage of dorsal root ganglia neurons mediated by CD8 T lymphocytes (Martinez et al., 2012). In SSc, the mechanism of neuropathy has not been elucidated, but acral vasospasm secondary to Raynaud phenomenon might be involved in its etiopathogenesis (Paik et al., 2016). Infiltration of the epineurium and perineurium by sarcoid granuloma supposedly causes axonal damage and neuropathy in sarcoidosis (Pirau and Lui, 2020), whereas both humoral and cellular abnormal immune responses might play a role in the development of neuropathy in BD (Emam, 2019). Apart from the vasculitis of vasa nervorum, eosinophilic infiltration and granuloma formation are involved in the pathogenesis of EGPA-related neuropathy (Collins, 2012). In cryoglobulinemia, either cryoglobulin precipitation with subsequent vessel occlusion or immune complex deposition along myelin occurs (Collins, 2012). A direct pathogenic role of antisulfatide antibodies and GM1-ganglioside antibodies has also been proposed (Blaes, 2015). Up to 32% of patients with connective tissue disorders have increased levels of serum anti-nerve growth factor antibodies, which correlate with high disease activity and severe nervous system manifestations (Snoussi et al., 2019). On the other hand, an increased expression of nerve growth factor occurs in painful vasculitic neuropathies (Blaes, 2015).

Axonal Degeneration

The axons play a significant role in long-distance neuronal communication through action potential initiation and propagation and action potential-mediated transmitter release. The vasculitic neuropathies lead to nerve ischemia and consecutive focal and asymmetrical axonal loss in a specific spatial distribution–it is likely to be centrofascicular in the proximal areas and multifocal/diffuse in distal ones because of twisted nerve fibers (Sampaio et al., 2011; Collins et al., 2013). Axonal degeneration occurs mostly in large sensory and motor myelinated fibers (Sampaio et al., 2011; Suppiah et al., 2011) and is responsible for the length-dependent pattern of the disease, affecting the longest nerves from distal extremities. There is a reciprocal link between the axons and the vasa nervorum. On one hand, as already mentioned, inflammatory damage of vessel walls and blood flow restriction promote axonal ischemia and loss. Since axonal degeneration is associated with increased permeability of the perineurium, it has been suggested that the axon might be responsible for producing diffusible factors that maintain the tight intercellular junctions (by regulating the synthesis of intercellular junctional proteins) in the perineurium (Weerasuriya and Mizisin, 2011). This could indicate that axonal degeneration is not merely a final path in the etiopathogenic process of vasculitic neuropathy. However, this hypothesis needs to be tested.

CLINICAL PRESENTATION

In immune axonal neuropathy related to SARDs, the clinical presentation ranges from asymptomatic to very aggressive forms of neuropathy leading to significant disability (Blaes, 2015).

Clinical Patterns of Immune Axonal Neuropathy in Systemic Autoimmune Rheumatic Diseases

Sensorimotor polyneuropathy is the main phenotype of neuropathy in collagen vascular diseases and the second most common presentation of vasculitic neuropathy in primary systemic vasculitides (Bril and Katzberg, 2014; Blaes, 2015). These patients present with chronic distal symmetrical sensorimotor symptoms. A pure sensory or motor presentation is rarely found (Blaes, 2015).

Mononeuritis multiplex is the classical presentation of vasculitic neuropathy, occurring in up to 65% of cases (Blaes, 2015). It is defined as an "acute or subacute involvement of multiple individual nerves serially or almost simultaneously" (Ropper et al., 2014). It usually presents with painful sensorimotor deficit in the distribution of a single peripheral nerve (Bril and Katzberg, 2014), the peroneal and tibial nerves being mostly affected, followed by the ulnar nerve (Blaes, 2015). The simultaneous or sequential multifocal involvement with overlapping clinical deficits might give the appearance of an asymmetrical polyneuropathy (Collins et al., 2013), but constitutional symptoms (i.e. fever, fatigue, weight loss) should raise suspicion of a vasculitic process. Constitutional symptoms accompany neurological dysfunction in up to 80% of patients with systemic vasculitis (Blaes, 2015).

Pure sensory neuropathy may also be a presentation of sensory neuronopathy (ganglionopathy) in SS or SLE (Martinez et al., 2012; Bril and Katzberg, 2014; Lefter et al., 2020). The manifestations of sensory neuronopathy are usually multifocal and spread toward both proximal and distal regions of the limbs. They comprise all sensory modalities (proprioception, vibration sense, fine touch, pain, temperature), with prominent gait ataxia as well as widespread areflexia and possible pseudoathetosis, pain and allodynia (Martinez et al., 2012). An acute onset with disabling manifestations is often encountered in SS-related ganglionopathy (Martinez et al., 2012). Pure sensory symptoms might also arise as a consequence of *small fiber neuropathy* in SS or sarcoidosis (Levine, 2018), usually with positive manifestations such as paresthesia, dysesthesia, hyperpathia, allodynia and hyperalgesia that are more severe in the evening and have a symmetrical length-dependent distribution–beginning in the feet and extending proximally (Hoeijmakers et al., 2012; Gondim et al., 2018). However, non-length-dependent and patchy symptoms (on the face, tongue, scalp, trunk) have also been reported (Hoeijmakers et al., 2012; Gondim et al., 2018). When present, negative symptoms include thermal sensory loss and numbness (Hoeijmakers et al., 2012).

Autonomic dysfunction alone or combined with sensory manifestations could also be the result of small fiber neuropathy (Bril and Katzberg, 2014). Although not a prominent feature of immune-mediated neuropathies related to SARDs, autonomic dysfunction can occur in SS, SLE and SSc (Adams et al., 2012). Autonomic dysfunction has clinical manifestations ranging from mild symptoms to pandysautonomia that can be life-threatening or severely affecting the quality of life. Clinical findings can be further classified into cardiovascular (at-rest tachycardia, orthostatic hypotension, silent myocardial ischemia), gastrointestinal (gastroparesis, diarrhea, constipation, fecal incontinence), genitourinary (neurogenic bladder, erectile dysfunction) and sudomotor manifestations (anhidrosis, excessive sweating, heat intolerance) as well as pupillary abnormalities (i.e. Argyll Robertson pupils) (Adams et al., 2012).

Cranial neuropathy might be encountered in SARDs in an isolated fashion or a multifocal distribution, but its etiopathogenesis is not always related to the vasculitic process–optic and olfactory nerves might be affected by granulomatous invasion, whereas basilar meningitis or other inflammatory processes might involve the rest of the cranial nerves (Wludarczyk and Szczeklik, 2016).

Acute motor axonal neuropathy (AMAN) and acute motor and sensory axonal neuropathy (AMSAN) are two variants of GBS rarely reported in SARDs, notably in LES (Santiago-Casas et al., 2013; Thakolwiboon et al., 2019). Acute motor axonal neuropathy presents as acute ascending symmetrical quadriparesis with occasional preservation of deep tendon reflexes, whereas AMSAN is a more severe form of AMAN, with superimposed sensory symptoms. It is important to recognize these entities since they might require a combination of IV immunoglobulin or plasma exchange and immunosuppressants (Ubogu et al., 2001; Santiago-Casas et al., 2013).

Asymptomatic neuropathy is a controversial entity detected only by nerve conduction studies and/or nerve biopsy performed in patients with systemic symptoms and laboratory findings suggestive of a systemic vasculitis. As already mentioned, neuropathy could serve as a diagnostic criterion for systemic vasculitides. Kurt et al. identified 21 patients with asymptomatic, biopsy-proven vasculitic neuropathy, out of which 20 had diffuse neuropathy involving both legs and one had mononeuritis multiplex (Kurt et al., 2015). Similar to other studies, they reported a prevalence of 7.8% of asymptomatic vasculitic neuropathies among patients with biopsy-proven vasculitis. Sural nerve conduction studies and biopsy were abnormal in all the cases, indicating a high sensitivity of these methods. Interestingly, the majority of these patients had biopsy-proven active vasculitis (Kurt et al., 2015). These data indicate the relevance of searching for neuropathy in the setting of a systemic vasculitis.

Types of Immune Axonal Neuropathy in Systemic Autoimmune Rheumatic Diseases

Axonal sensorimotor polyneuropathy is the main presentation of neuropathy in collagen vascular diseases (Bril and Katzberg, 2014) (**Table 1**).

Systemic lupus erythematosus affects the central and peripheral nervous system either independently or simultaneously (Bril and Katzberg, 2014)–neuropsychiatric events attributed to SLE emerge as primary manifestations of SLE and should be distinguished from complications of the disease (e.g. hypertension) and its therapy (e.g. diabetes,

TABLE 1 | Types and frequency of immune-mediated axonal neuropathy in SARDs. Legend: +++ - > mostly found, ++ - > frequently encountered, + - > moderately found,/ - > rarely encountered, sar - > sarcoidosis, cryo - > cryoglobulinemia, PNS - > peripheral nervous system.

Clinical presentation	SLE	RA	SS	aPL	SSc	Sar	BD	PAN	EGPA	GPA	MPA	Cryo
Sensorimotor polyneuropathy	+++	+++	/	+++	++	—	/	+++	+	+++	+	++
Pure sensory polyneuropathy	+	+++	/	++	++	—	/	—	+	—	—	+
Mononeuritis multiplex	++	++	/		/	—	/	+++	+++	+++	+++	+++
Sensory neuronopathy	/	—	+++	—	—	—	—	—	—	—	—	—
Small fiber neuropathy (sensory)	+	+	+++	++	+++	++	—	—	—	—	—	—
Autonomic involvement	+	+	+++	+++	+++	++	/	—	—	—	—	—
Cranial neuropathy	+		/(5th)		++(5th)	+++(7th)	/	+		+	+	
GBS axonal variants	/	—	/	—	—	—	—	—	—	—	—	—
PNS involvement	20–27%	15–70%	30–45%	35%	—	4–20%	—	65–85%	65–80%	5–50%	6–75%	30–70%

infections) or concurrent neuropsychiatric disease not related to lupus (Hanly, 2014). All axonal neuropathy phenotypes have been reported in SLE patients, namely axonal sensorimotor polyneuropathy, mononeuritis multiplex, cranial neuropathy, small fiber neuropathy, sensory neuronopathy (ganglionopathy), AMAN and AMSAN, reflecting the diverse mechanisms of neuropathy in this disease (Bril and Katzberg, 2014; Hanly, 2014). However, axonal sensorimotor polyneuropathy is the main presentation, followed by mononeuritis multiplex (Mizisin and Weerasuriya, 2011). Sensory loss involving vibratory and position senses is usually more prominent than motor deficit in axonal sensorimotor polyneuropathy (Ropper et al., 2014). Although axonal degeneration is the cardinal histopathological pattern (70–80%), demyelination can also occur (20%) (Ropper et al., 2014; Blaes, 2015). Neuropathy is rarely the inaugural manifestation in SLE and usually occurs in the advanced stages of the disease (Ropper et al., 2014) and correlates with disease activity (Mizisin and Weerasuriya, 2011). Interestingly, AMAN and AMSAN have been reported as initial manifestations of SLE in 4 cases and preceding the diagnosis of SLE in 2 cases (Thakolwiboon et al., 2019).

Rheumatoid arthritis involves the peripheral nervous system in up to 75% of cases. Neuropathy usually takes the form of an aggressive axonal sensorimotor polyneuropathy, but mononeuritis multiplex also manifests in up to 8% of patients with RA (Bril and Katzberg, 2014). One study found pure sensory polyneuropathy to be the most prevalent pattern of neuropathy in RA patients (Agarwal et al., 2008) and another one reported pure motor polyneuropathy in 15 patients with RA (Kaeley et al., 2019). Mononeuritis multiplex is sometimes not easily differentiated from entrapment mononeuropathy (secondary to thickened tendons and destructive joint lesions) or drug-induced neuropathy (Blaes, 2015). Neuropathy mostly occurs in strongly seropositive patients (Ropper et al., 2014) in the advanced stages of the disease (Bril and Katzberg, 2014), accompanying other extraarticular manifestations such as rheumatoid nodules and purpura (Ropper et al., 2014).

Sjögren's syndrome is an autoimmune disease mainly affecting the exocrine glands, therefore causing xerophthalmia and xerostomia. Extraglandular manifestations include peripheral neuropathies (2–64%), but only few of them are vasculitic (Blaes, 2015). SS has a wide spectrum of neuropathy phenotypes. Small fiber neuropathy is the most frequent finding, presenting with burning pain if sensory fibers in the skin are damaged and dysautonomia provided that autonomic fibers are involved (Bril and Katzberg, 2014). However, autonomic dysfunction is rarely inaugural and usually accompanies sensory symptoms (Adams et al., 2012). Sensory neuronopathy leading to sensory ataxia is also a common finding, as opposed to sensorimotor polyneuropathies that only occur in 1% of patients with SS (Bril and Katzberg, 2014); cranial neuropathy (especially trigeminal sensory neuropathy) and mononeuritis multiplex have been reported even more rarely (Bril and Katzberg, 2014).

Primary antiphospholipid syndrome associates neuropathy in up to 35% of cases according to Santos et al. (Santos et al., 2010). In their group of patients, the most common phenotype was sensorimotor polyneuropathy, followed by sensory polyneuropathy and carpal tunnel syndrome (Santos et al., 2010). Interestingly, most of the patients with electrophysiological findings compatible with neuropathy had no clinical symptoms or signs (Santos et al., 2010). Schofield identified 22 patients with aPS and autonomic neuropathy as the inaugural manifestation, out of which 71% also had sensory small fiber neuropathy (Schofield, 2017). Autonomic involvement was associated with significant thrombotic risk (Schofield, 2017).

Systemic sclerosis and localized scleroderma affect the peripheral nervous system in up to 30% of cases. Sensory symptoms and dysautonomia (including gut motility disturbance) are the most frequent complaints of patients with SSc (Blaes, 2015). Cranial nerve involvement occurs in almost 8% of patients with localized scleroderma, encompassing 7th, 3rd and 6th nerve palsies as well as trigeminal neuropathy (Amaral et al., 2013). Systemic sclerosis mostly features trigeminal neuropathy (16.52%), peripheral sensorimotor polyneuropathy (14.25%) and entrapment neuropathies (9.25%) and, to a lesser extent, symptomatic carpal tunnel syndrome (6.65%), ulnar nerve involvement (3.39%), mononeuritis multiplex (1.81%) and facial nerve damage (1.58%) (Amaral et al., 2013). Brachial plexopathy (0.68%), lumbar plexopathy (0.44%), 8th nerve (0.44%) as well as other cranial nerve (e.g. 6th, 9th, 12th nerve) involvement are rarely found in SSc (Amaral et al., 2013). Autonomic neuropathies have been reported in up to

80% of patients with SSc. Parasympathetic underactivity and sympathetic overdrive were most commonly encountered and could precede visceral fibrosis (Amaral et al., 2013). Nevertheless, Paik et al. (Paik et al., 2016) found that 35% of patients with SSc and peripheral neuropathy had an alternative cause for the nerve impairment, recommending screening for other etiologies since they might be reversed or potentially treatable.

In sarcoidosis, cranial neuropathy is the most common manifestation of peripheral nervous system involvement (Lacomis, 2011). Any cranial nerve could be affected, but facial nerves are most frequently involved, sometimes bilaterally (Lacomis, 2011). Heerfordt syndrome is a pathognomonic manifestation of sarcoidosis, including facial palsy combined with uveitis, chronic fever and parotid enlargement (Bril and Katzberg, 2014). Apart from the granulomatous infiltration and compression of nerves along their course, basilar leptomeningitis can also be responsible for cranial nerve palsies (Lacomis, 2011). Basilar leptomeningitis can have a monophasic, chronic or relapsing course, usually with a good outcome (Lacomis, 2011). Peripheral neuropathy occurs in 4–20% of patients with sarcoidosis and all axonal subtypes have been reported (Said et al., 2002; Lacomis, 2011). Out of these, mononeuropathies affecting ulnar and peroneal nerves were the most frequent (Lacomis, 2011). Peripheral neuropathy can occur at any stage of disease (Lacomis, 2011).

In BD, neurological involvement carries a bad prognosis (Emam, 2019). Cranial neuropathy and peripheral neuropathy are atypical presentations of BD and other plausible causes should be excluded in order to link them to BD, especially iatrogenic effects of colchicine or thalidomide (Siva and Saip, 2009; Dutra LAaB, 2016). Birol et al. found subclinical neuropathy in almost 77% of BD patients, with lower extremity nerves being more affected, especially sural and peroneal nerves (Birol et al., 2004). Sensory and motor components were equally involved according to the electrophysiological studies (Birol et al., 2004). Sensorimotor polyneuropathy, mononeuritis multiplex, autonomic dysfunction, sensory neuropathy with recurrent episodes of myositis and cranial neuropathy can sporadically occur in BD (Siva and Saip, 2009; Dutra LAaB, 2016).

As previously mentioned, primary systemic vasculitides are idiopathic inflammatory diseases of blood vessels that can virtually affect any organ or tissue in the body, including the peripheral nervous system (**Table 1**).

Polyarteritis nodosa is a primary systemic necrotizing vasculitis of the medium-sized vessels. Absence of glomerulonephritis, ANCA and small vessel involvement are its distinctive features. PAN might be either idiopathic or triggered by viral infections such as hepatitis B virus (HBV) (Collins et al., 2013). The peripheral nervous system is the most frequent target, the prevalence of neuropathy in HBV-associated PAN being even higher than in the idiopathic form (Collins et al., 2013). Neuropathy is the first clinical event in one third of PAN patients (Bril and Katzberg, 2014). Up to 72% of patients present with mononeuritis multiplex (mainly of the lower extremity) and less than 2% associate cranial nerve palsy (Hernández-Rodríguez et al., 2014). Mononeuritis multiplex in PAN usually has a sudden onset with pain or numbness in the distal part of a nerve and sensory or motor deficit in the distribution of the same nerve (Ropper et al., 2014). As mononeuritis multiplex in PAN features many small nerve infarctions, it might seem symmetrical and generalized, resembling a polyneuropathy (Ropper et al., 2014).

Eosinophilic granulomatosis with polyangiitis, formerly known as Churg Strauss syndrome, is an ANCA-associated primary systemic vasculitis (usually against myeloperoxidase: p-ANCA) of the small-to-medium sized vessels that presents with asthma, paranasal sinus abnormalities, non-fixed pulmonary infiltrates, blood eosinophilia and tissue eosinophilic invasion. Peripheral nervous system involvement occurs in up to 65% of patients and is preceded by constitutional symptoms, giving rise to different phenotypes, particularly mononeuritis multiplex, mononeuropathy or polyneuropathy (Bril and Katzberg, 2014; Ropper et al., 2014). The onset is often acute, with tingling or painful paresthesia in the distal parts of the lower limbs (Koike and Sobue, 2013).

Granulomatosis with polyangiitis, formerly known as Wegener's granulomatosis, is also an ANCA-associated primary systemic vasculitis (usually against proteinase 3: c-ANCA) of the small-to-medium sized vessels that primarily affects the upper and lower respiratory tract as well as renal glomeruli. Vasculitic neuropathy is the first clinical presentation in 8% of GPA patients (Suppiah et al., 2011) and is distributed as mononeuritis multiplex in most of the cases (Blaes, 2015). A distinctive feature of peripheral nervous system involvement is lower cranial nerve mononeuropathy (Ropper et al., 2014).

Conversely, MPA is a pauci-immune necrotizing vasculitis of lung and kidney capillaries mainly associated with p-ANCA that does not elicit granulomatous inflammation. Motor polyneuropathy and sensorimotor polyneuropathy are as frequent as in GPA (7%), whereas pure sensory neuropathy and cranial nerve palsy are far less commonly encountered (Suppiah et al., 2011). Instead, the clinical course of MPA shares many similarities with EGPA, with sensory impairment distributed as mononeuritis multiplex in the initial phase (Koike and Sobue, 2013).

Cryoglobulinemia is a paraproteinemic state that leads to a small-vessel immune-complex-mediated vasculitis. Its main clinical features are purpura, arthralgia and renal involvement. It might be classified into type I cryoglobulinemia associated with monoclonal immunoglobulins, type II cryoglobulinemia with both monoclonal and polyclonal immunoglobulins and type III cryoglobulinemia with polyclonal IgG. Type III is most frequently accompanied by peripheral nervous system involvement and is usually the consequence of a systemic disease, either an infection or a noninfectious inflammatory disorder (Bril and Katzberg, 2014). Painful mononeuritis multiplex is the main clinical presentation, but aggressive sensorimotor polyneuropathy is also encountered (Bril and Katzberg, 2014; Blaes, 2015). The course of the asymmetrical form is slower than in other diseases, with long "silent" periods between the attacks of mononeuropathy (Ropper et al., 2014). Interestingly, there is no relationship between the severity of neuropathy and the titer of serum cryoglobulins (Ropper et al., 2014).

TABLE 2 | Paraclinical tests and their utility in patients with SARDs and immune-mediated axonal neuropathies related to SARDs. Some tests are mandatory (routine blood tests, differential diagnosis of axonal neuropathies, electrophysiological testing), whereas others should be performed in selected cases, according to the clinical suspicion. Legend: abs - > antibodies, HbA1c - > glycated hemoglobin.

Paraclinical tests		Utility
Blood and urine tests	Complete blood count; erythrocyte sedimentation rate; C-reactive protein; fibrinogen; creatinine; blood urea nitrogen; electrolytes; urinalysis; transaminases; gamma-glutamyl transpeptidase; alkaline phosphatase; lactate dehydrogenase; creatine kinase	Activity and expansion of SARDs
	c-ANCA and *p*-ANCA; antinuclear abs; anti-double-stranded DNA abs; C_3; C_4; cryoglobulins; rheumatoid factor; anti-CCP abs; ACE; anti-ro/SSA and anti-La/SSB abs	Diagnosis of SARDs
	Hepatitis B surface antigen; hepatitis C abs; anti-HIV abs	Differential diagnosis of SARDs; Etiological diagnosis of neuropathy
	Fasting glucose; HbA1c; vitamin B_{12}; thyroid hormones; immunofixation electrophoresis; immunogram; β_2 microglobulin; anti-tissue transglutaminase abs; anti-borrelia burgdorferi abs; VDRL; toxicology testing; spot urine for porphobilinogen and total porphyrins	Differential diagnosis of immune-mediated axonal neuropathy related to SARDs
Electrophysiological testing	NCS; EMG	Diagnosis of axonal neuropathy Fiber type involvement Distribution of neuropathy Severity of neuropathy
	Nociceptive-evoked potentials; microneurography	Function of somatic small fibers
Imaging methods	Optical coherence tomography; sinus x-ray; echocardiography; abdominal ultrasound/CT; joint ultrasonography; contrast-enhanced brain MRI	Expansion of SARDs; Diagnosis of SARDs
	High resolution nerve sonography	Complementary role in mononeuropathy diagnosis
	Contrast-enhanced spine and limb MRI	Enhancement of nerve roots, plexuses and nerves can occur in sarcoidosis; hyperintense T2-weighted lesions and volumetric reduction of posterior columns can occur in chronic sensory neuronopathy
	Corneal confocal microscopy	Possible use in the diagnosis of sensory small fiber neuropathy
CSF analysis	NFL (also from serum)	Might differentiate active vasculitic neuropathy from non-vasculitic neuropathy
	Glucose (CSF:serum ratio); protein; cell count	Pleocytosis and hypoglycorrhachia could be found in sarcoidosis Pleocytosis might occur in AMAN
	Angiotensin-converting enzyme	Elevated values might occur in sarcoidosis
Biopsy	Nerve biopsy or combined nerve-muscle biopsy	"Gold standard" for the diagnosis of vasculitic neuropathy; should be performed when there is a high suspicion of vasculitis
	Skin biopsy with quantification of IENFD	Diagnosis of small fiber neuropathy Small fiber neuropathy progression and response to treatment Etiology of small fiber neuropathy
	Dorsal root ganglia excisional biopsy	Rarely performed for the diagnosis of sensory neuronopathy
Autonomic testing	Ewing battery test; QSART; TST; SSR; SVR; ARFS	Cardiovascular autonomic reflex and sudomotor and vasodilation function of autonomic fibers

PARACLINICAL FINDINGS

Although a peripheral nerve disorder is suspected based on history and physical examination, paraclinical tests are essential in making the final diagnosis of immune-mediated axonal neuropathies. **Table 2** provides information on laboratory tests and their utility in the diagnosis of immune-mediated neuropathies related to SARDs (**Table 2**).

Blood Tests and Imaging Methods

Blood and urine tests should be performed in suspected SARDs, both for establishing the diagnosis (and excluding differential diagnoses) and assessing disease activity and expansion. Routine blood tests and urinalysis could identify relevant findings such as cytopenia, eosinophilia, inflammatory biomarkers, proteinuria, elevated transaminases, cholestasis and elevated creatine kinase levels, whereas immunological tests such as autoantibodies support the diagnosis of SARDs (Bril and Katzberg, 2014; Blaes, 2015).

Relevant findings for SARDs diagnosis and expansion can also be detected by imaging modalities such as: optical coherence tomography–uveitis, optic neuropathy; sinus x-ray–sinusitis; chest x-ray/CT–chest infiltrates, lymphadenopathy, pleural effusion; echocardiography–pericardial effusion, Libman-Sacks endocarditis; abdominal ultrasound/CT–lymphadenopathy, hepatosplenomegaly; joint ultrasonography–arthritis, synovitis. A contrast-enhanced brain MRI might identify basal meningeal enhancement in sarcoidosis presenting with multiple cranial neuropathies (Pirau and Lui, 2020).

Nevertheless, we emphasize the fact that SARDs are usually diagnosed based on classification criteria (in the absence of diagnostic criteria), which means that exclusion of alternative diagnoses such as infections and malignancies is mandatory (Aggarwal et al., 2015). Moreover, other plausible causes for axonal neuropathy should be excluded before linking it to SARDs.

Electrophysiological Studies

In immune axonal neuropathies, electrodiagnosis reveals an axonal process, identifies the type of the affected fiber and indicates the distribution, course and severity of the disease (Karvelas et al., 2013).

Axonal degeneration impairs its function, leading to failure in properly conducting electrical signals to the recording electrode. Reduced sensory nerve action potentials (SNAPs) and compound muscle action potentials (CMAPs) amplitudes subsequently emerge, usually in a sequential manner–the sensory nerves are the first ones to display electrophysiological abnormalities, possibly because of their lack of compensatory reinnervation, whereas CMAP amplitudes can be normal until 75% of axons are affected as there is collateral sprouting in the motor nerves. However, axonal neuropathies may fail to show abnormalities on nerve conduction studies (NCS) in the early phases, exhibiting spontaneous muscle activity and aberrant motor unit action potential morphology on needle electromyography (EMG) instead. Since demyelinating features such as increased latencies, prolonged F waves or diminished conduction velocities might occur as a consequence of fast conducting fibers loss or demyelination secondary to prominent axonal loss, electrophysiological distinction between axonal and demyelinating processes might be a challenge (Karvelas et al., 2013). In this regard, Tankisi et al. (Tankisi et al., 2005) proposed a series of criteria for electrophysiological classification of polyneuropathies. According to them, a primarily axonal process requires the presence of at least two nerves (sensory and/or motor) fulfilling the criteria for axonal loss, namely a decrease in SNAP or CMAP amplitude with at least 2.5 standard deviations (SD) and a slight reduction in conduction velocity/distal motor latency by up to 2.5 SD and consistent EMG findings (Tankisi et al., 2005).

Standard electrophysiological studies indicate the fiber type involvement - motor or large sensory - by analyzing the SNAPs and CMAPs latencies and amplitudes. They do not directly assess the small sensory fibers responsible for pain/burning sensation in the extremities or small autonomic fibers and are expected to be normal in isolated involvement of these nerve fibers (Karvelas et al., 2013). An asymmetrical axonal sensory neuropathy without distal worsening gradient toward the legs is suggestive of sensory neuronopathy (ganglionopathy) (Martinez et al., 2012). Up to 18% of the patients also have reduced CMAP amplitude, especially at peroneal and tibial nerves, whereas EMG is usually normal in sensory neuronopathy (Martinez et al., 2012).

The distribution of neuropathy gives important clues regarding its etiopathogenesis. In mononeuritis multiplex multiple single nerves are affected either simultaneously or serially in an asymmetrical pattern. Chronic and severe vasculitis leads to axonal loss in multiple areas of a single nerve with eventual involvement of multiple nerves mimicking a distal symmetric polyneuropathy. In the initial phases of a distal symmetric neuropathy, the amplitudes of SNAPs and CMAPs are diminished in the distal lower limbs. As the disease progresses, similar abnormalities are likely to be found in the distal upper limbs. Moreover, a neurogenic pattern can be spotted on EMG.

The course and severity of neuropathy are assessed indirectly by electrophysiological studies. The severity of axon loss is well correlated with electrophysiological findings, but not with symptoms. Motor deficit is not clinically evident until 50% of the axons in the motor unit are damaged, but denervation with spontaneous muscle activity can be detected on EMG after minimal axonal degeneration. On the other hand, chronic neuropathies are likely to have collateral sprouting with fiber reinnervation expressed as abnormal motor unit action potential morphology (increased amplitude, duration and polyphasia) on EMG.

Since NCS are normal in small fiber neuropathy, other tests have been employed to assess the function of somatic and/or autonomic small fibers. Quantitative sensory testing (QST) assesses temperature thresholds by two methods: the method of levels and the method of limits (Hoeijmakers et al., 2012). In small fiber neuropathy, QST high thresholds are expected. However, QST specificity is low since central nervous system disorders such as multiple sclerosis and stroke might impair the results (Hoeijmakers et al., 2012). Another limit of QST is that the patient needs to be alert and cooperative (Hoeijmakers et al., 2012). Nociceptive-evoked potentials (laser-evoked potentials, contact-heat evoked potentials, pain-related evoked potentials, intraepidermal electrical stimulation) are elicited by selective stimulation of Aδ fibers and/or C-fibers (Hoeijmakers et al., 2012). Poor responses are correlated with the severity of the disease (Hoeijmakers et al., 2012). Microneurography provides direct measurement of sympathetic activity, but requires expert investigators and cooperative patients (Hoeijmakers et al., 2012). Autonomic testing such as the Ewing battery test for cardiovascular autonomic reflex and Quantitative Sudomotor Axon Reflex Test (QSART), Thermoregulatory Sweat Test (TST), Sympathetic Skin Response (SSR), Skin Vasomotor Reflex (SVR) as well as Axon Reflex Flare Size (ARFS) for sudomotor and vasodilation function could be used for assessing autonomic small fiber function (Hoeijmakers et al., 2012).

Cerebrospinal Fluid Analysis

Cerebrospinal fluid (CSF) analysis is not commonly recommended in neuropathies since it has a low diagnostic yield (except for demyelinating neuropathies) (England et al., 2009). However, serum neurofilament light (NFL), a structural protein specific to neurons that was previously proven indicative of axonal damage in central nervous system disorders such as multiple sclerosis, has displayed a 100% specificity and 82% sensitivity for a cut-off value of 155 pg/ml in discriminating between active vasculitic neuropathy and non-vasculitic neuropathy or systemic vasculitis without neuropathy (Bischof et al., 2018). Mariotto et al. (Mariotto et al., 2018) showed that serum and CSF NFL levels are increased not only in vasculitic neuropathies, but in many other types of acquired neuropathies irrespective of neurophysiological findings or clinical subtypes. Furthermore, they proved that serum NFL is correlated with disease activity and disability progression, subsequently extending the previous findings and suggesting a potential role for this biomarker in monitoring axonal damage and treatment

efficiency in peripheral nervous system disorders (Mariotto et al., 2018). In neurosarcoidosis, CSF analysis occasionally reveals elevated angiotensin-converting enzyme, pleocytosis and hypoglycorrhachia (Bril and Katzberg, 2014). In AMAN and AMSAN, CSF pleocytosis can occur (Bril and Katzberg, 2014).

Nerve Sonography and Magnetic Resonance Imaging

High resolution nerve sonography directly visualizes the peripheral nerves and provides data regarding their morphology. In addition to the well-known advantages of echography such as non-invasivity, low price and good tolerability, it provides an easy access to small fibers and many peripheral nerves since they display a superficial course, as well as a rapid assessment of a long nerve course (Goedee et al., 2013). Its complementary role in diagnostic approach has already been validated in mononeuropathies, but available data regarding polyneuropathies are still lacking. Information on vasculitic neuropathy is even more scarce, sometimes being obtained indirectly–for instance, Rajabally et al. (Rajabally et al., 2012) found that distal median nerve is significantly thicker in chronic inflammatory demyelinating polyneuropathy compared to vasculitic neuropathy. Nodora et al. (Nodera et al., 2006) reported a patient with vasculitic neuropathy who had multiple nerve hypertrophy, as suggested by bilateral enlargement (i.e. increased cross-sectional area) of the median, ulnar, tibial and cervical nerve roots that diminished after steroid treatment. Ito et al. (Ito et al., 2007) proved tibial nerve thickening and hypoechogenicity (possibly secondary to intraneural edema) in eight patients with vasculitic neuropathy. Data related to the size of fascicles, thickness of the epineurium or nerve vascularization are unavailable in the aforementioned studies. However, high resolution nerve sonography is to be considered in axonal neuropathies and should benefit from further quality research in order to be validated as a diagnostic tool, especially since electrophysiological studies are often not well tolerated because of intense pain (Goedee et al., 2013).

In sarcoidosis, apart from the basal meningeal enhancement already mentioned, contrast enhancement of nerve roots, plexuses and nerves can sometimes be identified on spine and limb MRI (Pirau and Lui, 2020). In chronic sensory neuronopathy, hyperintense T2-weighted lesions and volumetric reduction of posterior columns are evident due to dorsal root ganglia neuronal destruction with subsequent degeneration of their central projections (Martinez et al., 2012).

Nerve Biopsy

Nerve biopsy is indicated whenever there is a high suspicion of vasculitis but no supportive evidence from other paraclinical tests (Bril and Katzberg, 2014; Blaes, 2015). The classical histopathological findings of vasculitic neuropathy are: inflammatory infiltration of vasa nervorum with wall destruction, fibrinoid necrosis of the tunica media with fragmentation of the internal elastic lamina and centrofascicular axonal degeneration (Vallat et al., 2009; Collins et al., 2013). In older lesions, the fibrinoid necrosis is replaced by extensive fibrosis, but inflammatory cells are still present at the periphery (Vallat et al., 2009). There are three histopathological degrees of certainty for the diagnosis of vasculitic neuropathy: definite, probable and possible. The diagnosis of vasculitic neuropathy is certain when intramural vasa nervorum inflammation is associated with vascular wall damage in the absence of vasculitic mimicker (Collins et al., 2010). Vascular wall damage is reflected by either active lesions such as "fibrinoid necrosis, loss/disruption of endothelium, loss/fragmentation of internal elastic lamina, loss/fragmentation/separation of smooth muscle cells in media, acute thrombosis, vascular/perivascular hemorrhage or leukocytoclasia" or chronic lesions with signs of healing/repair, namely "intimal hyperplasia, fibrosis of media, adventitial/periadventitial fibrosis or chronic thrombosis with recanalization" (Collins et al., 2010). Some supportive criteria for the diagnosis of vasculitic neuropathy (also considered pathologic predictors of definite vasculitic neuropathy) have also been proposed, specifically "neovascularization, endoneurial hemorrhage, focal perineurial inflammation/degeneration/thickening, injury neuroma, microfasciculation, swollen axons filled with organelles and other axonal changes of acute ischemia" (Collins et al., 2010). Probable vasculitic neuropathy is suspected whenever predominant axonal changes occur in addition to both perivascular/vascular inflammation and vascular damage or "vascular deposition of complement/IgM/fibrinogen/hemosiderin, asymmetrical/multifocal nerve fiber loss/degeneration, prominent active axonal degeneration, myofiber necrosis, regeneration/infarcts in concomitant peroneus brevis muscle biopsy" (Collins et al., 2010). Predominant axonal changes associating either vascular inflammation, vascular damage or pathologic predictors of definite vasculitic neuropathy stand for a possible vasculitic neuropathy (Collins et al., 2010). **Figures 2–5** reveal some of the features commonly encountered in vasculitic neuropathy.

Histological proof is the "gold standard" for the diagnosis of vasculitic neuropathy. However, superficial nerve biopsy (sural nerve) has a sensitivity of only 50%, whereas combined nerve-muscle biopsy (superficial peroneal nerve/peroneus brevis muscle or sural nerve/anterior tibialis or gastrocnemius muscle) adds a 5.1% additional yield in clinically suspected vasculitic neuropathy and 15% in established vasculitic neuropathy (Collins et al., 2010; Vrancken et al., 2011). In this setting, histopathological predictors of vasculitis have been looked for. Immune deposits (immunoglobulin, complement, fibrinogen) have been detected by electron microscopy in epineurial vessel walls in up to 80% of patients with vasculitic neuropathy, but their specificity has been subject of debate since their presence might be the consequence of the disruption of blood-nerve interface. Collins et al. (Collins et al., 2013) hypothesized that a larger amount of immune proteins in the vessel walls might be more specific for a vasculitic process, hence a specific diagnosis might require a laboratory method that fails to identify low concentrations of these proteins. Therefore, they evaluated a cohort of patients with suspected vasculitic neuropathy undergoing combined nerve-muscle biopsy with direct immunofluorescence analysis (a less sensitive method) for detection of IgG, IgM and C_3 and

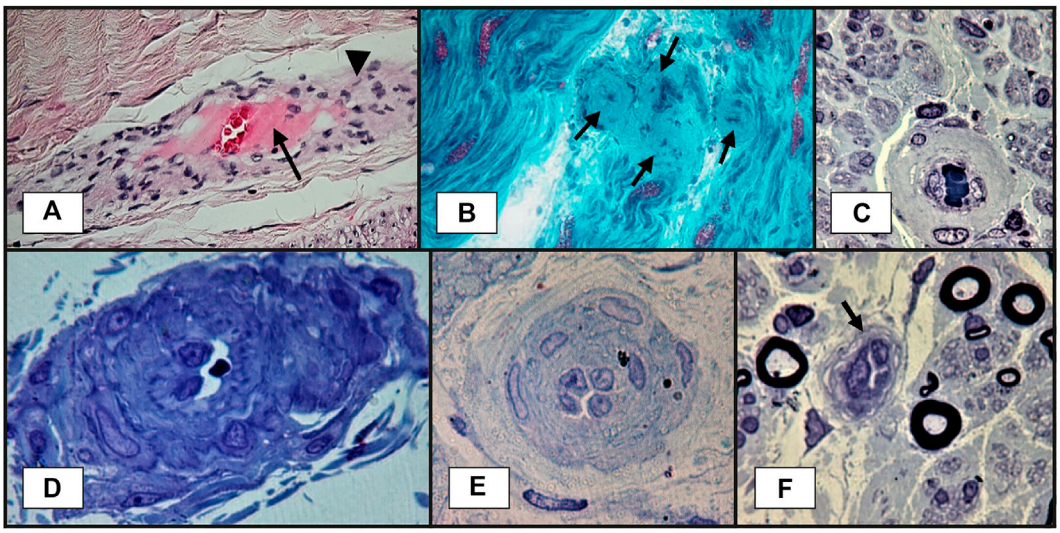

FIGURE 2 | Sural nerve biopsy showing vasa nervorum lesions suggestive of vasculitic neuropathy: **(A)**–transmural inflammation (arrowhead) and fibrinoid necrosis: thick layer in the center of the vessel, near lumen, in pink (arrow). This section is slightly oblique, so the vessel wall is elongated (paraffin embedded tissue section, H&E staining); **(B)**–blood vessel wall thickening, with marked luminal narrowing and presumptive fibrinoid necrosis (arrows) (longitudinal cryosection, modified Gömöri trichrome staining); **(C)**–thickened vessel wall in endoneurium (semithin section, epon embedding tissue, toluidine blue staining); **(D)**–a vessel with abnormal structure and thickened wall in epineurium. A narrowed lumen is observed (semithin section, epon embedding tissue, toluidine blue staining); **(E)**–a vessel with reactive endothelial cells, multilayered basal membrane and very narrow lumen (semithin section, epon embedding tissue, toluidine blue staining); **(F)**–a vessel with reactive endothelial cells and narrow lumen (arrow) (semithin section, epon embedding tissue, toluidine blue staining).

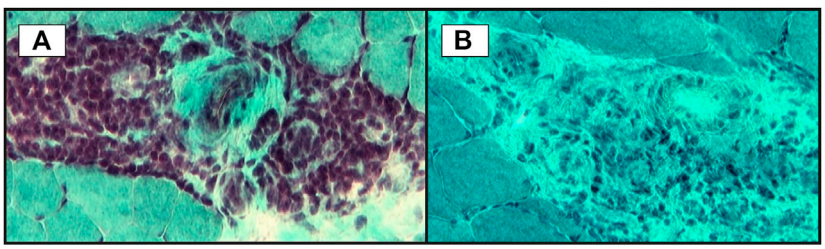

FIGURE 3 | Small vessels inflammation in skeletal muscle biopsy: **(A)**–significant perivascular inflammatory infiltrate; **(B)**–microvasculitis: some small vessels with perivascular inflammatory infiltrate (transversal cryosections, modified Gömöri trichrome staining).

demonstrated a 92% specificity of this method for the diagnosis of vasculitic neuropathy (Collins et al., 2010).

Skin biopsy is increasingly being used as an additional test for the diagnosis of small fiber neuropathy (Hoeijmakers et al., 2012). It employs morphometric evaluation of intraepidermal nerve fibers (the distal ends of axons originating from dorsal root ganglia and trigeminal ganglion that cross the dermo-epidermal junction and reach the epidermis) density (IENFD). Intraepidermal nerve fibers density is significantly reduced in small fiber neuropathy (Tesfaye et al., 2010). In addition to decreased IENFD, degenerative changes of IENF and dermal fibers could also be spotted (Hoeijmakers et al., 2012). Moreover, skin biopsy can also be used to evaluate autonomic structures and innervation in sweat glands and arrector pili muscles (Hoeijmakers et al., 2012). In diabetes mellitus and toxic neuropathies, IENF loss is an early feature of the disease, progresses with disease severity and may repair with proper management (Tesfaye et al., 2010; Hoeijmakers et al., 2012). Since damage of small nerve fibers is not disease-specific, these findings could also apply to immune-mediated small fiber neuropathy related to SARDs (Hoeijmakers et al., 2012). Skin biopsy can also identify the underlying cause of small fiber neuropathy when concurrent conditions such as diabetes mellitus emerge (Hoeijmakers et al., 2012). Perivascular inflammation and vascular injury point to SLE rather than diabetes mellitus (Hoeijmakers et al., 2012). Nevertheless, equivocal clinical-histological correlations have been reported, emphasizing the need for an accurate history taking and thorough neurological examination. For instance, decreased IENFD might arise as a result of distal damage to large sensory fibers (Gondim et al., 2018), but symptoms of small fiber involvement and normal NCS are highly suggestive of small fiber neuropathy (Levine, 2018). Corneal confocal microscopy is a non-invasive method that might be useful in the diagnosis of small fiber neuropathy

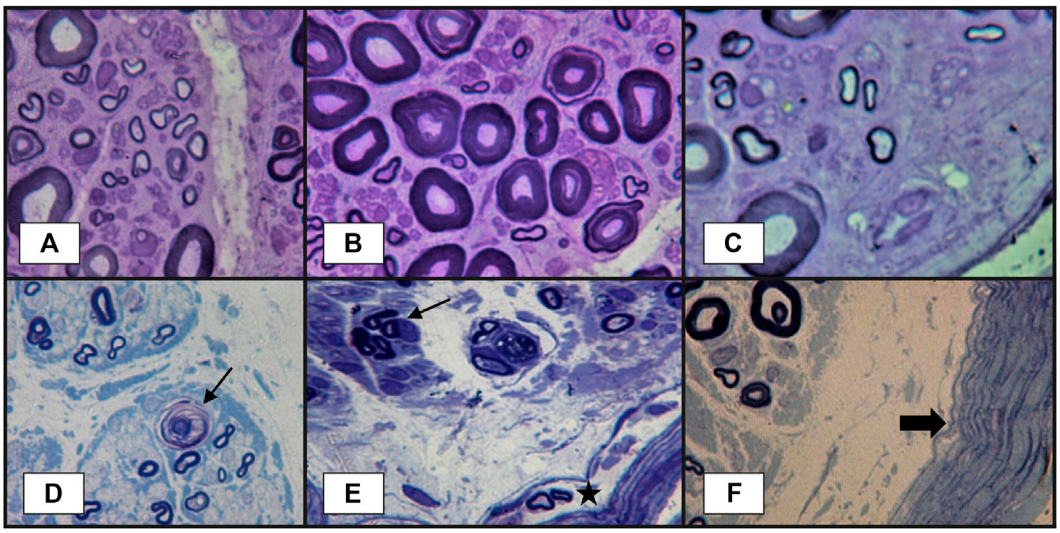

FIGURE 4 | Peripheral nerve lesions in vasculitic neuropathy: **(A–C)**–transverse semithin sections of sural nerve biopsy in a patient with severe acute axonal neuropathy, showing findings that are highly suggestive of vasculitic neuropathy: focal fiber damage in the same nerve fascicle with axonal degeneration in different zones (three images from the same semithin section), loss of large-caliber axons; **(D)**–another case more severely affected, with focal axonal loss, axonal degeneration (arrow) and subperineurial edema. Other abnormalities observed in vasculitic peripheral neuropathy, but without specificity, could be **(E)**–axonal los, axonal regeneration represented by the presence of a small group of axons with same caliber (arrow), some abnormal small myelinated axons in perineurium (star); **(F)**–thickened perineurium (thick arrow) with subperineurial marked edema (semithin sections, epon embedding tissue, toluidine blue staining).

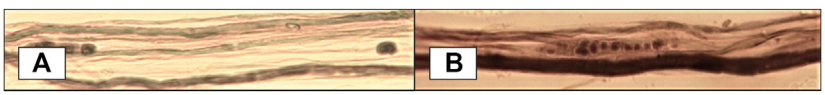

FIGURE 5 | Teased fiber studies showing axonal degeneration in dissociated myelinated fibers - fibers with myelin spheres and ovoids along with normally myelinated axons (osmium tetroxide).

(Hoeijmakers et al., 2012). Corneal fiber density seems to be inversely correlated with IENF loss in distal leg and disease severity (Hoeijmakers et al., 2012).

Dorsal root ganglia excisional biopsy with histological analysis reveals neuronal loss, the Nageotte nodules and mononuclear infiltrates in sensory neuronopathy (Martinez et al., 2012). However, this biopsy is rarely performed because is very invasive and requires trained neurosurgeons (Martinez et al., 2012).

We conclude that nerve biopsy is crucial for definite diagnosis in vasculitic neuropathies unless other examinations are conclusive. However, its low diagnostic yield in a phenotype not highly suggestive of a vasculitic neuropathy and the risks it implies (permanent hypoesthesia, wound infection and delayed healing or post-biopsy pain) require further research for identifying diagnostic biomarkers of vasculitic neuropathy with higher efficacy and safety profiles. Skin biopsy is the "gold standard" test for diagnosis of small fiber neuropathy. Dorsal root ganglia excisional biopsy is seldom performed for diagnosing sensory neuronopathy. Nerve biopsy is currently not recommended in other types of immune-mediated axonal neuropathy.

TREATMENT

Immunosuppressive and Immunomodulatory Treatment

Since neuropathy associated with SARDs is supposedly immune-mediated, its treatment aims for immunosuppression, likewise in other affected organs/tissues targeted by SARDs (lupus nephritis, rheumatoid lung disease, scleroderma-related interstitial lung disease, etc.). However, considering the low prevalence of systemic autoimmune diseases and the difficulty to conduct clinical trials, there is a scarcity of good evidence regarding their treatment, particularly when it comes to peripheral neurological involvement. Moreover, considering that peripheral neuropathy is usually overshadowed by life-threatening manifestations (pulmonary, renal, cardiac, central nervous system, severe thrombocytopenia or hemolytic anemia) or more disturbing symptoms (fever, polyarthritis, rash, malaise), treatment is generally directed toward these, whereas neuropathy is the main target only when it is an isolated manifestation or displays a severe and progressive course.

The guideline for the management of SLE with neuropsychiatric manifestations (Bertsias et al., 2010) states

that "glucocorticoids alone or with immunosuppressive therapy have been used with good results (60–75% response rate). Intravenous immunoglobulin, plasma exchange and rituximab have been used in severe cases", without listing any reference. Similarly, the recommendation regarding the treatment of peripheral neuropathy "Peripheral neuropathy: Combination therapy with glucocorticoids and immunosuppressive agents may be considered in severe cases" is rated with level A of evidence and class I recommendation (very strong), although the statement "may be considered" does not actually suggest a strong evidence. These features are inappropriate for a guideline and emphasize the lack of good quality data concerning immune-mediated neuropathy treatment. Furthermore, PubMed labels only one randomized controlled trial comparing IV cyclophosphamide with IV methylprednisolone in severe neurological manifestations of SLE, which reported only 7 patients with peripheral neuropathy out of 32 patients evaluated (Barile-Fabris et al., 2005). Additionally, there are only two retrospective observational studies regarding neurolupus, each evaluating 10 patients with neuropathy (Neuwelt et al., 1995; Fanouriakis et al., 2016), a restrospective case series of 10 patients with mononeuritis multiplex (Rivière et al., 2017) and various case reports. Generally, the cases describe patients who responded to an immunosuppressive drug or a combination therapy, sometimes following a lack of response to another immunosuppressive drug or combination, therefore providing no clear suggestion for a treatment algorithm, apart from the low evidence level (Constantin et al., 2020). Evidence is even more scarce for other SARDs that associate neuropathy, particularly RA, SS (Huma et al., 2020), PAN, ANCA-associated vasculitides or cryoglobulinemia.

Immunosuppressive treatment for immune-mediated axonal neuropathies related to SARDs consists of corticosteroids and cyclophosphamide, either in oral regimens or IV pulses. As in other organ involvement, rituximab and mycophenolate mofetil have been recently tried. Plasmapheresis is reserved for severe cases. Induction therapy for severe axonal immune-mediated neuropathy related to SARDs consists of prednisone 1 mg/kg (or methylprednisolone 7–15 mg/kg up to 1 g/day IV in severe cases of acute mononeuritis) plus either rituximab (off label) (375 mg/m^2/week, four weeks) or cyclophosphamide (15 mg/kg IV every 2 weeks for three doses, then every 3 weeks, 6 or 7 pulses). Provided that cyclophosphamide or rituximab are not tolerated or are unavailable, azathioprine or mycophenolate could be used instead (the latter off label). The dose of azathioprine is 2–2.5 mg/kg if thiopurine methyltransferase (an enzyme required for azathioprine metabolism) is present. Otherwise, the drug is very toxic and is restricted; if the enzyme assays are unavailable or too expensive, azathioprine 50 mg/day is administered and blood cell count is checked after one week–absence of leukopenia means that the enzyme is present, requiring full dosage afterward. For mycophenolate mofetil the induction dose is 2–3 g/day for 6 months (dose for induction in lupus nephritis) (Hahn et al., 2012). The maintenance therapy includes either azathioprine (dose mentioned above) or mycophenolate mofetil (1–1.5 g b. i.d) (Ong et al., 2005; Hahn et al., 2012).

Specific Advice for Each Disease/ Manifestation

Systemic lupus erythematosus: cyclophosphamide pulse should be administered monthly instead of every 2 and then 3 weeks. If secondary aPL is confirmed, anticoagulants or antiplatelet agents should be used.

Rheumatoid arthritis: if the patient is already treated with DMARDs (either methotrexate or leflunomide) or biological therapy, ceasing them is recommended.

Sjögren's syndrome: patients who do not respond adequately to symptomatic therapy could receive immunosuppressive medication, namely corticosteroids with azathioprine or rituximab. If cryoglobulinemic vasculitis (cryoglobulins can appear in SS) is suspected, immunosuppression should be more aggressive, with cyclophosphamide or rituximab. The same regimen applies for mononeuritis multiplex. In sensory neuronopathy, plasma exchange (5-9 sessions), IV immunoglobulin (3 cycles at 3 weeks interval) +/− rituximab, azathioprine (2–3 mg/kg/day) or TNFα antagonist infliximab (3 mg/kg in refractory cases) might have beneficial results (Martinez et al., 2012).

Sarcoidois: oral prednisone should be used in facial neuropathy (2 weeks) and peripheral neuropathy (4 weeks). For severe forms of neuropathy, IV methylprednisolone could be given for 3 days, followed by oral prednisone for 2–4 weeks, with subsequent tapering.

ANCA-associated vasculitides: acute-onset mononeuritis multiplex requires remission induction therapy as in vital organ involvement - high dose corticosteroids in combination with IV cyclophosphamide (3 pulses every 2 weeks, then 6–7 pulses every 3 weeks) or rituximab, as previously stated (Yates et al., 2016). In severe disease course, plasmapheresis could be added.

Polyarteritis nodosa: The "five factor score" that guides therapy in vasculitis does not include peripheral neuropathy. Corticosteroids and cyclophosphamide should be used for induction, while azathioprine or methotrexate maintain remission (De Virgilio et al., 2016). PAN secondary to hepatitis B virus infection requires treatment with lamivudine, short term use of corticosteroids and plasmapheresis in more severe cases.

Cryoglobulinemic vasculitis: rapidly progressive neuropathy is considered a feature of severe disease, requiring etiological treatment (most frequently, anti-hepatitis C) in addition to immunosuppressive therapy with rituximab alone or in combination with pulsed high-dose corticosteroids (instead of chronic use of low-medium doses); plasmapheresis should be performed in nonresponders, emergency situations or hyperviscosity syndrome (Pietrogrande et al., 2011).

Small fiber neuropathy: immunomodulatory therapy seems to show benefits in relieving symptoms (Hoeijmakers et al., 2012).

AMAN/AMSAN: apart from IV immunoglobulin or plasma exchange, immunosuppressants should also be used (IV methylprednisolone and high-dose cyclophosphamide).

Nevertheless, as previously mentioned, these recommendations are based on poor evidence (Benstead et al., 2014).

Analgesic Treatment

There are no studies specifically addressing pain treatment in immune-mediated neuropathy. Therefore, recommendations are extrapolated from diabetic peripheral neuropathy trials: pregabalin has consistent evidence with class I recommendation, whereas other drugs like gabapentin, duloxetine, venlafaxine, amitriptyline, valproate, opioids and capsaicin are probably effective and should be considered for treatment (class II recommendation for pain in diabetic neuropathy) (Bril et al., 2011).

PROGNOSIS

Although immune axonal neuropathy does not affect patient survival in SARDs, it has a major negative impact on daily activities and functionality level, with subsequent decrease in life quality (Koike and Sobue, 2013; Naddaf and Dyck, 2015). Apart from the unpleasant subjective experience (pain, paresthesia) that interferes with daily activities and significantly alters the quality of life (mood, sleep, etc.), these patients can have balance impairment leading to falls due to sensory and motor deficits. As expected, patients with active vasculitic neuropathy are more likely to have constitutional symptoms, active disease and multivisceral involvement (Suppiah et al., 2011).

CONCLUSION

Final Remarks

About 30–50% of patients with systemic vasculitis and 5–93% of those with connective tissue disorders have peripheral nervous system involvement (Blaes, 2015; Snoussi et al., 2019), either as inaugural presentation or throughout the course of the disease. It is mandatory to recognize and properly assess immune axonal neuropathy since it might be the only manifestation of an aggressive disease or cause significant distress to the patient. Moreover, appropriately classifying the underlying disorder assists the clinician in choosing the right treatment and influence the prognosis. Discovering new diagnostic biomarkers with high safety and efficacy profiles would be valuable since the diagnosis is sometimes difficult and delayed.

Future Perspectives

Considering the few trials directly addressing the effect of immunosuppression and immunomodulation on immune axonal neuropathy related to SARDs, current treatment strategies depend mainly on extrapolation from studies pertaining to other organ involvement such as lupus nephritis (Suppiah et al., 2011). High quality clinical research is required in order to provide indications and follow up guidelines for immunosuppressive therapies in immune axonal neuropathies associated with SARDs.

AUTHOR CONTRIBUTIONS

Conceptualization, CB, DT, and BOP; methodology, CB, DT, and EM; writing—original draft preparation, DT and CB; writing—review and editing, CB, DT, BOP, EM; visualization, DT and EM; supervision, CB and BOP; funding acquisition, BOP. All authors have read and agreed to the published version of the manuscript.

ACKNOWLEDGMENTS

We thank Sorin Brînduşescu and Adina Stroe for their valuable support in creating the graphic design.

REFERENCES

Adams, D., Cauquil, C., and Lozeron, P. (2012). Dysautonomies des neuropathies périphériques. *La Presse Médicale* 41 (11), 1128–1136. doi:10.1016/j.lpm.2012.05.030

Agarwal, V., Singh, R., Wiclaf, K. D., Chauhan, S., Tahlan, A., Ahuja, C. K., et al. (2008). A clinical, electrophysiological, and pathological study of neuropathy in rheumatoid arthritis. *Clin. Rheumatol.* 27 (7), 841–844. doi:10.1007/s10067-007-0804-x

Aggarwal, R., Ringold, S., Khanna, D., Neogi, T., Johnson, S. R., Miller, A., et al. (2015). Distinctions between diagnostic and classification criteria?. *Arthritis Care Res.* 67 (7), 891–897. doi:10.1002/acr.22583

Amaral, T. N., Peres, F. A., Lapa, A. T., Marques-Neto, J. F., and Appenzeller, S. (2013). Neurologic involvement in scleroderma: a systematic review. *Semin. Arthritis Rheum.* 43 (3), 335–347. doi:10.1016/j.semarthrit.2013.05.002

Barile-Fabris, L., Ariza-Andraca, R., Olguin-Ortega, L., Jara, L. J., Fraga-Mouret, A., Miranda-Limon, J. M., et al. (2005). Controlled clinical trial of IV cyclophosphamide versus IV methylprednisolone in severe neurological manifestations in systemic lupus erythematosus. *Ann. Rheum. Dis.* 64 (4), 620–625. doi:10.1136/ard.2004.025528

Benstead, T. J., Chalk, C. H., and Parks, N. E. (2014). Treatment for cryoglobulinemic and non-cryoglobulinemic peripheral neuropathy associated with hepatitis C virus infection. *Cochrane Database Syst. Rev.* (12), CD010404. doi:10.1002/14651858.CD010404.pub2

Bertsias, G. K., Ioannidis, J. P. A., Aringer, M., Bollen, E., Bombardieri, S., Bruce, I. N., et al. (2010). EULAR recommendations for the management of systemic lupus erythematosus with neuropsychiatric manifestations: report of a task force of the EULAR standing committee for clinical affairs. *Ann. Rheum. Dis.* 69 (12), 2074–2082. doi:10.1136/ard.2010.130476

Birol, A., Ulkatan, S., Koçak, M., and Erkek, E. (2004). Peripheral neuropathy in behçet's disease. *J. Dermatol.* 31 (6), 455–459. doi:10.1111/j.1346-8138.2004.tb00531.x

Bischof, A., Manigold, T., Barro, C., Heijnen, I., Berger, C. T., Derfuss, T., et al. (2018). Serum neurofilament light chain: a biomarker of neuronal injury in vasculitic neuropathy. *Ann. Rheum. Dis.* 77 (7), 1093–1094. doi:10.1136/annrheumdis-2017-212045

Blaes, F. (2015). Diagnosis and therapeutic options for peripheral vasculitic neuropathy. *Ther. Adv. Musculoskelet.* 7 (2), 45–55. doi:10.1177/1759720x14566617

Boissaud-Cooke, M., Pidgeon, T. E., and Tunstall, R. (2015). "The microcirculation of peripheral nerves: the vasa nervorum.," in *Nerves and nerve injuries. Vol 1: history, embryology, anatomy, imaging, and diagnostics*. Editors

R. Shane Tubbs, M. M. Shoja, N. Barbaro, E. Rizk, M. Loukas, and R. J. Spinner (Elsevier), 507–523.

Bril, V., and Katzberg, H. D. (2014). Acquired immune axonal neuropathies, *Continuum (Minneap Minn).* 20 (5 Peripheral Nervous System Disorders), 1261–1273. doi:10.1212/01.CON.0000455882.83803.72

Bril, V., England, J., Franklin, G. M., Backonja, M., Cohen, J., Del Toro, D., et al. (2011). Evidence-based guideline: treatment of painful diabetic neuropathy: report of the American academy of neurology, the American association of neuromuscular and electrodiagnostic medicine, and the American academy of physical medicine and rehabilitation. *Neurology* 76 (20), 1758–1765. doi:10.1212/wnl.0b013e3182166ebe

Collins, M. P., Arnold, W. D., and Kissel, J. T. (2013). The neuropathies of vasculitis. *Neurol. Clin.* 31 (2), 557–595. doi:10.1016/j.ncl.2013.01.007

Collins, M. P., Dyck, P. J. B., Gronseth, G. S., Guillevin, L., Hadden, R. D. M., Heuss, D., et al. (2010). Peripheral Nerve Society Guideline* on the classification, diagnosis, investigation, and immunosuppressive therapy of non-systemic vasculitic neuropathy: executive summary. *J. Peripher. Nerv Syst.* 15 (3), 176–184. doi:10.1111/j.1529-8027.2010.00281.x

Collins, M. P., Periquet-Collins, I., Sahenk, Z., and Kissel, J. T. (2010). Direct immunofluoresence in vasculitic neuropathy: specificity of vascular immune deposits. *Muscle Nerve* 42 (1), 62–69. doi:10.1002/mus.21639

Collins, M. P. (2012). The vasculitic neuropathies. *Curr. Opin. Neurol.* 25 (5), 573–585. doi:10.1097/wco.0b013e3283580432

Constantin, A., Năstase, D., Tulbă, D., Bălănescu, P., and Băicuș, C. (2020). Immunosuppressive therapy of systemic lupus erythematosus associated peripheral neuropathy: a systematic review. *Lupus* 29, 1509. doi:10.1177/0961203320948181

De Virgilio, A., Greco, A., Magliulo, G., Gallo, A., Ruoppolo, G., Conte, M., et al. (2016). Polyarteritis nodosa: a contemporary overview. *Autoimmun. Rev.* 15 (6), 564–570. doi:10.1016/j.autrev.2016.02.015

Doria, A., Zen, M., Bettio, S., Gatto, M., Bassi, N., Nalotto, L., et al. (2012). Autoinflammation and autoimmunity: bridging the divide. *Autoimmun. Rev.* 12 (1), 22–30. doi:10.1016/j.autrev.2012.07.018

Dutra LAaB, O. G. P. (2016). Neuro-Behçet's disease: a review of neurological manifestations and its treatment. *J. Vasculitis.* 2, 2. doi:10.4172/2471-9544.100112

Emam, H. M. (2019). Peripheral neuropathy IN BEHCET'S disease: clinical and neurophysiological study. *Cairo, Al-Azhar Med J.* 48 (8), 267-278. 10.12816/AMJ.2019.56680

England, J. D., Gronseth, G. S., Franklin, G., Carter, G. T., Kinsella, L. J., Cohen, J. A., et al. (2009). Evaluation of distal symmetric polyneuropathy: the role of autonomic testing, nerve biopsy, and skin biopsy (an evidence-based review). *Muscle Nerve* 39 (1), 106–115. doi:10.1002/mus.21227

Fanouriakis, A., Pamfil, C., Sidiropoulos, P., Damian, L., Flestea, A., Gusetu, G., et al. (2016). Cyclophosphamide in combination with glucocorticoids for severe neuropsychiatric systemic lupus erythematosus: a retrospective, observational two-centre study. *Lupus* 25 (6), 627–636. doi:10.1177/0961203315622821

Firestein, G. S., Budd, R. C., Gabriel, S. E., Koretzky, G. A., McInnes, I. B., and O'Dell, J. R. (n.d.). Firestein and Kelley's textbook of rheumatology2021. *Elsevier's Covid-19 Healthcare Hub*. 2, 336–339.

Fleetwood, T., Cantello, R., and Comi, C. (2018). Antiphospholipid syndrome and the neurologist: from pathogenesis to therapy. *Front. Neurol.* 9, 1001. doi:10.3389/fneur.2018.01001

Goedee, H. S., Brekelmans, G. J. F., van Asseldonk, J. T. H., Beekman, R., Mess, W. H., and Visser, L. H. (2013). High resolution sonography in the evaluation of the peripheral nervous system in polyneuropathy - a review of the literature. *Eur. J. Neurol.* 20 (10), 1342–1351. doi:10.1111/ene.12182

Gondim, F. d. A. A., Barreira, A. A., Claudino, R., Cruz, M. W., Cunha, F. M. B. d., Freitas, M. R. G. d., et al. (2018). Definition and diagnosis of small fiber neuropathy: consensus from the peripheral neuropathy scientific department of the Brazilian academy of neurology. *Arq. Neuro-psiquiatr.* 76 (3), 200–208. doi:10.1590/0004-282x20180015

Gwathmey, K. G., Burns, T. M., Collins, M. P., and Dyck, P. J. B. (2014). Vasculitic neuropathies. *Lancet Neurol.* 13 (1), 67–82. doi:10.1016/s1474-4422(13)70236-9

Hahn, B. H., McMahon, M. A., Wilkinson, A., Wallace, W. D., Daikh, D. I., Fitzgerald, J. D., et al. (2012). American College of Rheumatology guidelines for screening, treatment, and management of lupus nephritis. *Arthritis Care Res.* 64 (6), 797–808. doi:10.1002/acr.21664

Hanly, J. G. (2014). Diagnosis and management of neuropsychiatric SLE. *Nat. Rev. Rheumatol.* 10 (6), 338–347. doi:10.1038/nrrheum.2014.15

Hernández-Rodríguez, J., Alba, M. A., Prieto-González, S., and Cid, M. C. (2014). Diagnosis and classification of polyarteritis nodosa. *J. Autoimmun.* 48-49, 84–89. doi:10.1016/j.jaut.2014.01.029

Hoeijmakers, J. G., Faber, C. G., Lauria, G., Merkies, I. S., and Waxman, S. G. (2012). Small-fibre neuropathies-advances in diagnosis, pathophysiology and management. *Nat. Rev. Neurol.* 8 (7), 369–379. doi:10.1038/nrneurol.2012.97

Huma, A. C., Kecskes, E. M., Tulba, D., Balanescu, P., and Baicus, C. (2020). Immunosuppressive treatment for peripheral neuropathies in Sjogren's syndrome–a systematic review. *Rom. J. Intern. Med.* 58 (1), 5–12. doi:10.2478/rjim-2019-0022

Imam, M. H., Koriem, H. K., Hassan, M. M., El-Hadidi, A. S., and Ibrahim, N. A. (2019). Pattern of peripheral neuropathy in systemic lupus erythematosus: clinical, electrophysiological, and laboratory properties and their association with disease activity. *Egypt. Rheumatol. Rehabil.* 46 (4), 285–298. doi:10.4103/err.err_28_19

Ishibe, K., Tamatsu, Y., Miura, M., and Shimada, K. (2011). Morphological study of the vasa nervorum in the peripheral branch of human facial nerve. *Okajimas Folia Anat. Jpn.* 88 (3), 111–119. doi:10.2535/ofaj.88.111

Ito, T., Kijima, M., Watanabe, T., Sakuta, M., and Nishiyama, K. (2007). Ultrasonography of the tibial nerve in vasculitic neuropathy. *Muscle Nerve* 35 (3), 379–382. doi:10.1002/mus.20673

Jennette, J. C., Falk, R. J., Bacon, P. A., Basu, N., Cid, M. C., Ferrario, F., et al. (2012). 2012 revised international chapel hill consensus conference nomenclature of vasculitides. *Arthritis Rheum.* 65 (1), 1–11. doi:10.1002/art.37715

Kaeley, N., Ahmad, S., Pathania, M., and Kakkar, R. (2019). Prevalence and patterns of peripheral neuropathy in patients of rheumatoid arthritis. *J. Fam. Med Prim Care* 8 (1), 22–26. doi:10.4103/jfmpc.jfmpc_260_18

Karvelas, K., Rydberg, L., and Oswald, M. (2013). Electrodiagnostics and clinical correlates in acquired polyneuropathies. *PM&R* 5 (5 Suppl. l), S56–S62. doi:10.1016/j.pmrj.2013.03.030

Koike, H., and Sobue, G. (2013). Clinicopathological features of neuropathy in anti-neutrophil cytoplasmic antibody-associated vasculitis. *Clin. Exp. Nephrol.* 17 (5), 683–685. doi:10.1007/s10157-012-0767-3

Kurt, S., Alsharabati, M., Lu, L., Claussen, G. C., and Oh, S. J. (2015). Asymptomatic vasculitic neuropathy. *Muscle Nerve* 52 (1), 34–38. doi:10.1002/mus.24494

Lacomis, D. (2011). Neurosarcoidosis. *Current Neuropharmacology.* 9 (3), 429–436. doi:10.2174/157015911796557975

Lefter, S., Monaghan, B., McNamara, B., and Regan, M. J. (2020). Acute severe sensory ganglionopathy in systemic lupus erythematous. *Neuromuscul. Disord.* 30 (8), 701–706. doi:10.1016/j.nmd.2020.07.002

Levine, T. D. (2018). Small fiber neuropathy: disease classification beyond pain and burning. *J. Cent. Nerv Syst. Dis.* 10, 1179573518771703. doi:10.1177/1179573518771703

Lightfoot, R. W., Jr., Michel, B. A., Bloch, D. A., Hunder, G. G., Zvaifler, N. J., McShane, D. J., et al. (1990). The American College of Rheumatology 1990 criteria for the classification of polyarteritis nodosa. *Arthritis Rheum.* 33 (8), 1088–1093. doi:10.1002/art.1780330805

Mariotto, S., Farinazzo, A., Magliozzi, R., Alberti, D., Monaco, S., and Ferrari, S. (2018). Serum and cerebrospinal neurofilament light chain levels in patients with acquired peripheral neuropathies. *J. Peripher. Nerv Syst.* 23 (3), 174–177. doi:10.1111/jns.12279

Martinez, A. R., Nunes, M. B., Nucci, A., and Franca, M. C., Jr. (2012). Sensory neuronopathy and autoimmune diseases. *Autoimmune Dis.* 2012, 873587. doi:10.1155/2012/873587

Masi, A. T., Hunder, G. G., Lie, J. T., Michel, B. A., Bloch, D. A., Arend, W. P., et al. (1990). The American College of Rheumatology 1990 criteria for the classification of Churg-Strauss syndrome (allergic granulomatosis and angiitis). *Arthritis Rheum.* 33 (8), 1094–1100. doi:10.1002/art.1780330806

Mizisin, A. P., and Weerasuriya, A. (2011). Homeostatic regulation of the endoneurial microenvironment during development, aging and in response to trauma, disease and toxic insult. *Acta Neuropathol.* 121 (3), 291–312. doi:10.1007/s00401-010-0783-x

Naddaf, E., and Dyck, P. J. (2015). Vasculitic neuropathies. *Curr. Treat. Options. Neurol.* 17 (10), 374. doi:10.1007/s11940-015-0374-1

Neuwelt, C. M., Lacks, S., Kaye, B. R., Ellman, J. B., and Borenstein, D. G. (1995). Role of intravenous cyclophosphamide in the treatment of severe neuropsychiatric systemic lupus erythematosus. *Am. J. Med.* 98 (1), 32–41. doi:10.1016/s0002-9343(99)80078-3

Nodera, H., Sato, K., Terasawa, Y., Takamatsu, N., and Kaji, R. (2006). High-resolution sonography detects inflammatory changes in vasculitic neuropathy. *Muscle Nerve* 34 (3), 380–381. doi:10.1002/mus.20582

Ong, L. M., Hooi, L. S., Lim, T. O., Goh, B. L., Ahmad, G., Ghazalli, R., et al. (2005). Randomized controlled trial of pulse intravenous cyclophosphamide versus mycophenolate mofetil in the induction therapy of proliferative lupus nephritis. *Nephrology* 10 (5), 504–510. doi:10.1111/j.1440-1797.2005.00444.x

Paik, J. J., Mammen, A. L., Wigley, F. M., Shah, A. A., Hummers, L. K., and Polydefkis, M. (2016). Symptomatic and electrodiagnostic features of peripheral neuropathy in scleroderma. *Arthritis Care Res.* 68 (8), 1150–1157. doi:10.1002/acr.22818

Petri, M., Orbai, A. M., Alarcón, G. S., Gordon, C., Merrill, J. T., Fortin, P. R., et al. (2012). Derivation and validation of the Systemic Lupus International Collaborating Clinics classification criteria for systemic lupus erythematosus. *Arthritis Rheum.* 64 (8), 2677–2686. doi:10.1002/art.34473

Pietrogrande, M., De Vita, S., Zignego, A. L., Pioltelli, P., Sansonno, D., Sollima, S., et al. (2011). Recommendations for the management of mixed cryoglobulinemia syndrome in hepatitis C virus-infected patients. *Autoimmun. Rev.* 10 (8), 444–454. doi:10.1016/j.autrev.2011.01.008

Pirau, L., and Lui, F. (2020). *Neurosarcoidosis. StatPearls. Treasure island (FL).*

Rajabally, Y. A., Morlese, J., Kathuria, D., and Khan, A. (2012). Median nerve ultrasonography in distinguishing neuropathy sub-types: a pilot study. *Acta Neurol. Scand.* 125 (4), 254–259. doi:10.1111/j.1600-0404.2011.01527.x

Rivière, E., Cohen Aubart, F., Maisonobe, T., Maurier, F., Richez, C., Gombert, B., et al. (2017). Clinicopathological features of multiple mononeuropathy associated with systemic lupus erythematosus: a multicenter study. *J. Neurol.* 264 (6), 1218–1226. doi:10.1007/s00415-017-8519-7

Ropper, A. H., Samuels, M. A., and Klein, J. P. (2014). *Asymmetrical and Multifocal Polyneuropathies (Mononeuropathy, or Mononeuritis Multiplex)*. Adams and Victor's Principles of Neurology. 10th Edn: McGraw-Hill Education Medical; 2014. 1341–1343.

Said, G., Lacroix, C., Plante-Bordeneuve, V., Le Page, L., Pico, F., Presles, O., et al. (2002). Nerve granulomas and vasculitis in sarcoid peripheral neuropathy: a clinicopathological study of 11 patients. *Brain* 125 (Pt 2), 264–275. doi:10.1093/brain/awf027

Sampaio, L., Silva, L. G., Terroso, G., Nadais, G., Mariz, E., and Ventura, F. (2011). Vasculitic neuropathy. *Acta Reumatol Port* 36 (2), 102–109.

Santiago-Casas, Y., Peredo, R., and Vilá, L. (2013). Efficacy of low-dose intravenous cyclophosphamide in systemic lupus erythematosus presenting with Guillain-Barré syndrome-like acute axonal neuropathies: report of two cases. *Lupus* 22 (3), 324–327. doi:10.1177/0961203313476358

Santos, M., de Carvalho, J., Brotto, M., Bonfa, E., and Rocha, F. (2010). Peripheral neuropathy in patients with primary antiphospholipid (Hughes') syndrome. *Lupus* 19 (5), 583–590. doi:10.1177/0961203309354541

Schofield, J. R. (2017). Autonomic neuropathy-in its many guises-as the initial manifestation of the antiphospholipid syndrome. *Immunol. Res.* 65 (2), 532–542. doi:10.1007/s12026-016-8889-4

Siva, A., and Saip, S. (2009). The spectrum of nervous system involvement in Behçet's syndrome and its differential diagnosis. *J. Neurol.* 256 (4), 513–529. doi:10.1007/s00415-009-0145-6

Snoussi, M., Frickha, F., and Bahloul, Z. (2019). "Peripheral neuropathy in connective tissue diseases," in *Demystifying polyneuropathy: IntechOpen*. Editor P. B. Ambrosi, 568.

Starshinova, A. A., Malkova, A. M., Basantsova, N. Y., Zinchenko, Y. S., Kudryavtsev, I. V., Ershov, G. A., et al. (2019). Sarcoidosis as an autoimmune disease. *Front. Immunol.* 10, 2933. doi:10.3389/fimmu.2019.02933

Suppiah, R., Hadden, R. D. M., Batra, R., Arden, N. K., Collins, M. P., Guillevin, L., et al. (2011). Peripheral neuropathy in ANCA-associated vasculitis: outcomes from the European Vasculitis Study Group trials. *Rheumatology* 50 (12), 2214–2222. doi:10.1093/rheumatology/ker266

Tankisi, H., Pugdahl, K., Fuglsang-Frederiksen, A., Johnsen, B., de Carvalho, M., Fawcett, P. R. W., et al. (2005). Pathophysiology inferred from electrodiagnostic nerve tests and classification of polyneuropathies. Suggested guidelines. *Clin. Neurophysiol.* 116 (7), 1571–1580. doi:10.1016/j.clinph.2005.04.003

Tesfaye, S., Boulton, A. J. M., Dyck, P. J., Freeman, R., Horowitz, M., Kempler, P., et al. (2010). Diabetic neuropathies: update on definitions, diagnostic criteria, estimation of severity, and treatments. *Diabetes Care* 33 (10), 2285–2293. doi:10.2337/dc10-1303

Thakolwiboon, S., Karukote, A., and Sohn, G. (2019). Acute motor-sensory axonal neuropathy associated with systemic lupus erythematosus. *Baylor Univ. Med. Cent. Proc.* 32 (4), 610–613. doi:10.1080/08998280.2019.1647715

Ubogu, E. E., Zaidat, O. O., and Suarez, J. I. (2001). Acute motor-sensory axonal neuropathy associated with active systemic lupus erythematosus and anticardiolipin antibodies. *JCR: J. Clin. Rheumatol.* 7 (5), 326–331. doi:10.1097/00124743-200110000-00014

Vallat, J.-M., Vital, A., Magy, L., Martin-Negrier, M.-L., and Vital, C. (2009). An update on nerve biopsy. *J. Neuropathol. Exp. Neurol.* 68 (8), 833–844. doi:10.1097/nen.0b013e3181af2b9c

Vrancken, A. F. J. E., Gathier, C. S., Cats, E. A., Notermans, N. C., and Collins, M. P. (2011). The additional yield of combined nerve/muscle biopsy in vasculitic neuropathy. *Eur. J. Neurol.* 18 (1), 49–58. doi:10.1111/j.1468-1331.2010.03041.x

Vrancken, A. F. J. E., and Said, G. (2013). Vasculitic neuropathy. *Handb Clin. Neurol.* 115, 463–483. doi:10.1016/b978-0-444-52902-2.00026-6

Weerasuriya, A., and Mizisin, A. P. (2011). The blood-nerve barrier: structure and functional significance. *Methods Mol. Biol.* 686, 149–173. doi:10.1007/978-1-60761-938-3_6

Wludarczyk, A., and Szczeklik, W. (2016). Neurological manifestations in ANCA-associated vasculitis - assessment and treatment. *Expert Rev. Neurotherapeutics* 16 (8), 861–863. doi:10.1586/14737175.2016.1165095

Yates, M., Watts, R. A., Bajema, I. M., Cid, M. C., Crestani, B., Hauser, T., et al. (2016). EULAR/ERA-EDTA recommendations for the management of ANCA-associated vasculitis. *Ann. Rheum. Dis.* 75 (9), 1583–1594. doi:10.1136/annrheumdis-2016-209133

Conflict of Interest: The authors declare that the research was conducted in the absence of any commercial or financial relationships that could be construed as a potential conflict of interest.

frontiers in Pharmacology

REVIEW
published: 07 March 2022
doi: 10.3389/fphar.2022.745658

Pruritus: A Sensory Symptom Generated in Cutaneous Immuno-Neuronal Crosstalk

*Attila Gábor Szöllősi[1], Attila Oláh[2], Erika Lisztes[2], Zoltán Griger[3] and Balázs István Tóth[2]**

[1]Department of Immunology, Faculty of Medicine, University of Debrecen, Debrecen, Hungary, [2]Department of Physiology, Faculty of Medicine, University of Debrecen, Debrecen, Hungary, [3]Division of Clinical Immunology, Department of Internal Medicine, Faculty of Medicine, University of Debrecen, Debrecen, Hungary

Pruritus or itch generated in the skin is one of the most widespread symptoms associated with various dermatological and systemic (immunological) conditions. Although many details about the molecular mechanisms of the development of both acute and chronic itch were uncovered in the last 2 decades, our understanding is still incomplete and the clinical management of pruritic conditions is one of the biggest challenges in daily dermatological practice. Recent research revealed molecular interactions between pruriceptive sensory neurons and surrounding cutaneous cell types including keratinocytes, as well as resident and transient cells of innate and adaptive immunity. Especially in inflammatory conditions, these cutaneous cells can produce various mediators, which can contribute to the excitation of pruriceptive sensory fibers resulting in itch sensation. There also exists significant communication in the opposite direction: sensory neurons can release mediators that maintain an inflamed, pruritic tissue-environment. In this review, we summarize the current knowledge about the sensory transduction of pruritus detailing the local intercellular interactions that generate itch. We especially emphasize the role of various pruritic mediators in the bidirectional crosstalk between cutaneous non-neuronal cells and sensory fibers. We also list various dermatoses and immunological conditions associated with itch, and discuss the potential immune-neuronal interactions promoting the development of pruritus in the particular diseases. These data may unveil putative new targets for antipruritic pharmacological interventions.

Keywords: itch, molecular transduction of pruritus, sensory neurons, inflammation, skin, cytokines, dermatoses

OPEN ACCESS

Edited by:
Imola Wilhelm,
Biological Research Centre, Hungary

Reviewed by:
Wolfgang Bäumer,
Freie Universität Berlin, Germany
Laurent Misery,
Université de Bretagne Occidentale, France

****Correspondence:***
Balázs István Tóth
toth.istvan@med.unideb.hu

Specialty section:
This article was submitted to Inflammation Pharmacology, a section of the journal Frontiers in Pharmacology

Received: *22 July 2021*
Accepted: *07 February 2022*
Published: *07 March 2022*

Citation:
Szöllősi AG, Oláh A, Lisztes E, Griger Z and Tóth BI (2022) Pruritus: A Sensory Symptom Generated in Cutaneous Immuno-Neuronal Crosstalk. Front. Pharmacol. 13:745658. doi: 10.3389/fphar.2022.745658

THE CUTANEOUS ITCH

General Introduction

Itch is a common somatosensory modality well-known from the everyday life. It was defined as an "unpleasant sensation that elicits the desire or reflex to scratch" by Samuel Hafenreffer in the 17th century (Ikoma et al., 2006, p. 535), which is a pragmatic and valid definition even today. Our knowledge has been hugely expanded since Hafenreffer's definition and, especially in the last 2 decades, we reached a deeper insight into the molecular and cellular details of how itch is generated, yet our understanding is far from complete. Although itch in general is not a life-threatening situation, the clinical management of itching conditions is still one of the biggest challenges of daily dermatological practice. Treatment of chronic itch (lasting longer than 6 weeks) remains an unmet medical challenge in many instances, affecting millions of people worldwide. According to

epidemiological results the prevalence of chronic itch in the general population is between 8–28% (Weisshaar and Dalgard, 2009; Leader et al., 2015). Based on these data, it is not surprising that the socioeconomic burden of chronic pruritus is comparable to that of chronic pain. Development of effective treatments is mainly impaired by our lack of understanding of the signaling pathways underlying pruriception, especially in chronic itch, where itch develops and is maintained (at least partly) independently of external stimuli.

Itch can be classified into four categories based on both the different mechanisms by which it may be generated, and by taking into account their clinical appearence (Paus et al., 2006; Bíró et al., 2007; Ständer et al., 2007; Tóth et al., 2015; Dong and Dong, 2018). **Pruriceptive itch** is peripherally induced itch generated in the skin. In this case, itch is evoked by locally released pruritogens exciting the pruriceptive nerve endings in the skin. The release of these chemical mediators can be triggered acutely by external irritants (e.g. insect bite, poisonous plants or skin sensitizers) or may be related to various, typically inflammatory skin conditions which can affect an extended area of the skin, and is likely to be chronic. **Neurogenic itch** is also evoked by the (peripheral) excitation of itch sensitive neurons, but in this case the triggering pruritic mediators stem from a "central source" and their production is related to systemic diseases, such as kidney failure, hepatic conditions or immunological diseases. In contrast, **neuropathic itch** is due to a damage of the itch processing neural network at any level. It can be associated with peripheral neuropathies (e.g. postherpetic neuropathy), nerve compression or irritation (e.g. in notalgia paresthetica) or certain brain lesions and tumors. Finally, **psychogenic itch** is related to psychiatric disorders or psychological conditions like phobias, obsessive-compulsive disorder or psychotic diseases. In this review, we focus on the role of peripheral interactions in the generation of pruritus, therefore, mainly discussing cases of pruriceptive and some neurogenic pruritus as these are evoked by the excitation of pruriceptive cutaneous nerve endings.

Sensing Pruritus

Pruriceptive Fibers of the Skin

The sensory transduction of pruritus, i.e. how propagating action potentials are generated by pruritic stimuli, is realized by exciting a subpopulation of cutaneous bare nerve endings which also express molecular markers typical of nociceptors. Therefore, pruriceptive fibers are generally considered a subpopulation of nociceptors, the selective activation of which results in itch sensation. This is in contrast to a general activation of nociceptors that results in nociception and evokes pain. This is postulated as the selectivity theory of itch, a nowadays generally accepted description of the relation between pruriception and nociception (LaMotte et al., 2014). This is also supported by the findings that depletion of nociceptors by overdosing transient receptor potential 1 (TRPV1) agonists (Cavanaugh et al., 2009; Imamachi et al., 2009) or genetic ablation of TRPV1-lineage nociceptive neurons of the dorsal root ganglia (DRGs) resulted in a dramatic reduction of both nociception and pruriception (Mishra et al., 2011; Mishra and Hoon, 2013). However, intense efforts were taken to identify molecular markers of a "labelled line" for pruriception. Among primary sensory neurons of the DRGs, a few molecular markers were identified which are believed to be (more or less) specifically expressed by pruriceptive sensory neurons. For example, specific neurotransmitters can be released from the central terminal of the pruriceptive sensory neurons which may differentiate these neurons from the nociceptor population. The fact that the ablation of gastrin releasing peptide receptor expressing (GRPR+) neurons–or only the GRPR molecules from the spinal cord–strongly inhibited pruritogen evoked scratching behavior without affecting acute nociception suggested that gastrin releasing peptide (GRP) may be a neurotransmitter released selectively from itch sensitive sensory neurons of DRGs. GRP was indeed detected in peripheral sensory neurons (Sun and Chen, 2007; Barry et al., 2016, 2020) and its expression was found to be elevated in chronic itch conditions in mice (Zhao et al., 2013) and primates (Nattkemper et al., 2013). The optogenic activation of GRP expressing cutaneous sensory fibers resulted in itch behavior, and chemically induced itch was attenuated by conditional deletion of GRP from DRG neurons (Barry et al., 2020). However, other studies resulted in controversial findings as they could not (or hardly) detect GRP in peripheral sensory neurons, rather localized it in the spinal cord, expressed by higher order neurons in the itch pathway (Fleming et al., 2012; Mishra and Hoon, 2013; Sun et al., 2017). Other studies argue for the role of natriuretic polypeptide b (NPPB) as a peripheral itch specific neurotransmitter. It was shown to be expressed in a subpopulation of DRG neurons and its genetic deletion, as well as ablating its receptor, dramatically decreased scratching behavior induced by various pruritogens (Mishra and Hoon, 2013). Moreover, members of Mas1-related G protein-coupled receptors (MRGPRs) were also identified as markers of itch specific neurons (Liu et al., 2009; Liu and Dong, 2015). In mouse, MRGPRs are coded by an extended gene cluster and divided into several subfamilies. However, in human, there are only four members of the family identified, marked as MRGPRX1-4, which do not form orthologous pairs with rodent counterparts (Dong et al., 2001; Lembo et al., 2002). Some MRGPRs, expressed exclusively in skin innervating fibers, are not only markers of pruriceptive neurons, but also serve as receptors for pruritic ligands. Especially the role of MRGPRA3, MRGPRC11 and MRGPRD, as well as the human MRGPRX1 were described to be involved in various forms of non-histaminergic itch. Interestingly, MRGPRA3 and MRGPRD display non-overlapping expression in pruriceptive neurons and are activated by different pruritic ligands, suggesting the existence of different labeled lines even within the non-histaminergic itch sensing neuron population (Liu et al., 2009, Liu et al., 2012 Q.; Han et al., 2013; Liu and Dong, 2015).

Recently, large scale transcriptome profiling studies also characterized and classified somatosensory neurons in an unbiased manner and identified different neuronal subpopulations potentially responsible for pruriception based on their specific expression patterns. Following single cell RNA-Seq, Usoskin et al. (2015) identified 11 clusters of somatosensory neurons by principal component analysis.

Among them, itch associated markers (*Mrgpr*s, *Nppb*, histamine receptors (*Hr*s) serotonin receptors (*Htr*s) endothelin receptor A (*Ednra*), etc.) were highly and selectively enriched in the NP1-3 clusters which represents a fraction of the unmyelinated, small size neurons expressing the classical markers of non-peptidergic sensory neurons. Interestingly, within these clusters, marked inhomogeneity was found in the expression of particular pruritic markers, e. g. *Nppb* and IL-31 receptor (*Il31ra*) were highly expressed in the NP3 cluster, or *Mrgpra3* and *Mrgprd* displayed highest expression in different clusters, in line with previous data from "biased" studies. Clustering somatosensory neurons using a similar approach, Chiu et al. (2014) also identified a specific subset of DRG neurons highly expressing *Nppb* and *Il31ra* genes within the $Trpv1^{+}$ $Nav1.8/1.9^{+}$ nociceptor population. Interestingly, these cells were mainly negative for isolectin B4 (IB4), a classical marker of non-peptidergic nociceptors (Priestley, 2009). Most recently, a similar single neuron RNAseq transcriptome profiling identified that the neuronal clusters described in mice are highly conserved in non-human primates (Kupari et al., 2021). The NP1-3 classes were also identified in rhesus macaque expressing, among others, *MRGPRX1-4* in NP1-NP2 clusters and *HR1* in NP3. However, there are some remarkable interspecies differences in the expression of individual genes within some clusters. For example, although somatostatine (*SST*), Janus kinase 1 (*JAK1*), *IL31RA*, Oncostatin M receptor β (*OSMRβ*), and Sphingosine-1-phosphate receptor 1 (*S1PR1*) were highly expressed in the NP3 cluster in both mice and macaque, *Nppb,* serotonin receptor 1F (*HTR1F*), and neurotensin (*NTS*) were specifically expressed only in mice whereas the expression of some other genes were mainly restricted to primates (Kupari et al., 2021). In a current study, Nguyen et al. (2021) classified human DRG neurons based on single nucleus RNA sequencing and supported their analysis with multiplex *in situ* hybridization. They grouped the sensory neurons into 15 classes (H1-H15) that mainly matched the previously described mouse clusters, but they also identified some human-specific classes which does not have a clear mouse counterpart. From the point of view of itch, H10 and H11 classes seem to be the most relevant. The expression pattern of these classes resembled to the mouse NP1-3 classes, likely representing non-peptidergic pruriceptive neurons. Neurons in the H11 class highly expressed *OSMRβ*, *JAK1* and *SST* especially similarly to NP3 mouse neurons, whereas *MRGPRX1* was found mainly in H10 as its counterpart genes are characteristic for NP2 mouse cells. However, both human classes also expressed markers characteristic for NP1 group in mice, and in general, the *in situ* hybridization indicated that H10 and H11 are relatively heterogeneous classes of sensory neurons. Interestingly, some H10 neurons co-expressed the low-threshold mechanosensitive ion channel *PIEZO2* with pruriceptive markers that was not found in mice. Thus, it is tempting to consider these cells as the mediators of the human mechanically evoked itch (Nguyen et al., 2021). It is important to mention that these data revealed remarkable differences in the expression of growth factor receptors between the corresponding neuron classes of mice and human, suggesting that the development and differentiation of the analogue somatosensory neurons might be controlled by different mechanisms in rodent and human (Nguyen et al., 2021).

Phenomenologically, pruriceptive fibers can be characterized by their (electro)physiological properties in humans (Schmelz, 2015). The unmyelinated C fibers innervating the skin contains mechanosensitive polymodal nociceptors responding to mechanical, chemical and thermal stimuli, and less numerous mechano-insensitive nociceptive fibers, as well (Schmidt et al., 1995, 1997, 2002). In this latter, mechano-insensitive group, a subset of neurons are identified by their marked responses to the prototypic itch mediator histamine, suggesting that they form an "itch-sensitive" population within the primary afferents. These histamine-sensitive sensory neurons were characterized by low conduction velocity, high transcutaneous electrical threshold, large receptive field and poor two point discrimination threshold for histamine-induced itch (Wahlgren and Ekblom, 1996; Schmelz et al., 1997, 2000, 2003; Schmidt et al., 2002; Schmelz and Schmidt, 2010). A distinct group of histamine insensitive pruriceptive afferents was also proposed by the experiments demonstrating that low intensity-high frequency focal electrical stimulation evoked itch sensation without causing erythema, which erythema is a characteristic consequence of the axon reflex activated by exciting the histamine sensitive fibers (Ikoma et al., 2005; Steinhoff et al., 2006). In contrast to histamine, the pruritic spicules of the cowhage (*Mucuna pruriens*) pod activated a subgroup of mechanosensitive nociceptive afferents and not the mechano-insensitive ones (Namer et al., 2008). Moreover, the involvement of nociceptive, myelinated A-fibers was also demonstrated in the itch sensation evoked by cowhage (Ringkamp et al., 2011).

These human data are in good accordance to the above mentioned rodent results describing distinct sub-groups of pruriceptive fibers within the nociceptor population. Indeed, results of rodent behavior experiments on pruriception can be successfully translated to human itch sensation, especially with the use of advanced experimental paradigms which are able to discriminate between nociception and pruriception in mice, like the cheek test or calf injection model. In the cheek model, compounds are injected into the cheek of the animals which results in wiping with the forelimb or scratching with the hind limb in case of algogens and pruritogens, respectively. Similarly, calf injection resulting in pain and itch will induce selectively licking and biting responses, respectively (Shimada and LaMotte, 2008; LaMotte et al., 2011, 2014). These techniques were found to be very useful to discriminate between pruriception and nociception and identifying the selective molecular events in the sensory transduction on pruritus.

Mechanisms of the Sensory Transduction in Pruritus

The activation of the above detailed pruriceptive primary sensory neurons is responsible for the sensory transduction of itch, which is the first step of pruriception, (i.e. the neural processing of the information which finally will result in itch sensation). The pruritic sensory transduction is typically initiated by chemical mediators acting on their receptors expressed by the cutaneous sensory terminals. During the molecular events of the sensory transduction of itch, pruritic mediators typically bind to a

metabotropic receptor which initiates the activation of intracellular signaling pathways resulting in the opening of some ion channels responsible for the generator potential which finally evokes the discharge of the neuron (Tóth et al., 2015, 2020; Dong and Dong, 2018).

The ion channels involved in the initial depolarization are considered as molecular integrators and amplifiers of pruriception. The best studied of these ion channels mostly belong to the transient receptor potential (TRP) family of ion channels and show significant overlap with those involved in nociception. The pruriceptive role of the thermosensitive nociceptors TRPV1 and transient receptor potential ankyrin 1 (TRPA1) is the most characterized on sensory neurons (Wilson and Bautista, 2014, 201; Schmelz, 2015; Tóth et al., 2015, 2020). The role of TRPV1 was described primarily in the transduction of histamine induced pruritus, but it is involved in some forms of non-histaminergic pruritus as well (Imamachi et al., 2009; Dong and Dong, 2018). In contrast, TRPA1 is a general integrator in the transduction of itch induced by various non-histaminergic mediators (Wilson et al., 2011; Wilson et al., 2013; Lieu et al., 2014; Wilson and Bautista, 2014). Although histaminergic and non-histaminergic forms of pruritus signal via different pathways and may be transmitted by selective labeled lines, the partially overlapping expression of TRPV1 and TRPA1 is more widespread in sensory afferents and is not restricted to pruriceptors. Beyond their role in pruriception, they are thermosensitive and can mediate different forms of nociception as well: e.g. TRPV1 is a central molecule of inflammatory warm hyperalgesia and TRPA1 plays a role in cold and mechanical hyperalgesia (Tominaga et al., 1998; Caterina et al., 2000; da Costa et al., 2010; Julius, 2013; Vriens et al., 2014). However, in certain cases, TRPA1 and TRPV1 can play a synergistic role in the same process. They were recently shown as key transducers of heat-pain together with transient receptor potential melastatin 3 (TRPM3), another thermosensitive nociceptor TRP channel significantly co-expressed with TRPV1 and TRPA1. Interestingly, despite their co-expression and functional overlap in thermal nociception (Vandewauw et al., 2018; Held and Tóth, 2021), TRPM3 is not involved in transduction of pruritus evoked by either histamine or serotonin (5-HT) and endothelin-1 (ET-1) (Kelemen et al., 2021). These data suggests, that individual TRP channels, even if coexpressed by some sensory neurons, can play selective roles in certain forms of pruriception or nociception. Even different sensations evoked by the same substance can be mediated by different TRP channels: Sphingosine 1-phosphate (S1P) activates S1P receptor 3 (S1PR3) which induces both itch and pain. However, itch transduction is due to activation of TRPA1 *via* $G_{\beta\gamma}$ signaling pathway but pain transduction realized by TRPV1 activation *via* PLC mediated signal transduction (Hill et al., 2018).

Beyond TRPV1 and TRPA1, other ion channels can integrate the effect of pruritogens. Recently, TRPV4 was described to mediate (at least some forms of) 5-HT evoked itch and cellular responses of DRG neurons (Akiyama et al., 2016). Beyond TRP channels, the Ca^{2+}-activated chloride channel anoctamine 1 (ANO1/TMEM16A) (Yang et al., 2008) was proposed to mediate the activation of C fibers by chloroquine, a strongly pruritic antimalarial drug activating MrgprA3 (Ru et al., 2017). Similar to TRP channels, ANO1 is a thermosensitive nociceptor, as well: it can be activated by noxious warm temperature and mediates nociceptive responses in thermal pain models. Although ANO1 is a chloride channel, its activation can result in depolarization and consequent discharge of DRG neurons due to their relatively higher intracellular Cl^- concentration in physiological circumstances and it can contribute to the neural depolarization induced by ET-1 and histamine (Cho et al., 2012). Interestingly ANO1 can also amplify the neural activity elicited by depolarizing nociceptive Ca^{2+}-permeable cationic channels. In nociceptors, Ca^{2+} influx via TRPV1 was demonstrated to activate ANO1, strongly exacerbating TRPV1 induced depolarization and nociception (Takayama et al., 2015, 2019). Similarly, TRPV4 can be also coupled to ANO1 as reported in secretory cells (Takayama et al., 2014; Derouiche et al., 2018).

Receptors for Pruritogens in Sensory Fibers

The activation of the above listed neuronal ion channels can be initiated by several receptors of the cutaneous pruriceptive nerve endings which are sensitive for the peripherally released pruritic mediators (**Table 1**). The most well-known, "traditional" pruritogenic mediator histamine binds to its G protein coupled ***histamine receptors*** (H1R, H3R, and H4R) that are linked to pruritus and expressed on the cutaneous sensory fibers (Panula et al., 2015) (Rossbach et al., 2011). Of these, activation of H1R and H4R excites pruriceptors resulting in itch. H1R signalizes via $G_{q/11}$ proteins (Panula et al., 2015), and is shown to activate phospholipase C β3 (PLCβ3) and consequently TRPV1 (Han et al., 2006). Pharmacological data also support the involvement of phospholipase A2 and lipoxygenases in the H1R-induced activation of TRPV1 (Kim et al., 2004). H4R can also activate TRPV1 via a PLC-mediated pathway (Jian et al., 2016). Moreover, the role of protein kinase C δ (PKCδ) was also described in the activation of pruriceptors by histamine but not by non-histaminergic pruritogens (Valtcheva et al., 2015). In contrast, the activation of H3R, which is known as an inhibitory histamine receptor transmitting negative feedback on histamine release (Panula et al., 2015), seems to inhibit histamine-induced pruritic responses as its inverse agonists can evoke both activation of pruriceptive neurons and itch (Rossbach et al., 2011).

5-HT is also a potent pruritogen in both humans and rodents (Weisshaar et al., 1997; Akiyama et al., 2010; Dong and Dong, 2018), which can activate several ***5-HT receptors*** expressed by sensory nerve endings. Among them, pharmacological activators of 5-HT_{2A} and 5-HT_7 were shown to sensitize TRPV1 responses via PKC- and PKA-dependent pathways (Ohta et al., 2006). In contrast, the genetic ablation of the ionotropic 5-HT3A did not affect 5-HT evoked behavioral responses, while the lack of PLCβ3 diminished it. This further supports the role of the metabotropic 5-HT receptors and related signaling pathways in pruriception. However, genetic deletion of TRPV1 did not influence the 5-HT-induced responses which were mainly abolished in the absence of TRPV1 expressing sensory neurons arguing for the role of an

TABLE 1 | Cutaneous pruritic mediators stimulating sensory nerve endings

Pruritic mediator	Potential sources	Potential targets on sensory fibers: Receptors, signal transduction, cellular responses
Histamine	Mast cells, basophils	H1R → G_q → PLCβ3/PLA2 → TRPV1 H4R → PLC → TRPV1 Further potential elements of transduction: PKCδ, lipoxygenase
Serotonin	Mast cells, keratinocytes	5-HTR7 → TRPA1 TRPV4
Endothelin 1	Keratinocytes	ET_A → PLCβ3 → TRPA1 Role of ERK1/2?
Proteases → BAM8-22, SLIGRL/SLIGKV	Mast cells, keratinocytes	(mouse) MRGPRC11 → $G_{\alpha q}$ → TRPA1 (human) MRGPRX1/MRGPRX2
TSLP	Keratinocytes	IL7Rα-TSLPR → TRPA1
IL-31	Mast cells	IL-31RA-OSMRβ → ERK1/2 → TRPA1/TRPV1
IL-33	Keratinocytes	IL-1RAcP-ST2 → TRPA1/TRPV1
IL-13	T_h2 type immune response	IL-13Rα1 → JAK1 → ?sensitization/activation?
IL-4	T_h2 type immune response	IL-4Rα → JAK1 → ?sensitization/activation?
CXCL10	Neutrophils, Keratinocytes	CXCR3 → Ca^{2+}-regulated Cl^- channels
LTC4	Various leukocytes, especially in T_h2 type immune response	$CysLT_2R$ → TRPA1/TRPV1
S1P	Erythrocytes, Endothelial cells, Mast cells, Dendritic cells; increased in inflammation	S1PR3 → $G_{\beta\gamma}$ → TRPA1 → itch (High concentration of S1P: S1PR3 → PLC → TRPV1 → pain)
Periostin	Keratinocytes, Fibroblasts	integrin $\alpha_V\beta3$ → TRPA1/TRPV1
(ds)RNA/hairpin structures of self-RNA	Tissue damage?	TLR3

alternative ion channel in the 5-HT signaling pathway in TRPV1+ neurons (Imamachi et al., 2009). Indeed, studies of gene deleted animals provided evidence for the role of 5-HT_7 receptor in mediating acute serotonergic itch via consequent TRPA1 activation (Morita et al., 2015). Moreover, as mentioned above, TRPV4 was also described as a component in the transduction of serotonergic itch in sensory neurons (Akiyama et al., 2016).

The otherwise vasoconstrictive peptide ET-1 acts as an effective endogenously produced itch mediator, although ET-1 can also induce nociception (Hans et al., 2009; Gomes et al., 2012; Kido-Nakahara et al., 2014). Sensory neurons express mainly the ***ET receptor A*** (***ET_A***) (Khodorova et al., 2009) which signals partly via a G_q-related pathway stimulating PLCβ (Khodorova et al., 2009; Davenport et al., 2016). In nociceptors, ET_A activation by endothelin results in increase in intracellular Ca^{2+} concentration which activates PKC resulting in the potentiation of TRPV1 responses (Plant et al., 2007). The pruritic signaling also starts from ET_A (McQueen et al., 2007), and involves PLCβ3, but endothelin-evoked itch is independent of TRPV1 (Imamachi et al., 2009). It is strongly reduced by genetic deletion or pharmacological blockade of TRPA1 (Kido-Nakahara et al., 2014), although there is some controversy about the role of this ion channel in ET-1-induced scratching (Liang et al., 2011). Moreover, the role of extracellular signal-regulated kinases ERK1/2 was also proposed in the ET_A induced pruritic responses. ET-1-induced scratching is negatively regulated by the endothelin-converting enzyme 1 (ECE1) co-expressed with ET_A in somatosensory neurons (Kido-Nakahara et al., 2014).

As mentioned above, ***MRGPRs*** serve not only as markers of the pruriceptive fibers but also as receptors for some non-histaminergic pruritogens. As their name indicates, they are G protein-coupled receptors that signal mainly via the G_q pathway, resulting in Ca^{2+} release from intracellular stores. The deletion of a gene cluster of 12 *Mrgpr* genes in mice resulted in impaired itch evoked by selected non-histaminergic pruritogens: the antimalarial drug chloroquine was identified to activate MRGPRA3, and bovine adrenal medulla 8-22 (BAM8-22, a proenkephalin A-derived peptide) and SLIGRL (a peptide product cleaved from the protease activated receptor 2, PAR2) stimulate MRGPRC11. These receptors were shown to signal *via* $G_{\alpha q11}$ activating TRPA1 (and not TRPV1) (Lembo et al., 2002; Liu et al., 2009, 2011; Wilson et al., 2011; Liu and Dong, 2015). However, a recent study challenged the role of TRPA1 in mediating chloroquine-induced itch, and suggested the role of the calcium-activated chloride channel ANO1/TMEM16A as a downstream target of the chloroquine-induced PLCβ-mediated signaling resulting in depolarization and consequent discharge of sensory fibers (Ru et al., 2017). Importantly, these mouse Mrgpr ligands are also pruritogenic in humans, activating MRGPRX1

TABLE 2 | Overview of the potential pathogenesis of itch in selected pruritic diseases and pathological conditions.

Disease	Factors potentially involved in the pathogenesis of pruritus
Irritant contact dermatitis (ICD)	Keratinocyte injury and barrier damage → inflammatory response, T_h1 cytokines
Allergic contact dermatitis (ACD)	Allergen specific, T cell mediated inflammatory responses, typically T_h2 type → 5-HT↑, ET-1↑, TSLP↑, CXCL10↑, IL-33↑
Urticaria	IgE, degranulation of mast cells, dysregulation of basophils and eosinophils → histamine↑, other pruritic mediators
Atopic dermatitis (AD)	Barrier disturbances, vicious itch-scratch cycle → irritant and allergen permeation↑ Type 2 inflammation: IL-4↑, IL-13↑, IL-31↑, TSLP↑ Dysregulation of cutaneous signaling pathways: opioid, cannabinoid, neuropepitide (SP→NKR1) signaling Innervation density↑ Inflammatory lipid mediators↑ Periostin synthesis↑ (linked to type 2 inflammation)
Psoriasis	T_h17↑ → IL-17↑, IL22↑ IL31↑, TSLP↑, SP↑, NPY↓ NGF↑ → innervation density↑
Prurigo nodularis	Innervation density↑ → SP↑, CGRP↑ Eosinophils↑, mast cells↑, T cells↑ → IL4↑, VIP↑, histamine↑ prostaglandins↑
Cutaneous T-cell lymphoma	IL-31↑, IL-31RA↑, OSMRβ↑ IL-4?, IL-13?, SP?
Dermatomyositis	$CD4^+$ cells↑ → IL-31↑, IL-31RA↑
Systemic sclerosis	Neuropathic component: Destruction of sensory fibers by accumulating collagen, and later regeneration by the inflammatory milieu Mast cells↑, histamine↑
Chronic renal failure	Eosinophils↑, mast cells↑, histamine↑, tryptase↑, inflammation↑ Peripheral neuropathy Imbalance of μ- and κ -opioid receptor activity
Cholestatic liver diseases	Endogenous opioids↑, histamine↑, serotonin↑, lysophosphatidic acid↑ (→TRPV1), bilirubin↑, bile acids↑ Lysophosphatidylcholine → TRPV4 (epidermis) → miR-146a↑ → neural TRPV1 activation↑ Bile acids↑ → TGR5 → TRPA1 (mouse) Bile acids↑ → MRGPRX4 (human) BAM8-22↑ → MRGPRX1/MRGPRC11↑ → TRPA1

(chloroquine and BAM8-22) and MRGPRX2 (SLIGKV, the human analog of the SLIGRL) (Liu et al., 2009, 2011; Sikand et al., 2011; Liu and Dong, 2015). Moreover, in humans, MRGPRX4 also induces pruritic signal transduction *via* G_q/PLC pathway upon activation by bile acids (Yu et al., 2019). Interestingly, in mice, bile acids activate another G-protein coupled receptor, the ***G-protein-coupled bile acid receptor 1*** (***TGR5***) in sensory afferents, which also signals via TRPA1 and evokes itch (Alemi et al., 2013; Lieu et al., 2014). Next to the above MRGPRs, the activation of MRGPRD by β-alanine can also induce itch. Similar to the previously mentioned receptors, MRGPRD activates TRPA1, albeit via a PKA-dependent manner (Liu Q. et al., 2012; Wang et al., 2019).

Although several cytokines, especially T_h2-associated ones, are involved in the development of pruritus and itchy (dermatological) disorders, only some of them can directly excite pruriceptive nerve endings *via* ***cytokine receptors***. Neural cytokine receptors can influence the responsiveness of the sensory fibers even if their activation does not initiate immediate action potential firing. Therefore, they can contribute to the development of chronic itch characteristic of several of the most prevalent dermatological conditions (Storan et al., 2015). One of the most well-established pruritic cytokines is IL-31 which activates a subpopulation of sensory neurons via a *receptor heterodimer composed of IL-31 receptor A (IL-31RA) and Oncostatin M receptor β (OSMRβ)* (Cevikbas et al., 2014; Datsi et al., 2021). IL-31RA activation induces signal transduction through the activation of ERK1/2 and both TRPV1 and TRPA1 (Cevikbas et al., 2014). Sensory neurons also express receptors of other T_h2-type cytokines, like IL-4 (*IL-4Rα*) and IL-13 (*IL-13Rα1*). Interestingly, although IL-4 and IL-13 also activate a small percentage of pruriceptive fibers in both mice and humans, they did not evoke acute itching, in contrast to IL-31. However, they sensitized the sensory neurons toward histamine and other pruritogens, and increased the intensity of histamine-evoked itch. These responses were mediated by IL-4Rα and downstream JAK1 signaling (Oetjen et al., 2017). A recent report raised some controversy about the itch-inducing effect of IL-4 and IL-13 demonstrating that they can evoke even acute itch if applied at lower concentration. A potential explanation might be that higher concentration of the cytokines saturates the JAK1 pathway, and induces negative feedback reactions (Campion et al., 2019). Sensory neurons also express the receptor of thymic stromal lymphopoietin (TSLP), which is another pruritic T_h2-type cytokine produced by various epithelial cells, including epidermal keratinocytes

(Wilson et al., 2013; Varricchi et al., 2018). It activates a small population of the cutaneous nerve endings expressing the heteromeric *TSLP receptor composed of IL7 receptor alpha (IL7Rα) and TSLP-specific receptor chain (TSLPR) chains*. The activation of TSLP receptor evokes itch via TRPA1 (Wilson et al., 2013). *IL-1 receptor accessory protein (IL-1RAcP) and a membrane-bound IL-33–specific ST2 form a heteromeric receptor* for IL-33, and both subunits can be found in the membrane of pruriceptive nerve endings. IL-33 is a pro-inflammatory cytokine, which can activate sensory neurons *via* ST2 receptor involving both TRPA1 and TRPV1. These IL-33-induced signaling pathways evoked itch in an urushiol-induced allergic contact dermatitis model (Liu et al., 2016; Topal et al., 2020). In early phase of AD and contact hypersensitivity model of allergic contact dermatitis, *CXC chemokine receptor 3 (CXCR3)* was found to be upregulated in pruriceptive neurons as was its ligand CXCL10 in the surrounding tissue. In these models, antagonist of CXCR3 inhibited spontaneous disease-related itch (Qu et al., 2015, 3; Walsh et al., 2019). Pharmacological evidence suggests that CXCR3 may signal via a Ca^{2+}-regulated chloride channel (Qu et al., 2017).

Toll-like receptors (***TLRs***) belong to pattern recognition receptors that are activated by exogenous pathogen- or endogenous danger-associated molecular patterns (PAMPs or DAMPs, respectively). Expressed in various immune cells and peripheral tissues, they are key players in initiating innate immune responses. Among them, TLR3 and TLR7 are expressed in sensory neurons and have been suggested to play roles in the development of pruritus (Taves and Ji, 2015; Dong and Dong, 2018). TLR3 activation by its ligand polyinosinic-polycytidylic acid (poly I:C) evoked action potential firing in sensory neurons and induced acute scratching behavior. Moreover, TLR3 was found to be important in the development of both histaminergic and non-histaminergic itch as both were markedly decreased in *Tlr3* knock out animals (Liu T. et al., 2012). Like TLR3, TLR7 was also detected in peripheral sensory neurons of the DRGs and TLR7 activators evoked acute itching in a TLR7-dependent manner. Moreover, the TLR7 agonist imiquimod induced discharge of DRG neurons in wild type, but not in $Tlr7^{-/-}$ mice (Liu et al., 2010). Although both TLR3 and TLR7 are mostly known to be localized in intracellular membranes, it is proposed that they can be expressed in the surface membrane of the sensory neurons, and are thereby available for extracellular ligands (Taves and Ji, 2015). However, the role of TLR7 was questioned by another study indicating that imiquimod-induced scratching as well as neuronal responses are independent of TLR7, but may be due to the inhibition of background or voltage-gated potassium channels of the somatosensory neurons (Kim et al., 2011; Lee et al., 2012). Moreover, imiquimod was recently shown to directly activate ***TRPA1*** which, in sensory neurons, may initiate immediate acute itch (Esancy et al., 2018; Kemény et al., 2018).

Recently, the extracellular matrix protein periostin was shown to activate the receptor ***integrin $\alpha_V\beta3$*** on the surface of DRG neurons resulting in itch behavior in mice. The periostin induced, integrin $\alpha_V\beta3$-dependent itch was strongly reduced in mice lacking TRPA1 and TRPV1 ion channels, and NPPB suggesting that these ion channels and neurotransmitters of the pruriceptive neurons are involved in the periostin evoked itch. However, the signaling pathway connecting the integrin $\alpha_V\beta3$ to TRP channels is still under investigation (Mishra et al., 2020; Hashimoto et al., 2021a).

As mentioned above, the activation of ***Sphingosine 1-phosphate receptor 3*** (***S1PR3***) by S1P can also initiate itch activating TRPA1 via $G_{\beta\gamma}$ signal transduction. However, the same receptor can also activate TRPV1 *via* PLC dependent signaling but this pathway results in nociception and can only be activated by higher S1P concentration (Hill et al., 2018).

Somatosensory neurons also express ***Lysophosphatidic acid receptor 5*** (***LPA5***), a receptor for lysophosphatidic acid (LPA), that mediates LPA evoked itch (Kittaka et al., 2017; Yamanoi et al., 2019). In the LPA5 signaling pathway, LPA can be (re-) generated intracellularly mainly via phospholipase D (PLD), but PLA_2 and PLC can be also involved. Finally, intracellular LPA can directly activate TRPV1 and TRPA1 resulting in the excitation of the pruriceptive neurons (Nieto-Posadas et al., 2011; Kittaka et al., 2017).

Currently, ***cysteinyl leukotriene receptor 2*** (***$CysLT_2R$***), the receptor of the cysteinyl leukotriene C4 (LTC4), was described as a highly expressed receptor in sensory neurons. $CysLT_2R$ was detected especially in the subset of NP3 cluster DRG neurons, strongly coexpressed with *Il31ra* and *Nppb*. Its activation by LTC4 induced acute scratching behavior via $CysLT_2R$. Although it was not investigated whether $CysLT_2R$ activates DRG neurons or not, and the downstream signaling pathway is also largely unknown, LTC4-induced scratching was diminished in *Trpv1* knock out mice and in the presence of TRPA1 antagonist suggesting that both ion channels can mediate the effect (Voisin et al., 2021).

Urokinase plasminogen activator receptor (***U-PAR***) was also reported in a subset of DRG neurons and its agonist serpin E1 evoked Ca^{2+} transients in DRG neurons as well as itching in mice, but the mechanism of action and the related signaling pathway is largely unknown (Larkin et al., 2021).

Cutaneous Pruritic Crosstalk

Recent advances in the field have shown that itch does not necessarily start at the level of the nerves, but can also be initiated by non-neuronal elements in the skin. In this section we will list the possible contribution of cutaneous cells to the development of itch through mediator release (skin-nerve axis), as well as the role of factors released by nerves that act locally to propagate both the release of pruritogens and local inflammation (nerve-skin axis) (**Figure 1**).

Keratinocytes' Contribution to Itch

Keratinocytes were classically considered to be important in forming and maintaining the skin barrier. This view has been supplemented by numerous observations, including the fact that keratinocytes express sensory receptors, among others TRP channels (Denda et al., 2001; Inoue et al., 2002; Peier et al., 2002; Bodó et al., 2004; Chung et al., 2004) and that they can actively secrete various substances that communicate with neighboring cells and nerve endings, including ATP (Denda and Denda, 2007; Mandadi et al., 2009; Mihara et al., 2011),

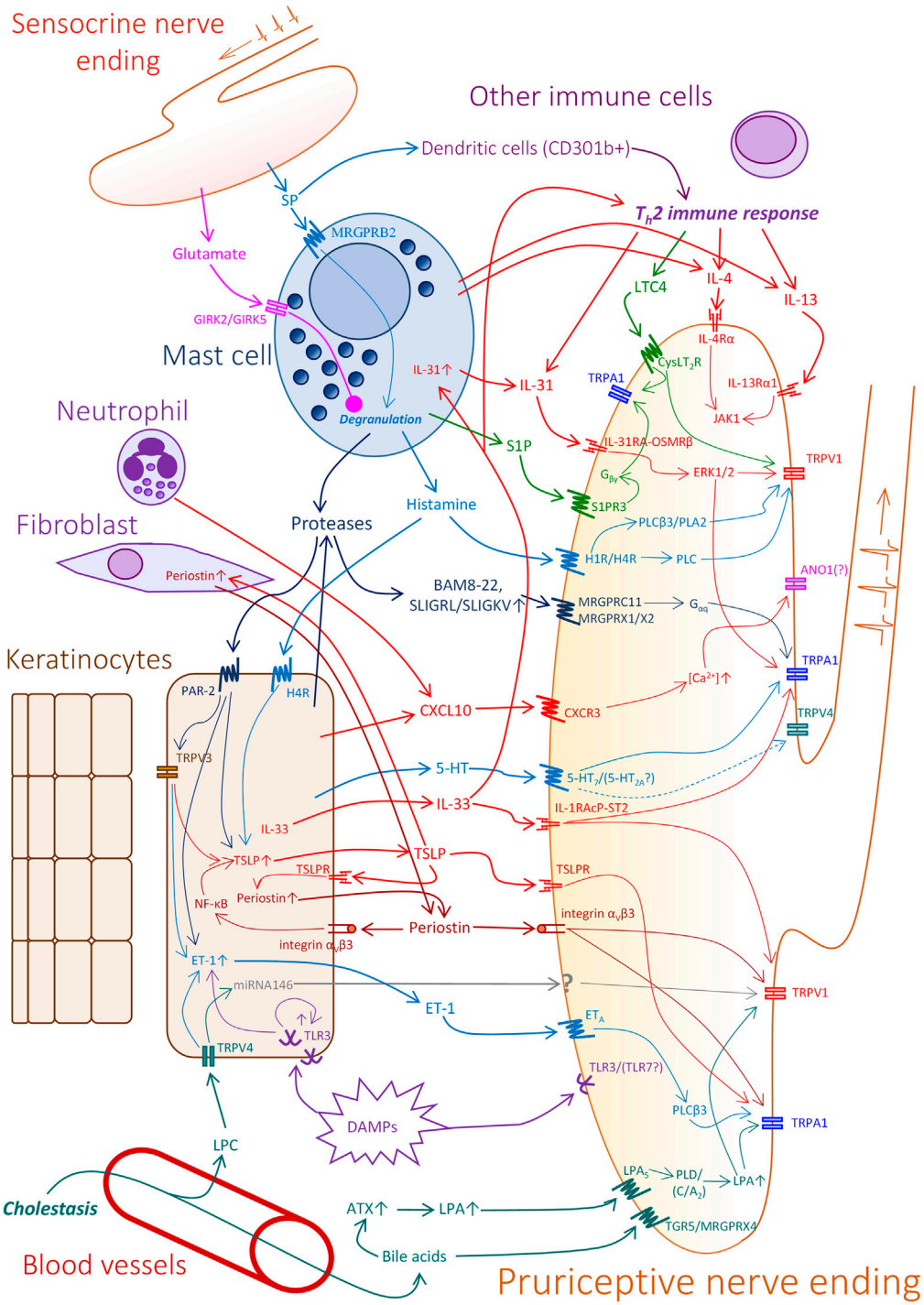

FIGURE 1 | Potential elements and mechanisms in pruritic cutaneous crosstalk. In the skin, products of keratinocytes, mast cells, several immune cells, and additional metabolic and tissue factors can contribute to the excitation of pruriceptive sensory nerve endings. Moreover, sensory terminals can also release pro- and anti-pruritic factors. Note, that the sensory nerve ending in the figure represents a hypothetic pruriceptor demonstrating the expression of several receptors and signaling

(*Continued*)

FIGURE 1 | pathways which may be expressed by different individual sensory neurons. For more detailed explanation, please see the text. Abbreviations: *5-HT*–Serotonin, *5-HT$_{2A/7}$*—Serotonin receptor$_{2A/7}$, *ANO1*—Anoctamine 1, *ATX*–Autotaxin, *CXCL10*—C-X-C motif chemokine ligand 10, *CXCR3*—C-X-C Motif Chemokine Receptor 3, *DAMPs*—Damage associated molecular patterns, *CysLT2R*—cysteinyl leukotriene receptor 2, *ERK1/2*—Extracellular signal-regulated kinase 1/2, *ET-1*—Endothelin 1, *ET$_A$*—Endothelin receptor A, *GIRK2/5*—glutamate ionotropic receptor kainate type subunit 2/5, *IL-13Rα1*—Interleukin 13 receptor, alpha 1, *IL-1RAcP-ST2*—IL-1 receptor accessory protein - ST2 heterodimer, *IL-31RA-OSMRβ*—IL-31 receptor A- Oncostatin M receptor β heterodimer, *IL-4Rα*—Interleukin 4 receptor, *JAK1*—Janus kinase 1, *LPA*—Lysophosphatidic acid, *LPA$_5$*—Lysophosphatidic acid receptor 5, *LPC*—lysophosphatidylcholine, *LTC4*—cysteinyl leukotriene C4, *MRGPRB2/C11/X1/X2/X4*—Mas-related G-protein-coupled receptor B2/C11/X1/X2/X4, *NF-κB*—nuclear factor kappa-light-chain-enhancer of activated B cells, *PLD/C/Cβ3/A$_2$*—phospholipase D/C/Cβ3/A$_2$, *S1P* - Sphingosine 1-phosphate, *S1P3R*—Sphingosine 1-phosphate receptor 3, *SP*—Substance P, *TGR5*—G-protein-coupled bile acid receptor 1 (Takeda G protein-coupled receptor 5), *TLR3/7*—Toll-like receptor 3/7, *TRPA1/V1/V3/V4*—Transient receptor potential Ankyrin 1/Vanilloid 1/Vanilloid 3/Vanilloid 4, *TSLP*—Thymic stromal lymphopoietin, *TSLPR*—Thymic stromal lymphopoietin receptor.

dopamine (Fuziwara et al., 2005) and glutamate (Fuziwara et al., 2003). Based on these results keratinocytes can be considered as the forefront of the sensory nervous system (Denda et al., 2007).

In terms of itch sensation, the triggers that can elicit the release of pruritogens from keratinocytes are still not fully known. Keratinocytes express multiple receptors that have been implicated in itch induction, including PAR2 (Buhl et al., 2020), TLR3 (Szöllősi et al., 2019), H1 and H4 receptors (Gschwandtner et al., 2008; Schaper et al., 2016), ET_A and endothelin receptor B (ET_B) (Tsuboi et al., 1995), 5-HT receptors (Lundeberg et al., 2002; Slominski et al., 2003), OSMRβ (Boniface et al., 2007; Kato et al., 2014), integrin $\alpha_V\beta3$ (Masuoka et al., 2012), TSLPR (Mishra et al., 2020), as well as neuropeptide receptors (Sandoval-Talamantes et al., 2020), and two members of the transient receptor potential vanilloid (TRPV) family, TRPV3 and 4 (Peier et al., 2002; Sokabe et al., 2010; Mihara et al., 2011; Tóth et al., 2014; Szöllősi et al., 2018). While we have evidence that the receptors listed above are all functionally expressed by keratinocytes, their role in the development and propagation of itch is less well-defined. In general we can classify them into two large groups: receptors that influence the barrier forming function of keratinocytes, and those that cause the cells to secrete factors that can activate pruritic nerve endings. The former may be considered as an indirect mechanism of itch induction, since impaired barrier function leads to increased transepidermal water loss, dry skin, and an increased likelihood of exogenous pruritogens penetrating the stratum corneum (Yosipovitch et al., 2019). The latter can be considered a direct mechanism of itch signaling, where the activated keratinocytes secrete signaling molecules (IL-33, TSLP and ET-1) known to activate pruritic nerve fibers.

The indirect path of itch induction as mentioned above is dependent on the disruption of the epidermal barrier. This is usually accompanied by the production of pro-inflammatory cytokines (e.g. IL-6) and chemokines (e.g. CXCL-8, CCL17/TARC, CCL19/MIP-3β, CCL22/MDC, CCL23/MIP-3, CCL4/MIP-1β and CXCL1/GRO1α) (Cornelissen et al., 2012; Kabashima, 2013; Lee et al., 2013), as well as nerve growth factor (NGF) by keratinocytes. The combined effect of these factors is recruitment of further inflammatory cells to the skin, and in the case of chronic pruritus, increased density of nerve fibers and response in the affected area (Buhl et al., 2020). The disruption of the epidermal barrier can occur through increased keratinocyte proliferation (as caused by agonists of H4R (Glatzer et al., 2013), TLR3 (Szöllősi et al., 2019), periostin (Masuoka et al., 2012), and neuropeptides (Sandoval-Talamantes et al., 2020)), through disruption of the differentiation process, by the production of matrix metallopeptidase 9 (MMP9), which can drive recruitment of immune cells to the skin [as caused by agonists to H1 (Gschwandtner et al., 2013; Chen J. et al., 2021)], and the increased production of antimicrobial peptides, a common characteristic of inflammatory skin diseases [as seen after OSMRβ activation (Boniface et al., 2007)]. TRPV3, a non-selective calcium-permeable channel first identified in keratinocytes (Peier et al., 2002), was linked to pruritus based on the consequence of gain-of-function mutations in the channel. These lead to the hairless and pruritic dermatitis phenotype of DS-*Nh* mice (Yoshioka et al., 2009) and to the development of Olmsted syndrome in humans, which is characterized by palmoplantar keratoderma and periorificial plaques, as well as hair and nail malformities, pain and itch (Lin et al., 2012). Conversely, the activation of TRPV4 accelerates barrier recovery, and the formation of intercellular junctions between keratinocytes since this channel is co-localized to adherent junction proteins such as E-cadherin and β-catenin. The role of TRPV4 in the development of itch is more nuanced however, since it has also been linked to regulation serotonin and histamine release as well as a consequent development of itch (Chen et al., 2016; Luo et al., 2018; Boudaka et al., 2020).

Of the above listed mediators, their involvement in direct keratinocyte-nerve communication has been proven for H4R (Schaper et al., 2016), PAR2 (Kempkes et al., 2014; Buhl et al., 2020) TLR3 (Szöllősi et al., 2019) and both TRPV3 (Seo et al., 2020) and TRPV4 (Moore et al., 2013). To date the major pruritic mediators that can directly activate pruritic nerve endings released by keratinocytes are TSLP, periostin, ET-1, IL-33 and most recently BNP. On keratinocytes histamine dominantly acts through the H4 receptor and increases the release of TSLP subsequently to poly I:C stimulation in both murine and human cells (Schaper et al., 2016). TSLP secretion has also been observed after activation of all the above mentioned receptors with the exception of TRPV4, which solidifies its role as one of the most important skin-derived pruritic mediators (Kinoshita et al., 2009; Wilson et al., 2013; Park et al., 2017). Furthermore, TSLP (and other T_h2 cytokines) can induce periostin secretion and periostin can stimulate further TSLP release potentially establishing another pruritic positive feedback (Masuoka et al., 2012; Mishra et al., 2020; Hashimoto et al., 2021a). One of the most potent keratinocyte-derived pruritic mediators is ET-1 (Kido-Nakahara et al., 2014), the production of which can be initiated by PAR2 (Buhl et al., 2020), TLR3 (Szöllősi

et al., 2019), TRPV3 (Zhao et al., 2020), and TRPV4 (Chen et al., 2016) activation. IL-33 is a member of the IL-1 inflammatory cytokine family, and is constitutively expressed in the nucleus of keratinocytes, and acts as an alarmin that is released upon inflammation or cellular damage (Moussion et al., 2008). While first shown to act on cells of the innate and adaptive arm of the immune system [specifically mast cells, type 2 innate lymphoid cells, basophils and type 2 T helper cells (Kondo et al., 2008)], the receptor of IL-33, ST2 is also expressed on sensory nerve endings in the skin and its activation leads to an itch response in mice, as discussed above (Liu et al., 2016). Moreover, IL-33 is upregulated in atopic dermatitis (AD) lesions which may contribute to its pruritic phenotype (Imai, 2019).

As seen above the contribution of keratinocytes to itch sensation is multifaceted, and this is further complicated by the interplay between these receptors in the keratinocytes themselves. PAR2 has been shown to signal through TRPV3 (Zhao et al., 2020), the expression of TLR3 is increased upon TLR3 activation (forming a positive feedback loop that could be a major factor in the chronification of itch (Szöllősi et al., 2019)), and the effect of histamine is also potentiated through TLR3 (Schaper et al., 2016). This is also compounded by the crosstalk between keratinocytes and immune cells, as detailed below.

Immune Cells

Mast cells have long been considered to be a central player in the pathogenesis of itch, mainly through their release of histamine. Histamine is the main mediator responsible for acute itch, by activating the H1 and H4 receptors on sensory nerves (Shim and Oh, 2008). Mast cells also release a wide array of other signaling molecules including cytokines and chemokines, and have recently been shown to contribute to non-histaminergic itch as well (Meixiong et al., 2019a) through these mediators. The direct role of mast cells in itch transduction is further supported by their close proximity to afferent nerves in the skin (Bienenstock et al., 1991). The most important cytokines known to directly activate pruritogenic nerves are IL-4, IL-13 and IL-31, all of which are associated with T_h2 cells and which can be released from mast cells, among others. Other sources of these cytokines include natural killer cells, basophils and eosinophils, although the contribution of these latter cell populations to itch is not well defined.

The role of T_h2 cells in pruritic skin diseases, especially in AD, is well documented (Gandhi et al., 2017), and forms the basis for some of the most effective treatments of itch in AD (Ruzicka et al., 2017; Gooderham et al., 2018; Bawany et al., 2020). Dupilumab inhibits the effect of IL-4 and IL-13 by blocking the IL-4α subunit which is shared by both cytokines, while Nemolizumab targets IL-31RA to block the effect of IL-31 (Ruzicka et al., 2017). IL-4 and IL-13 act both as amplifiers of T_h2 responses that contribute to the upkeep of the environment that promotes pruritic signaling (Furue et al., 2019), and as direct activators of pruritic nerve endings (Campion et al., 2019). IL-31 acts on both keratinocytes and sensory nerves (Sonkoly et al., 2006), although its direct link to itch is only proven in mice, since in humans it does not induce immediate, only delayed itch responses (Hawro et al., 2014). Nevertheless, Nemolizumab has been proven to be efficacious in the treatment of AD (Ruzicka et al., 2017), which hints that in humans IL-31 acts indirectly to induce itch.

An indirect contribution of the abovementioned cytokines to the development of chronic itch is their contribution to barrier dysfunction, by the downregulation of skin barrier proteins in keratinocytes (Kim et al., 2008). Since this may lead to the release of TSLP that strengthens T_h2 cell functions (Kitajima et al., 2011), we can once again see a possible positive feedback loop that may lead to the chronification of itch. Keratinocytes may also produce IL-33, which also leads to T_h2 polarization in AD (Imai, 2019), and results in IL-31 secretion from mast cells (Petra et al., 2018). Recently, next to its direct pruritogenic effect, the role of the extracellular matrix protein periostin emerged as a regulator of barrier functions, and an amplifier of T_h2 responses, as well (Hashimoto et al., 2021a).

Neurogenic Pruritus – Role of Sensory Neurons in the Establishment of a Pruritus-Prone Local Milieu

The crucial role of the cutaneous immune cells and keratinocytes in the establishment of a local pruritic environment via the secretion of mediators that signal toward the itch-detecting sensory fibers in various skin conditions is unquestionable. However, emerging evidence supports the concept that this is not a one-way interaction, but rather a local pruritic intercellular network between the sensory neurons and the peripheral cells, in which the neurons can also actively take part by influencing the function of the neighboring cells, and thereby contributing to the development of an inflamed, pro-pruritic local tissue micromilieu. The "classical" concept of neurogenic inflammation has been known since the '60s, when Miklós Jancsó and his colleagues showed that the excitation of capsaicin-sensitive nerve endings causes local inflammation (Jancsó et al., 1967, 1968). Later research described the "sensocrine" function of the sensory neurons by which they release neuropeptides such as substance P (SP) and calcitonin gene related peptide (CGRP), as well as glutamate, ATP, chemokine (C–C motif) ligand 2 (CCL2), colony stimulating factor 1 (CSF-1) and other mediators, including even micro-RNAs at the peripheral nerve endings. These sensory neuron-derived mediators can influence the local barrier and immune functions as well as inflammatory responses (Shouman and Benarroch, 2021). As time passes, more and more specific "neuron-to-periphery" interactions are identified, and some of them are likely to have an impact on the development of pruritus.

Neuropeptides released from the sensory nerve endings, especially from C-fibers, can target keratinocytes, dermal endothelial cells, mast cells, Langerhans cells, and lymphocytes as well. For example, SP can increase histamine and TNFα release from mast cells, IL-1, IL-6 and IL-8 production in keratinocytes, or IL-8 production in dermal microvascular endothelial cells, all contributing to local inflammation (Ansel et al., 1997; Choi and Di Nardo, 2018; Shouman and Benarroch, 2021). In contrast to the inflammatory role of SP, the effect of CGRP is more ambiguous. It can activate mast cells, evoke vasodilation (Ansel et al., 1997; Choi and Di Nardo, 2018; Shouman and Benarroch, 2021), and shift Langerhans cells-initiated immune responses toward T_h2 direction (Ding et al., 2008), but it was also

found to inhibit 5-HT- or histamine-induced inflammatory responses (Granstein et al., 2015), as well as the T_h2 cytokine production in type 2 innate lymphoid cells (Wallrapp et al., 2019). Somatostatin is also released from the peripheral sensory endings, but it evokes rather anti-inflammatory responses (Szolcsányi et al., 1998; Helyes et al., 2004, 2009).

As described above, T_h2 cell mediated immune responses play a crucial role in the development and maintenance of a pruritic tissue environment. It was shown in a mouse AD model that substance P-dependent neurogenic inflammation mediated the stress-evoked shift in the cutaneous cytokine profile toward T_h2 cytokines (Pavlovic et al., 2008). Moreover, sensory neuron-derived SP can regulate allergic responses as well. It was recently described that allergen house dust mite proteases activate TRPV1 expressing sensory neurons resulting in SP release, and SP then induces mast cell degranulation *via* MRGPRB2 (Serhan et al., 2019). Another recent study also demonstrated that intradermal injection of protease allergens initiated not only immediate itch and pain behavior, but stimulated SP (and inhibited CGRP) release from TRPV1 expressing sensory fibers. The released SP activated the CD301b + dendritic cells and induced their migration to draining lymph nodes, where these cells were responsible for T_h2-differentiation. It was found that ablation or pharmacological blockade of allergen responder TRPV1+ sensory neurons decreased allergen-induced T_h2 cell differentiation and related IL-4 and IL-13 expression (Perner et al., 2020). Moreover, CGRP released from cutaneous sensory nerve endings was also described to stimulate CD301b+ dendritic cells to produce IL-23 in murine skin, which resulted in increased IL-17A production of γδT cells (Kashem et al., 2015).

Importantly, cutaneous sensory neurons can not only initiate but also suppress this inflammatory, pruritic environment. In contrast to neuropeptides, some non-peptidergic fibers expressing MRGPRD can negatively regulate mast cells *via* glutamate release, which likely acts via an ionotropic glutamate receptor heterodimer composed of glutamate ionotropic receptor kainate type subunit 2 (GIRK2/GLUR6) and GIRK5 expressed by mast cells (Zhang et al., 2021).

PRURITIC DISEASES

Pruritus is a common symptom of several dermatological and systemic diseases with the involvement of the above discussed cutaneous immuno-neuronal crosstalk. In the next part of our review, we provide a concise summary of some of these diseases and the potential mechanisms which can lead to the development of the pruritic symptoms (**Table 2**).

Dermatological Diseases

Contact Dermatitis

There are two forms of contact dermatitis to distinguish: irritant and allergic contact dermatitis (ICD and ACD, respectively). In case of ICD, the primary cause is a (chronic) exposure to irritants that causes epidermal barrier perturbation. Epidermal keratinocytes are the primary targets of the irritants. Upon exposure, they subsequently synthesize and release pro-inflammatory cytokines that are not biased toward T_h2-mediated immune responses. Indeed, the infiltrating T cells rather belong to the T_h1 class and especially IL-2, IFNγ, IL-1α, IL-1β, IL-6, CXCL-8, TNFα, GMCSF, and VEGF are upregulated in the skin (Lisby and Baadsgaard, 2006; Lee et al., 2013). Importantly, different irritants can differentially affect cytokine levels, and can evoke various biological responses in keratinocytes ranging from hyperproliferation to necrotic cell death. Itch is a common symptom in ICD, but pain-like sensations (e.g., stinging or burning) are also often observed (Lisby and Baadsgaard, 2006; Bains et al., 2019). In contrast, ACD is a delayed, type 4 hypersensitivity reaction, i.e., an antigen-specific T-cell mediated inflammatory response to repeated exposure. It is composed of two distinct immunological phases, i.e., the sensitization and the elicitation or effector phase. In the sensitization phase, the haptens penetrate the epidermal barrier, and establish direct contacts with various skin components including MHC molecules expressed by epidermal Langerhans cells resulting in the activation of said cells. Activated, allergen-presenting Langerhans cells travel to the draining lymph nodes to be recognized by specific T cells. This process is associated with a cascade of cytokine production that stimulates the proliferation of the specific allergen-recognizing T cells which finally enter the circulation in high numbers. Upon a repeated allergen contact, the effector phase is initiated. The activated antigen presenting cells recruit the circulating primed T cells that will locally be activated by the allergens and will subsequently release large amounts of inflammatory cytokines thereby contributing to the local inflammation. This reaction typically peaks in 12–48 h after the allergen exposure. This process involves both type 1 and type 2 cytokines, which, beyond the inflammatory responses, can initiate ACD-associated sensory phenomena, like itch (Rustemeyer et al., 2006; Leonard and Guttman-Yassky, 2019).

A recent study compared itch and pain behavior, and scored the accompanying inflammation in mouse hypersensitivity models of ICD and ACD. The authors applied the same topical challenge for both conditions, using the hapten squaric acid dibutylester (SADBE; challenge with 1% solution on three consecutive days). The two experimental protocols only differed in the sensitization phase, when SADBE was applied to the abdominal skin of the animals belonging to the ACD group, whereas ICD mice as well as members of the control group received acetone. Finally, both group was challenged with 1% SADBE on the tested skin area (cheek or calf). It was found, that both ICD and ACD are characterized by itch- and pain-related behavior, inflammatory symptoms and pro-inflammatory cytokine production, but in general, both the sensory symptoms as well as the inflammatory features are stronger in ACD than in ICD. However, C-X-C motif chemokine ligand 10 (CXCL10) was elevated only in ACD (Zhang et al., 2019). Moreover, in SADBE-induced murine ACD, chemokine receptor CXCR3, which serves as the receptor of CXCL10, was upregulated in the DRG and its pharmacological inhibition attenuated spontaneous itch, but not pain. Injected CXCL10, on the other hand, evoked itch-, but not pain-related behavior in ACD mice (Qu et al., 2015).

Importantly, the exact pathomechanism, the cytokine production, and T-cell polarization in contact dermatitis largely depend on the allergen both in humans and in mice (Dhingra et al., 2014; Leonard and Guttman-Yassky, 2019). For example, nickel induces T_h1-biased responses with certain T_h17 and T_h22 elements, whereas house dust mite elicits T_h2-polarized responses with additional T_h9 and T_h17/T_h22 activation, and fragrance allergens cause T_h2/T_h22 skewed immune responses (Dhingra et al., 2014; Malik et al., 2017; Leonard and Guttman-Yassky, 2019). Allergen-specific reactions were also identified in skin biopsies after food patch tests applied in delayed-type hypersensitivity food reaction. For example, besides T_h17 polarization, peanut, but not beef or codfish, was also characterized by increased IL-33 expression (Ungar et al., 2017; Leonard and Guttman-Yassky, 2019). In mouse pruritic ACD models, the generally used oxazolone induced a mixed T_h1/T_h2 response with elevated level of 5-HT, ET-1, and substance P, but not TSLP. In contrast, the poison ivy-driven allergen urushiol resulted in T_h2-biased responses associated with increased IL-33, TSLP, 5-HT, and ET-1 expression without affecting substance P (Liu et al., 2016, 2019). These mediators are capable of activating their own receptors in the itch-sensitive sensory neurons that transduce the pruritic signals likely via TRPA1 in oxazolone- and urushiol-induced ACD (Liu et al., 2013).

Urticaria

Chronic urticaria (CU) is characterized by the occurrence of weals (hives), angioedema, or both for more than 6 weeks, and is usually accompanied by severe pruritus (Gonçalo et al., 2021). It is estimated to affect ~1% of the population, and it may significantly impair quality of life (Gonçalo et al., 2021). Although the signaling pathways involved in the development of itch in CU are not completely explored, pathological degranulation of dermal mast cells as well as dysregulation of basophil and eosinophil granulocytes and the subsequent histamine release appear to be central players in the process (Hon et al., 2021).

Indeed, the classical symptoms of urticaria are well-modelled by intradermal histamine injection. Besides pruritus, locally applied histamine also causes increased vascular permeability and development of edema (weal), as well as local vasodilation resulting in dermal hyperaemia (erythema), which latest is a consequence of neuropeptide release (SP and CGRP) from the activated mechano-insensitive, peptidergic C fibers. These symptoms are specifically related to histamine and are not associated to non-histaminergic itch (Andersen et al., 2015). Although urticaria is mainly characterized by a histaminergic nature, clinical data indicate that both histaminergic and non-histaminergic components may be involved in the development of pruritus in CU. Indeed, second generation antihistamines are recommended to be the first choice to alleviate itch (Hon et al., 2019), and, if they remain ineffective in spite of the elevation of their dose, administration of IgE-neutralizing antibodies (e.g., Omalizumab or the more effective Ligelizumab) (Wedi, 2020), corticosteroids, leukotriene receptor antagonists (e.g., montelukast), Cyclosporine A, or even certain antidepressants and anti-inflammatory drugs should be considered (Hon et al., 2019).

Importantly, recent research suggests that other mast cell and basophil granulocyte-related targets may also become useful tools in the treatment of CU. These include spleen tyrosine kinase (SYK; a down-stream target of the high-affinity IgE receptor FcεR1α), Bruton tyrosine kinase (BTK; an important regulator of IgE-independent mast cell activation), CRTh2 (a receptor for PGD2 expressed among others on mast cells), as well as H4 histamine and MRGPRX2 receptors (Hon et al., 2021). Last, but not least, besides the aforementioned biological drugs targeting mostly mast cells and basophils, eosinophil-targeting [e.g., ones neutralizing IL-5 [mepolizumab and reslizumab] or IL-5 receptor (benralizumab)], and other antibodies (interfering with the signaling of IL-1, IL-4, and TNF-α) also showed promising effects in clinical trials [for details, see (Hon et al., 2021)].

Atopic Dermatitis

AD is a chronic, inflammatory skin disease affecting ca. 20% of children and ca. 10% of adults in the industrial countries (Langan et al., 2020). Based on the symptoms and certain aspects of the pathogenesis, it can be classified into two major subtypes, i.e., "extrinsic" and "intrinsic" AD (Czarnowicki et al., 2019). The extrinsic endotype is more common. It usually develops on an atopic background, and it is characterized by eosinophilia, high serum IgE level, and greater filaggrin mutation rate as compared to the intrinsic endotype that exhibits female predominance, delayed onset, as well as lack of atopic background, and is characterized by a relatively more preserved barrier function, normal serum IgE level, and an increased prevalence of metal contact hypersensitivity (Czarnowicki et al., 2019). Importantly, the existence of intra-endotype variations in the immune polarization and epidermal barrier function is also well-described across different races (Czarnowicki et al., 2019). However, despite of the aforementioned complexity, it is well-evidenced that disturbance of each element of the complex cutaneous barrier (i.e., physicochemical, immunological and microbiological) (Proksch et al., 2008; Jensen and Proksch, 2009) is a key contributor in the development of AD (Bieber, 2008; Griffiths et al., 2017). Although clinical symptoms of the disease may exhibit a great inter-individual heterogeneity (Langan et al., 2020), development of eczematous lesions, intense pruritus, and a chronic or relapsing disease course are characteristic features of AD.

Of great importance, itch is not only one of the most unpleasant symptoms of AD, but, *via* the "itch-scratch cycle", it also contributes to the pathogenesis of the disease by damaging the epidermal barrier, and facilitating the permeation of allergens and irritants (Mack and Kim, 2018; Furue et al., 2020; Langan et al., 2020; Nakahara et al., 2021). Thus, alleviating itch could be much more than a mere symptomatic treatment in AD. Research efforts of the last decades have highlighted the role of several itch mediators and pathways in AD-related pruritus (Langan et al., 2020; Umehara et al., 2021). Indeed, periostin (Mishra et al., 2020) and type 2 cytokines (e.g., IL-4, IL-13, IL-31, and TSLP) (Yang and Kim, 2019) and most especially, the IL-4—neuronal IL-4 receptor interaction, together with the subsequent JAK-1

signaling appear to be key players in the process (Cevikbas et al., 2014; Oetjen et al., 2017), whereas histamine and its key pruritic receptors are likely to be of inferior significance (Umehara et al., 2021). Indeed, "classical" anti-histamines targeting H1R failed to be effective as "add-on" therapy in eczema (Matterne et al., 2019), although recently, promising results were published with H4R antagonists (Werfel et al., 2019) and combination of H1R and H4R antagonists (Köchling et al., 2017). On the other hand, dupilumab (a human monoclonal antibody blocking the effects of IL-4 and IL-13 and thereby interfering with the activation of T_h2 cells and group 2 innate lymphoid cells (Beck et al., 2014; Imai et al., 2021)) monotherapy was greatly efficient in reducing Eczema Area and Severity Index (EASI) and pruritus scores in a double-blind placebo-controlled trial involving patients with moderate-to-severe AD (Beck et al., 2014). Likewise, nemolizumab (CIM331), a humanized antibody against interleukin-31 receptor A could also significantly improve pruritus in patients with moderate-to-severe AD in a phase 2, randomized, double-blind, placebo-controlled study (Ruzicka et al., 2017).

Recent pieces of evidence argue that dysregulation of other signaling pathways (e.g., cutaneous cannabinoid (Tóth et al., 2019), and opioidergic signaling (Slominski, 2015; Bigliardi et al., 2016)) may also contribute to AD-related pruritus. Indeed, CB_1 and CB_2 cannabinoid receptors, as well as κ-opioid receptor (KOR) were found to be significantly downregulated in the lesional skin of AD patients suffering from severe itch as compared to the non-itchy, non-lesional skin of the patients (RNAseq) (Nattkemper et al., 2018). In line with these data, KOR, as well as dynorphin A 1-17 and dynorphin A 1-8 were found to be down-regulated in the lesional epidermis of AD patients (Tominaga et al., 2007), and topically applied nalfurafine (a selective KOR agonist) alleviated itch in AD (Inui, 2015; Elliott et al., 2016). Moreover, the serum concentration of β-endorphin (an endogenous opioid exhibiting higher affinity towards the "pro-pruritic" μ-opioid receptor) was found to be elevated in AD, and its level correlated with the severity of itch (Lee et al., 2006). Taken together, these pieces of evidence suggest that dysregulation of homeostatic cutaneous cannabinoid and opioid signaling may contribute to the development of pruritus in AD.

Importantly, several other peptide and lipid signaling pathways were also suggested to be involved in the development of AD-related itch. Indeed, both the number of mast cell–sensory nerve contacts, as well as the number of SP and CGRP positive nerve fibers were elevated in the lesional epidermis of AD patients as compared to healthy controls (Järvikallio et al., 2003). Moreover, the NKR1 antagonist aprepitant was found to exert significant anti-pruritic effects in AD suggesting that the SP–NKR1 pathway is also important in AD-related itch (Ständer et al., 2010). Moreover, 12/15-LOX and COX pathways were also found to be dysregulated in the lesional skin of AD patients leading to the elevation of the levels of several potentially pruritogenic lipid mediators, including 12-hydroxy-eicosatetraenoic acid (12-HETE), leukotriene B4 (LTB4), thromboxane B2 (TXB2), prostaglandin (PG) E2, and PGF2 (Töröcsik et al., 2019).

Last, but not least, it should also be noted that TRPV3 is a potent promoter of the production and release of various pro-inflammatory regulators on multiple cell types of the human skin, including keratinocytes and sebocytes (Szöllősi et al., 2018; Szántó et al., 2019), and is likely to play a role in dry skin dermatoses (Szántó et al., 2019), including AD as well as AD-related pruritus. Indeed, PAR2 and TRPV3 were shown to be up-regulated in skin biopsies of AD patients (Zhao et al., 2020). Activation of PAR2 on epidermal keratinocytes was shown to influence Ca^{2+}-homeostasis of the cells *via* STIM1-Orai1 interaction, resulting in TSLP release leading to itch (Wilson et al., 2013). More recently, it has also been demonstrated that the ability of keratinocyte PAR2 activation to evoke TSLP release and subsequent itch can be abrogated by the genetic deletion of TRPV3, arguing that the two receptors may cooperate in mediating itch in AD (Zhao et al., 2020). Finally, according to a recent study, the IL-31-induced BNP-release from the sensory neurons increases TRPV3 expression and activity on epidermal keratinocytes in a natriuretic peptide receptor 1 (NPR1)-dependent manner. Enhanced activity of TRPV3 in turn led to elevated SERPIN E1 [a.k.a. plasminogen activator inhibitor 1; an adipokine expressed in keratinocytes as well (Kovács et al., 2020)] release that evoked itch (Larkin et al., 2021). Thus, abrogation of TRPV3 activity promises to be a powerful tool to alleviate itch in AD.

Psoriasis Vulgaris

Psoriasis is a common inflammatory skin disease affecting 1–3% of the world population (Szepietowski and Reich, 2016) characterized by sharply demarcated, erythematous, pruritic plaques covered in grey scales that can cover large areas on the extensor surfaces of the limbs, the trunk, and the scalp (Rendon and Schäkel, 2019). Even though the name derives from the Greek word for itch (psora), pruritus has long been an overlooked aspect of the disease, even though 60–90% of psoriatic patients report itch as one of their symptoms. Indeed, many report pruritus as the most bothersome of their symptoms (Komiya et al., 2020). The treatment of pruritus in psoriatic disease poses an unmet need, since antihistamines are generally considered to have only moderate effects, and the exact cause of itch remains unknown in psoriatic lesions (Domagała et al., 2017).

Psoriasis can easily be considered an immuno-epithelial disease, since the main driving factor of plaque development is the production of IL-17 and IL-22 by T_h17 cells, which is initiated by TNFα and IL-23 from dendritic cells (Zheng et al., 2007). These cytokines have not been linked directly to pruritus, and it is likely that itch develops as a secondary consequence of the disease, instead of being a primary symptom that leads to the development of the psoriatic plaques. Nevertheless monoclonal antibody treatment targeting IL-17 has been reported to improve itch in psoriasis (Bushmakin et al., 2015; Strober et al., 2016; Kimball et al., 2018).

The role of multiple pruritic mediators have been investigated in psoriasis, including neuropeptides, nerve growth factor, IL-31, and TSLP (Komiya et al., 2020). Neuropeptides, specifically SP and Neuropeptide Y (NPY), have been implicated in the pruritus found in psoriasis. The levels of SP (Saraceno et al., 2006), as well

as the number of SP + fibers in pruritic psoriatic lesions (Nakamura et al., 2003) is increased, and serlopitant, an antagonist of the neurokinin-1 receptor, was effective against chronic itch (Yosipovitch et al., 2018). Interestingly, the effect of SP on murine dorsal root ganglia was found to be more dependent on MrgprA1 (Azimi et al., 2017), so it is possible that in humans SP also acts on MRGPRX2, which is also highly expressed in psoriatic lesions (Nattkemper et al., 2018). NPY, on the other hand is found at lower levels in psoriatic patients with pruritus (Reich et al., 2007), which is possibly explained by the finding that it suppresses mechanical itch transmission in wild-type mice (Acton et al., 2019). NGF expression was also found to be higher in psoriatic lesions, as well as the expression of the NGF receptor tropomyosin-receptor A, both of which correlated with the intensity of pruritus (Nakamura et al., 2003).

Multiple lines of evidence support the role of two classically AD-linked cytokines, TSLP and IL-31 in psoriasis. The serum level of both TSLP and IL-31 is elevated in patients with pruritic psoriasis (Narbutt et al., 2013; Suwarsa et al., 2019), as well the number of IL-31-immunoreactive mast cells at lesional sites (Niyonsaba et al., 2010), while TSLP expression is increased in the epidermis of psoriatic lesions (Volpe et al., 2014). TSLP has also been linked more directly to scalp psoriasis (Volpe et al., 2014).

The sphingolipid metabolite S1P is also associated to psoriasis. S1P, similar to IL-23, primes the maturation of T_h17 cells via S1PR1 (Huang et al., 2007; Liao et al., 2007). Indeed, in psoriasis, elevated plasma S1P level was reported (Checa et al., 2015; Myśliwiec et al., 2017), which may stimulate pruriceptive fibers via S1PR3 (Hill et al., 2018), as discussed above.

The involvement of the nervous system in the pathogenesis of the disease has been suspected for some time. Multiple reports (Raychaudhuri and Farber, 1993; Zhu et al., 2016; Onderdijk et al., 2017; Keçici et al., 2018; Qin et al., 2021) showed that denervation of the skin on one side of the body can lead to the clearance of the lesions, and that stress can exacerbate the disease (Harvima et al., 1993; Singh et al., 1999). The mechanisms behind these observations were considered to be both increased local production of neuropeptides (Hosoi et al., 1993), and changes in the density of innervation in psoriatic lesions. Interestingly, both increased (Naukkarinen et al., 1991) and decreased innervation have been reported (Pergolizzi et al., 1998), as well as some reports that found no significant differences (Di Francesco et al., 1978; Armagni et al., 1979). Since, as mentioned above epidermal keratinocytes in psoriasis produce increased levels of NGF (Pincelli, 2000), it is logical to assume that this would influence the growth of nerves (Kou et al., 2012). Applying a selective optogenetic stimulation of TRPV1+ cutaneous nerve endings in mice resulted in the development of type 17 inflammatory response associated with histological features that highly resembled the imiquimod-induced psoriasiform lesions. The ablation of TRPV1+ sensory fibers attenuated these responses clearly indicating that psoriasiform symptoms can develop on neurogenic inflammatory background (Cohen et al., 2019).

Prurigo Nodularis

Prurigo nodularis is a chronic inflammatory skin disease characterized by multiple extremely pruritic lesions commonly found on the trunk and the extensor surfaces of the extremities (Mullins et al., 2021). Prurigo nodularis commonly occurs with other diseases, including AD, xerosis cutis, excoriation disorder, hypertension, type II diabetes mellitus, chronic kidney disease, HIV infection, substance-use disorders, mood disorders, and obesity (Mullins et al., 2021; Pereira et al., 2021). The exact pathophysiology of the disease is still unknown, but a strong neural component is likely based on increased number of protein gene product 9.5 immunoreactive nerve fibers and increased expression of SP and CGRP in the lesions (Abadía Molina et al., 1992; Lee and Shumack, 2005). Both neuropeptides stimulate local immune responses and promote endothelial cell proliferation through the release of vascular endothelial growth factor, and further increase in the number of nerve fibers through NGF production (Choi and Di Nardo, 2018). In terms of the immune system, lesional skin in PN contains a dense infiltrate of eosinophils, mast cells and T cells. These cells contribute multiple cytokines to the inflammatory milieu of the lesions, including IL-4 and VIP from eosinophils (who can also contribute NGF and SP) (Johansson et al., 2000), IL-31 from T lymphocytes and macrophages (Hashimoto et al., 2021b) and histamine and prostaglandins from mast cells (Zeidler et al., 2018).

Cutaneous T-Cell Lymphoma

Cutaneous T-cell lymphoma is typically divided into two common subtypes: mycosis fungoides (MF) and its leukemic variant, Sézary syndrome (SS). Pruritus affects a large population (approximately 88%) of both subtypes, and the severity of itch increases in late-stage disease, as well as being higher in general in SS (Vij and Duvic, 2012; Nattkemper et al., 2016). Pruritus in these patients responds poorly to treatment, which is unsurprising considering the fact the exact mechanism behind it is still unknown. Various mediators have implicated, although mostly based on empirical experience in a limited number of patients.

IL-31 levels are higher in sera of patients with MF and SS (Ohmatsu et al., 2012; Malek et al., 2015), although other results show contradictory results (Möbs et al., 2015). It is also unclear whether the IL-31 serum levels correlate with disease or pruritus severity (Malek et al., 2015). IL-31 expression locally in the skin is also increased, as well as the level of IL-31RA and OSMRβ (Nattkemper et al., 2016).

IL-4 and IL-13 may also play important roles in itch in these patients, since dupilimab significantly reduced itch in a patient with SS (Steck et al., 2020). SP may also be involved in itch in both SS and MF, since multiple reports show that the NK_1 receptor antagonist aprepritant showed some efficacy in alleviating pruritus (Duval and Dubertret, 2009; Booken et al., 2011; Ladizinski et al., 2012; Torres et al., 2012; Song et al., 2017).

Selected Systemic Diseases and Pathological Conditions

Dermatomyositis

Dermatomyositis (DM) is a rare heterogeneous systemic autoimmune connective tissue disease, which is a subtype of idiopathic inflammatory myopathies. DM might have a wide

variety of clinical manifestations including lung, joint, esophageal and cardiac findings; however, its hallmark features are the characteristic skin manifestations and progressive symmetrical muscle weakness (Griger et al., 2017). Based on data from question surveys, the majority of the patients (84.6–90.4%) suffers from pruritus (Shirani et al., 2004; Kim et al., 2018) which has a significant impact on quality of life (QoL). It seems that the severity of pruritus significantly correlates with disease activity, but the pathogenesis of DM-related itch is poorly understood. One small retrospective study (Khanna et al., 2020) found that there is a trend between histopathologic presence of eosinophils in skin biopsies, and pruritus. Recently, it was shown that IL-31 and IL-31RA gene expression in lesional skin was upregulated compared with either non-lesional skin or that from healthy controls (Kim et al., 2018). IL-31 mRNA expression also positively correlated with itch score and immunoreactivity for IL-31 and IL-31RA was greater in lesional skin. Furthermore, lesional DM skin contained significantly more IL-31-producing cells, of which $CD4^+$ cells were the most abundant IL-31-expressing cell type (Kim et al., 2018). Importantly, lenabasum (a.k.a. JBT-101 or ajulemic acid), an investigational, non-psychotropic, orally bioavailable CB_2 receptor agonist with remarkable anti-inflammatory potential, was recently found to significantly downregulate IL-31 in CpG-stimulated PBMCs *in vitro* (Kim et al., 2018). These data indicate that lenabasum may have potential as a new therapy for DM and DM-related itch; its efficiency is also currently being tested in a phase 3 clinical trial (NCT03813160).

Systemic Sclerosis

Systemic sclerosis (SSc) is a rare and complex chronic autoimmune connective tissue disease characterized by Raynaud's phenomenon (RP), nailfold capillary changes, excessive production of collagen, manifested as skin thickening and fibrosis of internal organs such as the lungs, heart, gastrointestinal tract, and kidneys. Clinically, patients can be subdivided into limited cutaneous SSc (lcSSc) and diffuse cutaneous SSc (dcSSc) forms. Pruritus represents a common, but infrequently reported skin symptom in SSc, with a prevalence of 43–62% (El-Baalbaki et al., 2010; Razykov et al., 2013; Théréné et al., 2017). It is significantly associated with greater skin and gastrointestinal involvement (Razykov et al., 2013) as well as worse mental status, physical function, and disability (El-Baalbaki et al., 2010).

The pathophysiology of pruritus in patients with SSc is unknown. Pruritus could arise either from 1) abnormalities of nerve fiber endings in SSc skin, 2) from the presence of an excess of mast cells, and/or 3) from the release of local mediators in the skin. The role of chemokines (derived not only from mast cells, but possibly also from other perivascular immune cells) on SSc itch is also of interest (Frech and Baron, 2013). Previous clinical observations in SSc, namely that pruritus is associated with sensory symptoms that predominate in the extremities and non-sclerotic areas, argue for a neuropathic component of pruritus (Théréné et al., 2017). The compression of small nerve fibers by thickened and/or dense collagen might contribute to the neuropathic component. A reduction of sensory and autonomic innervation in both sclerotic and apparently uninvolved skin has been reported in SSc (Provitera et al., 2005) with mast cell association early in the pathologic process. In addition, an inflammatory and immunological component of neuropathic pruritus had also been adduced by regeneration of C-fibers after destruction by collagen deposition and increasing sensitization of itch fibers by inflammatory mediators (Haber et al., 2016). On the other hand, elevated levels of histamine were found in 56% of patients with SSc and was more common in patients with diffuse disease (74%), in contrast to limited disease (31%), thus mast cells and histamine could also be the part of the pathogenesis of SSc-related itch (Falanga et al., 1990).

Chronic Renal Failure

Chronic renal failure is a worldwide public health problem with a global prevalence rate of 13.4% (Hill et al., 2016). Based on data of a multicenter study from 18,801 hemodialysis patients, moderate to extreme pruritus was experienced by 42% (Pisoni et al., 2006). The importance of pruritus is underlined not only because of poorer quality of life of the patients, but pruritus in HD patients was significantly associated with a 17% higher mortality risk (Pisoni et al., 2006). Although the association between chronic renal failure and skin itching has been recognized for more than a century, the exact pathogenesis of pruritus in renal failure remains poorly understood. It seems that uremic pruritus cannot be caused by a single factor, whereas many metabolic factors have been implicated in the pathogenesis of itching. Based on the existing literature, 4 general theories have emerged: 1) toxin deposition, 2) peripheral neuropathy, 3) immune system dysregulation, and 4) opioid imbalance (Verduzco and Shirazian, 2020).

The initial theory of chronic renal failure associated pruritus pathogenesis is deposition of pruritogenic toxins in the skin, like uremic compounds, vitamin A, calcium, phosphorus, and magnesium. This theory is mainly based on early observations, like pruritus is associated with underdialysis, improvement of pruritus after treatment of high calcium, parathormone and phosphorus level (Hampers et al., 1968; Hiroshige et al., 1995; Kimata et al., 2014; Mettang and Kremer, 2015), but further studies have not confirmed these associations (Shirazian et al., 2013). It is currently thought that underdialysis and toxin deposition may cause pruritus in a subset of patients, which should resolve with adequate dialysis. The second theory is based on the fact that in patients with chronic dialysis, there is a high prevalence of peripheral neuropathy and autonomic dysfunction, which could lead to abnormal skin innervation and nerve conduction resulting itch sensation. The pruritus in uremic patients occurred significantly more frequently in patients with paresthesia (Verduzco and Shirazian, 2020) and gabapentin, a drug approved for the treatment of epilepsy and neuropathic pain significantly reduced pruritus score, supporting the neuropathic hypothesis of uremic pruritus (Gunal et al., 2004).

The elevated levels of pro-inflammatory cytokines and inflammatory markers (C-reactive protein, IL-6, and IL-2) in patients with severe pruritus argue for the hypothesis that dysregulation of the immune system underlies pruritus in

kidney disease (Kimmel et al., 2006; Narita et al., 2006). It is further supported by the fact that after kidney transplantation patients do not complain about pruritus as long as immunosuppressive therapy, including cyclosporine or tacrolimus is administered, even when a substantial loss of transplant function has occurred (Mettang et al., 2002). In addition, in small randomized trials thalidomide and tacrolimus ointment were effective in the therapy of uremic pruritus (Silva et al., 1994; Pauli-Magnus et al., 2000). However the effectivity of this latter compound was not proved by another vehicle controlled study (Duque et al., 2005). Increased levels of eosinophils, mast cells, histamine and tryptase have also been found in patients with uremic pruritus, which might draw attention to this hypothesis (Francos et al., 1991; Dugas-Breit et al., 2005).

Finally, the alteration of the opioid pathway, modulation of its receptors and cellular processes might also affect chronic renal failure associated pruritus. Overstimulation of central μ-opioid receptors, antagonism of peripheral κ-opioid receptors, or an imbalance of stimulation and antagonism of μ- and κ -opioid receptors causes itching (Tey and Yosipovitch, 2011; Verduzco and Shirazian, 2020). In a recently published double blind, randomized trial, difelikefalin, a peripherally restricted and selective agonist of κ opioid receptors, had a significant reduction in itch intensity and improved itch-related quality of life as compared with those who received placebo in patients undergoing hemodialysis who had moderate-to-severe pruritus (Fishbane et al., 2020). In addition, nalfurafine hydrochloride, an κ-opioid-selective agonist, has been officially approved for resistant pruritus in HD patients on the basis of a well-evidenced clinical trial in Japan (Inui, 2015).

Cholestatic Liver Diseases

Pruritus is a common and debilitating symptom in patients with *cholestatic liver pathology* such as cholangiocellular (primary biliary cholangitis, primary sclerosing cholangitis), obstructive biliary (gallstone diseases, pancreatic head carcinoma, etc.,) and hepatocellular (pregnancy related cholestasis, viral hepatitis) diseases. The pathogenesis of itch in cholestatic disease remains elusive and is likely multifactorial, while the mechanisms of HCV-associated pruritus are attributed to HCV induced cholestasis and the induction of interferon stimulated genes as a result of viral overload (Alhmada et al., 2017). Numerous candidate pruritogens are present in bile and upregulated in cholestatic patients, including endogenous opioids, histamine, serotonin, lysophosphatidic acid (LPA), bilirubin, and bile acids (BA) (Beuers et al., 2014). These substances might interact with the nerve endings of the skin and induce the sensation of itching. One of these key factors is Autotaxin (ATX), whose elevated activity in patients' sera may be a consequence of HCV-induced chronic liver diseases and has a crucial role in the synthesis of LPA (Ikeda et al., 2009). Under pathological conditions elevated bile salts in patient's tissues and sera are able to signal the activation of ATX-LPA signaling (Nguyen et al., 2014), leading to the accumulation of LPA, which can initiate the pruritus via its receptor LPA_5 (Yamanoi et al., 2019). LPA is able to trigger the activation of TRPV1 and TRPA1 (Nieto-Posadas et al., 2011; Kittaka et al., 2017) and regulation of LPA by PI3k, protein kinase A (PKA) and C (PKC)-dependent mechanisms has been reported (Kassmann et al., 2013). Most recently, the LPA precursor lysophosphatidylcholine (LPC) was shown to directly bind to and activate epidermal TRPV4 resulting in the release of a micro RNA (miR-146a) which activates pruriceptive cutaneous nerve endings eliciting itch. The miR-146 evoked neural activation depended on TRPV1 activation, although the exact mechanism is not discovered yet. Importantly from a clinical point of view, elevated levels of LPC and miR-146 were found in pruritic primary biliary cholangitis patients compared to non-itching patients and the concentration of both LPC and miR-146a correlated with the severity of itch, although in another sample, there was no significant difference between primary biliary cholangitis patients and healthy subjects (Chen Y. et al., 2021).

Furthermore, animal experiments revealed that BAs activate TGR5 on sensory nerves. TGR5 is a G_s protein coupled bile acid receptor that is known to regulate metabolic processes in several tissues (Guo et al., 2016), which stimulates the release of neuropeptides in the spinal cord that transmit itch and analgesia (Alemi et al., 2013). It was found that TRPA1 is involved in this BA-evoked, TGR5-dependent pruritus in mice (Lieu et al., 2014). However, recently, experiments based on expression characterizations as well as functional assays revealed that TGR5 is not expressed in human DRG neurons and does not directly mediate itch sensation in human (Yu et al., 2019). Instead, it was proved, using humanized mouse models and calcium imaging, that the human sensory neuron-expressed MRGPRX4 is a novel bile acid receptor. The data suggest that targeting MRGPRX4 is a promising strategy for alleviating cholestatic itch (Meixiong et al., 2019b; Yu et al., 2019). Moreover, in a mouse biliary duct ligation model of cholestasis, that induced spontaneous itching, an increased expression of BAM8-22 was detected in the skin, and its receptor MRGPRX1/MRGPRC11 and the related TRPA1 were also upregulated in the sensory neurons of the DRGs. In this model, the number of the BAM8-22 responsive neurons was increased and BAM8-22 seemed to potentiate the spontaneous itching behavior suggesting that peripheral BAM8-22 may also mediate cholestatic itch (Sanjel et al., 2019). However, the recent recommendations for the treatment of cholestasis associated pruritus are based on 1) ursodeoxycholic acid (UDCA), which enhances biliary secretion of bile salts and other cholephiles; 2) the non-absorbable anion exchange resin cholestyramine, which binds a wide variety of amphiphilic molecules in the small intestinal lumen, increasing the bile excretion; 3) the potent pregnane X receptor agonist rifampicin, altering the metabolism of the presumed pruritogens in the liver and/or the gut by biotransformation and 4) opioid antagonists such as naltrexone and serotonin reuptake inhibitors such as sertraline, affecting the endogenous opioidergic and serotonergic system (European Association for the Study of the Liver, 2009; Bergasa, 2011; Kremer et al., 2011; Beuers et al., 2014).

THERAPEUTIC CONCLUSIONS

No universal itch-specific therapy has been established to date. The European guideline on chronic pruritus recommends several

therapeutic options including diseases specific and various sympthomatic interventions based on a careful diagnosis and several individual factors (Weisshaar et al., 2019). The application of these diverse clinical approaches in different diseases and increasing evidence from recent research suggest that the anti-pruritic philosophers' stone probably does not even exist. Inefficiency of antihistamines is well-established in several cases, and often-used immunosuppressants, for example glucocorticoids or calcineurin inhibitors are far from being specific in targeting pruritus or any specific pruritic disorders. They evoke their beneficial effect by generally suppressing immune responses, including several local immune-neuronal interactions characteristic for individual pathologies (Buddenkotte and Steinhoff, 2010). Specifically targeting this intercellular crosstalk locally in the skin may provide a highly specific and effective therapeutic approach with fewer side effects. The possible targets can be the pruritic mediators, their receptors and the related signaling pathways carefully chosen in light of the underlying pathology. The putative efficiency of such a selective approach is supported by several successful attempts using monoclonal neutralizing antibodies targeting T_h2 and T_h17 cytokines or their receptors e.g., in the treatment of AD and psoriasis, respectively (Fourzali et al., 2020; Zhang and He, 2020; Garcovich et al., 2021). The related signal transduction of these receptors can also be successfully targeted e.g., by JAK or phosphodiesterase 4 inhibitors (Fourzali et al., 2020; Soeberdt et al., 2020). Future alternative targets may be neural receptors (e.g., MRGPRs), signaling molecules, and ion channels (e.g., TRP channels) involved in the transduction of itch (Buddenkotte and Steinhoff, 2010; Tóth et al., 2015; Moore et al., 2018; Xie and Hu, 2018; Golpanian and Yosipovitch, 2020). However, the investigation of the specificity of these novel methods requires a cautious approach since certain molecular elements may overlap with different sensory transduction systems. For example, TRPV1 and TRPA1 are known not only as pruritic ion channels, but they also take part in temperature sensation and regulation, as well as in nociception (Vriens et al., 2014; Moore et al., 2018). Therefore, better understanding of the cutaneous pruritic interactions and identification of novel therapeutic targets are of great importance in current pruritus research.

AUTHOR CONTRIBUTIONS

AGS and BIT contributed to the conceptualization and design. AGS, AO, EL, ZG, and BIT wrote sections and drafted the original manuscript. AGS, AO, ZG, and BIT reviewed and edited the final version. BIT was responsible for project administration and funding acquisition. All authors have critically reviewed and approved the final version of the manuscript. All listed authors qualify for authorship and all authors qualifying for authorship are listed above.

FUNDING

The presented work was supported by Hungarian research grants of the National Research, Development and Innovation Office (NRDIO 120187, 134235, 134725, 134791, 134993, EFOP-3.6.3-VEKOP-16-2017-00009, and GINOP-2.3.2-15-2016-00050). AGS, AO, and BIT were awarded the János Bolyai Research Scholarship of the Hungarian Academy of Sciences. AGS, AO, and BIT were supported by the New National Excellence Program of the Ministry for Innovation and Technology from the source of the National Research, Development and Innovation Fund (ÚNKP-20-5-DE-100, ÚNKP-21-5-DE-465 and ÚNKP-21-5-DE-491, respectively).

REFERENCES

Abadía Molina, F., Burrows, N. P., Jones, R. R., Terenghi, G., and Polak, J. M. (1992). Increased Sensory Neuropeptides in Nodular Prurigo: a Quantitative Immunohistochemical Analysis. *Br. J. Dermatol.* 127, 344–351. doi:10.1111/j.1365-2133.1992.tb00452.x

Acton, D., Ren, X., Di Costanzo, S., Dalet, A., Bourane, S., Bertocchi, I., et al. (2019). Spinal Neuropeptide Y1 Receptor-Expressing Neurons Form an Essential Excitatory Pathway for Mechanical Itch. *Cell Rep* 28, 625–e6. e6. doi:10.1016/j.celrep.2019.06.033

Akiyama, T., Carstens, M. I., and Carstens, E. (2010). Enhanced Scratching Evoked by PAR-2 Agonist and 5-HT but Not Histamine in a Mouse Model of Chronic Dry Skin Itch. *Pain* 151, 378–383. doi:10.1016/j.pain.2010.07.024

Akiyama, T., Ivanov, M., Nagamine, M., Davoodi, A., Carstens, M. I., Ikoma, A., et al. (2016). Involvement of TRPV4 in Serotonin-Evoked Scratching. *J. Invest. Dermatol.* 136, 154–160. doi:10.1038/JID.2015.388

Alemi, F., Kwon, E., Poole, D. P., Lieu, T., Lyo, V., Cattaruzza, F., et al. (2013). The TGR5 Receptor Mediates Bile Acid-Induced Itch and Analgesia. *J. Clin. Invest.* 123, 1513–1530. doi:10.1172/JCI64551

Alhmada, Y., Selimovic, D., Murad, F., Hassan, S. L., Haikel, Y., Megahed, M., et al. (2017). Hepatitis C Virus-Associated Pruritus: Etiopathogenesis and Therapeutic Strategies. *World J. Gastroenterol.* 23, 743–750. doi:10.3748/wjg.v23.i5.743

Andersen, H. H., Elberling, J., and Arendt-Nielsen, L. (2015). Human Surrogate Models of Histaminergic and Non-histaminergic Itch. *Acta Derm Venereol.* 95, 771–777. doi:10.2340/00015555-2146

Ansel, J. C., Armstrong, C. A., Song, I., Quinlan, K. L., Olerud, J. E., Caughman, S. W., et al. (1997). Interactions of the Skin and Nervous System. *J. Investig. Dermatol. Symp. Proc.* 2, 23–26. doi:10.1038/jidsymp.1997.6

Armagni, C., di Francesco, C., Schaltegger, H., and Krebs, A. (1979). Electron Microscopy Studies on Dermal Nerves in Psoriatic Plaques. *Acta Derm Venereol. Suppl. (Stockh)* 87, 68–70.

Azimi, E., Reddy, V. B., Pereira, P. J. S., Talbot, S., Woolf, C. J., and Lerner, E. A. (2017). Substance P Activates Mas-Related G Protein-Coupled Receptors to Induce Itch. *J. Allergy Clin. Immunol.* 140, 447–e3. e3. doi:10.1016/j.jaci.2016.12.980

Bains, S. N., Nash, P., and Fonacier, L. (2019). Irritant Contact Dermatitis. *Clin. Rev. Allergy Immunol.* 56, 99–109. doi:10.1007/s12016-018-8713-0

Barry, D. M., Li, H., Liu, X. Y., Shen, K. F., Liu, X. T., Wu, Z. Y., et al. (2016). Critical Evaluation of the Expression of Gastrin-Releasing Peptide in Dorsal Root Ganglia and Spinal Cord. *Mol. Pain* 12. doi:10.1177/1744806916643724

Barry, D. M., Liu, X. T., Liu, B., Liu, X. Y., Gao, F., Zeng, X., et al. (2020). Exploration of Sensory and Spinal Neurons Expressing Gastrin-Releasing Peptide in Itch and Pain Related Behaviors. *Nat. Commun.* 11, 1397. doi:10.1038/s41467-020-15230-y

Bawany, F., Franco, A. I., and Beck, L. A. (2020). Dupilumab: One Therapy to Treat Multiple Atopic Diseases. *JAAD Case Rep.* 6, 1150–1152. doi:10.1016/j.jdcr.2020.08.036

Beck, L. A., Thaçi, D., Hamilton, J. D., Graham, N. M., Bieber, T., Rocklin, R., et al. (2014). Dupilumab Treatment in Adults with Moderate-To-Severe Atopic Dermatitis. *N. Engl. J. Med.* 371, 130–139. doi:10.1056/NEJMoa1314768

Bergasa, N. V. (2011). The Itch of Liver Disease. *Semin. Cutan. Med. Surg.* 30, 93–98. doi:10.1016/j.sder.2011.04.009

Beuers, U., Kremer, A. E., Bolier, R., and Elferink, R. P. (2014). Pruritus in Cholestasis: Facts and Fiction. *Hepatology* 60, 399–407. doi:10.1002/hep.26909

Bieber, T. (2008). Atopic Dermatitis. *N. Engl. J. Med.* 358, 1483–1494. doi:10.1056/NEJMra074081

Bienenstock, J., MacQueen, G., Sestini, P., Marshall, J. S., Stead, R. H., and Perdue, M. H. (1991). Mast Cell/nerve Interactions *In Vitro* and *In Vivo*. *Am. Rev. Respir. Dis.* 143, S55–S58. doi:10.1164/ajrccm/143.3_Pt_2.S55

Bigliardi, P. L., Dancik, Y., Neumann, C., and Bigliardi-Qi, M. (2016). Opioids and Skin Homeostasis, Regeneration and Ageing - What's the Evidence? *Exp. Dermatol.* 25, 586–591. doi:10.1111/exd.13021

Bíró, T., Tóth, B. I., Marincsák, R., Dobrosi, N., Géczy, T., and Paus, R. (2007). TRP Channels as Novel Players in the Pathogenesis and Therapy of Itch. *Biochim. Biophys. Acta (Bba) - Mol. Basis Dis.* 1772, 1004–1021. doi:10.1016/j.bbadis.2007.03.002

Bodó, E., Kovács, I., Telek, A., Varga, A., Paus, R., Kovács, L., et al. (2004). Vanilloid Receptor-1 (VR1) Is Widely Expressed on Various Epithelial and Mesenchymal Cell Types of Human Skin. *J. Invest. Dermatol.* 123, 410–413. doi:10.1111/j.0022-202X.2004.23209.x

Boniface, K., Diveu, C., Morel, F., Pedretti, N., Froger, J., Ravon, E., et al. (2007). Oncostatin M Secreted by Skin Infiltrating T Lymphocytes Is a Potent Keratinocyte Activator Involved in Skin Inflammation. *J. Immunol.* 178, 4615–4622. doi:10.4049/jimmunol.178.7.4615

Booken, N., Heck, M., Nicolay, J. P., Klemke, C. D., Goerdt, S., and Utikal, J. (2011). Oral Aprepitant in the Therapy of Refractory Pruritus in Erythrodermic Cutaneous T-Cell Lymphoma. *Br. J. Dermatol.* 164, 665–667. doi:10.1111/j.1365-2133.2010.10108.x

Boudaka, A., Al-Yazeedi, M., and Al-Lawati, I. (2020). Role of Transient Receptor Potential Vanilloid 4 Channel in Skin Physiology and Pathology. *Sultan Qaboos Univ. Med. J.* 20, e138–e146. doi:10.18295/squmj.2020.20.02.003

Buddenkotte, J., and Steinhoff, M. (2010). Pathophysiology and Therapy of Pruritus in Allergic and Atopic Diseases. *Allergy* 65, 805–821. doi:10.1111/j.1398-9995.2010.01995.x

Buhl, T., Ikoma, A., Kempkes, C., Cevikbas, F., Sulk, M., Buddenkotte, J., et al. (2020). Protease-Activated Receptor-2 Regulates Neuro-Epidermal Communication in Atopic Dermatitis. *Front. Immunol.* 11, 1740. doi:10.3389/fimmu.2020.01740

Bushmakin, A. G., Mamolo, C., Cappelleri, J. C., and Stewart, M. (2015). The Relationship between Pruritus and the Clinical Signs of Psoriasis in Patients Receiving Tofacitinib. *J. Dermatolog Treat.* 26, 19–22. doi:10.3109/09546634.2013.861891

Campion, M., Smith, L., Gatault, S., Métais, C., Buddenkotte, J., and Steinhoff, M. (2019). Interleukin-4 and Interleukin-13 Evoke Scratching Behaviour in Mice. *Exp. Dermatol.* 28, 1501–1504. doi:10.1111/exd.14034

Caterina, M. J., Leffler, A., Malmberg, A. B., Martin, W. J., Trafton, J., Petersen-Zeitz, K. R., et al. (2000). Impaired Nociception and Pain Sensation in Mice Lacking the Capsaicin Receptor. *Science* 288, 306–313. doi:10.1126/science.288.5464.306

Cavanaugh, D. J., Lee, H., Lo, L., Shields, S. D., Zylka, M. J., Basbaum, A. I., et al. (2009). Distinct Subsets of Unmyelinated Primary Sensory Fibers Mediate Behavioral Responses to Noxious thermal and Mechanical Stimuli. *Proc. Natl. Acad. Sci. U S A.* 106, 9075–9080. doi:10.1073/pnas.0901507106

Cevikbas, F., Wang, X., Akiyama, T., Kempkes, C., Savinko, T., Antal, A., et al. (2014). A Sensory Neuron-Expressed IL-31 Receptor Mediates T Helper Cell-dependent Itch: Involvement of TRPV1 and TRPA1. *J. Allergy Clin. Immunol.* 133, 448–460. doi:10.1016/j.jaci.2013.10.048

Checa, A., Xu, N., Sar, D. G., Haeggström, J. Z., Ståhle, M., and Wheelock, C. E. (2015). Circulating Levels of Sphingosine-1-Phosphate Are Elevated in Severe, but Not Mild Psoriasis and Are Unresponsive to Anti-TNF-α Treatment. *Sci. Rep.* 5, 12017. doi:10.1038/srep12017

Chen, J., Zhu, Z., Li, Q., Lin, Y., Dang, E., Meng, H., et al. (2021a). Neutrophils Enhance Cutaneous Vascular Dilation and Permeability to Aggravate Psoriasis by Releasing Matrix Metallopeptidase 9. *J. Invest. Dermatol.* 141, 787–799. doi:10.1016/j.jid.2020.07.028

Chen, Y., Fang, Q., Wang, Z., Zhang, J. Y., MacLeod, A. S., Hall, R. P., et al. (2016). Transient Receptor Potential Vanilloid 4 Ion Channel Functions as a Pruriceptor in Epidermal Keratinocytes to Evoke Histaminergic Itch. *J. Biol. Chem.* 291, 10252–10262. doi:10.1074/jbc.M116.716464

Chen, Y., Wang, Z.-L., Yeo, M., Zhang, Q.-J., López-Romero, A. E., Ding, H.-P., et al. (2021b). Epithelia-Sensory Neuron Cross Talk Underlies Cholestatic Itch Induced by Lysophosphatidylcholine. *Gastroenterology* 161, 301–317. doi:10.1053/j.gastro.2021.03.049

Chiu, I. M., Barrett, L. B., Williams, E. K., Strochlic, D. E., Lee, S., Weyer, A. D., et al. (2014). Transcriptional Profiling at Whole Population and Single Cell Levels Reveals Somatosensory Neuron Molecular Diversity. *eLife* 3, e04660. doi:10.7554/eLife.04660

Cho, H., Yang, Y. D., Lee, J., Lee, B., Kim, T., Jang, Y., et al. (2012). The Calcium-Activated Chloride Channel Anoctamin 1 Acts as a Heat Sensor in Nociceptive Neurons. *Nat. Neurosci.* 15, 1015–1021. doi:10.1038/nn.3111

Choi, J. E., and Di Nardo, A. (2018). Skin Neurogenic Inflammation. *Semin. Immunopathol* 40, 249–259. doi:10.1007/s00281-018-0675-z

Chung, M. K., Lee, H., Mizuno, A., Suzuki, M., and Caterina, M. J. (2004). TRPV3 and TRPV4 Mediate Warmth-Evoked Currents in Primary Mouse Keratinocytes. *J. Biol. Chem.* 279, 21569–21575. doi:10.1074/jbc.M401872200

Cohen, J. A., Edwards, T. N., Liu, A. W., Hirai, T., Jones, M. R., Wu, J., et al. (2019). Cutaneous TRPV1+ Neurons Trigger Protective Innate Type 17 Anticipatory Immunity. *Cell* 178, 919–e14. e14. doi:10.1016/j.cell.2019.06.022

Cornelissen, C., Marquardt, Y., Czaja, K., Wenzel, J., Frank, J., Lüscher-Firzlaff, J., et al. (2012). IL-31 Regulates Differentiation and Filaggrin Expression in Human Organotypic Skin Models. *J. Allergy Clin. Immunol.* 129, 426433–426438. e1–8. doi:10.1016/j.jaci.2011.10.042

Czarnowicki, T., He, H., Krueger, J. G., and Guttman-Yassky, E. (2019). Atopic Dermatitis Endotypes and Implications for Targeted Therapeutics. *J. Allergy Clin. Immunol.* 143, 1–11. doi:10.1016/j.jaci.2018.10.032

da Costa, D. S., Meotti, F. C., Andrade, E. L., Leal, P. C., Motta, E. M., and Calixto, J. B. (2010). The Involvement of the Transient Receptor Potential A1 (TRPA1) in the Maintenance of Mechanical and Cold Hyperalgesia in Persistent Inflammation. *Pain* 148, 431–437. doi:10.1016/j.pain.2009.12.002

Datsi, A., Steinhoff, M., Ahmad, F., Alam, M., and Buddenkotte, J. (2021). Interleukin-31: The "itchy" Cytokine in Inflammation and Therapy. *Allergy* 76, 2982–2997. doi:10.1111/all.14791

Davenport, A. P., Hyndman, K. A., Dhaun, N., Southan, C., Kohan, D. E., Pollock, J. S., et al. (2016). Endothelin. *Pharmacol. Rev.* 68, 357–418. doi:10.1124/pr.115.011833

Denda, M., and Denda, S. (2007). Air-exposed Keratinocytes Exhibited Intracellular Calcium Oscillation. *Skin Res. Technol.* 13, 195–201. doi:10.1111/j.1600-0846.2007.00210.x

Denda, M., Fuziwara, S., Inoue, K., Denda, S., Akamatsu, H., Tomitaka, A., et al. (2001). Immunoreactivity of VR1 on Epidermal Keratinocyte of Human Skin. *Biochem. Biophys. Res. Commun.* 285, 1250–1252. doi:10.1006/bbrc.2001.5299

Denda, M., Nakatani, M., Ikeyama, K., Tsutsumi, M., and Denda, S. (2007). Epidermal Keratinocytes as the Forefront of the Sensory System. *Exp. Dermatol.* 16, 157–161. doi:10.1111/j.1600-0625.2006.00529.x

Derouiche, S., Takayama, Y., Murakami, M., and Tominaga, M. (2018). TRPV4 Heats up ANO1-dependent Exocrine Gland Fluid Secretion. *FASEB J.* 32, 1841–1854. doi:10.1096/fj.201700954R

Dhingra, N., Shemer, A., Correa da Rosa, J., Rozenblit, M., Fuentes-Duculan, J., Gittler, J. K., et al. (2014). Molecular Profiling of Contact Dermatitis Skin Identifies Allergen-dependent Differences in Immune Response. *J. Allergy Clin. Immunol.* 134, 362–372. doi:10.1016/j.jaci.2014.03.009

Di Francesco, C., Meier, C., Schaltegger, H., and Krebs, A. (1978). Qualitative and Quantitative Investigations of the Skin Nerves of Patients with Psoriasis Light- and Electronmicroscopical Study (Author's Transl). *Arch. Dermatol. Res.* 262, 177–184. doi:10.1007/BF00455388

Ding, W., Stohl, L. L., Wagner, J. A., and Granstein, R. D. (2008). Calcitonin Gene-Related Peptide Biases Langerhans Cells toward Th2-type Immunity. *J. Immunol.* 181, 6020–6026. doi:10.4049/jimmunol.181.9.6020

Domagała, A., Szepietowski, J., and Reich, A. (2017). Antihistamines in the Treatment of Pruritus in Psoriasis. *Postepy Dermatol. Alergol* 34, 457–463. doi:10.5114/ada.2017.71112

Dong, X., and Dong, X. (2018). Peripheral and Central Mechanisms of Itch. *Neuron* 98, 482–494. doi:10.1016/j.neuron.2018.03.023

Dong, X., Han, S., Zylka, M. J., Simon, M. I., and Anderson, D. J. (2001). A Diverse Family of GPCRs Expressed in Specific Subsets of Nociceptive Sensory Neurons. *Cell* 106, 619–632. doi:10.1016/s0092-8674(01)00483-4

Dugas-Breit, S., Schöpf, P., Dugas, M., Schiffl, H., Ruëff, F., and Przybilla, B. (2005). Baseline Serum Levels of Mast Cell Tryptase Are Raised in Hemodialysis

Patients and Associated with Severity of Pruritus. *J. Dtsch Dermatol. Ges* 3, 343–347. doi:10.1111/j.1610-0387.2005.05706.x

Duque, M. I., Yosipovitch, G., Fleischer, A. B., Willard, J., and Freedman, B. I. (2005). Lack of Efficacy of Tacrolimus Ointment 0.1% for Treatment of Hemodialysis-Related Pruritus: a Randomized, Double-Blind, Vehicle-Controlled Study. *J. Am. Acad. Dermatol.* 52, 519–521. doi:10.1016/j.jaad.2004.08.050

Duval, A., and Dubertret, L. (2009). Aprepitant as an Antipruritic Agent? *N. Engl. J. Med.* 361, 1415–1416. doi:10.1056/NEJMc0906670

El-Baalbaki, G., Razykov, I., Hudson, M., Bassel, M., Baron, M., Thombs, B. D., et al. (2010). Association of Pruritus with Quality of Life and Disability in Systemic Sclerosis. *Arthritis Care Res. (Hoboken)* 62, 1489–1495. doi:10.1002/acr.20257

Elliott, G., Vanwersch, R., Soeberdt, M., Metze, D., Lotts, T., Ständer, S., et al. (2016). Topical Nalfurafine Exhibits Anti-inflammatory and Anti-pruritic Effects in a Murine Model of AD. *J. Dermatol. Sci.* 84, 351–354. doi:10.1016/j.jdermsci.2016.09.008

Esancy, K., Condon, L., Feng, J., Kimball, C., Curtright, A., and Dhaka, A. (2018). A Zebrafish and Mouse Model for Selective Pruritus via Direct Activation of TRPA1. *Elife* 7. doi:10.7554/eLife.32036

European Association for the Study of the Liver (2009). EASL Clinical Practice Guidelines: Management of Cholestatic Liver Diseases. *J. Hepatol.* 51, 237–267. doi:10.1016/j.jhep.2009.04.009

Falanga, V., Soter, N. A., Altman, R. D., and Kerdel, F. A. (1990). Elevated Plasma Histamine Levels in Systemic Sclerosis (Scleroderma). *Arch. Dermatol.* 126, 336–338. doi:10.1001/archderm.1990.01670270068011

Fishbane, S., Jamal, A., Munera, C., Wen, W., and Menzaghi, F.KALM-1 Trial Investigators (2020). A Phase 3 Trial of Difelikefalin in Hemodialysis Patients with Pruritus. *N. Engl. J. Med.* 382, 222–232. doi:10.1056/NEJMoa1912770

Fleming, M. S., Ramos, D., Han, S. B., Zhao, J., Son, Y. J., and Luo, W. (2012). The Majority of Dorsal Spinal Cord Gastrin Releasing Peptide Is Synthesized Locally whereas Neuromedin B Is Highly Expressed in Pain- and Itch-Sensing Somatosensory Neurons. *Mol. Pain* 8, 52. doi:10.1186/1744-8069-8-52

Fourzali, K., Golpanian, R. S., and Yosipovitch, G. (2020). Emerging Drugs for the Treatment of Chronic Pruritic Diseases. *Expert Opin. Emerg. Drugs* 25, 273–284. doi:10.1080/14728214.2020.1801632

Francos, G. C., Kauh, Y. C., Gittlen, S. D., Schulman, E. S., Besarab, A., Goyal, S., et al. (1991). Elevated Plasma Histamine in Chronic Uremia. Effects of Ketotifen on Pruritus. *Int. J. Dermatol.* 30, 884–889. doi:10.1111/j.1365-4362.1991.tb04360.x

Frech, T. M., and Baron, M. (2013). Understanding Itch in Systemic Sclerosis in Order to Improve Patient Quality of Life. *Clin. Exp. Rheumatol.* 31, 81–88.

Furue, K., Ulzii, D., Tanaka, Y., Ito, T., Tsuji, G., Kido-Nakahara, M., et al. (2020). Pathogenic Implication of Epidermal Scratch Injury in Psoriasis and Atopic Dermatitis. *J. Dermatol.* 47, 979–988. doi:10.1111/1346-8138.15507

Furue, M., Ulzii, D., Vu, Y. H., Tsuji, G., Kido-Nakahara, M., and Nakahara, T. (2019). Pathogenesis of Atopic Dermatitis: Current Paradigm. *Iran J. Immunol.* 16, 97–107. doi:10.22034/IJI.2019.80253

Fuziwara, S., Inoue, K., and Denda, M. (2003). NMDA-type Glutamate Receptor Is Associated with Cutaneous Barrier Homeostasis. *J. Invest. Dermatol.* 120, 1023–1029. doi:10.1046/j.1523-1747.2003.12238.x

Fuziwara, S., Suzuki, A., Inoue, K., and Denda, M. (2005). Dopamine D2-like Receptor Agonists Accelerate Barrier Repair and Inhibit the Epidermal Hyperplasia Induced by Barrier Disruption. *J. Invest. Dermatol.* 125, 783–789. doi:10.1111/j.0022-202X.2005.23873.x

Gandhi, N. A., Pirozzi, G., and Graham, N. M. H. (2017). Commonality of the IL-4/IL-13 Pathway in Atopic Diseases. *Expert Rev. Clin. Immunol.* 13, 425–437. doi:10.1080/1744666X.2017.1298443

Garcovich, S., Maurelli, M., Gisondi, P., Peris, K., Yosipovitch, G., and Girolomoni, G. (2021). Pruritus as a Distinctive Feature of Type 2 Inflammation. *Vaccines (Basel)* 9, 303. doi:10.3390/vaccines9030303

Glatzer, F., Gschwandtner, M., Ehling, S., Rossbach, K., Janik, K., Klos, A., et al. (2013). Histamine Induces Proliferation in Keratinocytes from Patients with Atopic Dermatitis through the Histamine 4 Receptor. *J. Allergy Clin. Immunol.* 132, 1358–1367. doi:10.1016/j.jaci.2013.06.023

Golpanian, R. S., and Yosipovitch, G. (2020). Current and Emerging Systemic Treatments Targeting the Neural System for Chronic Pruritus. *Expert Opin. Pharmacother.* 21, 1629–1636. doi:10.1080/14656566.2020.1775815

Gomes, L. O., Hara, D. B., and Rae, G. A. (2012). Endothelin-1 Induces Itch and Pain in the Mouse Cheek Model. *Life Sci.* 91, 628–633. doi:10.1016/j.lfs.2012.03.020

Gonçalo, M., Gimenéz-Arnau, A., Al-Ahmad, M., Ben-Shoshan, M., Bernstein, J. A., Ensina, L. F., et al. (2021). The Global burden of Chronic Urticaria for the Patient and Society*. *Br. J. Dermatol.* 184, 226–236. doi:10.1111/bjd.19561

Gooderham, M. J., Hong, H. C., Eshtiaghi, P., and Papp, K. A. (2018). Dupilumab: A Review of its Use in the Treatment of Atopic Dermatitis. *J. Am. Acad. Dermatol.* 78, S28–S36. doi:10.1016/j.jaad.2017.12.022

Granstein, R. D., Wagner, J. A., Stohl, L. L., and Ding, W. (2015). Calcitonin Gene-Related Peptide: Key Regulator of Cutaneous Immunity. *Acta Physiol. (Oxf)* 213, 586–594. doi:10.1111/apha.12442

Griffiths, C. E., van de Kerkhof, P., and Czarnecka-Operacz, M. (2017). Psoriasis and Atopic Dermatitis. *Dermatol. Ther. (Heidelb)* 7, 31–41. doi:10.1007/s13555-016-0167-9

Griger, Z., Nagy-Vincze, M., and Dankó, K. (2017). Pharmacological Management of Dermatomyositis. *Expert Rev. Clin. Pharmacol.* 10, 1109–1118. doi:10.1080/17512433.2017.1353910

Gschwandtner, M., Mildner, M., Mlitz, V., Gruber, F., Eckhart, L., Werfel, T., et al. (2013). Histamine Suppresses Epidermal Keratinocyte Differentiation and Impairs Skin Barrier Function in a Human Skin Model. *Allergy* 68, 37–47. doi:10.1111/all.12051

Gschwandtner, M., Purwar, R., Wittmann, M., Bäumer, W., Kietzmann, M., Werfel, T., et al. (2008). Histamine Upregulates Keratinocyte MMP-9 Production via the Histamine H1 Receptor. *J. Invest. Dermatol.* 128, 2783–2791. doi:10.1038/jid.2008.153

Gunal, A. I., Ozalp, G., Yoldas, T. K., Gunal, S. Y., Kirciman, E., and Celiker, H. (2004). Gabapentin Therapy for Pruritus in Haemodialysis Patients: a Randomized, Placebo-Controlled, Double-Blind Trial. *Nephrol. Dial. Transpl.* 19, 3137–3139. doi:10.1093/ndt/gfh496

Guo, C., Chen, W. D., and Wang, Y. D. (2016). TGR5, Not Only a Metabolic Regulator. *Front. Physiol.* 7, 646. doi:10.3389/fphys.2016.00646

Haber, J. S., Valdes-Rodriguez, R., and Yosipovitch, G. (2016). Chronic Pruritus and Connective Tissue Disorders: Review, Gaps, and Future Directions. *Am. J. Clin. Dermatol.* 17, 445–449. doi:10.1007/s40257-016-0201-9

Hampers, C. L., Katz, A. I., Wilson, R. E., and Merrill, J. P. (1968). Disappearance of "Uremic" Itching after Subtotal Parathyroidectomy. *N. Engl. J. Med.* 279, 695–697. doi:10.1056/NEJM196809262791307

Han, L., Ma, C., Liu, Q., Weng, H. J., Cui, Y., Tang, Z., et al. (2013). A Subpopulation of Nociceptors Specifically Linked to Itch. *Nat. Neurosci.* 16, 174–182. doi:10.1038/nn.3289

Han, S. K., Mancino, V., and Simon, M. I. (2006). Phospholipase Cbeta 3 Mediates the Scratching Response Activated by the Histamine H1 Receptor on C-Fiber Nociceptive Neurons. *Neuron* 52, 691–703. doi:10.1016/j.neuron.2006.09.036

Hans, G., Schmidt, B. L., and Strichartz, G. (2009). Nociceptive Sensitization by Endothelin-1. *Brain Res. Rev.* 60, 36–42. doi:10.1016/j.brainresrev.2008.12.008

Harvima, I. T., Viinamäki, H., Naukkarinen, A., Paukkonen, K., Neittaanmäki, H., Harvima, R. J., et al. (1993). Association of Cutaneous Mast Cells and Sensory Nerves with Psychic Stress in Psoriasis. *Psychother Psychosom* 60, 168–176. doi:10.1159/000288690

Hashimoto, T., Mishra, S. K., Olivry, T., and Yosipovitch, G. (2021a). Periostin, an Emerging Player in Itch Sensation. *J. Invest. Dermatol.* 141, 2338–2343. doi:10.1016/j.jid.2021.03.009

Hashimoto, T., Nattkemper, L. A., Kim, H. S., Kursewicz, C. D., Fowler, E., Shah, S. M., et al. (2021b). Itch Intensity in Prurigo Nodularis Is Closely Related to Dermal Interleukin-31, Oncostatin M, IL-31 Receptor Alpha and Oncostatin M Receptor Beta. *Exp. Dermatol.* 30, 804–810. doi:10.1111/exd.14279

Hawro, T., Saluja, R., Weller, K., Altrichter, S., Metz, M., and Maurer, M. (2014). Interleukin-31 Does Not Induce Immediate Itch in Atopic Dermatitis Patients and Healthy Controls after Skin challenge. *Allergy* 69, 113–117. doi:10.1111/all.12316

Held, K., and Tóth, B. I. (2021). TRPM3 in Brain (Patho)Physiology. *Front Cel Dev Biol* 9, 635659. doi:10.3389/fcell.2021.635659

Helyes, Z., Pintér, E., Sándor, K., Elekes, K., Bánvölgyi, A., Keszthelyi, D., et al. (2009). Impaired Defense Mechanism against Inflammation, Hyperalgesia, and Airway Hyperreactivity in Somatostatin 4 Receptor Gene-Deleted Mice. *Proc. Natl. Acad. Sci. U S A.* 106, 13088–13093. doi:10.1073/pnas.0900681106

Helyes, Z., Szabó, A., Németh, J., Jakab, B., Pintér, E., Bánvölgyi, A., et al. (2004). Antiinflammatory and Analgesic Effects of Somatostatin Released from

Capsaicin-Sensitive Sensory Nerve Terminals in a Freund's Adjuvant-Induced Chronic Arthritis Model in the Rat. *Arthritis Rheum.* 50, 1677–1685. doi:10.1002/art.20184

Hill, N. R., Fatoba, S. T., Oke, J. L., Hirst, J. A., O'Callaghan, C. A., Lasserson, D. S., et al. (2016). Global Prevalence of Chronic Kidney Disease - A Systematic Review and Meta-Analysis. *PLoS One* 11, e0158765. doi:10.1371/journal.pone.0158765

Hill, R. Z., Morita, T., Brem, R. B., and Bautista, D. M. (2018). S1PR3 Mediates Itch and Pain via Distinct TRP Channel-dependent Pathways. *J. Neurosci.* 38, 7833–7843. doi:10.1523/JNEUROSCI.1266-18.2018

Hiroshige, K., Kabashima, N., Takasugi, M., and Kuroiwa, A. (1995). Optimal Dialysis Improves Uremic Pruritus. *Am. J. Kidney Dis.* 25, 413–419. doi:10.1016/0272-6386(95)90102-7

Hon, K. L., Leung, A. K. C., Ng, W. G. G., and Loo, S. K. (2019). Chronic Urticaria: An Overview of Treatment and Recent Patents. *Recent Pat Inflamm. Allergy Drug Discov.* 13, 27–37. doi:10.2174/1872213X13666190328164931

Hon, K. L., Li, J. T. S., Leung, A. K. C., and Lee, V. W. Y. (2021). Current and Emerging Pharmacotherapy for Chronic Spontaneous Urticaria: a Focus on Non-biological Therapeutics. *Expert Opin. Pharmacother.* 22, 497–509. doi:10.1080/14656566.2020.1829593

Hosoi, J., Murphy, G. F., Egan, C. L., Lerner, E. A., Grabbe, S., Asahina, A., et al. (1993). Regulation of Langerhans Cell Function by Nerves Containing Calcitonin Gene-Related Peptide. *Nature* 363, 159–163. doi:10.1038/363159a0

Huang, M. C., Watson, S. R., Liao, J. J., and Goetzl, E. J. (2007). Th17 Augmentation in OTII TCR Plus T Cell-Selective Type 1 Sphingosine 1-phosphate Receptor Double Transgenic Mice. *J. Immunol.* 178, 6806–6813. doi:10.4049/jimmunol.178.11.6806

Ikeda, H., Watanabe, N., Nakamura, K., Kume, Y., Nakai, Y., Fujishiro, M., et al. (2009). Significance of Serum Autotaxin Activity in Gastrointestinal Disease. *Rinsho Byori* 57, 445–449.

Ikoma, A., Handwerker, H., Miyachi, Y., and Schmelz, M. (2005). Electrically Evoked Itch in Humans. *Pain* 113, 148–154. doi:10.1016/j.pain.2004.10.003

Ikoma, A., Steinhoff, M., Ständer, S., Yosipovitch, G., and Schmelz, M. (2006). The Neurobiology of Itch. *Nat. Rev. Neurosci.* 7, 535–547. doi:10.1038/nrn1950

Imai, Y. (2019). Interleukin-33 in Atopic Dermatitis. *J. Dermatol. Sci.* 96, 2–7. doi:10.1016/j.jdermsci.2019.08.006

Imai, Y., Kusakabe, M., Nagai, M., Yasuda, K., and Yamanishi, K. (2021). Dupilumab Effects on Innate Lymphoid Cell and Helper T Cell Populations in Patients with Atopic Dermatitis. *JID Innov.* 1, 100003. doi:10.1016/j.xjidi.2021.100003

Imamachi, N., Park, G. H., Lee, H., Anderson, D. J., Simon, M. I., Basbaum, A. I., et al. (2009). TRPV1-expressing Primary Afferents Generate Behavioral Responses to Pruritogens via Multiple Mechanisms. *Proc. Natl. Acad. Sci. U S A.* 106, 11330–11335. doi:10.1073/pnas.0905605106

Inoue, K., Koizumi, S., Fuziwara, S., Denda, S., Inoue, K., and Denda, M. (2002). Functional Vanilloid Receptors in Cultured normal Human Epidermal Keratinocytes. *Biochem. Biophys. Res. Commun.* 291, 124–129. doi:10.1006/bbrc.2002.6393

Inui, S. (2015). Nalfurafine Hydrochloride to Treat Pruritus: a Review. *Clin. Cosmet. Investig. Dermatol.* 8, 249–255. doi:10.2147/CCID.S55942

Jancsó, N., Jancsó-gábor, A., and Szolcsányi, J. (1967). Direct Evidence for Neurogenic Inflammation and its Prevention by Denervation and by Pretreatment with Capsaicin. *Br. J. Pharmacol. Chemother.* 31, 138–151. doi:10.1111/j.1476-5381.1967.tb01984.x

Jancsó, N., Jancsó-gábor, A., and Szolcsányi, J. (1968). The Role of Sensory Nerve Endings in Neurogenic Inflammation Induced in Human Skin and in the Eye and Paw of the Rat. *Br. J. Pharmacol. Chemother.* 33, 32–41. doi:10.1111/j.1476-5381.1968.tb00471.x

Järvikallio, A., Harvima, I. T., and Naukkarinen, A. (2003). Mast Cells, Nerves and Neuropeptides in Atopic Dermatitis and Nummular Eczema. *Arch. Dermatol. Res.* 295, 2–7. doi:10.1007/s00403-002-0378-z

Jensen, J. M., and Proksch, E. (2009). The Skin's Barrier. *G Ital. Dermatol. Venereol.* 144, 689–700.

Jian, T., Yang, N., Yang, Y., Zhu, C., Yuan, X., Yu, G., et al. (2016). TRPV1 and PLC Participate in Histamine H4 Receptor-Induced Itch. *Neural Plast.* 2016, 1682972. doi:10.1155/2016/1682972

Johansson, O., Liang, Y., Marcusson, J. A., and Reimert, C. M. (2000). Eosinophil Cationic Protein- and Eosinophil-Derived Neurotoxin/eosinophil Protein X-Immunoreactive Eosinophils in Prurigo Nodularis. *Arch. Dermatol. Res.* 292, 371–378. doi:10.1007/s004030000142

Julius, D. (2013). TRP Channels and Pain. *Annu. Rev. Cell Dev. Biol.* 29, 355–384. doi:10.1146/annurev-cellbio-101011-155833

Kabashima, K. (2013). New Concept of the Pathogenesis of Atopic Dermatitis: Interplay Among the Barrier, Allergy, and Pruritus as a trinity. *J. Dermatol. Sci.* 70, 3–11. doi:10.1016/j.jdermsci.2013.02.001

Kashem, S. W., Riedl, M. S., Yao, C., Honda, C. N., Vulchanova, L., and Kaplan, D. H. (2015). Nociceptive Sensory Fibers Drive Interleukin-23 Production from CD301b+ Dermal Dendritic Cells and Drive Protective Cutaneous Immunity. *Immunity* 43, 515–526. doi:10.1016/j.immuni.2015.08.016

Kassmann, M., Harteneck, C., Zhu, Z., Nürnberg, B., Tepel, M., and Gollasch, M. (2013). Transient Receptor Potential Vanilloid 1 (TRPV1), TRPV4, and the Kidney. *Acta Physiol. (Oxf)* 207, 546–564. doi:10.1111/apha.12051

Kato, A., Fujii, E., Watanabe, T., Takashima, Y., Matsushita, H., Furuhashi, T., et al. (2014). Distribution of IL-31 and its Receptor Expressing Cells in Skin of Atopic Dermatitis. *J. Dermatol. Sci.* 74, 229–235. doi:10.1016/j.jdermsci.2014.02.009

Kelemen, B., Pinto, S., Kim, N., Lisztes, E., Hanyicska, M., Vladár, A., et al. (2021). The TRPM3 Ion Channel Mediates Nociception but Not Itch Evoked by Endogenous Pruritogenic Mediators. *Biochem. Pharmacol.* 183, 114310. doi:10.1016/j.bcp.2020.114310

Kemény, Á., Kodji, X., Horváth, S., Komlódi, R., Szőke, É., Sándor, Z., et al. (2018). TRPA1 Acts in a Protective Manner in Imiquimod-Induced Psoriasiform Dermatitis in Mice. *J. Invest. Dermatol.* 138, 1774–1784. doi:10.1016/j.jid.2018.02.040

Kempkes, C., Buddenkotte, J., Cevikbas, F., Buhl, T., and Steinhoff, M. (2014). "Role of PAR-2 in Neuroimmune Communication and Itch," in Itch: Mechanisms And Treatment *Frontiers in Neuroscience*. Editors E. Carstens and T. Akiyama (Boca Raton (FL): CRC Press/Taylor & Francis). Available at: http://www.ncbi.nlm.nih.gov/books/NBK200911/(Accessed April 12, 2021).

Keçici, A. S., Göktay, F., Tutkavul, K., Güneş, P., and Yaşar, Ş. (2018). Unilateral Improvement of Nail Psoriasis with Denervation Injury. *Clin. Exp. Dermatol.* 43, 339–341. doi:10.1111/ced.13337

Khanna, U., Vaughan, H., North, J., and Haemel, A. (2020). Quantitative Assessment of Eosinophils in Dermatomyositis Skin Biopsies with Correlation of Eosinophils to Pruritus and Other Clinical Features. *Am. J. Dermatopathol* 43, 287–290. doi:10.1097/DAD.0000000000001765

Khodorova, A., Montmayeur, J. P., and Strichartz, G. (2009). Endothelin Receptors and Pain. *J. Pain* 10, 4–28. doi:10.1016/j.jpain.2008.09.009

Kido-Nakahara, M., Buddenkotte, J., Kempkes, C., Ikoma, A., Cevikbas, F., Akiyama, T., et al. (2014). Neural Peptidase Endothelin-Converting Enzyme 1 Regulates Endothelin 1-induced Pruritus. *J. Clin. Invest.* 124, 2683–2695. doi:10.1172/JCI67323

Kim, B. E., Leung, D. Y., Boguniewicz, M., and Howell, M. D. (2008). Loricrin and Involucrin Expression Is Down-Regulated by Th2 Cytokines through STAT-6. *Clin. Immunol.* 126, 332–337. doi:10.1016/j.clim.2007.11.006

Kim, B. M., Lee, S. H., Shim, W. S., and Oh, U. (2004). Histamine-induced Ca(2+) Influx via the PLA(2)/lipoxygenase/TRPV1 Pathway in Rat Sensory Neurons. *Neurosci. Lett.* 361, 159–162. doi:10.1016/j.neulet.2004.01.019

Kim, H. J., Zeidi, M., Bonciani, D., Pena, S. M., Tiao, J., Sahu, S., et al. (2018). Itch in Dermatomyositis: the Role of Increased Skin Interleukin-31. *Br. J. Dermatol.* 179, 669–678. doi:10.1111/bjd.16498

Kim, S. J., Park, G. H., Kim, D., Lee, J., Min, H., Wall, E., et al. (2011). Analysis of Cellular and Behavioral Responses to Imiquimod Reveals a Unique Itch Pathway in Transient Receptor Potential Vanilloid 1 (TRPV1)-Expressing Neurons. *Proc. Natl. Acad. Sci. U S A.* 108, 3371–3376. doi:10.1073/pnas.1019755108

Kimata, N., Fuller, D. S., Saito, A., Akizawa, T., Fukuhara, S., Pisoni, R. L., et al. (2014). Pruritus in Hemodialysis Patients: Results from the Japanese Dialysis Outcomes and Practice Patterns Study (JDOPPS). *Hemodial Int.* 18, 657–667. doi:10.1111/hdi.12158

Kimball, A. B., Luger, T., Gottlieb, A., Puig, L., Kaufmann, R., Burge, R., et al. (2018). Long-term Impact of Ixekizumab on Psoriasis Itch Severity: Results from a Phase III Clinical Trial and Long-Term Extension. *Acta Derm Venereol.* 98, 98–102. doi:10.2340/00015555-2801

Kimmel, M., Alscher, D. M., Dunst, R., Braun, N., Machleidt, C., Kiefer, T., et al. (2006). The Role of Micro-inflammation in the Pathogenesis of Uraemic Pruritus in Haemodialysis Patients. *Nephrol. Dial. Transpl.* 21, 749–755. doi:10.1093/ndt/gfi204

Kinoshita, H., Takai, T., Le, T. A., Kamijo, S., Wang, X. L., Ushio, H., et al. (2009). Cytokine Milieu Modulates Release of Thymic Stromal Lymphopoietin from

Human Keratinocytes Stimulated with Double-Stranded RNA. *J. Allergy Clin. Immunol.* 123, 179–186. doi:10.1016/j.jaci.2008.10.008

Kitajima, M., Lee, H. C., Nakayama, T., and Ziegler, S. F. (2011). TSLP Enhances the Function of Helper Type 2 Cells. *Eur. J. Immunol.* 41, 1862–1871. doi:10.1002/eji.201041195

Kittaka, H., Uchida, K., Fukuta, N., and Tominaga, M. (2017). Lysophosphatidic Acid-Induced Itch Is Mediated by Signalling of LPA5 Receptor, Phospholipase D and TRPA1/TRPV1. *J. Physiol.* 595, 2681–2698. doi:10.1113/JP273961

Köchling, H., Schaper, K., Wilzopolski, J., Gutzmer, R., Werfel, T., Bäumer, W., et al. (2017). Combined Treatment with H1 and H4 Receptor Antagonists Reduces Inflammation in a Mouse Model of Atopic Dermatitis. *J. Dermatol. Sci.* 87, 130–137. doi:10.1016/j.jdermsci.2017.04.004

Komiya, E., Tominaga, M., Kamata, Y., Suga, Y., and Takamori, K. (2020). Molecular and Cellular Mechanisms of Itch in Psoriasis. *Int. J. Mol. Sci.* 21. doi:10.3390/ijms21218406

Kondo, Y., Yoshimoto, T., Yasuda, K., Futatsugi-Yumikura, S., Morimoto, M., Hayashi, N., et al. (2008). Administration of IL-33 Induces Airway Hyperresponsiveness and Goblet Cell Hyperplasia in the Lungs in the Absence of Adaptive Immune System. *Int. Immunol.* 20, 791–800. doi:10.1093/intimm/dxn037

Kou, K., Nakamura, F., Aihara, M., Chen, H., Seto, K., Komori-Yamaguchi, J., et al. (2012). Decreased Expression of semaphorin-3A, a Neurite-Collapsing Factor, Is Associated with Itch in Psoriatic Skin. *Acta Derm Venereol.* 92, 521–528. doi:10.2340/00015555-1350

Kovács, D., Fazekas, F., Oláh, A., and Törőcsik, D. (2020). Adipokines in the Skin and in Dermatological Diseases. *Ijms* 21, 9048. doi:10.3390/ijms21239048

Kremer, A. E., Oude Elferink, R. P., and Beuers, U. (2011). Pathophysiology and Current Management of Pruritus in Liver Disease. *Clin. Res. Hepatol. Gastroenterol.* 35, 89–97. doi:10.1016/j.clinre.2010.10.007

Kupari, J., Usoskin, D., Parisien, M., Lou, D., Hu, Y., Fatt, M., et al. (2021). Single Cell Transcriptomics of Primate Sensory Neurons Identifies Cell Types Associated with Chronic Pain. *Nat. Commun.* 12, 1510. doi:10.1038/s41467-021-21725-z

Ladizinski, B., Bazakas, A., and Olsen, E. A. (2012). Aprepitant: a Novel Neurokinin-1 Receptor/substance P Antagonist as Antipruritic Therapy in Cutaneous T-Cell Lymphoma. *J. Am. Acad. Dermatol.* 67, e198–9. doi:10.1016/j.jaad.2012.02.008

LaMotte, R. H., Dong, X., and Ringkamp, M. (2014). Sensory Neurons and Circuits Mediating Itch. *Nat. Rev. Neurosci.* 15, 19–31. doi:10.1038/nrn3641

LaMotte, R. H., Shimada, S. G., and Sikand, P. (2011). Mouse Models of Acute, Chemical Itch and Pain in Humans. *Exp. Dermatol.* 20, 778–782. doi:10.1111/j.1600-0625.2011.01367.x

Langan, S. M., Irvine, A. D., and Weidinger, S. (2020). Atopic Dermatitis. *Lancet* 396, 345–360. doi:10.1016/S0140-6736(20)31286-1

Larkin, C., Chen, W., Szabó, I. L., Shan, C., Dajnoki, Z., Szegedi, A., et al. (2021). Novel Insights into the TRPV3-Mediated Itch in Atopic Dermatitis. *J. Allergy Clin. Immunol.* 147, 1110–e5. e5. doi:10.1016/j.jaci.2020.09.028

Leader, B., Carr, C. W., and Chen, S. C. (2015). Pruritus Epidemiology and Quality of Life. *Handb Exp. Pharmacol.* 226, 15–38. doi:10.1007/978-3-662-44605-8_2

Lee, C. H., Chuang, H. Y., Shih, C. C., Jong, S. B., Chang, C. H., and Yu, H. S. (2006). Transepidermal Water Loss, Serum IgE and Beta-Endorphin as Important and Independent Biological Markers for Development of Itch Intensity in Atopic Dermatitis. *Br. J. Dermatol.* 154, 1100–1107. doi:10.1111/j.1365-2133.2006.07191.x

Lee, H. Y., Stieger, M., Yawalkar, N., and Kakeda, M. (20132013). Cytokines and Chemokines in Irritant Contact Dermatitis. *Mediators Inflamm.* 2013, 1–7. doi:10.1155/2013/916497

Lee, J., Kim, T., Hong, J., Woo, J., Min, H., Hwang, E., et al. (2012). Imiquimod Enhances Excitability of Dorsal Root Ganglion Neurons by Inhibiting Background (K(2P)) and Voltage-Gated (K(v)1.1 and K(v)1.2) Potassium Channels. *Mol. Pain* 8, 2. doi:10.1186/1744-8069-8-2

Lee, M. R., and Shumack, S. (2005). Prurigo Nodularis: a Review. *Australas. J. Dermatol.* 46, 211–220. quiz 219–220. doi:10.1111/j.1440-0960.2005.00187.x

Lembo, P. M., Grazzini, E., Groblewski, T., O'Donnell, D., Roy, M. O., Zhang, J., et al. (2002). Proenkephalin A Gene Products Activate a New Family of Sensory Neuron--specific GPCRs. *Nat. Neurosci.* 5, 201–209. doi:10.1038/nn815

Leonard, A., and Guttman-Yassky, E. (2019). The Unique Molecular Signatures of Contact Dermatitis and Implications for Treatment. *Clin. Rev. Allergy Immunol.* 56, 1–8. doi:10.1007/s12016-018-8685-0

Liang, J., Ji, Q., and Ji, W. (2011). Role of Transient Receptor Potential Ankyrin Subfamily Member 1 in Pruritus Induced by Endothelin-1. *Neurosci. Lett.* 492, 175–178. doi:10.1016/j.neulet.2011.02.009

Liao, J. J., Huang, M. C., and Goetzl, E. J. (2007). Cutting Edge: Alternative Signaling of Th17 Cell Development by Sphingosine 1-phosphate. *J. Immunol.* 178, 5425–5428. doi:10.4049/jimmunol.178.9.5425

Lieu, T., Jayaweera, G., Zhao, P., Poole, D. P., Jensen, D., Grace, M., et al. (2014). The Bile Acid Receptor TGR5 Activates the TRPA1 Channel to Induce Itch in Mice. *Gastroenterology* 147, 1417–1428. doi:10.1053/j.gastro.2014.08.042

Lin, Z., Chen, Q., Lee, M., Cao, X., Zhang, J., Ma, D., et al. (2012). Exome Sequencing Reveals Mutations in TRPV3 as a Cause of Olmsted Syndrome. *Am. J. Hum. Genet.* 90, 558–564. doi:10.1016/j.ajhg.2012.02.006

Lisby, S., and Baadsgaard, O. (2006). "Mechanisms of Irritant Contact Dermatitis," in *Contact Dermatitis*. Editors P. J. Frosch, T. Menné, and J.-P. Lepoittevin (Berlin, Heidelberg: Springer), 69–82. doi:10.1007/3-540-31301-X_4

Liu, B., Escalera, J., Balakrishna, S., Fan, L., Caceres, A. I., Robinson, E., et al. (2013). TRPA1 Controls Inflammation and Pruritogen Responses in Allergic Contact Dermatitis. *FASEB J.* 27, 3549–3563. doi:10.1096/fj.13-229948

Liu, B., Tai, Y., Achanta, S., Kaelberer, M. M., Caceres, A. I., Shao, X., et al. (2016). IL-33/ST2 Signaling Excites Sensory Neurons and Mediates Itch Response in a Mouse Model of Poison Ivy Contact Allergy. *Proc. Natl. Acad. Sci. U S A.* 113, E7572–E7579. doi:10.1073/pnas.1606608113

Liu, B., Tai, Y., Liu, B., Caceres, A. I., Yin, C., and Jordt, S. E. (2019). Transcriptome Profiling Reveals Th2 Bias and Identifies Endogenous Itch Mediators in Poison Ivy Contact Dermatitis. *JCI Insight* 5, 124497. doi:10.1172/jci.insight.124497

Liu, Q., and Dong, X. (2015). The Role of the Mrgpr Receptor Family in Itch. *Handb Exp. Pharmacol.* 226, 71–88. doi:10.1007/978-3-662-44605-8_5

Liu, Q., Sikand, P., Ma, C., Tang, Z., Han, L., Li, Z., et al. (2012a). Mechanisms of Itch Evoked by β-alanine. *J. Neurosci.* 32, 14532–14537. doi:10.1523/JNEUROSCI.3509-12.2012

Liu, Q., Tang, Z., Surdenikova, L., Kim, S., Patel, K. N., Kim, A., et al. (2009). Sensory Neuron-specific GPCR Mrgprs Are Itch Receptors Mediating Chloroquine-Induced Pruritus. *Cell* 139, 1353–1365. doi:10.1016/j.cell.2009.11.034

Liu, Q., Weng, H. J., Patel, K. N., Tang, Z., Bai, H., Steinhoff, M., et al. (2011). The Distinct Roles of Two GPCRs, MrgprC11 and PAR2, in Itch and Hyperalgesia. *Sci. Signal.* 4, ra45. doi:10.1126/scisignal.2001925

Liu, T., Berta, T., Xu, Z. Z., Park, C. K., Zhang, L., Lü, N., et al. (2012b). TLR3 Deficiency Impairs Spinal Cord Synaptic Transmission, central Sensitization, and Pruritus in Mice. *J. Clin. Invest.* 122, 2195–2207. doi:10.1172/JCI45414

Liu, T., Xu, Z. Z., Park, C. K., Berta, T., and Ji, R. R. (2010). Toll-like Receptor 7 Mediates Pruritus. *Nat. Neurosci.* 13, 1460–1462. doi:10.1038/nn.2683

Lundeberg, L., El-Nour, H., Mohabbati, S., Morales, M., Azmitia, E., and Nordlind, K. (2002). Expression of Serotonin Receptors in Allergic Contact Eczematous Human Skin. *Arch. Dermatol. Res.* 294, 393–398. doi:10.1007/s00403-002-0350-y

Luo, J., Feng, J., Yu, G., Yang, P., Mack, M. R., Du, J., et al. (2018). Transient Receptor Potential Vanilloid 4-expressing Macrophages and Keratinocytes Contribute Differentially to Allergic and Nonallergic Chronic Itch. *J. Allergy Clin. Immunol.* 141, 608–e7. e7. doi:10.1016/j.jaci.2017.05.051

Mack, M. R., and Kim, B. S. (2018). The Itch-Scratch Cycle: A Neuroimmune Perspective. *Trends Immunol.* 39, 980–991. doi:10.1016/j.it.2018.10.001

Malek, M., Gleń, J., Rębała, K., Kowalczyk, A., Sobjanek, M., Nowicki, R., et al. (2015). Il-31 Does Not Correlate to Pruritus Related to Early Stage Cutaneous T-Cell Lymphomas but Is Involved in Pathogenesis of the Disease. *Acta Derm Venereol.* 95, 283–288. doi:10.2340/00015555-1958

Malik, K., Ungar, B., Garcet, S., Dutt, R., Dickstein, D., Zheng, X., et al. (2017). Dust Mite Induces Multiple Polar T Cell Axes in Human Skin. *Clin. Exp. Allergy* 47, 1648–1660. doi:10.1111/cea.13040

Mandadi, S., Sokabe, T., Shibasaki, K., Katanosaka, K., Mizuno, A., Moqrich, A., et al. (2009). TRPV3 in Keratinocytes Transmits Temperature Information to Sensory Neurons via ATP. *Pflugers Arch.* 458, 1093–1102. doi:10.1007/s00424-009-0703-x

Masuoka, M., Shiraishi, H., Ohta, S., Suzuki, S., Arima, K., Aoki, S., et al. (2012). Periostin Promotes Chronic Allergic Inflammation in Response to Th2 Cytokines. *J. Clin. Invest.* 122, 2590–2600. doi:10.1172/JCI58978

Matterne, U., Böhmer, M. M., Weisshaar, E., Jupiter, A., Carter, B., and Apfelbacher, C. J. (2019). Oral H1 Antihistamines as 'add-On' Therapy to

Topical Treatment for Eczema. *Cochrane Database Syst. Rev.* 1, CD012167. doi:10.1002/14651858.CD012167.pub2

McQueen, D. S., Noble, M. A., and Bond, S. M. (2007). Endothelin-1 Activates ETA Receptors to Cause Reflex Scratching in BALB/c Mice. *Br. J. Pharmacol.* 151, 278–284. doi:10.1038/sj.bjp.0707216

Meixiong, J., Anderson, M., Limjunyawong, N., Sabbagh, M. F., Hu, E., Mack, M. R., et al. (2019a). Activation of Mast-Cell-Expressed Mas-Related G-Protein-Coupled Receptors Drives Non-histaminergic Itch. *Immunity* 50, 1163–e5. e5. doi:10.1016/j.immuni.2019.03.013

Meixiong, J., Vasavda, C., Snyder, S. H., and Dong, X. (2019b). MRGPRX4 Is a G Protein-Coupled Receptor Activated by Bile Acids that May Contribute to Cholestatic Pruritus. *Proc. Natl. Acad. Sci. U S A.* 116, 10525–10530. doi:10.1073/pnas.1903316116

Mettang, T., and Kremer, A. E. (2015). Uremic Pruritus. *Kidney Int.* 87, 685–691. doi:10.1038/ki.2013.454

Mettang, T., Pauli-Magnus, C., and Alscher, D. M. (2002). Uraemic Pruritus-Nnew Perspectives and Insights from Recent Trials. *Nephrol. Dial. Transpl.* 17, 1558–1563. doi:10.1093/ndt/17.9.1558

Mihara, H., Boudaka, A., Sugiyama, T., Moriyama, Y., and Tominaga, M. (2011). Transient Receptor Potential Vanilloid 4 (TRPV4)-dependent Calcium Influx and ATP Release in Mouse Oesophageal Keratinocytes. *J. Physiol.* 589, 3471–3482. doi:10.1113/jphysiol.2011.207829

Mishra, S. K., and Hoon, M. A. (2013). The Cells and Circuitry for Itch Responses in Mice. *Science* 340, 968–971. doi:10.1126/science.1233765

Mishra, S. K., Tisel, S. M., Orestes, P., Bhangoo, S. K., and Hoon, M. A. (2011). TRPV1-lineage Neurons Are Required for thermal Sensation. *EMBO J.* 30, 582–593. doi:10.1038/emboj.2010.325

Mishra, S. K., Wheeler, J. J., Pitake, S., Ding, H., Jiang, C., Fukuyama, T., et al. (2020). Periostin Activation of Integrin Receptors on Sensory Neurons Induces Allergic Itch. *Cell Rep* 31, 107472. doi:10.1016/j.celrep.2020.03.036

Möbs, M., Gryzik, S., Haidar, A., Humme, D., Beyer, M., and Vandersee, S. (2015). Analysis of the IL-31 Pathway in Mycosis Fungoides and Sézary Syndrome. *Arch. Dermatol. Res.* 307, 479–485. doi:10.1007/s00403-014-1527-x

Moore, C., Cevikbas, F., Pasolli, H. A., Chen, Y., Kong, W., Kempkes, C., et al. (2013). UVB Radiation Generates Sunburn Pain and Affects Skin by Activating Epidermal TRPV4 Ion Channels and Triggering Endothelin-1 Signaling. *Proc. Natl. Acad. Sci. U S A.* 110, E3225–E3234. doi:10.1073/pnas.1312933110

Moore, C., Gupta, R., Jordt, S. E., Chen, Y., and Liedtke, W. B. (2018). Regulation of Pain and Itch by TRP Channels. *Neurosci. Bull.* 34, 120–142. doi:10.1007/s12264-017-0200-8

Morita, T., McClain, S. P., Batia, L. M., Pellegrino, M., Wilson, S. R., Kienzler, M. A., et al. (2015). HTR7 Mediates Serotonergic Acute and Chronic Itch. *Neuron* 87, 124–138. doi:10.1016/j.neuron.2015.05.044

Moussion, C., Ortega, N., and Girard, J. P. (2008). The IL-1-like Cytokine IL-33 Is Constitutively Expressed in the Nucleus of Endothelial Cells and Epithelial Cells *In Vivo*: a Novel 'alarmin'? *PLoS One* 3, e3331. doi:10.1371/journal.pone.0003331

Mullins, T. B., Sharma, P., Riley, C. A., and Sonthalia, S. (2021). "Prurigo Nodularis," in *StatPearls* (Treasure Island (FL): StatPearls Publishing). Available at: http://www.ncbi.nlm.nih.gov/books/NBK459204/(Accessed April 12, 2021).

Myśliwiec, H., Baran, A., Harasim-Symbor, E., Choromańska, B., Myśliwiec, P., Milewska, A. J., et al. (2017). Increase in Circulating Sphingosine-1-Phosphate and Decrease in Ceramide Levels in Psoriatic Patients. *Arch. Dermatol. Res.* 309, 79–86. doi:10.1007/s00403-016-1709-9

Nakahara, T., Kido-Nakahara, M., Tsuji, G., and Furue, M. (2021). Basics and Recent Advances in the Pathophysiology of Atopic Dermatitis. *J. Dermatol.* 48, 130–139. doi:10.1111/1346-8138.15664

Nakamura, M., Toyoda, M., and Morohashi, M. (2003). Pruritogenic Mediators in Psoriasis Vulgaris: Comparative Evaluation of Itch-Associated Cutaneous Factors. *Br. J. Dermatol.* 149, 718–730. doi:10.1046/j.1365-2133.2003.05586.x

Namer, B., Carr, R., Johanek, L. M., Schmelz, M., Handwerker, H. O., and Ringkamp, M. (2008). Separate Peripheral Pathways for Pruritus in Man. *J. Neurophysiol.* 100, 2062–2069. doi:10.1152/jn.90482.2008

Narbutt, J., Olejniczak, I., Sobolewska-Sztychny, D., Sysa-Jedrzejowska, A., Słowik-Kwiatkowska, I., Hawro, T., et al. (2013). Narrow Band Ultraviolet B Irradiations Cause Alteration in Interleukin-31 Serum Level in Psoriatic Patients. *Arch. Dermatol. Res.* 305, 191–195. doi:10.1007/s00403-012-1293-6

Narita, I., Alchi, B., Omori, K., Sato, F., Ajiro, J., Saga, D., et al. (2006). Etiology and Prognostic Significance of Severe Uremic Pruritus in Chronic Hemodialysis Patients. *Kidney Int.* 69, 1626–1632. doi:10.1038/sj.ki.5000251

Nattkemper, L. A., Martinez-Escala, M. E., Gelman, A. B., Singer, E. M., Rook, A. H., Guitart, J., et al. (2016). Cutaneous T-Cell Lymphoma and Pruritus: The Expression of IL-31 and its Receptors in the Skin. *Acta Derm Venereol.* 96, 894–898. doi:10.2340/00015555-2417

Nattkemper, L. A., Tey, H. L., Valdes-Rodriguez, R., Lee, H., Mollanazar, N. K., Albornoz, C., et al. (2018). The Genetics of Chronic Itch: Gene Expression in the Skin of Patients with Atopic Dermatitis and Psoriasis with Severe Itch. *J. Invest. Dermatol.* 138, 1311–1317. doi:10.1016/j.jid.2017.12.029

Nattkemper, L. A., Zhao, Z. Q., Nichols, A. J., Papoiu, A. D. P., Shively, C. A., Chen, Z. F., et al. (2013). Overexpression of the Gastrin-Releasing Peptide in Cutaneous Nerve Fibers and its Receptor in the Spinal Cord in Primates with Chronic Itch. *J. Invest. Dermatol.* 133, 2489–2492. doi:10.1038/jid.2013.166

Naukkarinen, A., Harvima, I. T., Aalto, M. L., Harvima, R. J., and Horsmanheimo, M. (1991). Quantitative Analysis of Contact Sites between Mast Cells and Sensory Nerves in Cutaneous Psoriasis and Lichen Planus Based on a Histochemical Double Staining Technique. *Arch. Dermatol. Res.* 283, 433–437. doi:10.1007/BF00371778

Nguyen, K. D., Sundaram, V., and Ayoub, W. S. (2014). Atypical Causes of Cholestasis. *World J. Gastroenterol.* 20, 9418–9426. doi:10.3748/wjg.v20.i28.9418

Nguyen, M. Q., von Buchholtz, L. J., Reker, A. N., Ryba, N. J., and Davidson, S. (2021). Single-nucleus Transcriptomic Analysis of Human Dorsal Root Ganglion Neurons. *eLife* 10, e71752. doi:10.7554/eLife.71752

Nieto-Posadas, A., Picazo-Juárez, G., Llorente, I., Jara-Oseguera, A., Morales-Lázaro, S., Escalante-Alcalde, D., et al. (2011). Lysophosphatidic Acid Directly Activates TRPV1 through a C-Terminal Binding Site. *Nat. Chem. Biol.* 8, 78–85. doi:10.1038/nchembio.712

Niyonsaba, F., Ushio, H., Hara, M., Yokoi, H., Tominaga, M., Takamori, K., et al. (2010). Antimicrobial Peptides Human Beta-Defensins and Cathelicidin LL-37 Induce the Secretion of a Pruritogenic Cytokine IL-31 by Human Mast Cells. *J. Immunol.* 184, 3526–3534. doi:10.4049/jimmunol.0900712

Oetjen, L. K., Mack, M. R., Feng, J., Whelan, T. M., Niu, H., Guo, C. J., et al. (2017). Sensory Neurons Co-opt Classical Immune Signaling Pathways to Mediate Chronic Itch. *Cell* 171, 217–e13. e13. doi:10.1016/j.cell.2017.08.006

Ohmatsu, H., Sugaya, M., Suga, H., Morimura, S., Miyagaki, T., Kai, H., et al. (2012). Serum IL-31 Levels Are Increased in Patients with Cutaneous T-Cell Lymphoma. *Acta Derm Venereol.* 92, 282–283. doi:10.2340/00015555-1345

Ohta, T., Ikemi, Y., Murakami, M., Imagawa, T., Otsuguro, K., and Ito, S. (2006). Potentiation of Transient Receptor Potential V1 Functions by the Activation of Metabotropic 5-HT Receptors in Rat Primary Sensory Neurons. *J. Physiol.* 576, 809–822. doi:10.1113/jphysiol.2006.112250

Onderdijk, A. J., Hekking-Weijma, I. M., Florencia, E. F., and Prens, E. P. (2017). Surgical Denervation in the Imiquimod-Induced Psoriasiform Mouse Model. *Methods Mol. Biol.* 1559, 75–81. doi:10.1007/978-1-4939-6786-5_6

Panula, P., Chazot, P. L., Cowart, M., Gutzmer, R., Leurs, R., Liu, W. L., et al. (2015). International Union of Basic and Clinical Pharmacology. XCVIII. Histamine Receptors. *Pharmacol. Rev.* 67, 601–655. doi:10.1124/pr.114.010249

Park, C. W., Kim, H. J., Choi, Y. W., Chung, B. Y., Woo, S. Y., Song, D. K., et al. (2017). TRPV3 Channel in Keratinocytes in Scars with Post-Burn Pruritus. *Int. J. Mol. Sci.* 18. doi:10.3390/ijms18112425

Pauli-Magnus, C., Klumpp, S., Alscher, D. M., Kuhlmann, U., and Mettang, T. (2000). Short-term Efficacy of Tacrolimus Ointment in Severe Uremic Pruritus. *Perit Dial. Int.* 20, 802–803.

Paus, R., Schmelz, M., Bíró, T., and Steinhoff, M. (2006). Frontiers in Pruritus Research: Scratching the Brain for More Effective Itch Therapy. *J. Clin. Invest.* 116, 1174–1186. doi:10.1172/JCI28553

Pavlovic, S., Daniltchenko, M., Tobin, D. J., Hagen, E., Hunt, S. P., Klapp, B. F., et al. (2008). Further Exploring the Brain-Skin Connection: Stress Worsens Dermatitis via Substance P-dependent Neurogenic Inflammation in Mice. *J. Invest. Dermatol.* 128, 434–446. doi:10.1038/sj.jid.5701079

Peier, A. M., Reeve, A. J., Andersson, D. A., Moqrich, A., Earley, T. J., Hergarden, A. C., et al. (2002). A Heat-Sensitive TRP Channel Expressed in Keratinocytes. *Science* 296, 2046–2049. doi:10.1126/science.1073140

Pereira, M., Zeidler, C., Wallengren, J., Halvorsen, J., Weisshaar, E., Garcovich, S., et al. (2021). Chronic Nodular Prurigo: A European Cross-Sectional Study of Patient Perspectives on Therapeutic Goals and Satisfaction. *Acta Derm Venereol.* 101, adv00403. doi:10.2340/00015555-3726

Pergolizzi, S., Vaccaro, M., Magaudda, L., Mondello, M. R., Arco, A., Bramanti, P., et al. (1998). Immunohistochemical Study of Epidermal Nerve Fibres in Involved and Uninvolved Psoriatic Skin Using Confocal Laser Scanning Microscopy. *Arch. Dermatol. Res.* 290, 483–489. doi:10.1007/s004030050340

Perner, C., Flayer, C. H., Zhu, X., Aderhold, P. A., Dewan, Z. N. A., Voisin, T., et al. (2020). Substance P Release by Sensory Neurons Triggers Dendritic Cell Migration and Initiates the Type-2 Immune Response to Allergens. *Immunity* 53, 1063–e7. e7. doi:10.1016/j.immuni.2020.10.001

Petra, A. I., Tsilioni, I., Taracanova, A., Katsarou-Katsari, A., and Theoharides, T. C. (2018). Interleukin 33 and Interleukin 4 Regulate Interleukin 31 Gene Expression and Secretion from Human Laboratory of Allergic Diseases 2 Mast Cells Stimulated by Substance P And/or Immunoglobulin E. *Allergy Asthma Proc.* 39, 153–160. doi:10.2500/aap.2018.38.4105

Pincelli, C. (2000). Nerve Growth Factor and Keratinocytes: a Role in Psoriasis. *Eur. J. Dermatol.* 10, 85–90.

Pisoni, R. L., Wikström, B., Elder, S. J., Akizawa, T., Asano, Y., Keen, M. L., et al. (2006). Pruritus in Haemodialysis Patients: International Results from the Dialysis Outcomes and Practice Patterns Study (DOPPS). *Nephrol. Dial. Transpl.* 21, 3495–3505. doi:10.1093/ndt/gfl461

Plant, T. D., Zöllner, C., Kepura, F., Mousa, S. S., Eichhorst, J., Schaefer, M., et al. (2007). Endothelin Potentiates TRPV1 via ETA Receptor-Mediated Activation of Protein Kinase C. *Mol. Pain* 3, 35. doi:10.1186/1744-8069-3-35

Priestley, J. V. (2009). "Neuropeptides: Sensory Systems," in *Encyclopedia of Neuroscience*. Editor L. R. Squire (Oxford: Academic Press), 935–943. doi:10.1016/B978-008045046-9.01465-0

Proksch, E., Brandner, J. M., and Jensen, J. M. (2008). The Skin: an Indispensable Barrier. *Exp. Dermatol.* 17, 1063–1072. doi:10.1111/j.1600-0625.2008.00786.x

Provitera, V., Nolano, M., Pappone, N., di Girolamo, C., Stancanelli, A., Lullo, F., et al. (2005). Distal Degeneration of Sensory and Autonomic Cutaneous Nerve Fibres in Systemic Sclerosis. *Ann. Rheum. Dis.* 64, 1524–1526. doi:10.1136/ard.2005.038935

Qin, B., Sun, C., Chen, L., Wang, S., Yang, J., Xie, Z., et al. (2021). The Nerve Injuries Attenuate the Persistence of Psoriatic Lesions. *J. Dermatol. Sci.* 102, 85–93. doi:10.1016/j.jdermsci.2021.02.006

Qu, L., Fu, K., Shimada, S. G., and LaMotte, R. H. (2017). Cl- Channel Is Required for CXCL10-Induced Neuronal Activation and Itch Response in a Murine Model of Allergic Contact Dermatitis. *J. Neurophysiol.* 118, 619–624. doi:10.1152/jn.00187.2017

Qu, L., Fu, K., Yang, J., Shimada, S. G., and LaMotte, R. H. (2015). CXCR3 Chemokine Receptor Signaling Mediates Itch in Experimental Allergic Contact Dermatitis. *PAIN* 156, 1737–1746. doi:10.1097/j.pain.0000000000000208

Raychaudhuri, S. P., and Farber, E. M. (1993). Are Sensory Nerves Essential for the Development of Psoriatic Lesions? *J. Am. Acad. Dermatol.* 28, 488–489. doi:10.1016/s0190-9622(08)81760-4

Razykov, I., Levis, B., Hudson, M., Baron, M., and Thombs, B. D.Canadian Scleroderma Research Group (2013). Prevalence and Clinical Correlates of Pruritus in Patients with Systemic Sclerosis: an Updated Analysis of 959 Patients. *Rheumatology (Oxford)* 52, 2056–2061. doi:10.1093/rheumatology/ket275

Reich, A., Orda, A., Wiśnicka, B., and Szepietowski, J. C. (2007). Plasma Neuropeptides and Perception of Pruritus in Psoriasis. *Acta Derm Venereol.* 87, 299–304. doi:10.2340/00015555-0265

Rendon, A., and Schäkel, K. (2019). Psoriasis Pathogenesis and Treatment. *Int. J. Mol. Sci.* 20. doi:10.3390/ijms20061475

Ringkamp, M., Schepers, R. J., Shimada, S. G., Johanek, L. M., Hartke, T. V., Borzan, J., et al. (2011). A Role for Nociceptive, Myelinated Nerve Fibers in Itch Sensation. *J. Neurosci.* 31, 14841–14849. doi:10.1523/JNEUROSCI.3005-11.2011

Rossbach, K., Nassenstein, C., Gschwandtner, M., Schnell, D., Sander, K., Seifert, R., et al. (2011). Histamine H1, H3 and H4 Receptors Are Involved in Pruritus. *Neuroscience* 190, 89–102. doi:10.1016/j.neuroscience.2011.06.002

Ru, F., Sun, H., Jurcakova, D., Herbstsomer, R. A., Meixong, J., Dong, X., et al. (2017). Mechanisms of Pruritogen-Induced Activation of Itch Nerves in Isolated Mouse Skin. *J. Physiol.* 595, 3651–3666. doi:10.1113/JP273795

Rustemeyer, T., van Hoogstraten, I. M. W., von Blomberg, B. M. E., and Scheper, R. J. (2006). "Mechanisms in Allergic Contact Dermatitis," in *Contact Dermatitis*. Editors P. J. Frosch, T. Menné, and J.-P. Lepoittevin (Berlin, Heidelberg: Springer), 11–43. doi:10.1007/3-540-31301-X_2

Ruzicka, T., Hanifin, J. M., Furue, M., Pulka, G., Mlynarczyk, I., Wollenberg, A., et al. (2017). Anti-Interleukin-31 Receptor A Antibody for Atopic Dermatitis. *N. Engl. J. Med.* 376, 826–835. doi:10.1056/NEJMoa1606490

Sandoval-Talamantes, A. K., Gómez-González, B. A., Uriarte-Mayorga, D. F., Martínez-Guzman, M. A., Wheber-Hidalgo, K. A., and Alvarado-Navarro, A. (2020). Neurotransmitters, Neuropeptides and Their Receptors Interact with Immune Response in Healthy and Psoriatic Skin. *Neuropeptides* 79, 102004. doi:10.1016/j.npep.2019.102004

Sanjel, B., Maeng, H. J., and Shim, W. S. (2019). BAM8-22 and its Receptor MRGPRX1 May Attribute to Cholestatic Pruritus. *Sci. Rep.* 9, 10888. doi:10.1038/s41598-019-47267-5

Saraceno, R., Kleyn, C. E., Terenghi, G., and Griffiths, C. E. (2006). The Role of Neuropeptides in Psoriasis. *Br. J. Dermatol.* 155, 876–882. doi:10.1111/j.1365-2133.2006.07518.x

Schaper, K., Rossbach, K., Köther, B., Stark, H., Kietzmann, M., Werfel, T., et al. (2016). Stimulation of the Histamine 4 Receptor Upregulates Thymic Stromal Lymphopoietin (TSLP) in Human and Murine Keratinocytes. *Pharmacol. Res.* 113, 209–215. doi:10.1016/j.phrs.2016.08.001

Schmelz, M., Michael, K., Weidner, C., Schmidt, R., Torebjörk, H. E., and Handwerker, H. O. (2000). Which Nerve Fibers Mediate the Axon Reflex Flare in Human Skin? *Neuroreport* 11, 645–648. doi:10.1097/00001756-200002280-00041

Schmelz, M. (2015). Neurophysiology and Itch Pathways. *Handb Exp. Pharmacol.* 226, 39–55. doi:10.1007/978-3-662-44605-8_3

Schmelz, M., Schmidt, R., Bickel, A., Handwerker, H. O., and Torebjörk, H. E. (1997). Specific C-Receptors for Itch in Human Skin. *J. Neurosci.* 17, 8003–8008. doi:10.1523/jneurosci.17-20-08003.1997

Schmelz, M., and Schmidt, R. (2010). Microneurographic Single-Unit Recordings to Assess Receptive Properties of Afferent Human C-Fibers. *Neurosci. Lett.* 470, 158–161. doi:10.1016/j.neulet.2009.05.064

Schmelz, M., Schmidt, R., Weidner, C., Hilliges, M., Torebjork, H. E., and Handwerker, H. O. (2003). Chemical Response Pattern of Different Classes of C-Nociceptors to Pruritogens and Algogens. *J. Neurophysiol.* 89, 2441–2448. doi:10.1152/jn.01139.2002

Schmidt, R., Schmelz, M., Forster, C., Ringkamp, M., Torebjörk, E., and Handwerker, H. (1995). Novel Classes of Responsive and Unresponsive C Nociceptors in Human Skin. *J. Neurosci.* 15, 333–341. doi:10.1523/jneurosci.15-01-00333.1995

Schmidt, R., Schmelz, M., Ringkamp, M., Handwerker, H. O., and Torebjörk, H. E. (1997). Innervation Territories of Mechanically Activated C Nociceptor Units in Human Skin. *J. Neurophysiol.* 78, 2641–2648. doi:10.1152/jn.1997.78.5.2641

Schmidt, R., Schmelz, M., Weidner, C., Handwerker, H. O., and Torebjörk, H. E. (2002). Innervation Territories of Mechano-Insensitive C Nociceptors in Human Skin. *J. Neurophysiol.* 88, 1859–1866. doi:10.1152/jn.2002.88.4.1859

Seo, S. H., Kim, S., Kim, S. E., Chung, S., and Lee, S. E. (2020). Enhanced Thermal Sensitivity of TRPV3 in Keratinocytes Underlies Heat-Induced Pruritogen Release and Pruritus in Atopic Dermatitis. *J. Invest. Dermatol.* 140, 2199–e6. e6. doi:10.1016/j.jid.2020.02.028

Serhan, N., Basso, L., Sibilano, R., Petitfils, C., Meixiong, J., Bonnart, C., et al. (2019). House Dust Mites Activate Nociceptor-Mast Cell Clusters to Drive Type 2 Skin Inflammation. *Nat. Immunol.* 20, 1435–1443. doi:10.1038/s41590-019-0493-z

Shim, W. S., and Oh, U. (2008). Histamine-induced Itch and its Relationship with Pain. *Mol. Pain* 4, 29. doi:10.1186/1744-8069-4-29

Shimada, S. G., and LaMotte, R. H. (2008). Behavioral Differentiation between Itch and Pain in Mouse. *Pain* 139, 681–687. doi:10.1016/j.pain.2008.08.002

Shirani, Z., Kucenic, M. J., Carroll, C. L., Fleischer, A. B., Feldman, S. R., Yosipovitch, G., et al. (2004). Pruritus in Adult Dermatomyositis. *Clin. Exp. Dermatol.* 29, 273–276. doi:10.1111/j.1365-2230.2004.01510.x

Shirazian, S., Kline, M., Sakhiya, V., Schanler, M., Moledina, D., Patel, C., et al. (2013). Longitudinal Predictors of Uremic Pruritus. *J. Ren. Nutr.* 23, 428–431. doi:10.1053/j.jrn.2013.08.002

Shouman, K., and Benarroch, E. E. (2021). Peripheral Neuroimmune Interactions: Selected Review and Some Clinical Implications. *Clin. Auton. Res.* 31, 477–489. doi:10.1007/s10286-021-00787-5

Sikand, P., Dong, X., and LaMotte, R. H. (2011). BAM8-22 Peptide Produces Itch and Nociceptive Sensations in Humans Independent of Histamine Release. *J. Neurosci.* 31, 7563–7567. doi:10.1523/JNEUROSCI.1192-11.2011

Silva, S. R., Viana, P. C., Lugon, N. V., Hoette, M., Ruzany, F., and Lugon, J. R. (1994). Thalidomide for the Treatment of Uremic Pruritus: a Crossover Randomized Double-Blind Trial. *Nephron* 67, 270–273. doi:10.1159/000187978

Singh, L. K., Pang, X., Alexacos, N., Letourneau, R., and Theoharides, T. C. (1999). Acute Immobilization Stress Triggers Skin Mast Cell Degranulation via Corticotropin Releasing Hormone, Neurotensin, and Substance P: A Link to Neurogenic Skin Disorders. *Brain Behav. Immun.* 13, 225–239. doi:10.1006/brbi.1998.0541

Slominski, A., Pisarchik, A., Zbytek, B., Tobin, D. J., Kauser, S., and Wortsman, J. (2003). Functional Activity of Serotoninergic and Melatoninergic Systems Expressed in the Skin. *J. Cell Physiol* 196, 144–153. doi:10.1002/jcp.10287

Slominski, A. T. (2015). On the Role of the Endogenous Opioid System in Regulating Epidermal Homeostasis. *J. Invest. Dermatol.* 135, 333–334. doi:10.1038/jid.2014.458

Soeberdt, M., Kilic, A., and Abels, C. (2020). Small Molecule Drugs for the Treatment of Pruritus in Patients with Atopic Dermatitis. *Eur. J. Pharmacol.* 881, 173242. doi:10.1016/j.ejphar.2020.173242

Sokabe, T., Fukumi-Tominaga, T., Yonemura, S., Mizuno, A., and Tominaga, M. (2010). The TRPV4 Channel Contributes to Intercellular junction Formation in Keratinocytes. *J. Biol. Chem.* 285, 18749–18758. doi:10.1074/jbc.M110.103606

Song, J. S., Tawa, M., Chau, N. G., Kupper, T. S., and LeBoeuf, N. R. (2017). Aprepitant for Refractory Cutaneous T-Cell Lymphoma-Associated Pruritus: 4 Cases and a Review of the Literature. *BMC Cancer* 17, 200. doi:10.1186/s12885-017-3194-8

Sonkoly, E., Muller, A., Lauerma, A. I., Pivarcsi, A., Soto, H., Kemeny, L., et al. (2006). IL-31: a New Link between T Cells and Pruritus in Atopic Skin Inflammation. *J. Allergy Clin. Immunol.* 117, 411–417. doi:10.1016/j.jaci.2005.10.033

Ständer, S., Weisshaar, E., Mettang, T., Szepietowski, J. C., Carstens, E., Ikoma, A., et al. (2007). Clinical Classification of Itch: a Position Paper of the International Forum for the Study of Itch. *Acta Derm Venereol.* 87, 291–294. doi:10.2340/00015555-0305

Ständer, S., Siepmann, D., Herrgott, I., Sunderkötter, C., and Luger, T. A. (2010). Targeting the Neurokinin Receptor 1 with Aprepitant: A Novel Antipruritic Strategy. *PLOS ONE* 5, e10968. doi:10.1371/journal.pone.0010968

Steck, O., Bertschi, N. L., Luther, F., Berg, J., Winkel, D. J., Holbro, A., et al. (2020). Rapid and Sustained Control of Itch and Reduction in Th2 Bias by Dupilumab in a Patient with Sézary Syndrome. *J. Eur. Acad. Dermatol. Venereol.* 35, 1331–1337. doi:10.1111/jdv.17001

Steinhoff, M., Bienenstock, J., Schmelz, M., Maurer, M., Wei, E., and Bíró, T. (2006). Neurophysiological, Neuroimmunological, and Neuroendocrine Basis of Pruritus. *J. Invest. Dermatol.* 126, 1705–1718. doi:10.1038/sj.jid.5700231

Storan, E. R., O'Gorman, S. M., McDonald, I. D., and Steinhoff, M. (2015). Role of Cytokines and Chemokines in Itch. *Handb Exp. Pharmacol.* 226, 163–176. doi:10.1007/978-3-662-44605-8_9

Strober, B., Sigurgeirsson, B., Popp, G., Sinclair, R., Krell, J., Stonkus, S., et al. (2016). Secukinumab Improves Patient-Reported Psoriasis Symptoms of Itching, Pain, and Scaling: Results of Two Phase 3, Randomized, Placebo-Controlled Clinical Trials. *Int. J. Dermatol.* 55, 401–407. doi:10.1111/ijd.13236

Sun, S., Xu, Q., Guo, C., Guan, Y., Liu, Q., and Dong, X. (2017). Leaky Gate Model: Intensity-dependent Coding of Pain and Itch in the Spinal Cord. *Neuron* 93, 840–e5. e5. doi:10.1016/j.neuron.2017.01.012

Sun, Y. G., and Chen, Z. F. (2007). A Gastrin-Releasing Peptide Receptor Mediates the Itch Sensation in the Spinal Cord. *Nature* 448, 700–703. doi:10.1038/nature06029

Suwarsa, O., Dharmadji, H. P., Sutedja, E., Herlina, L., Sori, P. R., Hindritiani, R., et al. (2019). Skin Tissue Expression and Serum Level of Thymic Stromal Lymphopoietin in Patients with Psoriasis Vulgaris. *Dermatol. Rep.* 11, 8006. doi:10.4081/dr.2019.8006

Szántó, M., Oláh, A., Szöllősi, A. G., Tóth, K. F., Páyer, E., Czakó, N., et al. (2019). Activation of TRPV3 Inhibits Lipogenesis and Stimulates Production of Inflammatory Mediators in Human Sebocytes-A Putative Contributor to Dry Skin Dermatoses. *J. Invest. Dermatol.* 139, 250–253. doi:10.1016/j.jid.2018.07.015

Szepietowski, J. C., and Reich, A. (2016). Pruritus in Psoriasis: An Update. *Eur. J. Pain* 20, 41–46. doi:10.1002/ejp.768

Szolcsányi, J., Pintér, E., Helyes, Z., Oroszi, G., and Németh, J. (1998). Systemic Anti-inflammatory Effect Induced by Counter-irritation through a Local Release of Somatostatin from Nociceptors. *Br. J. Pharmacol.* 125, 916–922. doi:10.1038/sj.bjp.0702144

Szöllősi, A. G., McDonald, I., Szabó, I. L., Meng, J., van den Bogaard, E., and Steinhoff, M. (2019). TLR3 in Chronic Human Itch: A Keratinocyte-Associated Mechanism of Peripheral Itch Sensitization. *J. Invest. Dermatol.* 139, 2393–2396. e6. doi:10.1016/j.jid.2019.04.018

Szöllősi, A. G., Vasas, N., Angyal, Á., Kistamás, K., Nánási, P. P., Mihály, J., et al. (2018). Activation of TRPV3 Regulates Inflammatory Actions of Human Epidermal Keratinocytes. *J. Invest. Dermatol.* 138, 365–374. doi:10.1016/j.jid.2017.07.852

Takayama, Y., Derouiche, S., Maruyama, K., and Tominaga, M. (2019). Emerging Perspectives on Pain Management by Modulation of TRP Channels and ANO1. *Int. J. Mol. Sci.* 20. doi:10.3390/ijms20143411

Takayama, Y., Shibasaki, K., Suzuki, Y., Yamanaka, A., and Tominaga, M. (2014). Modulation of Water Efflux through Functional Interaction between TRPV4 and TMEM16A/anoctamin 1. *FASEB J.* 28, 2238–2248. doi:10.1096/fj.13-243436

Takayama, Y., Uta, D., Furue, H., and Tominaga, M. (2015). Pain-enhancing Mechanism through Interaction between TRPV1 and Anoctamin 1 in Sensory Neurons. *Proc. Natl. Acad. Sci. U S A.* 112, 5213–5218. doi:10.1073/pnas.1421507112

Taves, S., and Ji, R. R. (2015). Itch Control by Toll-like Receptors. *Handb Exp. Pharmacol.* 226, 135–150. doi:10.1007/978-3-662-44605-8_7

Tey, H. L., and Yosipovitch, G. (2011). Targeted Treatment of Pruritus: a Look into the Future. *Br. J. Dermatol.* 165, 5–17. doi:10.1111/j.1365-2133.2011.10217.x

Thériné, C., Brenaut, E., Sonbol, H., Pasquier, E., Saraux, A., Devauchelle, V., et al. (2017). Itch and Systemic Sclerosis: Frequency, Clinical Characteristics and Consequences. *Br. J. Dermatol.* 176, 1392–1393. doi:10.1111/bjd.14998

Tominaga, M., Caterina, M. J., Malmberg, A. B., Rosen, T. A., Gilbert, H., Skinner, K., et al. (1998). The Cloned Capsaicin Receptor Integrates Multiple Pain-Producing Stimuli. *Neuron* 21, 531–543. doi:10.1016/s0896-6273(00)80564-4

Tominaga, M., Ogawa, H., and Takamori, K. (2007). Possible Roles of Epidermal Opioid Systems in Pruritus of Atopic Dermatitis. *J. Invest. Dermatol.* 127, 2228–2235. doi:10.1038/sj.jid.5700942

Topal, F. A., Zuberbier, T., Makris, M. P., and Hofmann, M. (2020). The Role of IL-17, IL-23 and IL-31, IL-33 in Allergic Skin Diseases. *Curr. Opin. Allergy Clin. Immunol.* 20, 367–373. doi:10.1097/ACI.0000000000000658

Töröcsik, D., Weise, C., Gericke, J., Szegedi, A., Lucas, R., Mihaly, J., et al. (2019). Transcriptomic and Lipidomic Profiling of Eicosanoid/docosanoid Signalling in Affected and Non-affected Skin of Human Atopic Dermatitis Patients. *Exp. Dermatol.* 28, 177–189. doi:10.1111/exd.13867

Torres, T., Fernandes, I., Selores, M., Alves, R., and Lima, M. (2012). Aprepitant: Evidence of its Effectiveness in Patients with Refractory Pruritus Continues. *J. Am. Acad. Dermatol.* 66, e14–5. doi:10.1016/j.jaad.2011.01.016

Tóth, B. I., Oláh, A., Szöllősi, A. G., and Bíró, T. (2014). TRP Channels in the Skin. *Br. J. Pharmacol.* 171, 2568–2581. doi:10.1111/bph.12569

Tóth, B. I., Szallasi, A., and Bíró, T. (2015). Transient Receptor Potential Channels and Itch: How Deep Should We Scratch? *Handb Exp. Pharmacol.* 226, 89–133. doi:10.1007/978-3-662-44605-8_6

Tóth, B. I., Szöllősi, A. G., and Bíró, T. (2020). "TRP Channels in Itch and Pain," in *Itch and Pain. Similarities, Interactions, and Differences* (Washington, D.C.: IASP - Wolters Kluwer). Available at: https://shop.lww.com/Itch-and-Pain/p/9781975153038.

Tóth, K., Ádám, D., Bíró, T., and Oláh, A. (2019). Cannabinoid Signaling in the Skin: Therapeutic Potential of the "C(ut)annabinoid" System. *Molecules* 24, 918. doi:10.3390/molecules24050918

Tsuboi, R., Sato, C., Oshita, Y., Hama, H., Sakurai, T., Goto, K., et al. (1995). Ultraviolet B Irradiation Increases Endothelin-1 and Endothelin Receptor Expression in Cultured Human Keratinocytes. *FEBS Lett.* 371, 188–190. doi:10.1016/0014-5793(95)00912-s

Umehara, Y., Kiatsurayanon, C., Trujillo-Paez, J. V., Chieosilapatham, P., Peng, G., Yue, H., et al. (2021). Intractable Itch in Atopic Dermatitis: Causes and Treatments. *Biomedicines* 9. doi:10.3390/biomedicines9030229

Ungar, B., Correa da Rosa, J., Shemer, A., Czarnowicki, T., Estrada, Y. D., Fuentes-Duculan, J., et al. (2017). Patch Testing of Food Allergens Promotes Th17 and Th2 Responses with Increased IL-33: a Pilot Study. *Exp. Dermatol.* 26, 272–275. doi:10.1111/exd.13148

Usoskin, D., Furlan, A., Islam, S., Abdo, H., Lönnerberg, P., Lou, D., et al. (2015). Unbiased Classification of Sensory Neuron Types by Large-Scale Single-Cell RNA Sequencing. *Nat. Neurosci.* 18, 145–153. doi:10.1038/nn.3881

Valtcheva, M. V., Davidson, S., Zhao, C., Leitges, M., and Gereau, R. W. (2015). Protein Kinase Cδ Mediates Histamine-Evoked Itch and Responses in Pruriceptors. *Mol. Pain* 11, 1. doi:10.1186/1744-8069-11-1

Vandewauw, I., De Clercq, K., Mulier, M., Held, K., Pinto, S., Van Ranst, N., et al. (2018). A TRP Channel Trio Mediates Acute Noxious Heat Sensing. *Nature* 555, 662–666. doi:10.1038/nature26137

Varricchi, G., Pecoraro, A., Marone, G., Criscuolo, G., Spadaro, G., Genovese, A., et al. (2018). Thymic Stromal Lymphopoietin Isoforms, Inflammatory Disorders, and Cancer. *Front. Immunol.* 9, 1595. doi:10.3389/fimmu.2018.01595

Verduzco, H. A., and Shirazian, S. (2020). CKD-associated Pruritus: New Insights into Diagnosis, Pathogenesis, and Management. *Kidney Int. Rep.* 5, 1387–1402. doi:10.1016/j.ekir.2020.04.027

Vij, A., and Duvic, M. (2012). Prevalence and Severity of Pruritus in Cutaneous T Cell Lymphoma. *Int. J. Dermatol.* 51, 930–934. doi:10.1111/j.1365-4632.2011.05188.x

Voisin, T., Perner, C., Messou, M. A., Shiers, S., Ualiyeva, S., Kanaoka, Y., et al. (2021). The CysLT2R Receptor Mediates Leukotriene C4-Driven Acute and Chronic Itch. *Proc. Natl. Acad. Sci. U S A.* 118. doi:10.1073/pnas.2022087118

Volpe, E., Pattarini, L., Martinez-Cingolani, C., Meller, S., Donnadieu, M. H., Bogiatzi, S. I., et al. (2014). Thymic Stromal Lymphopoietin Links Keratinocytes and Dendritic Cell-Derived IL-23 in Patients with Psoriasis. *J. Allergy Clin. Immunol.* 134, 373–381. doi:10.1016/j.jaci.2014.04.022

Vriens, J., Nilius, B., and Voets, T. (2014). Peripheral Thermosensation in Mammals. *Nat. Rev. Neurosci.* 15, 573–589. doi:10.1038/nrn3784

Wahlgren, C. F., and Ekblom, A. (1996). Two-point Discrimination of Itch in Patients with Atopic Dermatitis and Healthy Subjects. *Acta Derm Venereol.* 76, 48–51. doi:10.2340/00015555764851

Wallrapp, A., Burkett, P. R., Riesenfeld, S. J., Kim, S. J., Christian, E., Abdulnour, R. E., et al. (2019). Calcitonin Gene-Related Peptide Negatively Regulates Alarmin-Driven Type 2 Innate Lymphoid Cell Responses. *Immunity* 51, 709–e6. e6. doi:10.1016/j.immuni.2019.09.005

Walsh, C. M., Hill, R. Z., Schwendinger-Schreck, J., Deguine, J., Brock, E. C., Kucirek, N., et al. (2019). Neutrophils Promote CXCR3-dependent Itch in the Development of Atopic Dermatitis. *eLife* 8, e48448. doi:10.7554/eLife.48448

Wang, C., Gu, L., Ruan, Y., Geng, X., Xu, M., Yang, N., et al. (2019). Facilitation of MrgprD by TRP-A1 Promotes Neuropathic Pain. *FASEB J.* 33, 1360–1373. doi:10.1096/fj.201800615RR

Wedi, B. (2020). Ligelizumab for the Treatment of Chronic Spontaneous Urticaria. *Expert Opin. Biol. Ther.* 20, 853–861. doi:10.1080/14712598.2020.1767061

Weisshaar, E., and Dalgard, F. (2009). Epidemiology of Itch: Adding to the burden of Skin Morbidity. *Acta Derm VenereolVenereol* 89, 339–350. doi:10.2340/00015555-0662

Weisshaar, E., Szepietowski, J. C., Dalgard, F. J., Garcovich, S., Gieler, U., Giménez-Arnau, A. M., et al. (2019). European S2k Guideline on Chronic Pruritus. *Acta Derm Venereol.* 99, 469–506. doi:10.2340/00015555-3164

Weisshaar, E., Ziethen, B., and Gollnick, H. (1997). Can a Serotonin Type 3 (5-HT3) Receptor Antagonist Reduce Experimentally-Induced Itch? *Inflamm. Res.* 46, 412–416. doi:10.1007/s000110050213

Werfel, T., Layton, G., Yeadon, M., Whitlock, L., Osterloh, I., Jimenez, P., et al. (2019). Efficacy and Safety of the Histamine H4 Receptor Antagonist ZPL-3893787 in Patients with Atopic Dermatitis. *J. Allergy Clin. Immunol.* 143, 1830–e4. e4. doi:10.1016/j.jaci.2018.07.047

Wilson, S. R., Gerhold, K. A., Bifolck-Fisher, A., Liu, Q., Patel, K. N., Dong, X., et al. (2011). TRPA1 Is Required for Histamine-independent, Mas-Related G Protein-Coupled Receptor-Mediated Itch. *Nat. Neurosci.* 14, 595–602. doi:10.1038/nn.2789

Wilson, S. R., Thé, L., Batia, L. M., Beattie, K., Katibah, G. E., McClain, S. P., et al. (2013). The Epithelial Cell-Derived Atopic Dermatitis Cytokine TSLP Activates Neurons to Induce Itch. *Cell* 155, 285–295. doi:10.1016/j.cell.2013.08.057

Wilson, S. R., and Bautista, D. M. (2014). "Role of Transient Receptor Potential Channels in Acute and Chronic Itch," in Mechanisms And Treatment *Frontiers in Neuroscience*. Editors E. Carstens and T. Akiyama (Boca Raton (FL): CRC Press/Taylor & Francis). Available at: http://www.ncbi.nlm.nih.gov/books/NBK200927/(Accessed July 16, 2021).

Xie, Z., and Hu, H. (2018). TRP Channels as Drug Targets to Relieve Itch. *Pharmaceuticals (Basel)* 11. doi:10.3390/ph11040100

Yamanoi, Y., Kittaka, H., and Tominaga, M. (2019). Cheek Injection Model for Simultaneous Measurement of Pain and Itch-Related Behaviors. *JoVE* 151. doi:10.3791/58943

Yang, T. B., and Kim, B. S. (2019). Pruritus in Allergy and Immunology. *J. Allergy Clin. Immunol.* 144, 353–360. doi:10.1016/j.jaci.2019.06.016

Yang, Y. D., Cho, H., Koo, J. Y., Tak, M. H., Cho, Y., Shim, W. S., et al. (2008). TMEM16A Confers Receptor-Activated Calcium-dependent Chloride Conductance. *Nature* 455, 1210–1215. doi:10.1038/nature07313

Yoshioka, T., Imura, K., Asakawa, M., Suzuki, M., Oshima, I., Hirasawa, T., et al. (2009). Impact of the Gly573Ser Substitution in TRPV3 on the Development of Allergic and Pruritic Dermatitis in Mice. *J. Invest. Dermatol.* 129, 714–722. doi:10.1038/jid.2008.245

Yosipovitch, G., Misery, L., Proksch, E., Metz, M., Ständer, S., and Schmelz, M. (2019). Skin Barrier Damage and Itch: Review of Mechanisms, Topical Management and Future Directions. *Acta Derm Venereol.* 99, 1201–1209. doi:10.2340/00015555-3296

Yosipovitch, G., Ständer, S., Kerby, M. B., Larrick, J. W., Perlman, A. J., Schnipper, E. F., et al. (2018). Serlopitant for the Treatment of Chronic Pruritus: Results of a Randomized, Multicenter, Placebo-Controlled Phase 2 Clinical Trial. *J. Am. Acad. Dermatol.* 78, 882–e10. e10. doi:10.1016/j.jaad.2018.02.030

Yu, H., Zhao, T., Liu, S., Wu, Q., Johnson, O., Wu, Z., et al. (2019). MRGPRX4 Is a Bile Acid Receptor for Human Cholestatic Itch. *Elife* 8. doi:10.7554/eLife.48431

Zeidler, C., Yosipovitch, G., and Ständer, S. (2018). Prurigo Nodularis and its Management. *Dermatol. Clin.* 36, 189–197. doi:10.1016/j.det.2018.02.003

Zhang, S., Edwards, T. N., Chaudhri, V. K., Wu, J., Cohen, J. A., Hirai, T., et al. (2021). Nonpeptidergic Neurons Suppress Mast Cells via Glutamate to Maintain Skin Homeostasis. *Cell* 184, 2151–e16. e16. doi:10.1016/j.cell.2021.03.002

Zhang, X., and He, Y. (2020). The Role of Nociceptive Neurons in the Pathogenesis of Psoriasis. *Front. Immunol.* 11, 1984. doi:10.3389/fimmu.2020.01984

Zhang, Z., Malewicz, N. M., Xu, X., Pan, J., Kumowski, N., Zhu, T., et al. (2019). Differences in Itch and Pain Behaviors Accompanying the Irritant and Allergic Contact Dermatitis Produced by a Contact Allergen in Mice. *Pain Rep.* 4, e781. doi:10.1097/PR9.0000000000000781

Zhao, J., Munanairi, A., Liu, X. Y., Zhang, J., Hu, L., Hu, M., et al. (2020). PAR2 Mediates Itch via TRPV3 Signaling in Keratinocytes. *J. Invest. Dermatol.* 140, 1524–1532. doi:10.1016/j.jid.2020.01.012

Zhao, Z. Q., Huo, F. Q., Jeffry, J., Hampton, L., Demehri, S., Kim, S., et al. (2013). Chronic Itch Development in Sensory Neurons Requires BRAF Signaling Pathways. *J. Clin. Invest.* 123, 4769–4780. doi:10.1172/JCI70528

Zheng, Y., Danilenko, D. M., Valdez, P., Kasman, I., Eastham-Anderson, J., Wu, J., et al. (2007). Interleukin-22, a T(H)17 Cytokine, Mediates IL-23-induced Dermal Inflammation and Acanthosis. *Nature* 445, 648–651. doi:10.1038/nature05505

Zhu, T. H., Nakamura, M., Farahnik, B., Abrouk, M., Lee, K., Singh, R., et al. (2016). The Role of the Nervous System in the Pathophysiology of Psoriasis: A Review of Cases of Psoriasis Remission or Improvement Following Denervation Injury. *Am. J. Clin. Dermatol.* 17, 257–263. doi:10.1007/s40257-016-0183-7

Conflict of Interest: AO provides consultancy services to Monasterium Laboratory Skin & Hair Research Solutions GmbH.

The remaining authors declare that the research was conducted in the absence of any commercial or financial relationships that could be construed as a potential conflict of interest.

Publisher's Note: All claims expressed in this article are solely those of the authors and do not necessarily represent those of their affiliated organizations, or those of the publisher, the editors and the reviewers. Any product that may be evaluated in this article, or claim that may be made by its manufacturer, is not guaranteed or endorsed by the publisher.

Advantages of publishing in Frontiers

OPEN ACCESS
Articles are free to read for greatest visibility and readership

FAST PUBLICATION
Around 90 days from submission to decision

HIGH QUALITY PEER-REVIEW
Rigorous, collaborative, and constructive peer-review

TRANSPARENT PEER-REVIEW
Editors and reviewers acknowledged by name on published articles

Frontiers
Avenue du Tribunal-Fédéral 34
1005 Lausanne | Switzerland

Visit us: www.frontiersin.org
Contact us: frontiersin.org/about/contact

REPRODUCIBILITY OF RESEARCH
Support open data and methods to enhance research reproducibility

DIGITAL PUBLISHING
Articles designed for optimal readership across devices

FOLLOW US
@frontiersin

IMPACT METRICS
Advanced article metrics track visibility across digital media

EXTENSIVE PROMOTION
Marketing and promotion of impactful research

LOOP RESEARCH NETWORK
Our network increases your article's readership